

UNIVERSIDADE ESTADUAL DE CAMPINAS



Karina Carvalho Mancini

**ULTRA-ESTRUTURA E CITOQUÍMICA DOS
ESPERMATOZÓIDES EM *EUPTOIETA HEGESIA*
(INSECTA: LEPIDOPTERA) AO LONGO DOS TRATOS
REPRODUTORES MASCULINO E FEMININO**

Este exemplar corresponde à redação final
da tese defendida pelo(a) candidato (a)
Karina Carvalho
Mancini
e aprovada pela Comissão Julgadora.

Tese apresentada ao Instituto de Biologia da
Universidade Estadual de Campinas para
obtenção do título de Doutor em Ciências
Biológicas na área de Biologia Celular e
Estrutural.

A handwritten signature in cursive script, likely belonging to Mary Anne Heidi Dolder.

Orientação: Profa. Dra. Mary Anne Heidi Dolder

UNICAMP
BIBLIOTECA CENTRAL
SEÇÃO CIRCULANTE

UNIDADE	BC
Nº CHAMADA	M312u
V	EX
TOMBO BC/	56413
PROC.	16-124/03
C <input type="checkbox"/>	D <input checked="" type="checkbox"/>
PREÇO	R\$ 11,00
DATA	
Nº CPD	

CM001B9457-7

BIBD 305031

**FICHA CATALOGRÁFICA ELABORADA PELA
BIBLIOTECA DO INSTITUTO DE BIOLOGIA - UNICAMP**

M312u Mancini, Karina Carvalho
 Ultra-estrutura e citoquímica dos espermatozóides em *Euptoieta hegesia*
 (Insecta: Lepidoptera) ao longo dos tratos reprodutores masculino e feminino /
 Karina Carvalho Mancini. --
 Campinas, SP:[s.n], 2003.

Orientadora: Mary Anne Heidi Dolder
 Tese (doutorado) – Universidade Estadual de Campinas.
 Instituto de Biologia.

1. Espermatozóides. 2. Carboidrato. 3. Proteína. I. Dolder, Mary Anne Heidi.
- II. Universidade Estadual de Campinas. Instituto de Biologia. III. Título.

Data da Defesa: 27 / 08 / 2003

BANCA EXAMINADORA

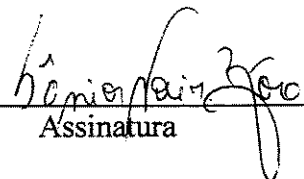
Profa. Dra. Mary Anne Heidi Dolder (Orientadora)


Assinatura

Prof. Dr. José Lino-Neto


Assinatura

Profa. Dra. Sonia Nair Bão


Assinatura

Profa. Dra. Marília Medeiros

Assinatura

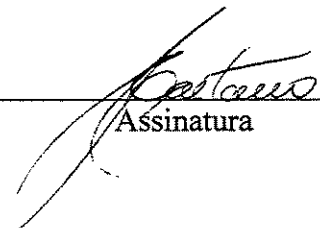
Profa. Dra. Doralice Maria Cella


Assinatura

Prof. Dr. Hernandes Faustino de Carvalho

Assinatura

Prof. Dr. Flávio Henrique Caetano


Assinatura

10033-904

AGRADECIMENTOS

Em primeiro lugar à minha orientadora e amiga *Mary Anne Heidi Dolder* que me acolheu em seu laboratório desde 1998 quando dei início a minha jornada em microscopia eletrônica.

Aos *professores que compuseram as bancas examinadoras* pelas correções e contribuições finais para a elaboração definitiva desta tese.

Aos *docentes do Departamento de Biologia Celular*, em especial àqueles com quem dividi espaço no primeiro piso e que tiveram que suportar as intermináveis conversas no laboratório e na sala da Heidi.

À *secretaria do Departamento de Biologia Celular*, em especial à *super secretária Lilian* que, exceto nos períodos de relatório CAPES, sempre me atendeu com absoluta precisão e competência.

A *CAPES e FAPESP* pelos auxílios financeiros para o desenvolvimento desta tese e pela aquisição dos meus dois maiores bens materiais.

Às meninas do Laboratório de Microscopia Eletrônica: *Antônia, Adriane e Aurora*, que sempre foram prestativas em arrumar o astigmatismo do microscópio, em revelar meus infindáveis negativos e em cortar meus piores blocos.

Ao pessoal da Pressing Works pela simpatia, eficiência e excelente qualidade das cópias fotográficas, além, é claro, de uma senhora paciência para reproduzir minhas centenas de pranchas.

À Professora *Sônia Nair Bão* que me iniciou na citoquímica ultra-estrutural e me auxiliou em várias etapas desta tese.

Ao pessoal do Laboratório da Dolder, mas em especial as amigas *Adê* e a *Zama*, que sempre me ajudaram, escutaram, fizeram rir, deram broncas e conselhos impagáveis. *Adê*, obrigada por funcionar como um rádio inúmeras vezes, pela companhia no laboratório, onde trocávamos nossas experiências citoquímicas, mas principalmente pela amizade e cumplicidade que construímos. *Zama*, obrigada pelo companheirismo que tivemos dentro e fora do laboratório, pelo acolhimento em seu apartamento e em Viçosa, mas

principalmente, obrigada por não me detetizar. Aproveito aqui para agradecer meu amigo *Gu Benevides*, agregado do laboratório da Dolder, pela amizade, carinho e incontáveis trocas de água. Como não mencionar o singular *José Lino-Neto*, com quem convivi no laboratório nos meus 3 primeiros anos no departamento. Sempre inventando (um verdadeiro MacGiver no laboratório), sempre trabalhando, sempre ocupado, mas também sempre muito prestativo, bem humorado, eficiente e otimista...não foi à toa que te escolhi agora.

Aos *colegas do Departamento de Biologia Celular*, mas em especial aos meus amigos de almoços, cafézinhos e afins... *Adê, Aninha, Klé, Paty e Oda*, obrigada pela eterna amizade. Vocês sabem o quanto foram, são e sempre serão importantes para mim.

Ao meu querido *André Victor Baku*, pelas incontáveis coletas de campo e por toda a ajuda na identificação e ecologia de borboletas. Obrigada pela paciência, carinho, compreensão, incentivo e confiança...aproveitei cada momento.

À minha *família*, pela paciência, incentivo, confiança e ajuda nestes anos em que trabalhei nesta tese sem fim. *Pai*, apesar de não entender muito bem o que estava acontecendo este tempo todo, sei que acreditou em mim. *Mãe*, obrigada pelas 'caronas' até a Unicamp, pelos lanchinhos e cafézinhos enquanto tentava trabalhar em casa. Aos dois, obrigada por absolutamente tudo. *Mila*, entre outras coisas, sou eternamente grata pela organização das minhas referências bibliográficas, que tento manter em ordem.

Enfim, a todos àqueles que, ao longo destes anos, de diferentes maneiras contribuíram para o desenvolvimento das próximas 200 páginas!

ÍNDICE

Resumo	1
Abstract	2
Introdução	3
<i>A ordem Lepidoptera</i>	
<i>Aspectos Gerais do Dimorfismo de Espermatozóides em Lepidoptera</i>	
<i>Controle da Espermatogênese Dicotômica em Lepidoptera</i>	
<i>Função dos espermatozóides apirenes e eupirenes e a evolução do polimorfismo</i>	
Objetivos Gerais	11
Referências Bibliográficas	12
Organização da Tese	18

Capítulo 1

Estrutura e Ultra-estrutura dos Espermatozóides Apirenes e Eupirenes ao Longo do Trato Reprodutor Masculino

- | | |
|--|----|
| 1.1. <i>Dichotomic spermiogenesis of Euptoieta hegesia (Lepidoptera: Nymphalidae)</i> | 20 |
| 1.2. <i>Ultrastructure of the apyrene and eupyrene spermatozoa from the seminal vesicle of Euptoieta hegesia (Lepidoptera: Nymphalidae)</i> | 46 |
| 1.3. <i>Sperm morphology and arrangement along the male reproductive tract of the butterfly Euptoieta hegesia (Lepidoptera: Nymphalidae)</i> | 55 |

Capítulo 2

Citoquímica Ultra-estrutural dos Espermatozóides Apirenes e Eupirene ao Longo do Trato Reprodutor Masculino

- | | |
|---|----|
| 2.1. <i>Protein detection in spermatids and spermatozoa of the butterfly Euptoieta hegesia (Lepidoptera: Nymphalidae)</i> | 83 |
|---|----|

2.2. Carbohydrate localization in apyrene and eupyrene spermatozoa of the butterfly <i>Euptoieta hegesia</i> (Lepidoptera: Nymphalidae)	108
2.3. Lectin binding sites on the spermatids and spermatozoa of <i>Euptoieta hegesia</i> (Lepidoptera: Nymphalidae)	128
2.4. Immunocytochemical Evidence of Tubulin Isoforms in Spermatids and Spermatozoa of <i>Euptoieta hegesia</i> (Lepidoptera: Nymphalidae)	146
 Capítulo 3	
Estrutura e Ultra-estrutura da Espermateca e dos Espermatozóides em Fêmeas	
3.1. Morphology of the spermatheca and the spermatozoa found in <i>Euptoieta hegesia</i> females (Lepidoptera: Nymphalidae)	169
 Capítulo 4 – Conclusões	 198

RESUMO

Borboletas e mariposas apresentam um dos casos mais evidentes de polimorfismo espermático, com a produção de dois tipos de espermatozóides: os apirenes e os eupirenes, que diferem em morfologia e função. Estudos ultra-estruturais descreveram a morfologia e organização de ambos os tipos de espermatozóides ao longo dos tratos reprodutores masculino e feminino da borboleta *Euptoieta hegesia*. Os espermatozóides apirenes extratesticulares adquirem membranas concêntricas externas provenientes do rearranjo da membrana plasmática. Já os eupirenes, adquirem um complexo envoltório que sofre modificações ao longo dos tratos reprodutores e parece ser parcialmente resultante do rearranjo dos apêndices laciniados. Foram usados também métodos citoquímicos, à saber: ácido fosfotúngstico-etanólico, ácido tânico, cuprolinic blue, vermelho de rutênio, tiosemicarbazida/proteinato de prata e lectinas. Apirenes e eupirenes apresentaram, diferencialmente, proteínas e carboidratos no lúmen dos microtúbulos e nos elementos de ligação do axonema, nas membranas e principalmente nas estruturas extra-celulares. Nos espermatozóides apirenes ainda foram detectados esses componentes no capuz anterior e nas regiões paracristalinas dos derivados mitocondriais. Nos espermatozóides eupirenes, os apêndices laciniados apresentaram, principalmente, componentes protéicos, enquanto os apêndices reticulados apresentaram carboidratos. Ambos os tipos de apêndices apresentaram organização paracristalina, formada por estruturas cilíndricas. Além disso, por meio da técnica de ácido tânico, foi verificada significativa similaridade entre os envoltórios apirenes e eupirenes, indicando uma possível origem comum. Com o uso de lectinas, os apêndices laciniados e os envoltórios apirenes e eupirenes apresentaram os mesmos glicoconjugados, sugerindo que os envoltórios se originaram do rearranjo destes apêndices. O método imunocitoquímico para detecção de tubulinas mostrou que os apêndices laciniados não são compostos microtubulares. No trato reprodutor feminino foram descritas as morfologias da spermateca e dos espermatozóides apirenes e eupirenes armazenados. O epitélio spermatecal, desconhecido na literatura, apresenta morfologia similar àquela encontrada em outras ordens de insetos.

ABSTRACT

Butterflies and moths present one of the most evident examples of sperm polymorphism, with the production of two types of spermatozoa: the apyrene and the eupyrene, that differ in functional and morphological characteristics. Ultrastructural studies were carried out to describe the morphology and organization of both sperm types along the male and female reproductive tracts of the butterfly *Euptoieta hegesia*. The extra-testicular apyrene spermatozoa acquire external concentric membranes as a result of the plasma membrane rearrangement. The eupyrene spermatozoa acquire a complex coat that is modified along the reproductive tracts and is apparently originates from the rearrangement of the laciniate appendages. Different cytochemical methods were applied: ethanol-fosfotungstic acid, tannic acid, cuproline blue, ruthenium red, tiosemicarbazide/silver proteinate and lectins. Both sperm types presented differences in the proteins and carbohydrates found in the microtubule lumens and in the links binding the axoneme, in the cellular membranes and, principally, in the extracellular structures. In apyrene sperm these components were detected in the anterior cap and in the paracrystalline cores of the mitochondrial derivatives. In the eupyrene sperm, the laciniate appendages were predominantly protein in composition, while the reticular appendages seem to be composed principally of carbohydrates. Both appendage types presented paracrystalline organization, made up of small cylindrical structures. With the tannic acid technique, a significant similarity was verified between the coats of both sperm types, indicating a possible common origin. With the lectin technique, the laciniate appendages and the coat of both sperm types were shown to contain the same glycoconjugates, suggesting that the coats are originated by reorganization of these appendages. The immunocytochemical method for tubulin detection demonstrated that the laciniate appendages are not microtubular structures. In the female reproductive tract, the morphology of the spermatheca was described as well as the apyrene and eupyrene spermatozoa, stored in this organ after mating. The morphology of the spermatheca epithelium, which had not been previously investigated for Lepidoptera, presented a somewhat similar organization to what is known for other insect.

INTRODUÇÃO

A ordem Lepidoptera

A ordem Lepidoptera representa um dos grupos mais importantes e mais bem estudados da Classe Insecta. Apresenta mais de 200.000 espécies, sendo considerada a terceira maior ordem de insetos e compreende dois grupos distintos: mariposas e borboletas. As mariposas são noturnas e vários de seus representantes são pragas na agricultura, causando grande impacto econômico ao homem. As borboletas são diurnas, apresentam grande diversidade de coloração nas asas, o que tornam seu estudo, observação e coleta mais fáceis. São especialmente importantes nos estudos de conservação, pois são excelentes indicadoras de qualidade ambiental e previsoras da biodiversidade local (Brown & Freitas, 1999). Além disso, têm contribuído para o desenvolvimento de vários ramos da Biologia, como Genética, Ecologia, Sistemática, Biogeografia e Morfologia.

Euptoieta hegesia é uma borboleta pertencente à família Nymphalidae. É uma espécie que habita tipicamente áreas abertas como pastos e campos, sendo facilmente encontrada em áreas urbanas, onde sua planta hospedeira larval, *Turnera ulmifolia*, se desenvolve em abundância. As larvas se desenvolvem em um mês e os adultos vivem até 14 dias (Schappert & Shore, 1998). *Euptoieta hegesia* pertence à subfamília Heliconiinae que são as borboletas com maior longevidade na fase adulta, resultando no desenvolvimento da espermatogênese ainda no adulto.

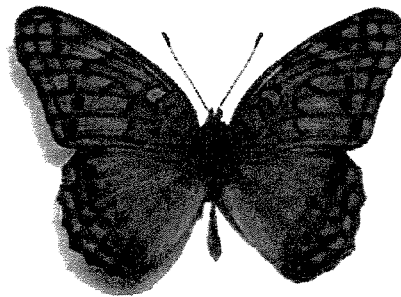


Figura 1: Macho de *Euptoieta hegesia*

Aspectos Gerais do Dimorfismo de Espermatozóides em Lepidoptera

O polimorfismo espermático, produção de diferentes tipos de espermatozóides por um mesmo indivíduo, é conhecido em grupos de invertebrados como gastrópodes (Hodgson, 1997) e artrópodes, onde se destacam as aranhas (Rosati *et al.*, 1970), os miriápodes (Jamieson, 1986) e os insetos (Sivinski, 1980). Nos insetos, estes espermatozóides podem variar em comprimento, como em Diptera e Hymenoptera; em morfologia, como em Hemiptera, Heteroptera e Hymenoptera; ou em número de cromossomos, como em Coleoptera (Jamieson, 1987; Jamieson *et al.*, 1999).

Na ordem Lepidoptera é encontrado o caso mais evidente de polimorfismo dentro dos insetos, que resulta em dois tipos de espermatozóides bastante distintos, denominados apirenes e eupirenes, que diferem em morfologia e função. O termo 'eupirene' refere-se aos espermatozóides com número haplóide de cromossomos, enquanto 'apirene' refere-se à ausência deste material cromatínico. Outra denominação encontrada é a de eu-espermatozóide (eupirene) e para-espermatozóide (apirene) (Healy & Jamieson, 1981). A primeira descrição do dimorfismo em Lepidoptera foi realizada por Meves (1903) e desde então tem se relatado a presença dos dois tipos de espermatozóides em todas as borboletas e mariposas analisadas, com exceção do gênero *Micropteryx* (Micropterigidae), um grupo basal no qual foram encontrados somente espermatozóides eupirenes (Sonnenschein & Hauser, 1990; Hamon & Chauvin, 1992).

Os espermatozóides apirenes não possuem núcleo, pois este é eliminado durante o processo de espermiogênese, e sua região anterior é composta exclusivamente por um capuz elétron denso que antecede o início do axonema (Riemann, 1970; Phillips 1971; Friedländer & Gitay 1972; Friedländer & Miesel, 1977; Lai-Fook, 1982; Medeiros, 1997; Medeiros & Silveira 1996; França & Báó, 2000). O flagelo é constituído por dois derivados mitocondriais, que possuem uma região paracristalina, e um axonema com arranjo do tipo 9+9+2, padrão em insetos, ou seja, 9 microtúbulos acessórios externos, 9 duplas de microtúbulos e 2 microtúbulos centrais (Phillips, 1970; Lai-Fook, 1982; Medeiros & Silveira, 1996; Kubo-Irie *et al.*, 1998; Garvey *et al.*, 2000).

Os espermatozóides eupirenes são mais complexos e, em geral, maiores em comprimento do que os apirenes. Possuem a região anterior composta por um acrossomo tubular localizado anterior e paralelamente a um núcleo alongado e compacto (Lai-Fook, 1982; Kubo-Irie *et al.*, 1998; França & Báó, 2000). O flagelo, assim como nos apirenes, é composto por dois derivados mitocondriais, que são maiores em dimensão do que aqueles dos apirenes e desprovidos de região paracristalina, e um axonema com arranjo do tipo 9+9+2 (Lai-Fook, 1982; Medeiros, 1986; Kubo-Irie *et al.*, 1998). Possuem ainda dois tipos de estruturas extracelulares denominadas de apêndices laciniados e reticulados que são exclusivos desta ordem. Estes apêndices eupirenes se estendem ao longo dos espermatozóides desde a região anterior, onde são mais desenvolvidos, até a extremidade posterior do flagelo, onde são menores (Phillips, 1971; Leviatan & Friedländer, 1979; Kubo-Irie *et al.*, 1998; França & Báó, 2000). Os apêndices laciniados representam uma manta radial estriada, composta de bandas elétron densas intercaladas a bandas elétron lúcidas, e estão presentes somente nos eupirenes intratesticulares (Phillips, 1971; Medeiros, 1986, 1997; Kubo-Irie *et al.*, 1998; França & Báó, 2000; Garvey *et al.*, 2000). O apêndice reticulado representa um bastão denso único que está presente nos eupirenes e se mantém durante o trato masculino (Lai-Fook, 1982; Riemann, 1970; Medeiros, 1986, 1997; Kubo-Irie *et al.*, 1998; Garvey *et al.*, 2000). Está localizado externa e paralelamente à membrana plasmática entre o axonema e um dos derivados mitocondriais.

Ao deixarem o testículo, tanto os espermatozóides apirenes quanto os eupirenes sofrem diversas modificações ultra-estruturais que são exclusivamente extracelulares. Os espermatozóides eupirenes perdem os apêndices laciniados ao mesmo tempo em que adquirem um complexo envoltório extracelular, formado por diferentes regiões elétron densas, com o apêndice reticulado externo (Riemann, 1970; Phillips, 1971; Riemann & Thorson, 1971; Lai-Fook, 1982; Kubo-Irie *et al.*, 1998; Garvey *et al.*, 2000). Os espermatozóides apirenes, por sua vez, sofrem modificações mais simples, adquirindo várias membranas concêntricas envolvendo toda membrana celular (Riemann, 1970; Phillips, 1971; Friedländer & Gitay, 1972; Lai-Fook, 1982; Kubo-Irie *et al.*, 1998; Garvey *et al.*, 2000).

Tanto os espermatozóides apirenes quanto os eupirenes são transferidos para a fêmea durante o processo de cópula. Os apirenes permanecem com a mesma morfologia encontrada nas regiões extra-testiculares, entretanto os eupirenes ainda apresentam modificações morfológicas (Riemann & Thorson, 1971; Friedländer & Gitay, 1972; Riemann & Gassner, 1973). Quando transferidos para a fêmea, esses espermatozóides não possuem mais o apêndice reticulado, restando somente uma pequena placa densa na região de contato com o envoltório (Riemann, 1970; Riemann & Thorson, 1971; Riemann & Gassner, 1973; Lai-Fook, 1982). Posteriormente, esses espermatozóides também perdem completamente o envoltório não restando nenhuma estrutura extracelular. Esta perda do envoltório antecede o processo de fertilização dos ovos, sugerindo assim que o envoltório não é necessário para o reconhecimento ou especificidade da ligação entre os gametas (Riemann & Thorson, 1971; Friedländer & Gitay, 1972; Medeiros, 1986).

Estudos que abordem a composição química das estruturas encontradas nos espermatozóides em Lepidoptera são bastante escassos (Friedländer, 1976; Friedländer & Gershon, 1978; Medeiros, 1997; França & Báó, 2000). Os trabalhos de Friedländer discutem a composição e origem dos apêndices laciniados, sugerindo, por meio de experimentos com vimbastina (Friedländer & Gershon, 1978), que tais estruturas sejam derivadas de microtúbulos citoplasmáticos. Medeiros (1997), utilizando a técnica de E-PTA para detecção de proteínas básicas, encontrou forte marcação no capuz, nas regiões paracristalinas dos derivados mitocondriais e nos microtúbulos acessórios dos espermatozóides apirenes. Nos espermatozóides eupirenes somente o apêndice reticulado apresentou reação positiva ao E-PTA. França & Báó (2000), também usando E-PTA, detectaram proteínas básicas no capuz, nas regiões paracristalinas dos derivados mitocondriais e em todos os elementos do axonema dos espermatozóides apirenes. Nos espermatozóides eupirenes o acrossomo tubular, o axonema e ambos os apêndices apresentaram reação positiva com esta técnica. Os resultados presentes na literatura são insuficientes para uma conclusão acerca da composição química das estruturas em ambos os espermatozóides, bem como da origem e função das estruturas extracelulares.

Controle da Espermatogênese Dicotômica em Lepidoptera

O processo de espermiogênese nos insetos tem início nos estágios de pré-pupa, pupa ou na fase adulta. Nos grupos cujas espécies possuem pouco tempo de vida adulta, como nos Ephemeroptera e Trichoptera, os testículos adultos apresentam somente espermatozóides, enquanto nas espécies de longa vida adulta os testículos apresentam uma contínua produção de espermatozóides, sendo encontradas assim várias fases pré- e pós-meióticas nos adultos (Wigglesworth, 1965). Em Lepidoptera, em decorrência da existência de um complexo dimorfismo espermático, existem muitas dúvidas com relação ao início do período de ambas as espermiogêneses bem como o controle envolvido em cada uma delas.

Os espermatozóides apirenes e eupirenes são derivados de espermatócitos bipotenciais que sofrem divisão meiótica originando assim estes dois tipos celulares (Friedländer, 1997). Apesar de ambos os tipos de espermatozóides serem encontrados simultaneamente nos adultos, são produzidos em fases diferentes do desenvolvimento. Em todas as espécies já estudadas, a espermiogênese eupirene inicia-se antes da apirene, porém a fase exata de início deste processo varia entre as espécies. De modo geral, a divisão meiótica eupirene tem início no último estágio larval enquanto que a divisão meiótica apirene inicia-se no final do último estágio larval ou começo do período de pupa (Holt & North, 1970; Riemann & Thorson, 1971; Leviatan & Friedländer, 1979; Friedländer & Benz, 1981; Katsuno, 1989; Friedländer, 1997; Kawamura & Sahara, 2002). Esses períodos variam em função da duração da vida adulta, e podem continuar ou não no adulto, ocorrendo desde espermatogônias até espermatozóides em espécies duradouras e somente espermatozóides em espécies efêmeras.

Os fatores que determinam a dicotomia espermática em Lepidoptera ainda não estão esclarecidos, entretanto a espermiogênese apirene parece estar relacionada diretamente com o período de pupa e indiretamente com a redução do hormônio juvenil (Jamieson *et al.*, 1999). Postula-se que a transição para o desenvolvimento de uma célula eupirene para apirene é causada por um fator presente na hemolinfa, denominado de fator indutor de espermatogênese apirene (ASIF), de origem e composição química desconhecidas, que se torna ativo no final do período larval ou de pré-pupa, quando tem início a meiose apirene

(Jans *et al.*, 1984; Friedländer, 1997). A espermiogênese eupirene é determinada nos estágios iniciais da ontogenia e sem uma influência hormonal, exceto pelo alongamento nuclear que parece estar relacionado com a redução do hormônio juvenil (Friedländer & Benz, 1981; Friedländer *et al.*, 1981). Nos núcleos eupirenes em processo de alongamento detectou-se que nucleoproteínas ricas em lisina são substituídas por nucleoproteínas ricas em arginina. O mesmo não ocorre nos núcleos apirenes, que não sofrem alongamento e ainda são posteriormente eliminados, onde somente nucleoproteínas ricas em lisina são detectadas. Esta distribuição protéica diferencial pode refletir em diferença funcional entre apirenes e eupirenes e pode, provavelmente, está relacionada com o controle dessa dicotomia em Lepidoptera (Friedländer & Hauschteck-Jungen, 1982).

Segundo Kawamura *et al.* (2003), a aplicação de glicose e ecdiosteróides em culturas de espermatócitos de *Bombyx mori* aumenta a produção de espermatozóides apirenes. Culturas in vitro de espermatócitos apresentam-se como importantes ferramentas para os estudos de compostos de controle da espermatogênese dimórfica (Goldschmidt, 1917; Schmidt & Williams, 1953; Yagi *et al.*, 1969; Kawamura & Sahara, 2002; Kawamura *et al.*, 2000, 2001, 2003).

Função dos espermatozóides apirenes e eupirenes e a evolução do polimorfismo

Tanto os espermatozóides eupirenes quanto os apirenes são produzidos em cistos dentro de folículos testiculares que desembocam nos ductos deferentes. Cada cisto é composto por aproximadamente 256 espermatozóides, como resultado de 8 divisões celulares (nos cistos apirenes este número pode sofrer variações) e não existe a ocorrência de cistos mistos, ou seja, encontram-se cistos exclusivamente com células apirene ou eupirenes (Phillips, 1971; Lai-Fook, 1982; Medeiros, 1986, 1997; Kubo-Irie *et al.*, 1998; França & Bão, 2000). A organização cística é perdida na região proximal dos ductos deferentes, assim, os espermatozóides apirenes ficam completamente dispersos pelo lúmen do ducto enquanto os espermatozóides eupirenes permanecem agregados ao longo de todo o trato masculino (Friedländer & Gitay, 1972; Phillips, 1971; Riemann, 1970; Riemann &

Thorson, 1971; Lai-Fook, 1982; Medeiros, 1986; Riemann & Giebultowicz, 1992; Kubo-Irie *et al.*, 1998; Friedländer *et al.*, 2001).

Ambos os tipos de espermatozóides são transferidos para a bursa copulatrix da fêmea durante a cópula e armazenados posteriormente na espermateca (Riemann, 1970; Phillips, 1971; Friedländer & Gitay, 1972; Lai-Fook, 1982), entretanto, somente os espermatozóides eupirenes são aptos a fertilizarem os ovos. Por não possuírem núcleo, os espermatozóides apirenes são responsáveis indiretamente por este processo, porém, sem a cooperação destes espermatozóides os eupirenes perdem sua capacidade de fertilização (Sahara & Kawamura, 2002).

Além da ordem Lepidoptera, outros grupos de invertebrados apresentam espécies onde o polimorfismo resulta em um tipo de espermatozóide que não é um gameta fertilizante, é o caso de *Goniobasis laqueata* (Molusca) (Woodward, 1940), *Pyrasus ebeninus* (Molusca) (Healy & Jamieson, 1981) e várias espécies do gênero *Drosophila* (Diptera) (Bressac *et al.*, 1991).

Os primeiros trabalhos com Lepidoptera atribuíam a função dos apirenes à dissociação dos feixes eupirenes ao longo do trato masculino (Riemann *et al.*, 1974; Katsuno, 1977; O sanai *et al.*, 1987) ou ao transporte dos eupirenes até o trato feminino (Iriki, 1941; Holt & North, 1970; Friedländer & Gitay, 1972; Friedländer & Miesel, 1977; Riemann, 1970). Estas hipóteses se baseavam no fato de os espermatozóides apirenes adquirirem motilidade no trato reprodutor masculino enquanto os eupirenes tornam-se móveis somente na fêmea, quando ativados por fosfatases alcalinas (Kinefuchi, 1978). Outra hipótese relaciona os espermatozóides apirenes à nutrição dos eupirenes na fêmea (Riemann & Gassner, 1973), devido à presença de inúmeras camadas extracelulares que serviriam como material de reserva dos apirenes para os eupirenes.

Atualmente, a hipótese mais aceita é a de que os espermatozóides apirenes e são envolvidos na competição espermática. Silberglie *et al.* (1984) propôs esta teoria pela primeira vez, através de análise da produção, fisiologia e comportamento dos apirenes e recentemente novos estudos têm corroborado esta hipótese (Gage, 1994; Snook, 1997, 1998; Wedell & Cook, 1998, 1999ab; Cook & Wedell, 1996, 1999). Swallow & Wilkinson (2002), em uma revisão sobre polimorfismo dos espermatozóides em insetos, separa a

teoria de competição espermática em 3 categorias, onde os apirenes exerceriam papel (1) na eliminação dos eupirenes pré-depositados na spermateca; (2) no preenchimento (cheap filler) da spermateca e (3) no bloqueio da spermateca.

Em Lepidoptera, a mistura de espermatozóides apirenes e eupirenes proveniente de diferentes cópulas em uma mesma fêmea é bastante comum. Desta forma, a hipótese mais aceita é de que os apirenes teriam a função de encher a spermateca, retardando a receptividade da fêmea para cópulas subsequentes e diminuindo o risco da competição de esperma, aumentando o sucesso da paternidade (Cook & Wedell, 1999). Assim, nas espécies que apresentam intensa competição, os machos transferem grande volume de esperma para a fêmea, na tentativa de aumentar seu sucesso no processo de fertilização. Watanabe *et al.* (2000) demonstraram que os espermatozóides apirenes são ejaculados antes dos eupirenes, pois já se encontram livres no trato masculino, são menores e apresentam maior mobilidade. Observa-se ainda que os machos podem variar o volume de esperma em resposta a intensidade da competição, quanto maior o risco de competição maior o volume (Wedell & Cook, 1998, 1999ab; Cook & Wedell 1996, 1999). Desta forma, fêmeas virgens recebem um pequeno volume de esperma com muita secreção; enquanto fêmeas não virgens recebem um volume maior de esperma, composto por um pequeno volume de eupirene, 10-15%, e um grande volume de apirene (Cook & Wedell, 1996, 1999; Wedell & Cook, 1998, 1999ab; Watanabe *et al.*, 2000).

A produção de espermatozóides é um processo com baixo custo energético, entretanto o polimorfismo espermático pode ser custoso. Então, quais forças evolutivas favorecem a produção e manutenção de espermatozóides não aptos a fertilização? No gênero *Drosophila*, onde o dimorfismo resulta em dois tipos de espermatozóides de comprimentos diferentes, a hipótese de competição de esperma ainda não foi testada (Snook, 1998). Entretanto, ao testar a significância filogenética de ambos os tipos de espermatozóides (longo e curto) encontrou-se correlação positiva para o espermatozóide longo e nenhuma correlação para o espermatozóide curto, sugerindo diferentes pressões de seleção para os dois tipos (Snook, 1997). Apesar da idéia sobre competição espermática ser a hipótese mais fundamentada e aceita acerca da função do heteromorfismo de espermatozóides em Lepidoptera, existem muitas dúvidas a respeito desta hipótese e muito

trabalho envolvendo morfologia, mobilidade e dinâmica de ambos os tipos de espermatozóides nos tratos masculinos e femininos bem como comportamento sexual de mariposas e borboletas.

OBJETIVOS GERAIS

Considerando a complexidade morfológica, organizacional e funcional que ocorre nos espermatozóides apirenes e eupirenes da ordem Lepidoptera, esta tese teve como objetivos principais:

- A descrição do processo de espermiogênese em ambos os tipos celulares;
- A caracterização morfológica ultra-estrutural destes espermatozóides ao longo de todo o trato reprodutor masculino;
- A análise citoquímica dos espermatozóides, com ênfase nas estruturas extracelulares de ambos os tipos de espermatozóides;
- A caracterização da morfologia da espermateca e dos espermatozóides armazenados em fêmeas;
- Uma contribuição para o entendimento do polimorfismo de espermatozóides em Lepidoptera.

REFERÊNCIAS BIBLIOGRÁFICAS

- Bressac, C., Joly, D., Devaux, J., Serres, C., Feneux, D. & Lachaise, D. 1991. Comparative kinetics of short and long sperm in the sperm dimorphic *Drosophila* species. **Cell Motil. Cytol.** 19: 269-274.
- Brown Jr., K.S. & Freitas, A. V. L. 1999. Lepidoptera. In: Joly, C. A. & Bicudo, C. E. M. (orgs.). **Biodiversidade do Estado de São Paulo, Brasil: síntese do conhecimento ao final do século XX. 5 – Invertebrados terrestres.** Brandão, C. R. F. & Cancellato, E. M. (eds.). pp. 225- 243. São Paulo (FAPESP).
- Cook, P. A. & Wedell, N. 1996. Ejaculate dynamics in butterflies: a strategy for maximizing fertilization success. **Proc. Royal Soc. London B** 263: 1047-1051.
- Cook, P. A. & Wedell, N. 1999. Non-fertile sperm delay female remating. **Nature** 397: 486.
- França, F. G. R. & Bão, S. N. 2000. Dimorphism in spermatozoa of *Anticarsia gemmatalis* Hübner, 1918 (Insecta, Lepidoptera, Noctuidae). **Braz. J. Morphol. Sci.** 17: 5-10.
- Friedländer, M. 1976. The role of transient perinuclear microtubules during spermiogenesis of the warehouse moth *Ephestia cautella*. **J. Submicrosc. Cytol.** 8: 319-326.
- Friedländer, M. 1997. Control of the eupyrene-apyrene sperm dimorphism in lepidoptera. **J. Insect Physiol.** 43: 1085-1092.
- Friedländer, M & Benz, G. 1981. The apyrene-eupyrene dichotomous spermatogenesis of Lepidoptera. Organ culture study on the timing of apyrene commitment in the codling moth. **Int. J. Invert. Reprod.** 3: 113-120.
- Friedländer, M. & Gershon, J. 1978. Reaction of surface lamella of moth spermatozoa to vinblastine. **J. Cell Sci.** 30: 353-361.
- Friedländer, M., Jeshtadi, A. & Reynolds, S. E. 2001. The structural mechanism of trypsin-induced intrinsic motility in *Manduca sexta* spermatozoa in vitro. **J. Insect Physiol.** 47: 245-255.
- Friedländer, M. & Gitay, H. 1972. The fate of the normal enucleated spermatozoa in inseminated female of the silkworm *Bombyx mori*. **J. Morphol.** 138: 121-129.

- Friedländer, M. & Miesel, S. 1977. Spermatid enucleation during the normal atypical spermiogenesis of the warehouse moth *Ephestia cautella*. **J. Submicrosc. Cytol.** 9: 173-185.
- Friedländer, M. & Hauschteck-Jungen, E. 1982. Differential basic nucleoprotein kinetics in the two kinds of Lepidoptera spermatids: nucleate (eupyrene) and anucleate (apyrene). **Chromosoma (Berlin)** 85:387-398.
- Friedländer, M., Jans, P. & Benz, G. 1981. Precocious reprogramming of eupyrene-apyrene spermatogenesis commitment induced by allatectomy of the penultimate larval instar in the moth *Actias selene*. **J. Insect Physiol.** 27: 267-269.
- Gage, M. J. G. 1994. Associations between body size, mating pattern, testis size and sperm lengths across butterflies. **Proc. Royal Soc. London B** 258: 247-254.
- Garvey, L. K., Gutierrez, G. M. & Krider, H. M. 2000. Ultrastructure and morphogenesis of the apyrene and eupyrene spermatozoa in the gypsy moth. **Ann. Entomol. Soc. Am.** 93: 1147-1155.
- Goldschmidt, R. 1917. Versuche zur Spermatogenese in vitro. **Arch. Zell.** 14: 421-450.
- Hamon, C., & Chauvin, G. 1992. Ultrastructural analysis of spermatozoa of *Korscheltellus lupulinus* L. (Lepidoptera: Hepialidae) and *Micropterix calthella* L. (Lepidoptera: Micropterigidae). **J. Insect Morphol. Embryol.** 21: 149-160.
- Healy, J. M. & Jamieson, B. G. M. 1981. An ultrastructural examination of developing and mature paraspermatozoa in *Pyrasmus ebeninus* (Mollusca, Gastropoda, Potamididae). **Zoomorphol.** 98: 101-119.
- Hodgson, A. N. 1997. Paraspermatogenesis in gastropod mollusks. **Invert. Reprod. Develop.** 31: 31-38.
- Holt, G. G. & North, D. T. 1970. Spermatogenesis in the cabbage looper *Trichoplusia ni* (Lepidoptera: Noctuidae). **Ann. Entomol. Soc. Am.** 63: 501-507.
- Iriki, S. 1941. On the function of apyrene spermatozoa in the silkworm. **Zool. Magaz. (Tokio)** 53: 123-144.
- Jamieson B. G. M., Dallai R. & Afzelius B. A. 1999. **Insects: their spermatozoa and phylogeny**. Enfield, New Hampshire (USA) Science Publishers, Inc.

- Jamieson, B. G. M. 1986. Onychophoran-euclitellate relationships: evidence from spermatozoal ultrastructure. **Zool. Scripta** 15: 141-155.
- Jans, P., Benz, G. & Friedländer, M. 1984. Apyrene spermatogenesis-inducing factor is present in the haemolymph the male and female pupae of the codling moth. **J. Insect Physiol.** 30: 495-497.
- Katsuno, S. 1977. Studies on eupyrene and apyrene spermatozoa in the silkworm *Bombyx mori* L. (Lepidoptera: Bombycidae) III. The post-testicular behavior of the spermatozoa at various stages from pupa to the adult. **Appl. Entomol. Zool.** 12: 241-247.
- Katsuno, S. 1989. Spermatogenesis and the abnormal germ cells in Bombycidae and Saturniidae. **J. Facul. Agric. Hokkaido Univ.** 64: 21-34.
- Kawamura, N. & Sahara, K. 2002. In vitro cultivation of spermatocysts to matured sperm in the silkworm *Bombyx mori*. **Develop. Growth Differ.** 44: 273-280.
- Kawamura, N., Sahara, K. & Fugo, H. 2003. Glucose and ecdysteroid increase apyrene sperm production in in vitro cultivation of spermatocysts of *Bombyx mori*. **J. Insect Physiol.** 49: 25-30.
- Kawamura, N., Yamashiki, N., Saitoh, H. & Sahara, K. 2000. Peristaltic squeezing of sperm bundles at the late stage of spermatogenesis in the silkworm, *Bombyx mori*. **J. Morphol.** 246: 53-58.
- Kawamura, N., Yamashiki, N., Saitoh, H. & Sahara, K. 2001. Significance of peristaltic squeezing of sperm bundles in the silkworm, *Bombyx mori*: Elimination of irregular eupyrene sperm nuclei of the triploid. **Zigote** 9: 159-166.
- Kinefuchi, H. 1978. Studies on eupyrene and apyrene spermatozoa of Lepidoptera. **Mem. Facul. Educ. Niigata Univ.** 19: 21-31.
- Kubo-Irie, M., Irie, M., Nakazawa, T. & Mohri, H. 1998. Morphological changes in eupyrene and apyrene spermatozoa in the reproductive tract of the male butterfly *Atrophaneura alcinous* Klug. **Invert. Reprod. Develop.** 34: 259-268.
- Lai-Fook, J. 1982. Structural comparison between eupyrene and apyrene spermiogenesis in *Calpodex ethlius* (Hesperiidae: Lepidoptera). **Can. J. Zool.** 60: 1216-1230.

- Leviatan, R. & Friedländer, M. 1979. The eupyrene-apyrene dichotomous spermatogenesis of Lepidoptera. I. The relationship with postembryonic development and the role of the decline in juvenile hormone titer toward pupation. **Develop. Biol.** 68: 515-524.
- Medeiros, M. 1986. **Caracterização ultra-estrutural de espermatozóides eupirenes e apirenes de *Alabama argillacea* Hübner, 1818 (Lepidoptera: Noctuidae), ao nível dos testículos e das vias genitais de imagos machos e fêmeas até a espermateca.** Dissertação de Mestrado, Instituto de Biologia, Universidade Estadual de Campinas.
- Medeiros, M. 1997. **Estudo ultra-estrutural da espermiogênese dicotômica de *Alabama argillacea* Hübner, 1818.** Dissertação de Doutorado, Instituto de Biociências, Universidade Estadual de São Paulo.
- Medeiros, M. & Silveira, M. 1996. Ultrastructural study of apyrene spermatozoa of *Alabama argillacea* (Insecta, Lepidoptera, Noctuidae) with tannic acid containing fixative. **J. Submicrosc. Cytol. Pathol.** 28: 133-140.
- Meves, F. 1903. Ueber den von La Valette Saint-George entdeckten Nebenkern (Mitochondrienkörper) des Samenzellen. **Arch. Mikrosk. Anat.** 56: 553-606.
- Osanai, M., Kasuga, H & Aigaki, T. 1987. Physiological role of apyrene spermatozoa of *Bombyx mori*. **Experientia** 43: 593-596.
- Phillips, D. M. 1970. Insect sperm: their structure and morphogenesis. **J. Cell Biol.** 44: 243-277.
- Phillips, D. M. 1971. Morphogenesis of the laciniate appendages of lepidopteran spermatozoa. **J. Ultrastruct. Res.** 34: 567-585.
- Riemann, J. G. 1970. Metamorphosis of sperm of the cabbage looper *Trichoplusia ni* during passage from the testes to the female spermatheca. In: Baccetti, B. **Comparative Spermatology**. Academic Press. New York. pp. 321-331.
- Riemann, J. G. & Gassner, G. 1973. Ultrastructure of Lepidopteran sperm within spermathecae. **Ann. Entomol. Soc. Am.** 66: 154-159.
- Riemann, J. G. & Giebultowicz, J. M. 1992. Sperm maturation in the *vasa deferentia* of the gypsy moth, *Lymantria dispar* L. (Lepidoptera: Lymantriidae). **Int. J. Insect Morphol. Embryol.** 21: 271-284.

- Riemann, J. G. & Thorson, B. J. 1971. Sperm maturation in the male and female genital tracts of *Anagasta kuhniella* (Lepidoptera: Pyralididae). **Int. J. Insect Morphol. Embryol.** 1: 11-19.
- Riemann, J. G., Thorson, B. J. & Ruud, R. L. 1974. Daily cycle of release of sperm from the testis of the mediterranea flour moth. **J. Insect Physiol.** 20: 195-207.
- Rosati, F., Baccetti, B. & Dallai, R. 1970, The spermatozoon of Arthropoda. X. Araneid and the lower myriapods. In: Baccetti, B. **Comparative Spermatology**. Academic Press. New York. pp. 247-254..
- Sahara, K. & Kawamura, N. 2002. Double copulation to a female with sterile diploid and polyploid increases fertility in *Bombyx mori*. **Zigote** 10: 23-29.
- Schappert, P. J. & Shore, J. S. 1998. Ecology, population biology and mortality of *Euptoietia hegesia* Cramer (Nymphalidae) on Jamaica. **J. Lepidop. Soc.** 52: 9-39.
- Schmidt, L. & Williams, C. M. 1953. Physiology of insect diapause. V. Assay of growth and differentiation hormone of Lepidoptera by the method of tissue culture. **Biol. Bull.** 105: 174-187.
- Silberglied, R. E., Shepherd, J. G. & Dickinson, J. L. 1984. Eunuchs: the role of apyrene sperm in lepidoptera? **Am. Nat.** 123: 255-265.
- Snook, R. R. 1997. Is the production of multiple sperm types adaptive? **Evolution** 51: 797-808.
- Snook, R. R. 1998. The risk of sperm competition and the evolution of sperm heteromorphism. **An. Behavior** 56: 1497-1507.
- Sonnenschein, M. & Hauser, C. L. 1990. Presence of only eupyrene spermatozoa in adult males of the genus *Micropteryx* Hubner and its phylogenetic significance. **Int. J. Insect Morphol. Embryol.** 19: 269-276.
- Sivinski, J. 1980. Sexual selection and insect sperm. **Florida Entomol.** 63: 99-111.
- Swallow, J. G. & Wilkinson, G. S. 2002 The long and short of sperm polymorphism in insect. **Biol. Res.** 77: 153-182.
- Watanabe, M., Bonno, M. & Hachisuka, A. 2000. Eupyrene sperm migrates to spermatheca after apyrene sperm in the swallowtail butterfly, *Papilio xuthus* L. (Lepidoptera: Papilionidae). **J. Ethol.** 18: 91-99.

- Wedell, N. & Cook, P. A. 1998. Determinants of paternity in a butterfly. **Proc. Royal Soc. London B** 265: 625-630.
- Wedell, N. & Cook, P. A. 1999a. Butterflies tailor their ejaculate in response to sperm competition risk and intensity. **Proc. Royal Soc. London B** 266: 1033-1039.
- Wedell, N. & Cook, P. A. 1999b. Strategic sperm allocation in the small white butterfly *Pieris rapae* (Lepidoptera: Pieridae). **Funct. Ecol.** 13: 85-93.
- Wigglesworth, V. B. 1965. **The principles of insect physiology**. Methuen and Co., London.
- Woodward, T. M. Jr. 1940. The function of the apyrene spermatozoa of *Goniobasis laqueata* (Say). **J. Exp. Zool.** 85: 103-125.
- Yagi, S., Kondo, E. & Fukuya, M. 1969. Hormonal effect on cultivated insect tissues, I. Effect of ectysterone on cultivated testes of diapausing rice stem borer larvae (Lepidoptera: Pyralidae). **Appl. Entomol. Zool.** 4: 70-78.

ORGANIZAÇÃO DA TESE

A tese está dividida em 4 capítulos cujos conteúdos apresentam-se em formato de manuscritos para publicação. O **Capítulo 1** refere-se à análise morfológica (estrutural e ultra-estrutural) dos espermatozóides apirenes e eupirenes ao longo do trato reprodutor masculino. O **Capítulo 2** aborda uma análise citoquímica ultra-estrutural dos espermatozóides apirenes e eupirenes pelo trato reprodutor masculino envolvendo a caracterização e distribuição de carboidratos e proteínas. O **Capítulo 3** trata da descrição ultra-estrutural da espermateca e dos espermatozóides aí armazenados. Finalmente, o **Capítulo 4** reúne as conclusões finais da presente tese.

CAPÍTULO 1

Estrutura e Ultra-estrutura dos Espermatozóides Apirenes e Eupirene ao Longo do Trato Reprodutor Masculino

1.1

Dichotomic spermiogenesis of Euptoieta hegesia (Lepidoptera: Nymphalidae)
(pp. 20-45)

1.2

*Ultrastructure of the apyrene and eupyrene spermatozoa from the seminal vesicle of
Euptoieta hegesia (Lepidoptera: Nymphalidae)*
(pp.46-54)

1.3

*Sperm morphology and arrangement along the male reproductive tract of the butterfly
Euptoieta hegesia (Lepidoptera: Nymphalidae)*
(pp.55-81)

1.1

**Dichotomic spermiogenesis of *Euptoieta hegesia*
(Lepidoptera: Nymphalidae)**

Mancini, K. and Dolder, H.

Running title: Spermiogenesis of *Euptoieta hegesia*

Abstract

Butterflies and moths produce two types of spermatozoa: anucleate (apyrene) and nucleate (eupyrene). These two spermiogenesis processes were analyzed in the male adult butterfly *Euptoieta hegesia* by light and transmission electron microscopy. It has a single fused testis with cysts that contain exclusively either apyrene or eupyrene cells. The main events of apyrene spermiogenesis are: micronuclei formation, transformation and elimination; dense cap formation; mitochondrial derivative development and tail elongation. Eupyrene spermiogenesis involves: acrosome formation; nuclear condensation and elongation; extracellular appendage development; mitochondrial derivative formation and tail elongation. Most research on lepidopteran spermatogenesis and spermiogenesis refers to larvae and pupae. This study describes these processes using only adult males of *E. hegesia*, because this species has a long adult time life and all cell stages can be found. The apyrene and eupyrene spermiogenesis of *E. hegesia* corroborates and complements the reports in the literature.

Key words: structure – ultrastructure – apyrene – eupyrene

Introduction

Sperm polymorphism exists in several invertebrate groups, like rotifers, turbellarians, mollusks and insects (Fain-Maurel, 1966). In insects, it occurs in many orders and the spermatozoa can differ in length (Diptera), chromosome number (Coleoptera) or morphology (Lepidoptera, Hemiptera, Heteroptera and Hymenoptera) (Jamieson, 1987; Jamieson *et al.* 1999). However, a well-known case of sperm polymorphism occurs in Lepidoptera, and results in the production of two types of morphologically and functionally different spermatozoa: the apyrene (anucleate) and the eupyrene (nucleate). This phenomenon has been reported for all the studied butterflies and moths species, except for the basal group of Micropterygidae, in which only eupyrene spermatozoa were found (Sonnenschein & Hauser, 1990; Hamon & Chauvin, 1992). The two types of spermatozoa differ in length, mitochondrial derivative structures and presence or absence of acrosome, glycocalyx and extracellular appendages and not only by the presence or absence of the nucleus.

Besides the morphological aspects, the apyrene and eupyrene sperm are functionally distinct. The eupyrene spermatozoa fertilize the egg while the apyrene spermatozoa may be only indirectly involved in this process, since they are devoid of nucleus. Some studies relate the function of apyrene spermatozoa to the eupyrene cyst dissociation (Osanai *et al.* 1987) or transport of eupyrene sperm bundles to the female tract (Riemann 1970; Friedländer & Gitay, 1972; Friedländer & Miesel, 1977). However, more recent experimental analyses have suggested that they are involved in sperm competition (Snook, 1997, 1998; Wedell and Cook, 1999a, b; Cook and Wedell, 1999), as proposed by Silberglied *et al.* (1984) and Drummond (1984).

Generally both types are produced at different ontogenetic developmental phases, as the eupyrene spermiogenesis begins before the apyrene, but both kinds of spermatozoa are found simultaneously in the adult (Leviatan & Friedländer, 1979; Friedländer & Benz, 1981; Katsuno, 1989). This study describes spermiogenesis using only adult males of *E. hegesia*, because this species has a long adult time life, about 14 days, and all cell stages can be found.

Materials & Methods

Approximately 50 adults of the butterfly *Euptoieta hegesia* were collected on the Campus of the Universidade Estadual de Campinas (SP – Brazil). Testes were dissected and processed for light and transmission electron microscopy.

Light Microscopy

The specimens were fixed in aqueous Bouin's solution for 12 hours at 4°C, rinsed in distilled water, dehydrated in ethanol and embedded in Technovit 7100 historesin. The tissues were sectioned at 1-2µm, mounted on microscope slides and stained with Toluidine Blue pH 4.0 or Harris's Hematoxylin.

Transmission Electron Microscopy

Testes were fixed overnight in a solution containing 2.5% glutaraldehyde, 0.2% picric acid, 3% sucrose in 0.1M sodium phosphate buffer at 4°C and pH 7.2. Tissue were post-fixed with 1% osmium tetroxide in the same buffer at 4°C, dehydrated in acetone and embedded in an Epoxy resin.

To obtain a good preservation of protein structures, tissues were fixed for three days in 2.5% glutaraldehyde and 1% tannic acid in 0.1 M phosphate buffer and contrasted for three hours with 1% aqueous uranyl acetate at room temperature. The specimens were dehydrated in acetone and included in an Epoxy resin (Dallai & Afzelius, 1990).

All the ultrathin sections (20-60nm) were stained with solutions of 2% uranyl acetate (20 min.) and 2% lead citrate (7 min.) and observed with a transmission electron microscope (Zeiss, Leo 906).

Results

Light microscopy

The adult male reproductive tract of *Euptoieta hegesia* contains a single, fused, red, spherical testis, which contains different developmental stages in pre- and post-meiotic division. The testis is formed by follicles, limited externally by tunic cells, which contain several cysts where apyrene and eupyrene spermatogenesis occurs (Fig. 1A). In these cysts, the germ cells are surrounded by somatic (cystic) cells (Figs. 1F and H) and divide synchronously, resulting in a uniform side-by-side organization of spermatids, all at the same stage of differentiation. The two types of spermatozoa are never produced in the same cyst.

Spermatogenesis advances in an apical-basal direction in the testis. The spermatogonia and spermatocyte cysts are at the testis periphery (Fig. 1A). The spermatogonia, which possess abundant dense cytoplasm and a spherical nuclei, forming dense, homogenous cysts (Figs. 1A-B). The spermatocytes are located around the cyst periphery; they contain a large amount of cytoplasm and a spherical nucleus with scattered dense chromatin aggregates and a prominent nucleolus (Fig. 1C).

Spermatids are uniformly distributed in large cysts and contain the 'Nebenkern' or mitochondrial complex (for review, see Pratt, 1962, 1970), from which the mitochondrial derivatives are formed during tail elongation (Fig. 1D).

The first evidence to distinguish apyrene to eupyrene spermatids in *E. hegesia* is the presence of atypical nuclei in apyrene cells, which appear as large dense, amorphous, spherical structures (Fig. 1E). In eupyrene spermatids, however, there is a typical nucleus that elongates and is compacted during spermiogenesis (Figs. 1G-H).

In the apyrene spermatozoa there is no nucleus at the anterior tip, since it was observed in the posterior tip of spermatid tails (Fig. 1F) ready to be eliminated. The eupyrene spermatozoa have very thin and compact head (Fig. 1H). Both apyrene and eupyrene sperm cysts are localized in the center of the testis and remain closely aligned (Fig. 1I).

Transmission Electron Microscopy

Apyrene Spermiogenesis

Early apyrene spermatids are characterized by a rounded shape, a large cytoplasmic volume and, principally, by the presence of several micronuclei, which are formed at the end of the second meiotic division (Fig. 2A). Initially, the micronuclei have an intact nuclear envelope, without pore complexes, surrounding clusters of dense chromatin (Fig. 2A). They have a heterogeneous chromatin distribution and are variable in size and chromatinic condensation, but become very dense during spermiogenesis. These micronuclei, dispersed in the cytoplasm, gradually degenerate, disorganizing both chromatin and nuclear envelope, forming an electron lucid degenerated ring (Figs. 2B-E). In the elongated spermatids, the micronuclei are eliminated in vesicles at the posterior tip of the tail together with the excess cytoplasm (Fig. 2F).

In the cytoplasm of early apyrene spermatids, with several micronuclei, there is a basal body (centriole), with a dense covering at the proximal end and the axoneme extending from the distal end (Fig. 2G). In elongated spermatids, this basal body is initially topped by a short and thin layer (Fig. 2H) that develops into a dense cap over the anterior tip of the apyrene spermatozoa (Figs. 2I-J). This dense cap has two distinct regions: a dense internal material and an external ring that extends over the initial portion of the axoneme (Fig. 2J). This anterior region of the elongated spermatids and spermatozoa is located outside of the cystic cells, in invaginations of the surface of the head cystic cell (Figs. 2H-J).

The flagellum contains an axoneme and two mitochondrial derivatives. The apyrene axoneme originates from the posterior tip of the basal body, beginning with the accessory microtubules (Fig. 2K), following by the peripheral doublets (Fig. 2L) and finally by the central ones (Fig. 2M). The accessory microtubules and one of the central ones are generally electron-dense (Figs. 2K, M, O and P). In early spermatids, the axoneme is composed of a 9+2 microtubule organization, with nine peripheral doublets and two central microtubules (Fig. 2N). In this formation, projections of the B-tubules of the doublets can

be seen where the accessory microtubules will be attached (Fig. 2N, inset), which leads to the definitive 9+9+2 axoneme arrangement (Figs. 2O-Q).

Besides the axoneme, the apyrene tail is composed of two mitochondrial derivatives, which develop from the "Nebenkern". In spermatids, with a 9+2 axoneme, the mitochondrial derivatives are located near to the axoneme (Fig. 2N) and are initially very large.

In elongated spermatids, with reduced cytoplasmic volume and 9+9+2 axoneme, the mitochondrial derivatives have a paracrystalline core and are surrounded by several microtubules (Fig. 2O). In the tail of late spermatids and spermatozoa, the mitochondrial derivatives present a well-defined paracrystalline core is visualized by tannic acid (Fig. 2Q). They appear at different levels below the anterior tip of the axoneme (Fig. 2J) and have the same shape (Figs. 2O, P and S). The presence of supernumerary microtubules is frequent in the late intratesticular apyrene spermatid (Fig. 2P).

In the posterior region of the spermatozoa, the mitochondrial derivatives end at different levels along the axoneme (1 and 2 in fig. 2R), which then disorganizes first by loss of the accessory microtubules (3 in fig. 2R), followed by the central ones and finally the doublets (4 and 5 in fig. 2R). The apyrene cyst ($n = 20$) contains 256 ± 3 cells (Fig. 2S).

Eupyrene Spermiogenesis

Abundant cytoplasm, a Nebenkern next to the spherical nucleus and an axoneme, which is attached to the nucleus, characterize the early eupyrene spermatids (Fig. 3A). In these cells, an acrosomal vesicle develops from the Golgi complex, close to the spherical nucleus and attached to the nuclear envelope, opposite to the axoneme (Figs. 3B-D). The vesicle presents, initially, a granular material (Fig. 3B) and then becomes a dense, compact, homogeneous structure (Fig. 3C) that contacts the plasma membrane next to a small dense extracellular cluster (Fig. 3D). In initial elongating spermatids, the acrosome becomes an elongated structure that is located above the axoneme (Fig. 3E), extending towards an attachment to a dense structure on the plasma membrane (Fig. 3F). It presents two different areas: a dense external ring with an internal mass (Fig. 3F). This tubular acrosome loses its

attachment to the nuclear envelope and migrates to the anterior region of the elongated spermatid, uniting with the plasma membrane (Fig. 3G). There is a single layer of microtubules surrounding this structure, presumed to contribute to the elongation process (Figs. 3H and 4A). The tubular acrosome complex comes to lie alongside the nucleus (Figs. 3J-M and 4A) and extends above it (Fig. 3H).

In the posterior head region, the acrosome has a dilated region with an internal mass (Fig. 3I). The attachment to the plasma membrane remains only during elongation (Figs. 3F-H and J). In the elongated spermatids and spermatozoa, the acrosome extends parallel to the nucleus with no membrane attachment (Figs. 3K-M).

Simultaneously to acrosome formation, the nucleus undergoes several changes as to its shape, chromatin and nuclear pores. In the initial spermatids, with an acrosomal vesicle, the nucleus is a large and spherical structure with dispersed chromatin (Figs. 3B-D). Later, the nucleus elongates and chromatin condenses, and contains several pore complexes in the region adjacent to the axoneme (Figs. 3E-G). This pore region will later be eliminated in the spermatozoon. The chromatin presents large and dense aggregates (Figs. 3F-G), then forms fibers (Figs. 3I-J) that become a homogeneous and compact material in the very elongated spermatids and the spermatozoa (Figs. 3K-M). The compacted nucleus extends parallel to the tubular acrosome (Fig. 4A) and laterally to the initial portion of the axoneme (Figs. 3I, 4B-C). In this elongated process there is also a single layer of microtubules that surrounds the nucleus (Figs. 3J-K and 4A). Besides the acrosome and nucleus, two types of extracellular appendages are observed, denominated reticular and laciniate appendages (Fig. 3M). Both extend to the tail and are well developed in the anterior region (Figs. 3M, 4C).

The reticular appendage is a single dense rod, which is formed in early spermatids. This structure can be used as a marker to distinguish early apyrene and eupyrene spermatid tail. Initially, in the tail, this appendage appears as a slender rod, which has an inner and outer regions (Fig. 4D). In the anterior region, during early acrosome formation, there is an apparent association between these structures at the plasma membrane (Figs. 3D-H and J). In late spermatids and spermatozoa the reticular appendage is large on the head (Figs. 3K-M, 4A, C and G) and compacted posteriorly (Figs. 4E-F, H-I), anchored by bridges to the plasma membrane (Figs. 4E and H).

The laciniate appendages are striated structures that surround the membrane. These structures are formed in the late spermatids, after the reticular appendage formation (Figs. 3L and 4F). Anteriorly, they almost cover all of the plasma membrane (Figs. 3M, 4C and G) while posteriorly they are attached only around the mitochondrial derivatives.

The tail contains an axoneme, two mitochondrial derivatives and the extracellular appendages. The mitochondrial derivatives are formed from the "Nebenkern" (Fig. 3A), as in the apyrene cell. The axoneme arises from the basal body, which is anchored to the nucleus on the side opposite to the acrosome in early spermatids (Fig. 3A). This basal body contains a dense mass that surrounds the microtubules (Fig. 4B). In spermatids, the tail has a abundant cytoplasm, 9+2 axoneme and two mitochondrial derivatives. With the assembly of the accessory microtubules, the axoneme acquires a 9+9+2 organization, similar to apyrene cells (Figs. 4C-I). The mitochondrial derivatives are large and still surrounded by microtubules at this stage (Figs. 4D-E).

In late spermatids and spermatozoa, the cytoplasm is reduced and the reticular appendage is completely extracellular, anchored on the membrane (Figs. 4E and H), and has a paracrystalline organization, detected by tannic acid (Figs. 4F and H). In the complete axoneme, the accessory and central microtubules are electron-dense (Fig. 4D and I). However, with tannic acid fixation the accessory microtubules are clear (Figs. 4E-F and H). The mitochondrial derivatives are closely associated and cytoplasmic microtubules are rare or absent (Figs. 4H-I). The eupyrene cysts contain 256 ± 3 cells (Fig. 4J).

Discussion

Spermiogenesis of *Euptoieta hegesia* is similar to that of other Lepidoptera species. In this insect order, sperm morphology is highly conserved between species and spermiogenesis follows a similar pattern.

Light Microscopy

There are many studies that describe lepidopteran spermatogenesis/spermiogenesis using light microscopy with thin sections or sperm suspension (Holt & North, 1970; Garbini & Imberski, 1977; Lai-Fook, 1982a; Scheepens & Wysoki, 1985; Corsatto-Alvarenga *et al.* 1987; Katsuno, 1989). All of these studies use larval stages, some of them use pupae also, but few studies are of adults, because the initial developmental stages warrant the presence of all germ cell types. In the present study, however, only adults were examined and all stages of spermatogenesis were found (Figs. 1A-I), which is possibly related to this species' longer lifetime. *Euptoieta hegesia* belongs to the Heliconiinae subfamily, which has a long adult lifetime and, therefore, the imago continues the spermatogenesis process, as observed in *Methona themisto* (Corsatto-Alvarenga *et al.* 1987) and *Calpodes ethlius* (Lai-Fook, 1982a).

The general testis organization described here, with several follicles containing apyrene and eupyrene cysts and the apical-basal direction of spermatogenesis, is similar to all species reported.

In sections of *E. hegesia* testis, the differentiation between apyrene and eupyrene cells was possible from the observations of the micronuclei in apyrene spermatids. In isolated cysts of *C. ethlius*, significant dimensional differences were found between apyrene and eupyrene cysts, which enabled their characterization already in the stage of secondary spermatocytes (Lai-Fook, 1982a).

Transmission Electron Microscopy

Apyrene Spermiogenesis

Loss of nucleus, Nebenkern modification, anterior dense cap formation and elongation of the tail are processes that describe the apyrene spermiogenesis. In *Alabama argillacea*, the apyrene spermiogenesis was divided into six stages (Medeiros, 1997), but we described their maturation continuously and did not find any sub-divisions in other studies.

The micronuclei morphology presents some variations between the species studied. In *Euptoieta hegesia*, they are heterogeneous as to size and their dense amorphous chromatin. In *Ephestia cautella* (Friedländer & Miesel, 1977), micronuclei are of two morphologically distinct types, as also occurs in *A. argillacea* (Medeiros, 1997). We believe that the difference observed in *E. hegesia* is related to the degeneration process and not to different types. The covering of the micronuclei by a membranous envelope, reported in *A. argillacea* (Medeiros, 1997), *E. cautella* (Friedländer & Miesel, 1977) and *C. ethlius* (Lai-Fook, 1982b) was not observed here.

The elimination of the micronuclei from the posterior tail region in *E. hegesia* was similar to that reported in *E. cautella* (Friedländer & Miesel, 1977), *C. ethlius* (Lai-Fook, 1982b) and *A. argillacea* (Medeiros, 1997). In *Bombyx mori* (Kawamura *et al.* 2000), peristaltic squeezing of sperm cysts was detected at the late stage of spermatogenesis. According to the authors, these contractions result in the discarding of the cytoplasm of eupyrene sperm and both cytoplasm and nuclei of the apyrene sperm, from the posterior end of the sperm.

The anterior dense cap of *E. hegesia* is similar to that observed in the majority of Lepidoptera species, including *Trichoplusia ni* (Riemann, 1970), *B. mori* (Friedländer & Gitay, 1972), *C. ethlius* (Lai-Fook, 1982b), *A. argillacea* (Medeiros & Silveira, 1996), *Atrophaneura alcinous* (Kubo-Irie *et al.* 1998) and many others species described by Jamieson (1987), Jamieson *et al.* (1999) and Phillips (1971). Although the structure is well known, the formation of the dense cap in apyrene spermatids, as shown in *E. hegesia*, was

observed only in *B. mori* (Friedländer & Wahrman, 1971) and *A. argillacea* (Medeiros, 1997).

The presence of a basal body below the dense cap and above the axoneme appears to be a characteristic feature of Lepidoptera order (Friedländer & Wahrman, 1971; Friedländer & Gitay, 1972; Lai-Fook, 1982b; Jamieson, 1987; Medeiros, 1997; Jamieson *et al.* 1999).

Both mitochondrial derivatives of *E. hegesia* apyrene sperm are smaller, albeit similar in diameter than eupyrene ones, and have paracrystalline core as also observed in *B. mori* (Friedländer & Gitay, 1972), *A. argillacea* (Medeiros & Silveira, 1996) and others species studied by Phillips (1971).

Eupyrene Spermiogenesis

Acrosome development, nuclear changes, Nebenkern modifications, extracellular appendage formation and elongation of the tail describe the events of eupyrene spermiogenesis.

The tubular acrosome of *Euptoieta hegesia* is similar to the description given for the majority of lepidopteran species (Lai-Fook, 1982b; Medeiros, 1997; Kubo-Irie *et al.* 1998). Its formation and migration to the membrane was described in *C. ethlius* (Lai-Fook, 1982b) in a process similar to that found in *E. hegesia*. The association between the acrosome and the plasma membrane by a small dense extracellular cluster, probably representing the early reticular appendage, was observed in *A. argillacea* (Medeiros, 1997), *B. mori* (Yasuzumi & Oura, 1964, 1965) and *C. ethlius* (Lai-Fook, 1982b).

As to the nuclear changes of *E. hegesia*, the chromatin has evenly distributed dense areas in early spermatids, followed by an arrangement in a fibrous network in elongating spermatids and finally becomes very dense, homogenous material in the spermatozoa. However, in *A. argillacea* (Medeiros, 1997), *C. ethlius* (Lai-Fook, 1982b) and *B. mori* (Friedländer & Wahrman, 1971; Wolf, 1992; Kawamura *et al.* 1998) the process of chromatin compaction begins at the nuclear periphery, different from that observed here.

The spermatid head alterations of *E. hegesia*, including acrosome, nucleus and basal body location, are similar to the observation of Zylberberg (1969); Friedländer & Wahrman (1971); Lai-Fook (1982b); Medeiros (1997) and Yamashiki & Kawamura (1997).

The laciniate and reticulate appendages are exclusive structures of the order Lepidoptera and are present in all species studied, except in the basal group of Micropterygidae (Sonnenschein & Hauser, 1990; Hamon & Chauvin, 1992). These extracellular appendages are morphologically very similar in the species studied.

The reticular appendage represents the principal characteristic for the differentiation of apyrene and eupyrene spermatid tail in early stages. The description of the modifications in this appendage during spermiogenesis in *E. hegesia* - including morphological, dimensional and organizational changes - was detailed above and is in agreement with the observations in *C. ethlius* (Lai-Fook, 1982b) and *A. argillacea* (Medeiros, 1986, 1997). The reticular paracrystalline structure, revealed by tannic acid, was reported in *A. argillacea* (Medeiros, 1997) and *Apopestes spectrum* (Jamieson *et al.*, 1999). We found, using tannic acid and cytochemical observations (unpublished), that the reticular appendage is composed of glycoproteins. In addition, we believe that it is involved in the eupyrene sperm packaging, maintaining the close association of spermatozoa.

The laciniate appendages assembled on the late spermatids also presented a regular structure with tannic acid. The number and shape of these structures vary in the species studied. A study on the effects of vinblastine in laciniate appendages of *Ephestia cautella*, demonstrate that these structures became poorly resolved and disappear, indicating the possible intracellular structure composed by tubulin (Friedländer & Gershon, 1978). In addition to this theory, in *E. hegesia* and *A. spectrum* (Jamieson *et al.*, 1999), using tannic acid (indicated for microtubules preservation) a good preservation and a regular structure was observed. However, we believe that these appendages are proteic but not composed by tubulin. As to function, we agree with Medeiros (1986, 1997), that they are involved in the organization of sperm sheaths, maintaining the close association between sperm cells.

In the axoneme, both mitochondrial derivatives of *E. hegesia* are equal in diameter, as *A. alcinous* (Kubo-Irie *et al.*, 1998). However, many species studied have unequal mitochondrial derivatives (Jamieson *et al.*, 1999). No paracrystalline core was reported in

eupyrene mitochondrial derivatives. The eupyrene cysts of *E. hegesia* have 256 sperm cells, as do *C. ethlius* (Lai-Fook, 1982b), *A. argillacea* (Medeiros, 1986, 1997), *A. alcinous* (Kubo-Irie *et al.*, 1998) and all species studied by Phillips (1971).

In conclusion, dichotomic spermiogenesis in the order Lepidoptera is a very complex process, which involves exclusive events that include loss of the nucleus and cap formation in apyrene spermiogenesis and development of elaborate extracellular appendages in eupyrene ones.

This study of dichotomic spermiogenesis of *E. hegesia* corroborates and complements the reports in the literature.

Acknowledgments

We would like to thank A. V. L. Freitas for supplying the butterflies. This research was supported by the Brazilian Agency FAPESP (98/03200-9 and 01/01049-6).

References

- Cook, P.A. and Wedell, N. 1999. Non-fertile sperm delay female remating. **Nature** **397**: 486.
- Corsatto-Alvarenga, L. B. F., Cestari, N. A. and Ribeiro, A. F. 1987. Apyrene and eupyrene spermatogenesis in *Methona themisto* (Lepidoptera: Ithomiinae). **Rev. Bras. Genet.** **10**: 655-672.
- Dallai, R. and Afzelius, B. A. 1990. Microtubular diversity in insect spermatozoa: results obtained with a new fixative. **J. Struct. Biol.** **103**: 164-179.
- Drummond, B. A. 1984. **Multiple mating and sperm competition in the lepidoptera**. In: **Sperm competition and the evolution of animal mating systems**. Smith RL (ed.) pp 291-370. Academic Press, London.

- Fain-Maurel, M. A. 1966. Acquisition récentes sur les spermatogénèses atypiques. **Ann. Biol.** **5**: 513-564.
- Friedländer, M. and Benz, G. 1981. The apyrene-eupyrene dichotomous spermatogenesis of Lepidoptera. Organ culture study on the timing of apyrene commitment in the codling moth. **Int. J. Invert. Reprod.** **3**: 113-120.
- Friedländer, M. and Gershon, J. 1978. Reaction of surface lamella of moth spermatozoa to vinblastine. **J. Cell. Sci.** **30**: 353-361.
- Friedländer, M. and Gitay, H. 1972. The fate of the normal anucleated spermatozoa in inseminated female of the silkworm *Bombyx mori*. **J. Morphol.** **138**: 121-129.
- Friedländer, M. and Miesel, S. 1977. Spermatid enucleation during the normal atypical spermiogenesis of the warehouse moth *Ephestia cautella*. **J. Submicrosc. Cytol.** **9**: 173-185.
- Friedländer, M. and Wahrman, J. 1971. The number of centrioles in insect sperm: a study in two kinds of differentiating silkworm spermatids. **J. Morphol.** **134**: 383-397.
- Garbini, C. P. and Imberski, R. B. 1977. Spermatogenesis in *Ephestia kuehniella* (Lepidoptera, Pyralididae). **Trans. Am. Microsc. Soc.** **96**: 189-203.
- Hamon, C. and Chauvin, G. 1992. Ultrastructural analysis of spermatozoa of *Korscheltellus lupulinus* L. (Lepidoptera: Hepialidae) and *Micropterix calthella* L. (Lepidoptera: Micropterigidae). **J. Insect Morphol. Embryol.** **21**: 149-160.
- Holt, G. G. and North, D. T. 1970. Spermatogenesis in the cabbage looper *Trichoplusia ni* (Lepidoptera: Noctuidae). **Ann. Entomol. Soc. Am.** **63**: 501-507.
- Jamieson, B. G. M. 1987. **The ultrastructure and phylogeny of insect spermatozoa.** Cambridge University Press. pp 253-272.
- Jamieson, B. G. M., Dallai, R. and Afzelius, B. A. 1999. **Insects: their spermatozoa and phylogeny.** Enfield, New Hampshire (USA): Science Publishers, Inc. 555p
- Katsuno, S. 1989. Spermatogenesis and the abnormal germ cells in Bombycidae and Saturniidae. **J. Fac. Agr. Hokkaido Univ.** **64**: 21-34.
- Kawamura, N., Yamashiki, N. and Bando, H. 1998. Behavior of mitochondria during eupyrene and apyrene spermatogenesis in the silkworm, *Bombyx mori* (Lepidoptera),

- investigated by fluorescence in situ hybridization and electron microscopy. **Protoplasma** **202**: 223-231.
- Kawamura, N., Yamashiki, N., Saitoh, H. and Sahara, K. 2000. Peristaltic squeezing of sperm bundles at the late stage of spermatogenesis in the silkworm, *Bombyx mori*. **J. Morphol.** **246**: 53-58.
- Kubo-Irie, M., Irie, M., Nakazawa, T. and Mohri, H. 1998. Morphological changes in apyrene and eupyrene spermatozoa in the reproductive tract of the male butterfly *Atrophaneura alcinous* Klug. **Invert. Reprod. Develop.** **34**: 259-269.
- Lai-Fook, J. 1982a. Testicular development and spermatogenesis in *Calpodas ethlius* Stoll (Hesperiidae: Lepidoptera). **Can. J. Zool.** **60**: 1161-1171.
- Lai-Fook, J. 1982b. Structural comparison between eupyrene and apyrene spermiogenesis in *Calpodas ethlius* (Hesperiidae: Lepidoptera). **Can. J. Zool.** **60**: 1216-1230.
- Leviatan, R. and Friedländer, M. 1979. The eupyrene-apyrene dichotomous spermatogenesis of Lepidoptera. I. The relationship with postembryonic development and the role of the decline in juvenile hormone titer toward pupation. **Develop. Biol.** **68**: 515-524.
- Medeiros, M. 1986. **Caracterização ultra-estrutural de espermatozóides eupirenes e apirenes de *Alabama argillacea* Hübner, 1818 (Lepidoptera: Noctuidae), ao nível dos testículos e das vias genitais de imagos machos e fêmeas até a espermateca.** (Master Thesis). Instituto de Biologia, Universidade Estadual de Campinas. 122p
- Medeiros, M. 1997. **Estudo ultra-estrutural da espermiogênese dicotômica de *Alabama argillacea* Hübner, 1818.** Tese (doutorado). Instituto de Biociências, Universidade Estadual de São Paulo. 142p
- Medeiros, M. and Silveira, M. 1996. Ultrastructural study of apyrene spermatozoa of *Alabama argillacea* (Insecta, Lepidoptera, Noctuidae) with tannic acid containing fixative. **J. Submicrosc. Cytol. Pathol.** **28**: 133-140.
- Phillips, D. M. 1971. Morphogenesis of the laciniate appendages of lepidopteran spermatozoa. **J. Ultrastruct. Res.** **34**: 567-585.

- Pratt, S. A. 1962. An electron microscope study of nebenkern formation and differentiation in spermatids of an hemipteran insect *Murgantia histrionica* (Hemiptera: Pentatomidae). **J. Morphol.** **126**: 31-66.
- Pratt, S. A. 1970. **Formation and differentiation of the nebenkern in spermatids of an hemipteran insect, *Murgantia histrionica*.** In: Baccetti, B. Comparative spermatology. Academic Press, New York. pp. 301-311.
- Osanai, M., Kasuga, H. and Aigaki, T. 1987. Physiological role of apyrene spermatozoa of *Bombyx mori*. **Experientia**, **43**: 593-596.
- Riemann, J. G. 1970. **Metamorphosis of the cabbage looper *Trichoplusia ni* during passage from the testes to the female spermatheca.** In: Comparative Spermatology. Baccetti, B. (ed.). pp. 321-331. Academic Press. New York.
- Scheepens, M. H. M. and Wysoki, M. 1985. Testicular development, spermatogenesis and chromosomes of *Boarmia selenaria* sciff (Lepidoptera: Geometridae). **Int. J. Invert. Reprod. Develop.** **8**: 337-348.
- Silberglied, R. E., Shepherd, J. G. and Dickinson, J. L. 1984. Eunuchs: the role of apyrene sperm in lepidoptera? **Am. Nat.** **123**: 255-265.
- Snook, R. R. 1997. Is the production of multiple sperm types adaptive? **Evolution** **51**: 797-808.
- Snook, R. R. 1998. The risk of sperm competition and the evolution of sperm heteromorphism. **An. Behav.** **56**: 1497-1507.
- Sonnenschein, M. and Hauser, C. L. 1990. Presence of only eupyrene spermatozoa in adult males of the genus *Micropteryx* Hubner and its phylogenetic significance. **Int. J. Insect Morphol. Embryol.** **19**: 269-276.
- Wedell, N. and Cook, P. A. 1999a. Butterflies tailor their ejaculate in response to sperm competition risk and intensity. **Proc. Roy. Soc. London B** **266**: 1033-1039.
- Wedell, N. and Cook, P. A. 1999b. Strategic sperm allocation in the Small White butterfly *Pieris rapae* (Lepidoptera: Pieridae). **Funct. Ecol.** **13**: 85-93.
- Wolf, K. W. 1992. Spindle membranes and microtubules are coordinately reduced in apyrene relative to eupyrene spermatocyte of *Inachis io* (Lepidoptera: Nymphalidae). **J. Submicrosc. Cytol. Pathol.** **24**: 381-394.

- Wolf, K. W., Baumgart, K. and Traut, W. 1987. Cytology of Lepidoptera. II. Fine structure of eupyrene primary spermatocytes in *Orgyia thyellina*. **Eur. J. Cell. Biol.** **44**: 57-67.
- Yamashiki, N. and Kawamura, N. 1997. Behaviors of nucleus, basal body and microtubules during eupyrene and apyrene spermiogenesis in the silkworm *Bombyx mori* (Lepidoptera). **Develop. Growth Differ.** **39**: 715-722.
- Yasuzumi, G. and Oura, C. 1964. Spermatogenesis in animals as revealed by electron microscopy. XIII. Formation of a tubular structure and two bands in the development spermatid of the silkworm *Bombyx mori* Linné. **Z. Zellforsch** **64**: 210-226.
- Yasuzumi, G. and Oura, C. 1965. Spermatogenesis in animals as revealed by electron microscopy. XIV. The fine structure of the clear band and tubular structure in late stages of development of spermatids of the silkworm *Bombyx mori* Linné. **Z. Zellforsch** **66**: 182-196.
- Zylberberg, L. 1969. Contribution a l'étude de la double spermatogenèse chez un lépidoptère (*Pieris brassicae* L., Pieridae). **Ann. Sci. Nat. Zool.** **11**: 569-626.

Figure Legends

Figures 1A-I: Light Microscopy of *Euptoieta hegesia* Testis

Fig. A: Follicles limited by the tunic (arrowhead) with several cysts in different developmental stages. (g) spermatogonia; (z) spermatozoon. 280x.

Fig. B: Dense spermatogonial cysts (g) in the testis periphery. 1100x.

Fig. C: Spermatocyte cysts with spherical nuclei (n) and evident nucleoli (arrow). 2800x.

Fig. D: Spermatid cyst with spherical nuclei (n) and "Nebenkern" (nk). 3300x.

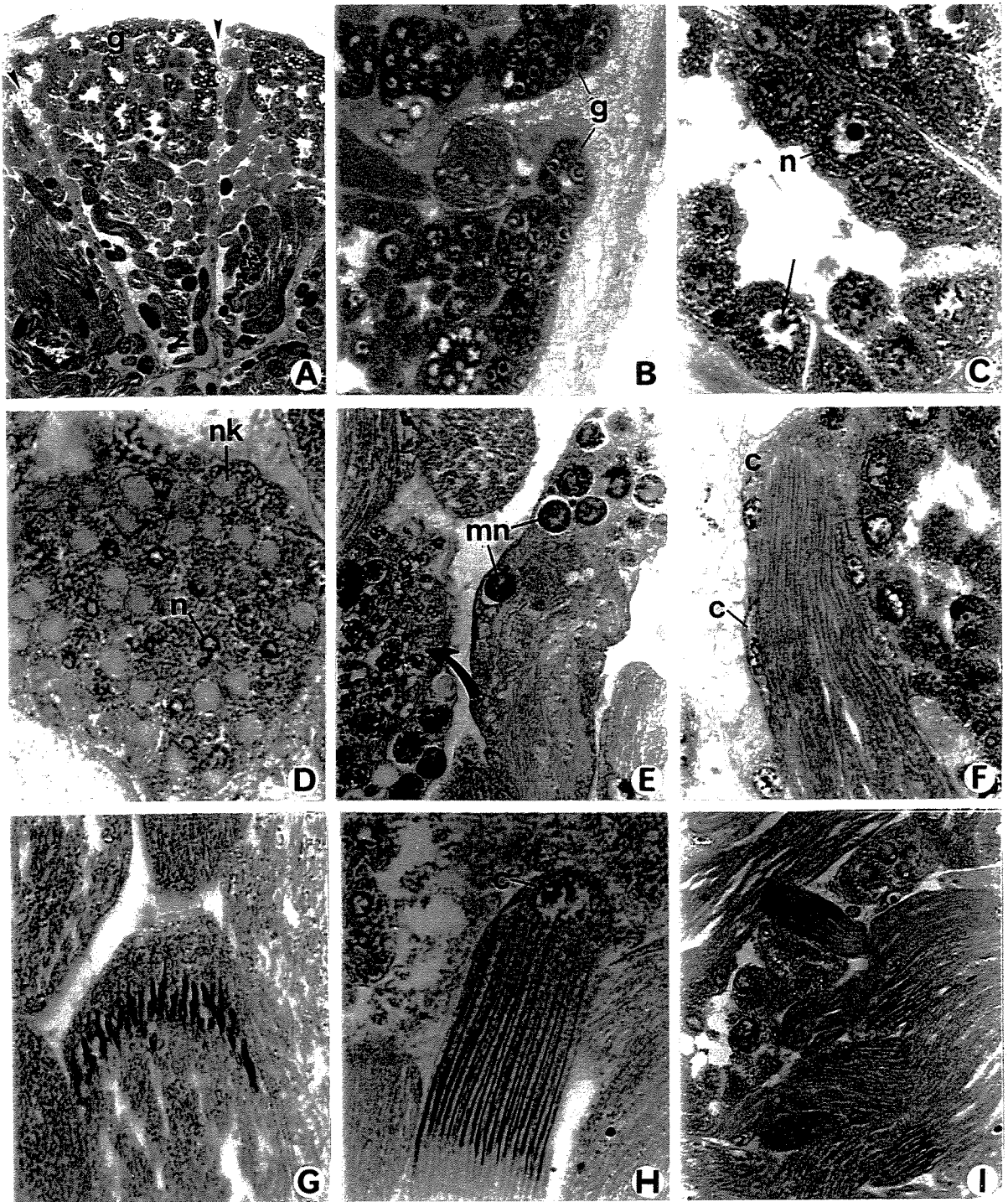
Fig. E: Elongated apyrene spermatid cyst with dense micronuclei (mn). Degenerating cytoplasm and nuclei (arrow). 2600x.

Fig. F: Apyrene spermatozoon cyst. Note the cystic cells (c) and the absence of a nucleus in the anterior region. 2600x.

Fig. G: Elongated eupyrene spermatids with their nuclei in compaction and elongation processes. 2800x.

Fig. H: Eupyrene spermatozoon cyst with very thin and compact nuclei. Note the cyst head cell (c). 3100x.

Fig. I: Eupyrene (with dense elongated nucleus) and apyrene (without nucleus) cysts in the center of the testis. 970x.



Figures 2A-S: Transmission Electron Microscopy of Apyrene Cells

Fig. A: Early apyrene spermatid with micronuclei (mn). 11500x.

Figs. B-E: Different micronuclei degeneration stages. Note the electron lucid degenerated ring (arrow). 12300x.

Fig. F: Micronuclei (mn) elimination in the spermatids' posterior tip. 14800x.

Fig. G: Longitudinal section of the axoneme formation of the early spermatid. Note the anterior dense basal body (b). 22000x.

Fig. H: Longitudinal section of the spermatids anterior tip with the early thin cap (c) above the axoneme (ax). 28000x.

Fig. I: Longitudinal section of the spermatozoon anterior dense cap. 47500x.

Fig. J: Transverse sections of the spermatozoon's anterior region showing progressively posterior levels (1-4). Note the anterior tip embedded in the cystic cell cytoplasm (c). Mitochondrial derivatives appear at different level (arrow). 22000x.

Figs. K-M: Transverse section of the proximal axoneme region, showing the emergence of accessory microtubules, followed by the doublets and, finally by the central ones, respectively (arrow) 49000x.

Fig. N: Spermatid tail with large cytoplasmic volume. The 9+2 axoneme (ax) with projections (arrow) and two mitochondrial derivatives (md). 34300x. Inset: the early 9+9+2 axoneme. 82.000x.

Fig. O: Late spermatid tail with 9+9+2 axoneme and mitochondrial derivatives with small paracrystalline cores (arrows). Microtubules (arrowhead). 61600x.

Figs. P-Q: Spermatozoon tail fixed by conventional and tannic acid methods, respectively, with differing densities in the axonemic microtubules (arrowhead). Mitochondrial derivatives (md) with paracrystalline core (arrow). Note the supernumerary microtubule (small arrow). 84000x. 95000x.

Fig. R: Transverse sections of the tail at progressively posterior levels (1-5) 35000x.

Fig. S: Apyrene cyst. 8500x.

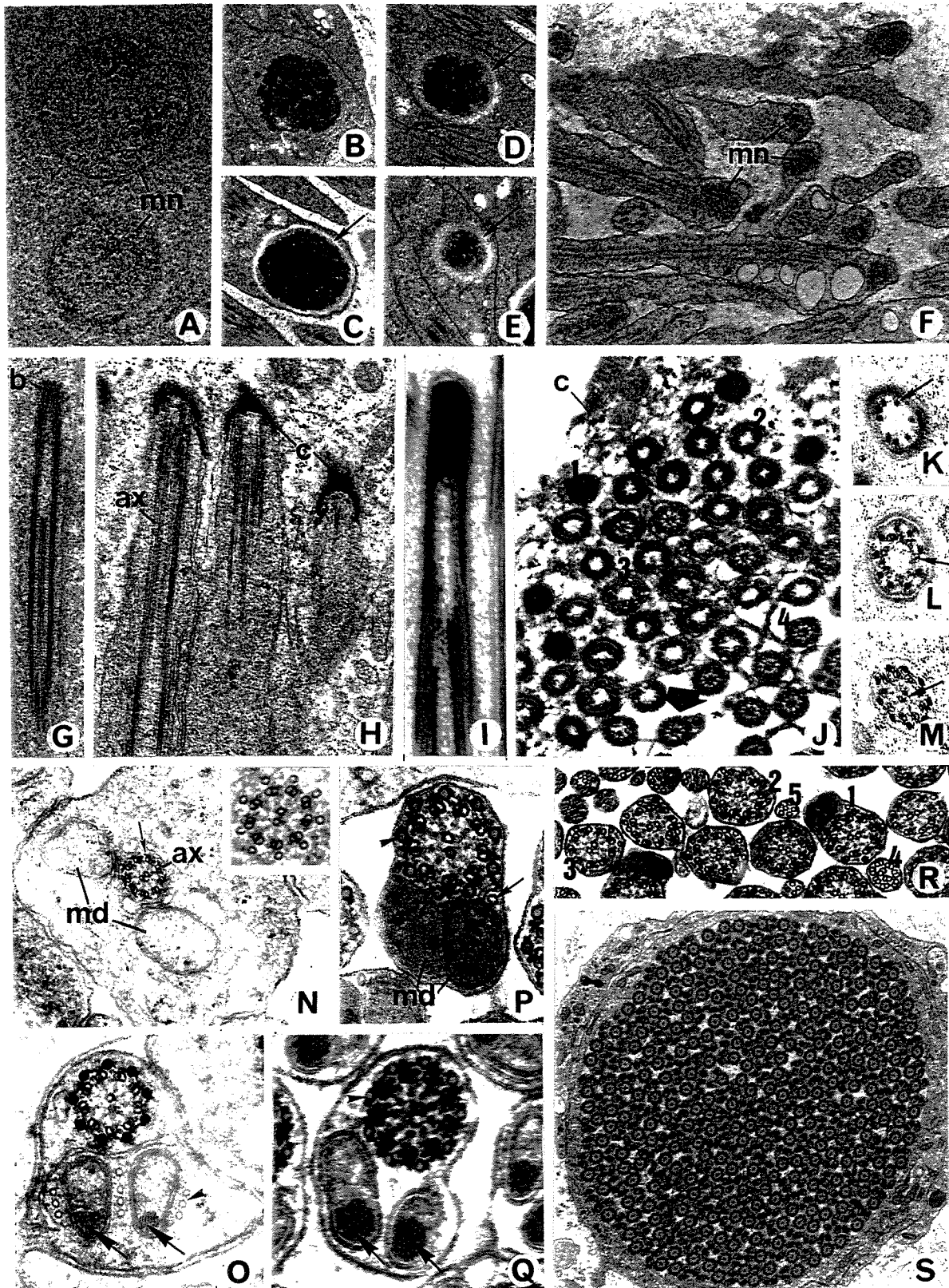


Figure 3A-M: Transmission Electron Microscopy of Eupyrene Cells

Fig. A: Early spermatid with spherical nucleus (n), axoneme (ax) attached posteriorly to the nucleus and Nebenkern (nk). 6.000x.

Figs. B-C: Spermatids with spherical nucleus (n) and acrosomal vesicle (av) attached anteriorly which is formed by the Golgi Complex (g). Mitochondrial derivatives (md). 10000x.

Fig. D: Acrosomal vesicle (av) attached to the nucleus (n) and to the plasma membrane (arrowhead). 28000x.

Fig. E: Elongated spermatid with axoneme (ax) and elongated acrosome (a) attached to the nucleus (n). Note the nuclear pore complexes (double arrowhead) and the reticular appendage (r). 10500x.

Fig. F: Elongated spermatid with tubular acrosome formation (a), attached to the nucleus (n) and plasma membrane (arrowhead). Note the presence of nuclear pore complexes (double arrowhead), the compacted chromatin and the acrosome mass (arrow). 22000x.

Fig. G: Elongating spermatid where the tubular acrosome (a) is not attached to the nucleus (n) but still remains attached to the plasma membrane (arrowhead). Note the presence of nuclear pore complexes (double arrowhead) and the compacting chromatin. 10500x.

Fig. H: Spermatid anterior tip with the tubular acrosome (a) surrounded by microtubules (small arrowhead) and attached to the plasma membrane (arrowhead). 38000x.

Fig. I: Longitudinal section of the nuclear base showing the dilated acrosome region (a) and the nucleus (n), which reaches alongside the axoneme (ax) and basal body (b). 31000x.

Fig. J-M: Transverse sections of different developmental stage (spermatids to spermatozoa) showing the chromatinic condensation and the changing appendages. Nucleus (n), acrosome (a), microtubules (arrowhead), reticular (r) and laciniate (l) appendages. 20000x. 40000x. 60000x. 60000x.

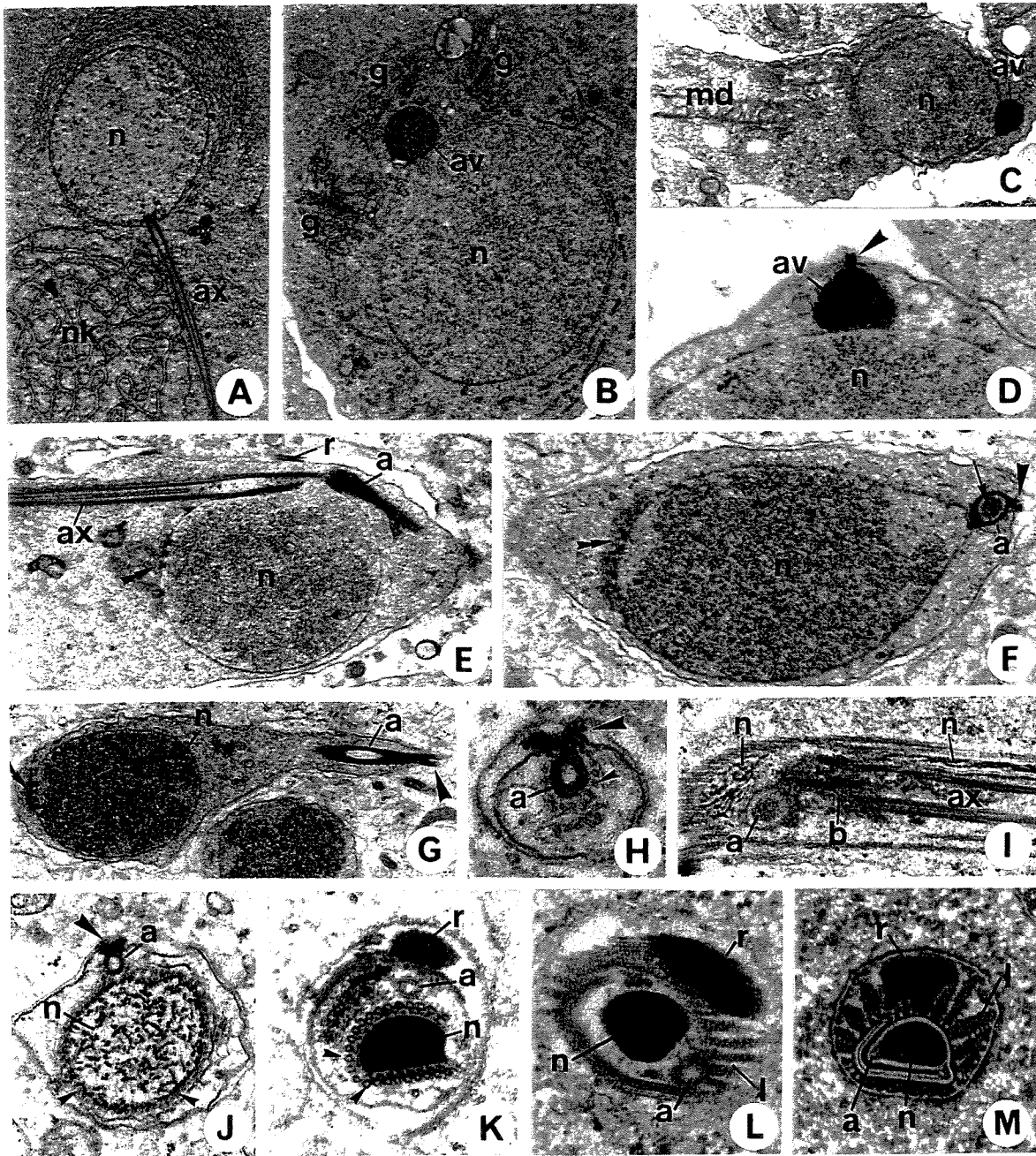


Figure 4A-J: Transmission Electron Microscopy of Eupyrene Cells

Fig. A: Longitudinal section of the anterior region showing the compacted nucleus (n) with several microtubules (arrowheads), tubular acrosome (a) and reticular appendage (r). 15000x.

Fig. B: Longitudinal section of the nucleus-tail transition region, showing the amorphous mass in and around the basal body (arrow), anterior to the axoneme (ax), and the nucleus (n) which comes to lie alongside the axoneme. 37000x.

Fig. C: Transverse sections of the nucleus-tail transition region showing the nucleus (n) with the centriole (c) and the axoneme (ax). Well developed laciniate (l) and reticular (r) appendages. 36000x.

Fig. D: Tail of the spermatid with 9+9+2 axoneme and two mitochondrial derivatives. The reticular appendage (r) possesses internal (arrow) and external regions. Note the microtubules (large double arrowhead) around the mitochondrial derivatives and the dense accessory (small double arrowhead) and central microtubules (arrowhead). 85000x.

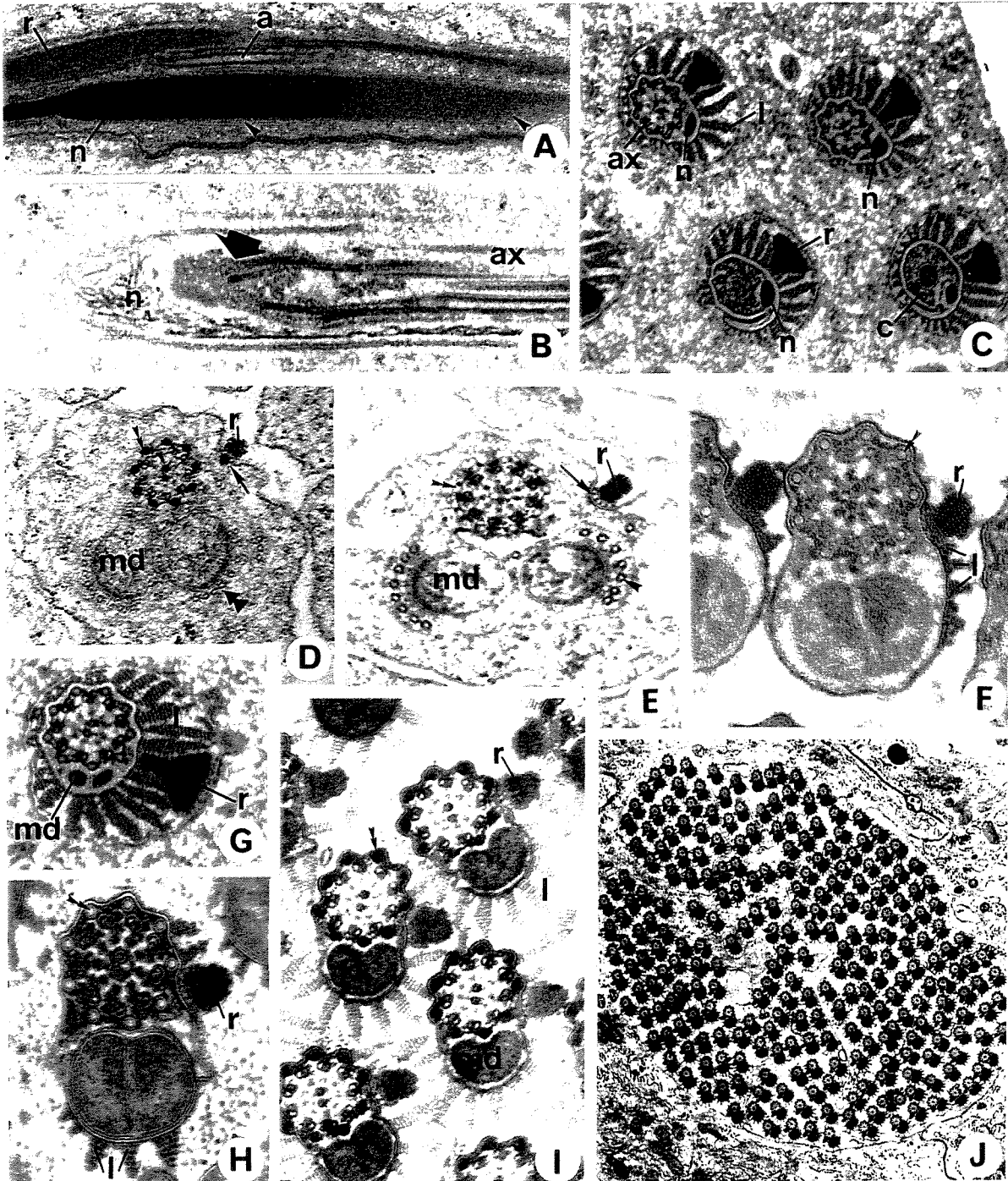
Fig. E: Tail of the spermatid with 9+9+2 axoneme and mitochondrial derivatives fixed with tannic acid. Note the microtubules (arrowhead) around the mitochondrial derivatives (md) and the electron lucid accessory microtubules (double arrowhead). Reticular appendage (r) with an external region anchored to the plasma membrane (arrow). 50000x.

Fig. F: Late spermatid fixed with tannic acid. Note the early laciniate appendage formation (l), the reticular appendage's paracrystalline arrangement (r) and the electron lucid accessory microtubules (double arrowhead). 65000x.

Fig. G: Spermatozoon in transverse section of the anterior axoneme region with well developed laciniate (l) and reticular (r) appendages, 9+9+2 axoneme and mitochondrial derivative tips (md). 60000x.

Fig. H-I: Spermatozoon tail fixed with tannic acid and conventional methods, respectively. Note the electron density difference between the axoneme microtubules (double arrowhead), and the morphology of the laciniate (l) and reticular (r) appendages. Mitochondrial derivatives (md). 60000x. 49000x.

Fig. J: Eupyrene cyst. 6000x.



1.2

Ultrastructure of the apyrene and eupyrene spermatozoa from the seminal vesicle of *Euptoieta hegesia* (Lepidoptera: Nymphalidae)

Mancini, K. and Dolder, H

Running title: Spermatozoa from seminal vesicle of *Euptoieta hegesia*

Ultrastructure of apyrene and eupyrene spermatozoa from the seminal vesicle of *Euptoieta hegesia* (Lepidoptera: Nymphalidae)

K. Mancini, H. Dolder

Abstract. The ultrastructure of the seminal vesicle's spermatozoa of the butterfly *Euptoieta hegesia* was analyzed. The apyrene spermatozoa measure about 300 µm in length and swim freely in a secretion. The anterior end consists in a cap with a cylindrical extension and a globular structure. The flagellum has a 9+9+2 axoneme, two mitochondrial derivatives with paracrystalline matrices and an external coat formed by concentric layers. The eupyrene spermatozoa measure about 550 µm in length and are grouped into bundles. The anterior end consists in an amorphous globule. Posterior to this globule, a coat with a dense material covers the spermatozoon where an acrosome and a nucleus appear. The flagellum has a 9+9+2 axoneme and two mitochondrial derivatives. External to the coat and attached to the dense material, there is a reticular appendage, which has a paracrystalline core and extends to the distal tip of the spermatozoon. © 2001 Harcourt Publishers Ltd

Keywords: ultrastructure, spermatozoa, Lepidoptera, seminal vesicle

Introduction

The lepidopteran order presents the most evident sperm polymorphism, which results in two types of spermatozoa: the apyrene and eupyrene ones.

The intratesticular apyrene spermatozoon has no nucleus (Friedländer & Miesel, 1977; Lai-Fook, 1982; Medeiros, 1997); in its place, the anterior region contains an electron dense cap (Phillips, 1970; Lai-Fook, 1982; Jamieson, 1987; Medeiros & Silveira, 1996; Kubo-Irie et al., 1998). The flagellum consists of a 9+9+2 axoneme and two mitochondrial derivatives.

The intratesticular eupyrene spermatozoon has an anterior region formed by an acrosome, a nucleus and, outside the membrane, two types of appendages, termed reticular and laciniate, extending the length of spermatozoon (Phillips, 1970, 1971; Leviatan & Friedländer, 1979; Medeiros, 1986; Kubo-Irie et al., 1998). The flagellum's components are the same as the apyrene spermatozoon, although they are structurally distinct.

The role of the apyrene sperm remains unclear, since they do not fertilize the eggs. Silberglid et al. (1984) proposed the hypothesis that they may be related to sperm competition. Recent experimental studies have given support to this hypothesis (Snook, 1997, 1998; Cook & Wedell, 1999; Wedell & Cook, 1999).

Sperm maturation in Lepidoptera involves several morphological and organizational modifications along the male reproductive tract, which may also contribute specific characteristics. Although the seminal vesicle is easily obtained from adult butterflies, only few studies show the ultrastructure of both types of sperm in the

¹Departamento de Biologia Celular, Instituto de Biologia, Universidade Estadual de Campinas – Unicamp, Campinas – SP, Brazil

Received 13 December 2000
Accepted 20 March 2001

Correspondence to: Dr Heidi Dolder, Departamento de Biologia Celular, Universidade Estadual de Campinas, CP 6109, 13083-970 Campinas, SP, Brazil. Tel/Fax: + 55 019 3788 7821; E-mail: heidi@unicamp.br

seminal vesicle (Phillips, 1971; Lai-Fook, 1982; Kubo-Irie, 1998).

Spermatozoal morphology has contributed to several taxonomic and phylogenetic studies in insects (Jamieson et al., 1999). Sperm ultrastructure has provided characters for the identification of orders, families and, in Hymenoptera, even sub-families and genus (Lino-Neto et al., 1999, 2000a, b). In Lepidoptera, sperm characters have sporadically been studied with this intention (Friedländer, 1983; Sonnenschein & Hauser, 1990).

The present work was carried out to obtain a detailed description of apyrene and eupyrene spermatozoa from the seminal vesicle of the adult male of the butterfly *Euptoieta hegesia*.

Materials and methods

Imagos of the butterfly *Euptoieta hegesia* were collected in the Campus of the Unicamp, Campinas, Brazil.

Light microscopy

Sperm suspensions from seminal vesicle and spermatheca were spread on microscope slides, fixed with a solution of 2.5% glutaraldehyde in 0.1 M phosphate buffer at room temperature and washed with running water. After drying at room temperature, the preparations were observed with a photomicroscope, equipped with phase contrast.

To measure the nucleus, some slides were stained for 30 min with 0.2 µg/ml 4,6-diamino-2-phenylindole (DAPI) in PBS buffer, washed with running water and immersed for 5 min in 0.1 M McIlvane buffer in the dark at room temperature. The slides were mounted and observed with a photomicroscope, equipped with a BP360–370 nm excitation filter.

Transmission electron microscopy

Seminal vesicles were fixed overnight with a solution containing 2.5% glutaraldehyde, 0.2% picric acid, 3% sucrose in 0.1 M phosphate buffer at 4°C. Specimens were post-fixed with 1% osmium tetroxide in the same buffer at 4°C, dehydrated in acetone and embedded in Epon 812 resin. Other seminal vesicles were fixed for three days with 2.5% glutaraldehyde and 1% tannic acid in 0.1 M phosphate buffer with daily changes and stained for three hours with 1% aqueous uranyl acetate at room temperature. The specimens were dehydrated in acetone and embedded in Epon 812 resin (Dallai & Afzelius, 1990).

Ruthenium red

Seminal vesicles were fixed for two hours with 2.5% glutaraldehyde in 0.1 M cacodylate buffer containing 1% ruthenium red, in the dark, at room temperature then washed in the same buffer. The specimens were post-fixed first for one hour with 1% osmium tetroxide in the 0.1 M cacodylate buffer, followed by 1% osmium

tetroxide containing 1% ruthenium red for one hour, in the dark, at room temperature and washed in 0.1 M cacodylate buffer, in the dark, at room temperature. Finally, the specimens were dehydrated in acetone and embedded in Epon 812 resin (modified from Souza, 1998).

All ultrathin sections were stained with uranyl acetate and lead citrate and observed with a transmission electron microscope.

Results

The apyrene spermatozoa of the butterfly *Euptoieta hegesia* are filiform and measure about 300 µm in length. They present a tapered posterior end and a truncated anterior end (Fig. 1). The apyrene spermatozoa swim freely in the accessory gland secretion (Fig. 2).

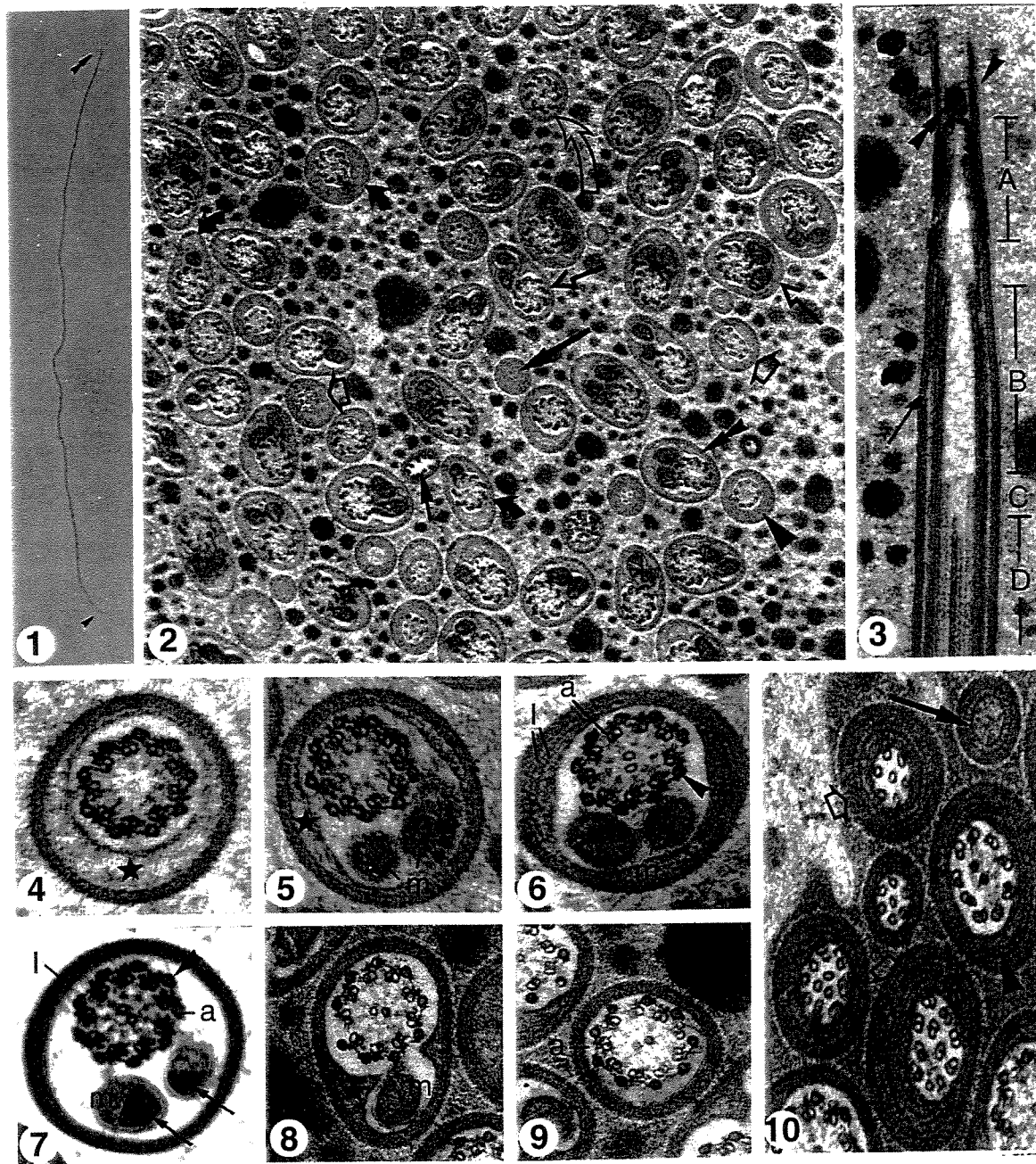
The anterior region includes a cap, a globular structure and a cylindrical structure (Fig. 29A). The cap measures about 0.6 µm in length and is covered by a membrane up to the beginning of the axoneme. The cylindrical structure surrounds the cap and extends about 0.36 µm above it. The globular structure measures about 0.14 µm in diameter and is located above the cap and inside the cylindrical structure (Fig. 3).

The axoneme contains a 9+9+2 microtubule arrangement. The accessory microtubules begin first (small arrow in Fig. 2; Figs 3 & 29B), followed by the doublets (1 µm below) (Figs 3 & 29C) and the central pair (0.2 µm below the doublets) (Fig. 3). The accessory microtubules are electron dense (Figs 6–9). The two mitochondrial derivatives, apparently begin together and above the two central microtubules of the axoneme (double arrowhead in Fig. 2; Figs 4, 5 & 29D), they are arranged in a V shape (Figs 5–7) and have a paracrystalline core (Fig. 7).

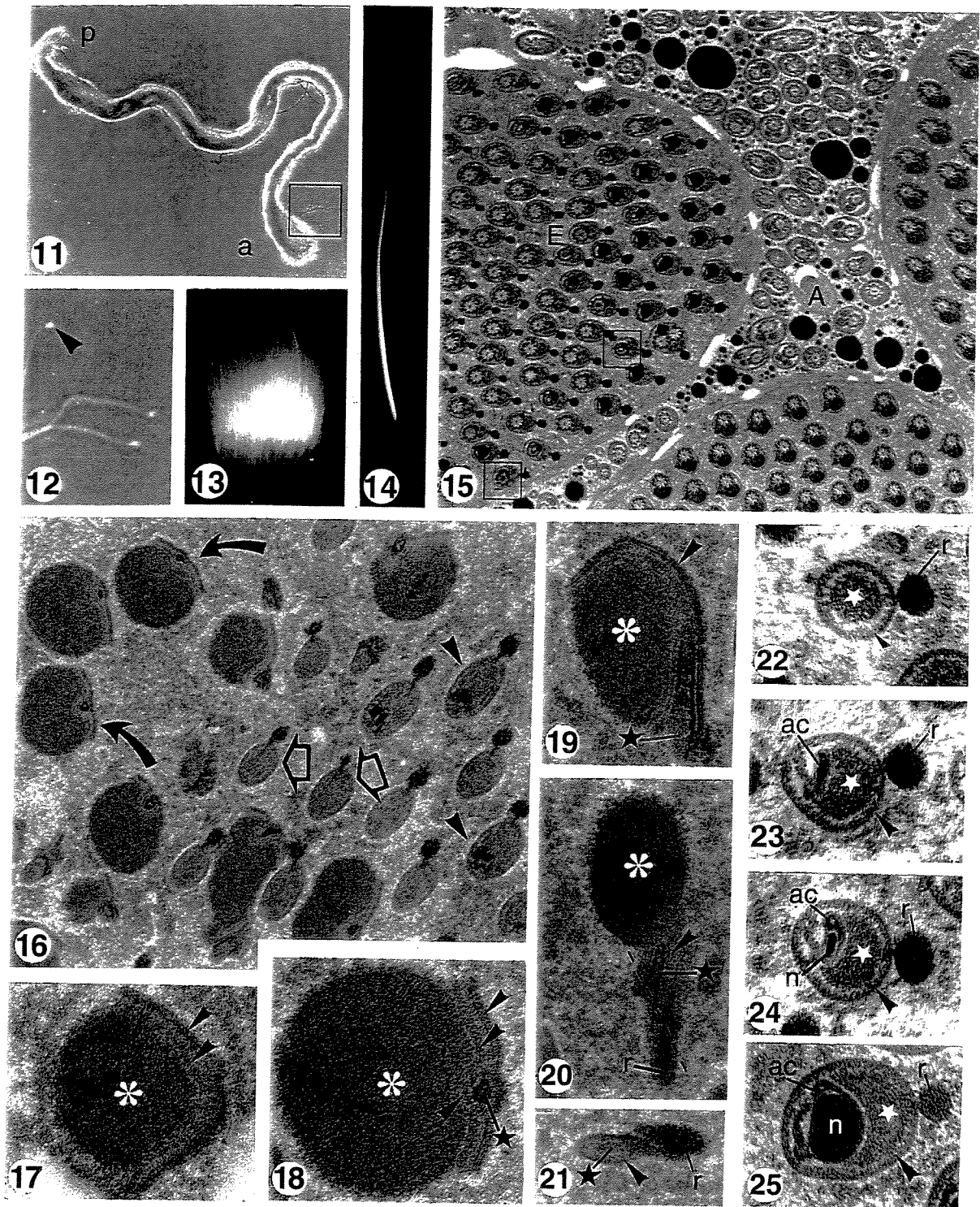
In the seminal vesicle, the apyrene sperm has several concentric layers outside the cellular membrane (Figs 4–10) and an irregular amorphous mass, which occupies the spaces between organelles internally to the membrane (star in the Figs 4, 5 & 8).

Posteriorly, the mitochondrial derivatives are the first structures to terminate and do so at different levels (curved arrow and white curved arrow in Fig. 2; Figs 8; 9 & 29E). In the axoneme, the accessory microtubules disappear first (arrowhead in Fig. 2; Figs 10 & 29F) followed by the central ones (white arrow in Fig. 2). The B-subtubules disorganize, leaving single microtubules (white arrow in Fig. 10 and Fig. 29G). At the posterior end, the spermatozoon tip is formed only by the concentric layers (large arrow in Fig. 2; Figs 10 & 29H).

The eupyrene spermatozoa, in light microscopy form bundles, which measure about 550 µm in length (Figs 11 & 13). The spermatozoon has a globular anterior structure (Figs 12, 16–18 & 30A) and a tapered posterior end (Figs 11 & 28). The spermatozoon (Figs 13 & 14) contains a thin nucleus measuring about 35 µm in length, which tapers toward the tip. No anterior globular region, such



Figs 1–10 Light (1) and transmission electron micrographs of the apyrene sperm in the seminal vesicle of *Euploietia hegesia*. (1) Phase contrast of apyrene spermatozoon showing the truncated anterior end (*double arrowhead*) and tapered posterior end (*arrowhead*) $\times 100$. (2) Cross-sections of apyrene spermatozoa at different levels immersed in secretion globules. The anterior to posterior end: axoneme formation (*small arrow*), flagellum with two mitochondrial derivatives and incomplete axoneme (*double arrowhead*), typical flagellum (*open arrows*), posterior region with one mitochondrial derivative (*curved arrow*), flagellum sectioned below of the mitochondrial derivative (*white curved arrow*), flagellum sectioned below of the accessory microtubules (*arrowhead*), disorganization of the axoneme (*white arrows*) and finally posterior end with concentric layers (*large arrow*) $\times 39\,500$. (3) Longitudinal section of the anterior end: (A) cap; (B) region with only accessory microtubules; (C) region with doublet microtubules and (D) region of the complete axoneme with a central pair. Globular structure (*double arrowhead*) anterior to the cap and cylindrical structure (*arrowhead*). A thick coat covers the spermatozoon (*arrow*) $\times 36\,000$. (4) & (5) Cross-section of the anterior region, at the level of the mitochondrial derivatives (m) $\times 79\,000$. (6) & (7) Cross-section of typical flagellum with axoneme (a), electron dense accessory microtubules (*arrowhead*) and two mitochondrial derivatives (m) with paracrystalline cores (*arrow*). (4) $\times 60\,000$. (5) $\times 72\,500$. (8)–(10) Cross-section of the posterior region. (8) flagellum sectioned posterior to the cap and cylindrical structure (*arrowhead*). A thick coat covers the spermatozoon (*arrow*) $\times 36\,000$. (9) flagellum sectioned posterior to both mitochondrial derivatives. (10) section showing the end of the accessory microtubules (*arrowhead*), the disorganization of the axoneme (*white arrow*) and the posterior end with concentric layers (*arrow*). (8) and (9) $\times 70\,000$. (10) $\times 86\,000$. (1) = concentric layers; (asterisk) = amorphous material.



Figs 11–25 Light (11–14) and transmission electron micrographs (15–25) of the eupyrene sperm in the seminal vesicle of *Euptoieta hegesia*. (11) & (12) Phase contrast of the eupyrene bundle. (11) showing the posterior (p) and anterior (a) ends. $\times 900$. (12) magnification of the square (11) showing the globular region (arrowhead). $\times 400$. (13) & (14) DAPI-stained fluorescence of the nuclear region in the seminal vesicle and in spermatheca, respectively. (13) $\times 800$. (14) $\times 2000$. (15) Cross-section of eupyrene bundle (E) and apyrene sperm (A) at different levels. In the square, nucleus–flagellum transition region. $\times 10\,000$. (16) Cross-section of the anterior end at different levels: globular region (curved arrow), anterior region above the nucleus (white arrow) and nuclear region (arrowhead) $\times 19\,000$. (17) & (18) Cross-sections of the anterior end with the globular amorphous mass (asterisk), a coat which, in this region

has a lamellar shape (*arrowhead*), and a dense material (*star*) within the sperm coat. (17) \times 46 500. (18) \times 58 500. (19) & (20) Longitudinal section of the anterior region showing the amorphous mass (*asterisk*), the coat (*arrowhead*), the dense material (*star*) and the reticular appendage (r). (19) \times 42 000. (20) \times 33 000. (21) & (22) Tangential section along the broken line in Figure 20 and cross section with the coat (*arrowhead*), the dense material (*star*) and the reticular appendage (r). (21) \times 33 000. (22) \times 50 000. (23)–(25) Cross-sections of the anterior region, showing the acrosome (ac) and nucleus (n). Dense material (*star*), coat (*arrowhead*) and reticular appendage (r). (23) and (24) \times 50 000. (25) \times 54 000. (22)–(24): Ruthenium red method.

as was found in the seminal vesicle, occurs in the spermatheca (Fig. 14).

Eupyrene spermatozoa bundles are formed by a matrix, which maintains the integrity of the spermatozoa bundle (Figs 13, 15 & 16). The globular end measures about 0.80 μ m in diameter and contains an amorphous mass.

A dense material, involved by a coat, appears adjacent to this amorphous mass (Figs 16, 18–20 & 30B) and covers all the spermatozoon (Figs 21–25 & 30A). This dense material is more abundant toward the posterior region (Figs 21–25 & 30A) and occupies the spaces between the coat and the sperm organelles, taking on a roughly crescent shape in cross sections (Figs 23–25 & 30C, D). In the medium flagellar region it is oval in cross section, compressed by the axoneme and mitochondrial derivatives (Figs 26–28 & 30E, F).

External to the coat there is a reticular appendage. This is a dense cylindrical structure, present only in the Lepidoptera order, that assembles just below the globular region (Figs 20–22 & 30A) and has a paracrystalline organization, seen only with tannic acid treatment (Fig. 27). The appendage measures 0.07 μ m in diameter in the anterior region, reducing its diameter towards the posterior region (Figs 21–28 & 30C–F). There is a connection between a reticular appendage and the dense material (Figs 26 & 27).

The tubular acrosome appears first inside the dense material (Figs 23 & 30A), followed by the nucleus, which lies laterally to the acrosome (Fig. 30A), and is tapered anteriorly (Fig. 24), large in the medium portion (Figs 25 & 30C) and truncated at the base, with a narrow crescent extending laterally along the axoneme base (Figs 15, 30A & D).

No centriolar adjunct was found. The axoneme, as in eupyrene spermatozoa, contains a 9+9+2 microtubule arrangement. The accessory and central microtubules are electron dense (Fig. 28). The A-subtubules and the central ones are electron dense when using tannic acid (Fig. 27). The two mitochondrial derivatives have the same diameter and shape (Figs 26 & 30E) and appear at different levels. At the posterior end, the mitochondrial derivatives terminate first at different levels, followed by the reticular appendage and the dense material. Finally the axoneme is disorganized, ending with the empty coat (Figs 28 & 30F–H).

Discussion

Apyrene spermatozoa

The anterior electron dense cap has been described from testicular spermatids and spermatozoa (Phillips, 1970;

Lai-Fook, 1982; Jamieson, 1987; Medeiros & Silveira, 1996; Kubo-Irie et al., 1998). These descriptions differ considerably from that of *E. hegesia* sperm in the seminal vesicle. The cap is usually described as a double layer, which forms a dense ring inside the plasma membrane, measuring 1 μ m in length with a thickness of 0.3 μ m (Jamieson, 1987; Medeiros & Silveira, 1996).

However, observations of *E. hegesia* testicular spermatozoa (unpublished observations) indicate an ultrastructure similar to that found by other authors, showing that structural modifications occur between the testis and the seminal vesicle. Friedländer and Gitay (1972) observed the cap in testicular and bursa copulatrix spermatozoa, where the latter are very similar to *E. hegesia* seminal vesicle spermatozoa. There is no evidence of a centriole in *E. hegesia*, nor in *Alabama argillacea* (Medeiros & Silveira, 1996) although there is in *Calpodethlius* (Lai-Fook, 1982).

The flagellum of apyrene spermatozoa is very similar in all species studied. However, the presence of an irregular dense material along the flagellum has only rarely been described (Phillips, 1970; Kubo-Irie et al., 1998). Medeiros and Silveira (1996) affirmed similar length of the two mitochondrial derivatives, while in *E. hegesia* the difference in length is very evident.

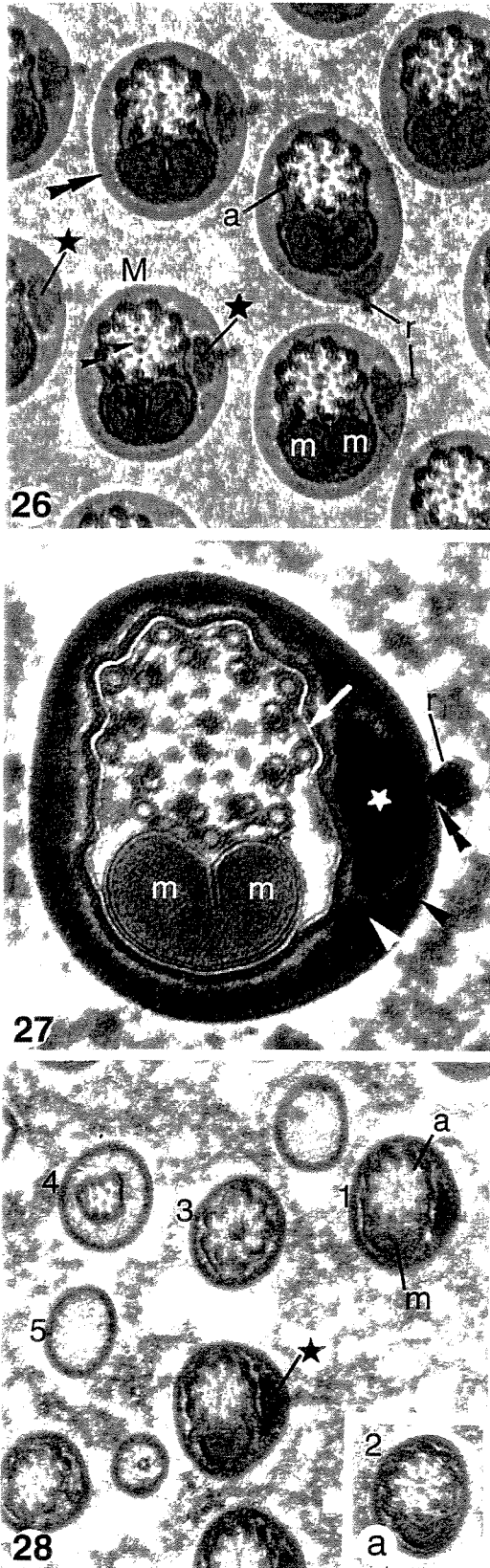
In *E. hegesia*, the accessory microtubules are the first to terminate distally, whereas Medeiros and Silveira (1996) found the accessory microtubules to extend most distally in *A. argillacea*.

Eupyrene spermatozoa

Sperm length varies considerably, from 300 μ m to 1 mm according to Phillips (1970), from 110 to 1267 μ m as described by Morrow and Gage (2000) and 1.6 mm in *C. ethlius* (Lai-Fook, 1982). According to recent studies, sperm length may be important in sperm competition, since the larger spermatozoa would be quicker and therefore more efficient to fertilize the egg (Gage, 1994; Morrow & Gage, 2000).

The presence of an anterior globular structure as found in *E. hegesia*, has not yet been observed in other species. This structure was found only on spermatozoa in the male, which means that it is temporary and not involved in egg recognition or fertilization.

The eupyrene spermatozoa have been described as having a remnant of the reticular appendage (Jamieson, 1987; Kubo-Irie et al., 1998) but our work has shown that this structure is well developed anteriorly, tapering to a small appendage in the tail as recounted for *C. ethlius* by Lai-Fook (1982). A bridge between the appendage and the dense material inside the sperm coat was also found



Figs 26–28 Eupyrene sperm in the seminal vesicle of *Euploietia hegesia*. (26) Typical flagella immersed in the bundle matrix (M). Electron density of the nine accessory and the central pair of microtubules (arrowhead) of the axoneme (a). Amorphous material (star), reticular appendage (r) and mitochondrial derivative (m). Notice the slipped position of the reticular appendage and the dense material that move together in one flagellum. $\times 48\,500$. (27) Cross-section of the flagellum showing the interruption (double arrowhead) of the coat (arrowhead) near the reticular appendage (r) and the dense material (star). Note the less dense surrounding layer (white arrowhead). Plasma membrane (white arrow) and mitochondrial derivative (m). $\times 128\,000$. (28) & (28a) Cross-section of the flagellum's posterior region at different levels (1–5). Axoneme (a), dense material (star) and one mitochondrial derivative (m). $\times 38\,000$.

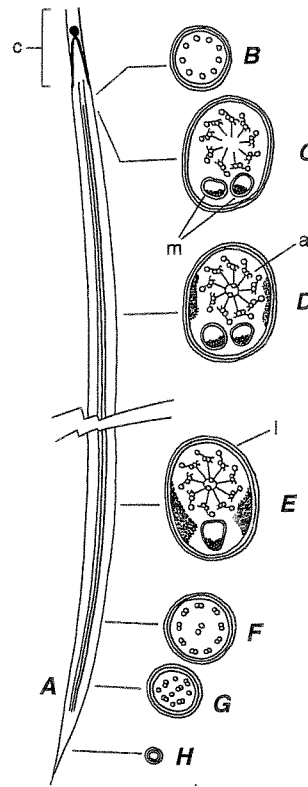


Fig. 29 Schematic diagram of an apyrene spermatozoon. Longitudinal (A) and transversal sections (B–H). Cap (c); axoneme (a); mitochondrial derivative (m); concentric layers (l).

in *A. argillacea* by Medeiros and Silveira (1996) who described it as a peduncle. A regular paracrystalline arrangement in this appendage was also noted by the above authors as well as in *Apopestes spectrum* (Jamieson et al., 1999), which shows the stability of this structure.

A centriolar adjunct is known in many insects as a structure that surrounds the centriole and sometimes part of the nucleus and apparently functions as a support for this transition region (Gatenby & Tamisian, 1959; Lino-Neto et al. 1999, 2000a). This structure does not exist in Lepidoptera and the necessary support is probably furnished by the fitting of the nucleus into the top

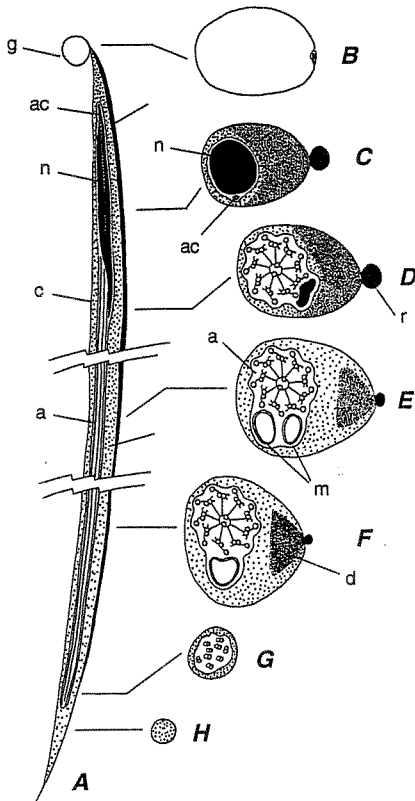


Fig. 30 Schematic diagram of an eupyrene spermatozoon. Longitudinal (A) and transversal sections (B–H). Globular structure (g); acrosome (ac); nucleus (n); axoneme (a); mitochondrial derivative (m); reticular appendage (r); dense material (d); coat (c).

and beside of the centriole, as well as by the dense material that fills the spaces between the organelles along the spermatozoon's entire length.

The electron density of the central and accessory microtubules of axonemes has been observed in many studies (Friedländer & Gitay, 1972; Lai-Fook, 1982; Riemann & Giebultowicz, 1992; Kubo-Irie et al., 1998). However, tannic acid treatment showed very dense central microtubules and the doublets' A tubules. This means that the accessory microtubules' contents are different from the central ones. In addition to this, Behnke and Forer (1967) showed that the axoneme's microtubules have different composition.

The present work did not find evidence that the rearrangement of material from the laciniate appendages resulted in the individual coat of the eupyrene spermatozoa, as stated by Phillips (1970), Lai-Fook (1982) and Riemann and Giebultowicz (1992).

The description of the head region by Lai-Fook (1982) is very similar to that in *E. hegesia*, but differs from that in Medeiros (1997), in which the reticular appendage is very small in proportion to the dense material inside the sperm coat, being the contrary to those of *E. hegesia*. The tubular form of the acrosome described in *E. hegesia* had

also been found by Kubo-Irie et al. (1998) and Lai-Fook (1982).

The lateral placement of the nucleus in relation to the acrosome and the axoneme also occurs in *A. alcinouis* (Kubo-Irie et al., 1998). Friedländer and Gitay (1972) described the proximal nuclear region as having a crescent shaped cross section, compressed between plasma membrane and the beginning of the axoneme, as seen in *E. hegesia*. In the literature, there is no step-by-step description of the flagellar tip, detailing the termination and disorganization of mitochondrial derivatives, axonemal microtubules and the coat.

ACKNOWLEDGEMENTS

We would like to thank A. V. L. Freitas for supplying the insects; and J. Lino-Neto and P. L. Moreira for their help in this publication. This research was supported by the Brazilian Agency CAPES.

REFERENCES

- Behnke, O. and Forer, A. 1967. Evidence for four classes of microtubules in individual cells. *J. Cell Sci.*, 2, 169–192.
- Cook, P.A. and Wedell, N. 1999. Non-fertile sperm delay female remating. *Nature*, 397, 486.
- Dallai, R. and Afzelius, B.A. 1990. Microtubular diversity in insect spermatozoa: results obtained with a new fixative. *J. Struct. Biol.*, 103, 164–179.
- Friedländer, M. 1983. Phylogenetic branching of Trichoptera and Lepidoptera – an ultrastructural analysis on comparative spermatology. *J. Ultrastruct. Res.*, 83, 141–147.
- Friedländer, M. and Gitay, H. 1972. The fate of the normal anucleated spermatozoa in inseminated female of the silkworm *Bombyx mori*. *J. Morphol.*, 138, 121–129.
- Friedländer, M. and Miesel, S. 1977. Spermatid anucleation during the normal atypical spermiogenesis of the warehouse moth *Ephestia cautella*. *J. Submicrosc. Cytol.*, 9, 173–185.
- Gage, M.J.G. 1994. Associations between body size, mating pattern, testis size and sperm lengths across butterflies. *Proc. R. Soc. Lond. B*, 258, 247–254.
- Gatenby, J.B. and Tahmisian, T.N. 1959. Centriole adjunct, centriole, mitochondria and ergastoplasm in orthopteran spermatogenesis. An electron microscopic study. *La Cellule*, 60, 103–134.
- Jamieson, B.G.M. 1987. The ultrastructure and phylogeny of insect spermatozoa. Cambridge University Press, Cambridge.
- Jamieson, B.G.M., Dallai R. and Afzelius, B.A. 1999. Insects: their spermatozoa and phylogeny. Science Publishers, Enfield, NH.
- Kubo-Irie, M., Irie, M., Nakazawa, T. and Mohri, H. 1998. Morphological changes in apyrene and eupyrene spermatozoa in the reproductive tract of the male butterfly *Atrophaneura alcinous*. *Klug. Invert. Reprod. Dev.*, 34, 259–269.
- Lai-Fook, J. 1982. Structural comparison between eupyrene and apyrene spermiogenesis in *Calpodex ethlius* (Hesperiidae: Lepidoptera). *Can. J. Zool.*, 60, 1216–1230.
- Leviatan, R. and Friedländer, M. 1979. The eupyrene-apyrene dichotomous spermatogenesis of Lepidoptera. I. The relationship with postembryonic development and the role of the decline in juvenile hormone titer toward pupation. *Develop. Biol.*, 68, 515–524.
- Lino-Neto, J., Bão, S.N. and Dolder, H. 1999. Structure and ultrastructure of the spermatozoa of *Bephratelloides pomorum* (Fabricius) (Hymenoptera: Eurytomidae). *Int. J. Insect Morphol. Embryol.*, 28, 253–259.
- Lino-Neto, J., Bão, S.N. and Dolder, H. 2000a. Structure and ultrastructure of the spermatozoa of *Trichogramma pretiosum* Riley and *Trichogramma atopovirilia* Oatman and Platner (Hymenoptera: Trichogrammatidae). *Acta Zool. (Stockh.)*, 81, 205–211.

- Lino-Neto, J., Bão, S.N. and Dolder, H. 2000b. Sperm ultrastructure of the honey bee (*Apis mellifera*) (L.) (Hymenoptera, Apidae) with emphasis on the nucleus-flagellum transition region. *Tissue & Cell*, 32, 322-327.
- Medeiros, M. 1986. Caracterização ultra-estrutural de espermatozoides eupirenes e apirenes de *Alabama argillacea* Hübner, 1818 (Lepidoptera: Noctuidae), ao nível dos testículos e das vias genitais de imagos machos e fêmeas até a espermateca. Tese (Mestrado). Instituto de Biologia, Universidade Estadual de Campinas.
- Medeiros, M. 1997. Estudo ultra-estrutural da espermiogênese dicotômica de *Alabama argillacea* Hübner, 1818. Tese (doutorado). Instituto de Biociências, Universidade Estadual de São Paulo.
- Medeiros, M. and Silveira, M. 1996. Ultrastructural study of apyrene spermatozoa of *Alabama argillacea* (Insecta, Lepidoptera, Noctuidae) with tannic acid containing fixative. *J. Submicrosc. Cytol. Pathol.*, 28, 133-140.
- Morrow, E.H. and Gage, M.J.G. 2000. The evolution of sperm length in moths. *Proc. R. Soc. Lond. B*, 267, 307-313.
- Phillips, D.M. 1970. Insect sperm: their structure and morphogenesis. *J. Cell Biol.*, 44, 243-277.
- Phillips, D.M. 1971. Morphogenesis of the laciniate appendages of lepidopteran spermatozoa. *J. Ultrastruct. Res.*, 34, 567-585.
- Riemann, J.G. and Giebultowicz, J.M. 1992. Sperm maturation in the vasa deferentia of the gypsy moth, *Lymantria dispar* L. (Lepidoptera: Lymantriidae). *Int. J. Insect Morphol. & Embryol.*, 21, 271-284.
- Silberglied, R.E., Shepherd, J.G. and Dickinson, J.L. 1984. Eunuchs: the role of apyrene sperm in Lepidoptera?. *Am. Nat.*, 123, 255-265.
- Sonnenschein, M. and Hauser, C.L. 1990. Presence of only eupyrene spermatozoa in adult males of the genus *Micropteryx* Hübner and its phylogenetic significance. *Int. J. Insect Morphol. & Embryol.*, 19, 269-276.
- Snook, R.R. 1997. Is the production of multiple sperm types adaptive?. *Evolution*, 51, 797-808.
- Snook, R.R. 1998. The risk of sperm competition and the evolution of sperm heteromorphism. *An. Behav.*, 56, 1497-1507.
- Souza, W., ed. 1998. Técnicas Básicas de Microscopia Eletrônica Aplicada às Ciências Biológicas. Sociedade Brasileira de Microscopia.
- Wedell, N. and Cook, P.A. 1999. Butterflies tailor their ejaculate in response to sperm competition risk and intensity. *Proc. R. Soc. Lond. B*, 266, 1033-1039.

1.3

**Sperm morphology and arrangement along the male reproductive tract of
the butterfly *Euptoieta hegesia* (Lepidoptera: Nymphalidae)**

Mancini, K. and Dolder, H.

Running title: Spermatozoa along the male reproductive tract of *Euptoieta hegesia*

Abstract

The present study was undertaken to describe the morphological and organizational modifications that occur in apyrene and eupyrene spermatozoa along the male adult reproductive tract of the butterfly, *Euptoieta hegesia*. Testis, deferent duct, seminal vesicle and ejaculatory duct were studied by Transmission Electron Microscopy. In the testis, both sperm types are organized into cysts; apyrene sperm are devoid of extracellular structures while eupyrene ones contain laciniate and reticular appendages. In the testis basal region, both sperm pass through an epithelial barrier and lose their cystic organization. From the deferent duct to the ejaculatory duct, apyrene sperm are dispersed in the lumen and acquire several concentric layers that are formed by the folding of their abundant cell membrane. The apyrene distribution observed here suggests that their functions include eupyrene transportation. Eupyrene sperm, however, remain aggregated along the tract. In the deferent duct, they are covered by a filamentous material, which develops into a homogeneous matrix surrounding the spermatozoa coat in the seminal vesicle and the ejaculatory duct. Eupyrene sperm undergo complex morphological changes that include the loss of laciniate appendages and the formation of a dense and heterogeneous extracellular coat. The formation of the matrix and the coat in eupyrene extratesticular sperm is related to the loss of laciniate appendages. These changes are exclusively extracellular and are probably important for sperm maturation.

Keywords: apyrene – eupyrene – spermatozoa – bundles

Introduction

Lepidoptera present a very evident sperm polymorphism, which results in the development of two morphologically and functionally distinct sperm types: apyrene and eupyrene sperm.

The first description of this sperm dimorphism was that by Meves (1903). Both sperm types were found in all butterflies and moths examined (Zylberberg 1969; Riemann 1970; Phillips 1970, 1971; Friedländer and Gitay, 1972; Lai-Fook 1982a, b; Jamieson 1987; Riemann and Giebultowicz, 1992; Kubo-Irie *et al.*, 1998; Jamieson *et al.*, 1999; Garvey *et al.*, 2000; Mancini and Dolder, 1999, 2001a). The exception is the basal group of Micropterigidae, in which only eupyrene sperm were reported (Sonnenschein and Hauser, 1990; Hamon and Chauvin, 1992).

The eupyrene sperm contains nucleus and acrosome and a flagellum made up of one axoneme and two mitochondrial derivatives. They also possess two extracellular appendages, exclusive to this order, which extend along the entire sperm length. The apyrene sperm is devoid of both nucleus and acrosome. The flagellum possesses one axoneme and two mitochondrial derivatives, which differ in shape and length in relation to the eupyrene one.

Both sperm are transferred to the female and then stored in the spermatheca (Riemann, 1970; Phillips, 1971; Riemann and Thorson, 1971; Friedländer and Gitay, 1972; Lai-Fook, 1982b; Friedländer *et al.*, 2001). However, only eupyrene sperm fertilize eggs. The apyrene sperm enter into this process indirectly to guarantee successful paternity with the eupyrene ones by participating in sperm competition (Silberglied *et al.*, 1984; Drummond 1984; Snook 1997, 1998; Wedell and Cook, 1999; Cook and Wedell, 1999).

The apyrene and eupyrene sperm bundles from the testis are first released into the deferent duct, then transferred into the seminal vesicle, and finally into the *ductus ejaculatorius*. This sperm release, from testes to the seminal vesicle is controlled by an intrinsic circadian mechanism located in the reproductive system (Riemann *et al.*, 1974; LaChance *et al.*, 1977; Giebultowicz *et al.*, 1988; Riemann and Giebultowicz, 1992; Giebultowicz and Zdarek, 1996; Giebultowicz and Brooks, 1998; Bebas *et al.*, 2001). A

photoreceptive circadian clock that is located in the reproductive system controls sperm release that appears to be important for post-testicular maturation of sperm, and, consequently, for male fertility (Riemann and Ruud, 1974; Giebultowicz *et al.*, 1990). This sperm movement, from the testis to the deferent duct, occurs in a daily rhythmic pattern, where the sperm bundles are released only during a period of a few hours in the evening. Sperm bundles remain in the deferent duct overnight, then, in the morning, are transferred to the seminal vesicle (Giebultowicz *et al.*, 1988, 1996; Giebultowicz and Zdarek, 1996; Giebultowicz and Brooks, 1998; Seth *et al.*, 2002).

Apyrene and eupyrene sperm released from the testis and pass through several organizational and morphological changes along the male and female tracts. The present study made a comparative description of these organizational and morphological modifications in apyrene and eupyrene sperm of the butterfly *Euptoieta hegesia*.

Materials and Methods

Adults of the butterfly *Euptoieta hegesia* were collected on the Campus of the Universidade Estadual de Campinas (São Paulo State – Brazil). Testis, deferent duct, seminal vesicle and ejaculatory duct were dissected in different periods of the day (early morning, early and late afternoon) and processed for Transmission Electron Microscopy.

(1) Most specimens were fixed in 2.5% glutaraldehyde, 4% paraformaldehyde, 1.5% sucrose, 5mM CaCl₂ in a 0.1M sodium phosphate buffer for 12 hours at 4°C. After fixation, they were rinsed in buffer, post-fixed in 1% osmium tetroxide for 3-5 hours at 4°C, dehydrated in acetone and finally embedded in Epoxy resin.

(2) In some cases, they were fixed in 2.5% glutaraldehyde, 1% tannic acid, 1.5% sucrose and 5mM CaCl₂, buffered with 0.1M sodium phosphate at pH 7.2 for three days at 4°C. After fixation, they were rinsed in buffer and block-stained in 1% uranyl acetate for 2 hours at room temperature (Dallai and Afzelius, 1990). They were dehydrated in acetone and embedded in Epoxy resin.

(3) Other samples were fixed in 2.5% glutaraldehyde, 0.2% cuproline blue, 0.2M $MgCl_2$, buffered with 0.05M sodium acetate for 24 hours at 4°C. After rinsing in buffer, they were post-fixed in 1% sodium tungstate in distilled water for 24 hours at 4°C. They were dehydrated in 30% ethanol in 1% sodium tungstate for 30 minutes at 4°C; 50% ethanol in 1% sodium tungstate overnight at 4°C; 70%-100% ethanol for 45 minutes (Modified from Scott *et al.*, 1989). Finally, they were embedded in Epoxy resin.

Ultra thin sections were stained with uranyl acetate and lead citrate.

Results

- Sperm Arrangement

The adult reproductive tract of *Euptoieta hegesia* is composed of a fused pair of testes connected to a pair of thin deferent duct. These ducts converge to the accessory glands to form a pair of seminal vesicle, which unite in a single, thin, long ejaculatory duct (fig. 1).

In the testis, apyrene and eupyrene cells are organized into cysts inside the lumen of the follicles. Eupyrene and apyrene cysts, sectioned in the head region, consist of approximately 256 sperm, however, sections of the tail regions of apyrene cyst show larger numbers of sperm (figs. 2A and C). The apyrene and eupyrene sperm heads are located inside of tubular invaginations of the cell membrane of the head cyst cell, which maintains these cells tightly packed, aligned and in the same developmental stages (fig. 2B). The cystic cells are rich in rough endoplasmic reticulum (figs. 2C and D).

In the basal region of the testis, near the deferent duct, apyrene and eupyrene compact cysts, with closely aligned spermatozoa, enlarge so that the spermatid cells are dispersed (figs. 2B-E), losing their regular arrangement. Apyrene cysts disorganize earlier than eupyrene ones (fig. 2B). Disorganized apyrene cysts contain several sperm cells with abundant intracellular material, still surrounded by the plasma membrane (fig. 2C), while eupyrene ones possess a filamentous material in which the sperm are embedded (figs. 2D

and E). Several apyrene spermatozoa can often be observed inside the broken eupyrene cysts (fig. 2E). The base of each follicle is separated from the lumen of the deferent duct by an epithelial barrier, which is penetrated by the apyrene and eupyrene sperm bundles during their release from the testis (fig. 2F). When apyrene sperm bundles pass through this barrier, they lose their cystic cells, and the spermatozoa are liberated directly into the deferent duct lumen. These spermatozoa continue aggregated for a short time, as long as their heads remain inside the tubular invaginations of the cell membrane of the head cyst cell (fig. 2G). When eupyrene sperm bundles pass through the barrier, some of the eupyrene cysts liberate their spermatozoa in the lumen, while others continue intact in the proximal deferent duct lumen (figs. 2H and I).

Despite the loss of the cystic envelope, eupyrene spermatozoa remain aggregated along the deferent duct (figs. 2J-K). The same aggregation does not occur with apyrene spermatozoa, which appear dispersed in the lumen (fig. 2I), and generally, near the microvilli (fig. 2K). It is common to find some apyrene spermatozoa next to the eupyrene groups.

In the medial region of the deferent duct, the aggregated eupyrene sperm are surrounded by filamentous material (fig. 2L), which latter is transformed into the matrix of eupyrene bundles, found in the seminal vesicle.

In the distal region of the deferent duct, several secretion granules were observed undergoing exocytosis from accessory gland cells. Apyrene spermatozoa are located next to the microvilli, where the granules are secreted (fig. 2M). Eupyrene bundles are well defined, with abundant fibrous material (fig. 2N).

In the seminal vesicle, the eupyrene bundle is completed and an amorphous matrix, without any cellular component, maintains the spermatozoa parallel and closely associated. Apyrene spermatozoa remain dispersed in the lumen, amid in the secretion (fig. 2O).

Finally, in the proximal region of the ejaculatory duct, sperm organization is similar to that observed in the seminal vesicle. There are some disrupted eupyrene bundles but, as a rule, the sperm aggregation is maintained. The apyrene sperm remain dispersed in the secretion (fig. 2P). No sperm were found in medial and distal regions of ejaculatory duct.

- Sperm Morphology

Simultaneously to the organizational modifications described above, apyrene and eupyrene spermatozoa undergo distinct and complex morphological changes.

In the testis, as described above, both spermatozoa types are arranged in cysts. Apyrene flagella of *E. hegesia* possess a 9+9+2 axoneme and two well-separated mitochondrial derivatives with the same shape (fig. 3A). Eupyrene flagella also have a 9+9+2 axoneme and two mitochondrial derivatives, however these are denser and closer, often appearing to be fused. Intratesticular eupyrene spermatozoa present, exclusively, two types of extracellular appendages, termed reticular and laciniate, that extend the entire sperm length.

The reticular appendage is a single dense rod located laterally at the junction of the axoneme and the mitochondrial derivatives. The laciniate appendages, which occur in variable number, are regularly spaced, pointed projections (fig. 3B).

In the basal testis region, where cyst disarrangement begins, eupyrene spermatozoa begin to lose their laciniate appendages. Some of them are cast off intact from the membrane, while others gradually disintegrate into filaments (fig. 3C).

In the proximal deferent duct region, apyrene spermatozoa are dispersed in the lumen and present an enlarged cell membrane (figs. 3D-H) originates the extracellular concentric layers, that later are found surrounding the plasma membrane (fig. 3P). Some apyrene spermatozoa present an abundant intracellular material and, consequently, the membrane is expanded (figs. 3D and F). The majority of the eupyrene spermatozoa in this region still possess a few laciniate appendages. Here a dense and amorphous material is observed to develop, that is, located between the cell membrane and the reticular appendage (figs. 3I and J).

In the medial deferent duct region, where fibrous material twisting around the eupyrene spermatozoa, these acquire a dense coat covering all the plasma membrane. The reticular appendage, which here is reduced in diameter, is external to this coat and no longer attached to the plasma membrane. Laciniate appendages are absent (fig. 3K).

Different developmental stages of spermatozoa occur mixed in the deferent duct.

Thus, there is a coexistence of apyrene spermatozoa with a newly forming concentric layer, together with apyrene spermatozoa, which have already formed this concentric layer (fig. 3L). Eupyrene aggregates in different stages of coat development also can be found in this region (fig. 3M).

In the seminal vesicle, eupyrene spermatozoa are grouped in bundles, with each spermatozoon covered by a coat, maintained in this formation by a matrix (fig. 3N). The coat contains three distinct regions (fig. 3O): an external layer, an amorphous material lining the external layer and a dense material located next to the reticular appendage, which remains external to the coat. These distinct regions were not previously observed in the deferent duct eupyrene spermatozoa (fig. 3K). Apyrene spermatozoa, in the seminal vesicle, are embedded in secretion and enveloped by well-formed concentric layers. Some of them contain irregular amorphous masses inside the layers (fig. 3P).

Apyrene and eupyrene spermatozoa from the ejaculatory duct are similar to those of the seminal vesicle.

Discussion

The morphology of the reproductive tract of *Euptoieta hegesia* is similar to other Lepidoptera species (Ehrlich, 1961; Kubo-Irie *et al.*, 1998; Justus and Mitchell, 1999) but differs as to the location of the seminal vesicle, which occurs at the junction of the deferent duct and the accessory glands. Therefore, it differs from the majority of the species studied (Riemann and Thorson, 1976; LaChance *et al.*, 1977; Lai-Fook, 1982b; Riemann and Giebultowicz, 1991; Giebultowicz *et al.*, 1988, 1996; 1997; Giebultowicz and Brooks, 1998).

Along the male reproductive tract of the butterfly *E. hegesia*, eupyrene and apyrene spermatozoa pass through several modifications of their organization and morphology, which distinguish the two sperm types (Mancini and Dolder, 1999). The morphological modifications are exclusively extracellular, associated to displacement, rearrangement and formation of new components, and not to the intracellular structures.

The eupyrene morphological and organizational modifications are more drastic than the apyrene ones. As a rule, when apyrene sperm bundles move through the base of the testis into a proximal deferent duct, most of the enclosing cyst cells are lysed, dispersing the spermatozoa, and an external sheath is formed over the plasma membrane of the individual sperm. No further morphological changes are seen in the individual apyrene sperm cells. However, eupyrene sperm undergo a series of organizational arrangements, remaining aggregated along the entire reproductive tract and forming elaborate extracellular structures. The elaborate changes that occur when the sperm move from the testes to the deferent duct and then to seminal vesicle were previously analyzed (Friedländer and Gitay, 1972; Phillips, 1971; Riemann, 1970; Riemann and Thorson, 1971; Lai-Fook 1982a; Riemann and Giebultowicz, 1992; Kubo-Irie *et al.*, 1998; Friedländer *et al.*, 2001).

Most of the *E. hegesia* sperm modifications (Mancini and Dolder, 1999, 2001b) are in agreement with reports of other Lepidoptera (Riemann 1970; Lai-Fook 1982a; Riemann and Giebultowicz, 1992; Kubo-Irie *et al.*, 1998; Garvey *et al.*, 2000).

Eupyrene and apyrene cysts of *E. hegesia* contain approximately 256 spermatozoa as occurs in the majority of Lepidoptera (Phillips 1971; Lai-Fook 1982a; Kubo-Irie *et al.*, 1998). Apyrene cysts showing larger numbers of flagella could be the result of folding or cyst fusion.

The epithelial barrier that separates the testicular follicles from the lumen of the deferent duct of *E. hegesia* was previous reported in other lepidoptera (Riemann and Thorson, 1971; Riemann and Giebultowicz, 1991; Giebultowicz *et al.*, 1997; Bebas *et al.*, 2001). These studies report that the apyrene and eupyrene sperm are released from the testis to the deferent duct according to a daily pattern of the circadian rhythm.

In *E. hegesia*, sperm release occurs first in apyrene spermatozoa, which immediately disperse in the deferent duct, followed by eupyrene spermatozoa, which remain aggregated along the entire male reproductive tract. This temporal cystic disorganization at the testicular base and proximal deferent duct regions has previously been reported by various authors (Riemann 1970; Riemann and Giebultowicz, 1991; Giebultowicz *et al.*, 1997; Bebas *et al.*, 2001).

In *E. hegesia*, the presence of a few apyrene sperm inside ruptured eupyrene cysts was commonly observed. The occurrence of the disorganized cysts, as well the close contact between sperm along the male tract, suggest that apyrene spermatozoa could be involved in liberation of the eupyrene sperm from their cysts, as well as in their transport along the reproductive tract. Various studies relate the function of apyrene spermatozoa to the transport of eupyrene sperm bundles to the female tract (Friedländer and Gitay, 1972; Friedländer and Miesel, 1977; Riemann 1970) and to their transport along the male tract (Osanai *et al.*, 1987a).

The apyrene and eupyrene sperm morphology of *E. hegesia* is similar to other Lepidoptera (Phillips 1971; Lai-Fook 1982a; Kubo-Irie *et al.*, 1998).

In the cystic cytoplasm of *E. hegesia*, there is a large quantity of rough endoplasmic reticulum. We believe that cystic cells may contribute to the appendage formation. Cytochemical studies have demonstrated the presence of carbohydrate and protein residues in these extracellular structures (Medeiros, 1986; França and Bão, 2000; Mancini and Dolder, in preparation).

There are several speculations about the fate of laciniate appendages in the extratesticular eupyrene sperm as being the origin of the eupyrene coat. In *E. hegesia*, as in other Lepidoptera, these appendages were broken down in the proximal deferent duct region, just as a fibrous material appeared surrounding the eupyrene sperm. At the same time, a dense coat was formed covering these spermatozoa (Mancini and Dolder, 2001b). According to Phillips (1971) and Riemann and Thorson (1971), in the deferent duct, laciniate appendages were rearranged to form the extracellular coat of both types of spermatozoa, possibly also contributing to the bundle's matrix. This hypothesis was partially accepted by other authors (Lai-Fook 1982a; Riemann and Giebultowicz, 1992; Kubo-Irie *et al.*, 1998). Laciniate appendages could contribute, in part, to both matrix and to the eupyrene coat, as suggested by the structural similarity between the filaments, which result from the laciniate appendage break down, and the matrix. Their break down occurs immediately before the appearance of these structures, suggesting a relationship between these two events. Also, the matrix skeleton is already present before the bundle reaches the secretory portions of the seminal vesicle (fig. 1L).

In *A. kuehniella*, *L. dispar* and *A. argillacea* (Riemann and Thorson, 1976; Riemann and Giebultowicz, 1992 and Medeiros 1986, respectively), apyrene spermatozoa in the deferent duct and seminal vesicle present short filaments (annulate rods) around the plasma membrane. In *E. hegesia*, gradual formation of concentric layers was observed but nothing similar to these filaments. Disorganized apyrene cysts present some spermatozoa with abundant clear intracellular material and, consequently, enlarged membranes. Similar structures were observed in apyrene sperm cells of the deferent duct proximal region. Images of folding cell membrane (figs. 3D-H) suggest that this is the origin of the concentric layers in *E. hegesia*.

With the fixations applied, no similarity was found between the extracellular coats of both extratesticular spermatozoa, as reported by other authors (Phillips 1971; Friedländer and Gitay, 1972; Riemann and Gassner, 1973; Riemann and Giebultowicz, 1992). Phillips (1971) proposes a common origin between these coats, but in *E. hegesia*, it is not probable.

The coexistence (in the same transverse section) of different apyrene developmental stages, with and without concentric layers, was previously reported (Kubo-Irie *et al.*, 1998). Similar events occur in eupyrene spermatozoa of *E. hegesia*. It is a result of apyrene and eupyrene cyst disorganization, which previously maintained the sperm cells aligned and in the same developmental stage.

Apyrene and eupyrene sperm organization and morphology in the seminal vesicle reported in *E. hegesia* (Mancini and Dolder, 2001a) is similar to the majority of the species studied (Medeiros 1986; Lai-Fook 1982a; Kubo-Irie *et al.*, 1998). When tannic acid fixative was used (fig. 3O), we identified, in the seminal vesicle an elaborate eupyrene coat composed of three distinct regions. These well defined regions apparently represent different protein components with various arrangements.

According to developmental stages (larva, pupa or imago) and during their lifetime, we believe there may be variations of all the events described along the reproductive tract. In the present study, only imagos of *E. hegesia* were analyzed and they possess a long adult lifetime, if compared with the majority of the species studied, which may account for some differences encountered.

In *E. hegesia*, sperm motility was not observed in the male tract but only in the female. According to Kinefuchi (1978), eupyrene sperm are immotile until activated by alkaline phosphatase in the female, whereas apyrene sperm are active in the semen. In *Bombyx mori* female, according to Osanai *et al.*, (1987b), apyrene sperm acquire motility first, then eupyrene bundles dissociate and the individual eupyrene sperm show a slow motility, and finally, the decapsulated eupyrene spermatozoa acquire high motility. These reports corroborated the hypothesis that the apyrene sperm help in eupyrene transport. Also in *Bombyx mori* (Kawamura *et al.*, 2000), peristaltic squeezing of sperm cysts was detected at late stages of spermatogenesis. These simple contractions would result in the discarding of cytoplasm from the posterior extremity of eupyrene sperm and both cytoplasm and nuclei from the apyrene ones, as suggested by these authors.

The functional significance of sperm organizational alterations, as well as of the morphological changes along the male reproductive tract possibly are related to sperm maturation, as occurs in mammals.

Acknowledgments

We would like to thank A. V. L. Freitas for supplying the butterflies. This research was supported by the Brazilian Agency FAPESP (01/01049-6).

References

- Bebas, P., Cymborowski, B. and Giebultowicz, J.M. 2001. Circadian rhythm of sperm release in males of the cotton leafworm, *Spodoptera littoralis*: in vivo and in vitro studies. **J. Insect Physiol.** 47: 859-866.
- Cook, P.A. and Wedell, N. 1999. Non-fertile sperm delay female remating. **Nature** 397: 486.

- Dallai, R. and Afzelius, B. A. 1990. Microtubular diversity in insect spermatozoa: results obtained with a new fixative. **J. Struct. Biol.** **103**: 164-179.
- Drummond, B.A. 1984. **Multiple mating and sperm competition in the lepidoptera**. In: Sperm competition and the evolution of animal mating systems, R.L. Smith (ed.), Academic Press, London. 1984, pp. 291-370.
- Ehrlich, P. 1961. Comparative morphology of the male reproductive system of the butterflies (Lepidoptera: Papilionoidea). **Microentomol.** **24**: 135-166.
- França, F. G. R. and Báo, S. N. 2000. Dimorphism in spermatozoa of *Anticarsia gemmatilis* Hübner, 1918 (Insecta, Lepidoptera, Noctuidae). **Braz. J. Morphol. Sci.** **17**: 5-10.
- Friedländer, M. and Gitay, H. 1972. The fate of the normal enucleated spermatozoa in inseminated female of the silkworm *Bombyx mori*. **J. Morphol.** **138**: 121-129.
- Friedländer, M., Jeshtadi, A. and Reynolds, S. E. 2001. The structural mechanism of trypsin-induced intrinsic motility in *Manduca sexta* spermatozoa in vitro. **J. Insect Physiol.** **47**: 245-255.
- Friedländer, M. and Miesel, S. 1977. Spermatid enucleation during the normal atypical spermiogenesis of the warehouse moth *Ephestia cautella*. **J. Submicrosc. Cytol.** **9**: 173-185.
- Garvey, L. K., Gutierrez, G. M., and Krider, H. M. 2000. Ultrastructure and morphogenesis of the apyrene and eupyrene spermatozoa in the Gypsy moth (Lepidoptera: Lymantriidae). **Ann. Entomol. Soc. Am.** **93**: 1147-1155.
- Giebultowicz, J.M., Bell, R.A. and Imberski, R.B. 1988. Circadian rhythm of sperm movement in the male reproductive tract of the gypsy moth, *Lymantria dispar*. **J. Insect Physiol.** **34**: 527-532.
- Giebultowicz, J.M., Blackburn, M.B., Thomas-Laemont, P.A., Weyda, F. and Raina, A.K. 1996. Daily rhythm in myogenic contractions of *vas deferens* associated with sperm release cycle in a moth. **J. Comp. Physiol.** **178**: 629-636.
- Giebultowicz, J.M. and Brooks, N.L. 1998. The circadian rhythm of sperm release in the codling moth, *Cydia pomonella*. **Entomol. Exp. Appl.** **88**: 229-234.

- Giebultowicz, J.M., Feldlaufer, M. and Gelman, D.B. 1990. Role of ecdysteroids in the regulation of sperm release from the testes of the gypsy moth, *Lymantria dispar*. **J. Insect Physiol.** **36**: 567-571.
- Giebultowicz, J.M., Weyda, F., Erbe, E.F. and Wergin, W.P. 1997. Circadian rhythm of sperm release in the gypsy moth, *Lymantria dispar*: ultrastructural study of transepithelial penetration of sperm bundles. **J. Insect Physiol.** **13**: 1133-1147.
- Giebultowicz, J.M. and Zdarek, J. 1996. The rhythm of sperm release from testis and mating flight are not correlated in *Lymantria* moths. **J. Insect Physiol.** **42**: 167-170.
- Hamon, C., and Chauvin, G. 1992. Ultrastructural analysis of spermatozoa of *Korscheltellus lupulinus* L. (Lepidoptera: Hepialidae) and *Micropterix calthella* L. (Lepidoptera: Micropterigidae). **J. Insect Morphol. Embryol.** **21**: 149-160.
- Jamieson, B. G. M. 1987. **The ultrastructure and phylogeny of insect spermatozoa.** Cambridge University Press.
- Jamieson, B. G. M., Dallai, R and Afzelius, B. A. 1999. **Insects: their spermatozoa and phylogeny.** Science Publishers, Inc., Enfield, New Hampshire, USA.
- Justus, K. A. And Mitchell, B. K. 1999. Reproductive morphology, copulation, and inter-population variation in the diamondback moth, *Plutella xylostella* (L.) (Lepidoptera: Plutellidae). **Int. J. Insect Morphol. Embryol.** **28**: 233-246.
- Kawamura, N., Yamashiki, N., Saitoh, H. and Sahara, K. 2000. Peristaltic squeezing of sperm bundles at the late stage of spermatogenesis in the silkworm, *Bombyx mori*. **J. Morphol.** **246**: 53-58.
- Kinefuchi, H. 1978. Studies on eupyrene and apyrene spermatozoa of Lepidoptera. **Mem. Facul. Educ. Niigata Univ.** **19**: 21-31.
- Kubo-Irie, M., Irie, M., Nakazawa, T. and Mohri, H. 1988. Morphological changes in apyrene and eupyrene spermatozoa in the reproductive tract of the male butterfly *Atrophaneura alcinous* Klug. **Invert. Reprod. Develop.** **34**: 259-269.
- LaChance, L.E., Richard, R.D. and Ruud, R.L. 1977. Movement of eupyrene sperm bundles from the testis and storage in the *ductus ejaculatorius* duplex of the male pink bollworm: effects of age, strain, irradiation, and light. **Ann. Entomol. Soc. Am.** **70**: 647-651.

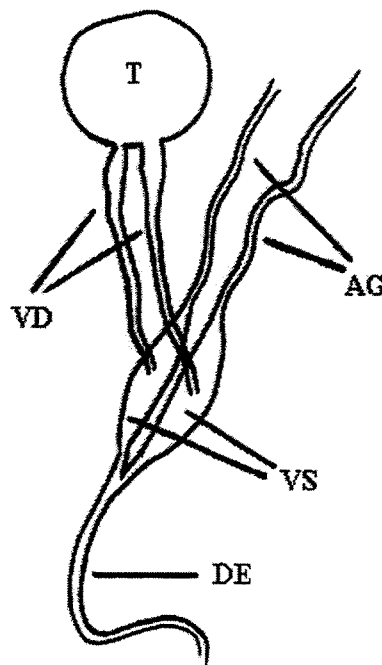
- Lai-Fook, J. 1982a. Structural comparison between eupyrene and apyrene spermiogenesis in *Calpodex ethlius* (Hesperiidae: Lepidoptera). **Can. J. Zool.** 60: 1216-1230.
- Lai-Fook, J. 1982b. The vasa deferentia of the male reproductive system of *Calpodex ethlius* (Hesperiidae: Lepidoptera). **Can. J. Zool.** 60:1172-1183.
- Mancini, K. and Dolder, H. 1999. Ultrastructural modifications in apyrene and eupyrene spermatozoa of *Euptoieta hegesia* (Lepidoptera: Nymphalidae) along the male reproductive tract. **Acta Microsc.** 567-568.
- Mancini, K. and Dolder, H. 2001a. Ultrastructure of apyrene and eupyrene spermatozoa from the seminal vesicle of *Euptoieta hegesia* (Lepidoptera: Nymphalidae). **Tissue and Cell** 33: 301-308.
- Mancini, K. and Dolder, H. 2001b. Extracellular appendages of Lepidopteran spermatozoa. **Acta Microsc.** 301-302.
- Medeiros, M. 1986. **Caracterização ultra-estrutural de espermatozoides eupirenes e apirenes de *Alabama argillacea* Hübner, 1818 (Lepidoptera: Noctuidae), ao nível dos testículos e das vias genitais de imagos machos e fêmeas até a espermateca.** Master Thesis, IB, Universidade Estadual de Campinas.
- Meves, F. 1903. Ueber den von La Valette Saint-George entdeckten Nebenkern (Mitochondrienkörper) des Samenzellen. **Archiv. für Mikrosk. Anat.** 56: 553-606.
- Osanai, M., Kasuga, H and Aigaki, T. 1987a. Physiological role of apyrene spermatozoa of *Bombyx mori*. **Experientia** 43: 593-596.
- Osanai, M., Kasuga, H and Aigaki, T. 1987b. Spermatophore and its structural changes with time in bursa copulatrix of the silkworm, *Bombyx mori*. **J. Morphol.** 193:1-11.
- Phillips, D. M. 1970. Insect sperm: their structure and morphogenesis. **J. Cell Biol.** 44: 243-277.
- Phillips, D. M. 1971. Morphogenesis of the laciniate appendages of Lepidopteran spermatozoa. **J. Ultrastruct. Res.** 34: 567-585.
- Riemann, J. G. 1970. **Metamorphosis of the cabbage looper *Trichoplusia ni* during passage from the testis to the female spermatheca.** In: Comparative Spermatology, B. Baccetti (ed.), Academic Press, New York, pp. 321-331.

- Riemann, J. G. and Gassner, G. 1973. Ultrastructure of Lepidopteran sperm within spermathecae. **An. Entomol. Soc. Am.** 66:154-159.
- Riemann, J. G. and Giebultowicz, J. M. 1991. Secretion in the upper *vas deferens* of the gypsy moth correlated with the circadian rhythm of sperm release from the testes. **J. Insect Physiol.** 37: 53-62.
- Riemann, J. G. and Giebultowicz, J. M. 1992. Sperm maturation in the *vasa deferentia* of the gypsy moth, *Lymantria dispar* L. (Lepidoptera: Lymantriidae). **Int. J. Insect Morphol. Embryol.** 21: 271-284.
- Riemann, J.G. and Ruud, R.L. 1974. Mediterranean flour moth: effects of continuous light on the reproductive capacity. **Ann. Entomol. Soc. Am.** 67: 857-860.
- Riemann, J. G. and Thorson, B. J. 1971. Sperm maturation in the male and female genital tracts of *Anagasta kuhniella* (Lepidoptera: Pyralididae). **Int. J. Insect Morphol. Embryol.** 1: 11-19.
- Riemann, J. G. and Thorson, B. J. 1976. Ultrastructure of the *vasa deferentia* of the mediterranean flour moth. **J. Morphol.** 129: 483-506.
- Riemann, J.G., Thorson, B.J. and Ruud, R.L. 1974. Daily cycle of release of sperm from the testes of Mediterranean flour moth. **J. Insect Physiol.** 20: 195-207.
- Scott, J. E., Haigh, M., Nusgens, B. and Lapière, C. M. 1989. Proteoglycan: collagen interactions in dermasparacti skin and tendon. An electron histochemical study using cupromeronic blue in a critical eletrolyte concentration method. **Matrix** 9: 437-442.
- Seth, R.K., Rao, D.K. and Reynolds, S.E. 2002. Movement of spermatozoa in the reproductive tract of adult male *Spodoptera litura*: daily rhythm of sperm descent and the effect of light regime on male reproduction. **J. Insect Physiol.** 48: 119-131.
- Silberglied, R.E., Shepherd, J.G. and Dickinson, J.L. 1984. Eunuchs: the role of apyrene sperm in lepidoptera? **Am. Nat.** 123: 255-265.
- Snook, R.R. 1997. Is the production of multiple sperm types adaptive? **Evolution** 51: 797-808.
- Snook, R.R. 1998. The risk of sperm competition and the evolution of sperm heteromorphism. **An. Behav.** 56: 1497-1507.

- Sonnenschein, M. and Hauser, C. L. 1990. Presence of only eupyrene spermatozoa in adult males of the genus *Micropteryx* Hubner and its phylogenetic significance. **Int. J. Insect Morphol. Embryol.** 19: 269-276.
- Wedell, N. and Cook, P.A. 1999. Butterflies tailor their ejaculate in response to sperm competition risk and intensity. **Proc. Royal Soc. London B** 266: 1033-1039.
- Zylberberg, L. 1969. Contribution a l'étude de la double spermatogenèse chez un lépidoptère (*Pieris brassicae* L., Pieridae). **Ann. Sci. Nat., Zool.** 11: 569-626.

Figure Legends

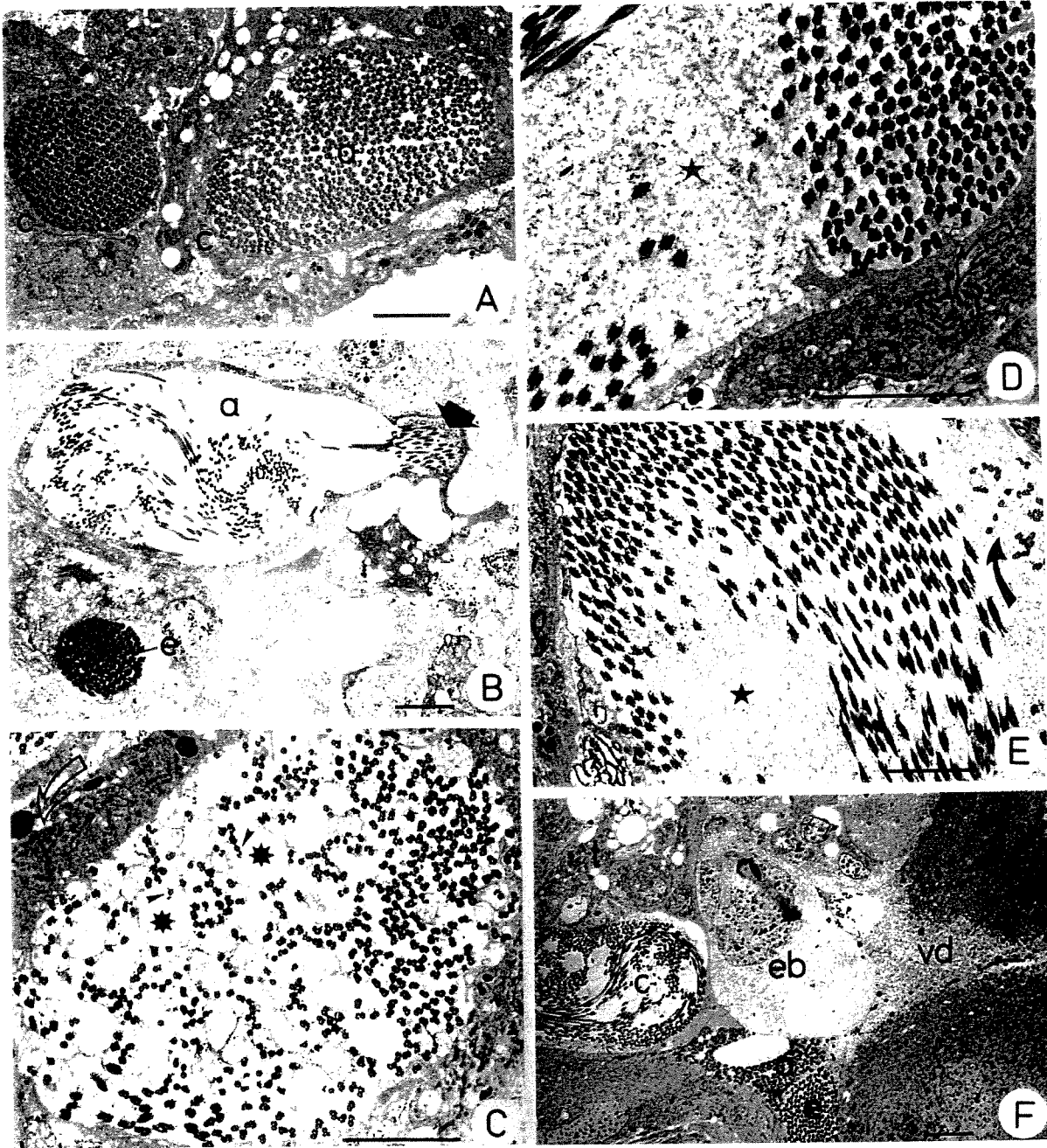
Figure 1: Schematic representation of the male reproductive system of *Euptoieta hegesia*. Fused testis (T); deferent duct (VD), seminal vesicle (VS); accessory glands (AG) and ejaculatory duct (DE).



Figures 2A-F: Apyrene and Eupyrene sperm arrangement

- (A) Apyrene (a) and Eupyrene (e) sperm testicular cysts surrounded by cystic cells (c). Compare the dimensions of these cysts.
- (B) Compact eupyrene (e) cyst and a disorganized apyrene (a) one, with sperm cells' anterior portions embedded in the cystic cell (arrow).
- (C) Disorganized apyrene cyst. Several spermatozoa (arrowheads) possess abundant clear intracellular material (asterisk). Rough endoplasmic reticulum (open arrow).
- (D) and (E) Ruptured eupyrene cysts with filamentous material (star) and apyrene sperm (arrow) dispersed inside the cyst. Rough endoplasmic reticulum (open arrow in D).
- (F) Epithelial barrier (eb) that separates the testis base (t) from the deferent duct lumen (vd). Note the testicular cyst (c) above the barrier and the apyrene (a) and eupyrene (e) bundles that pass through this barrier.

Scale bars: 5 μ m



Figures 2G-L: Apyrene and Eupyrene sperm arrangement

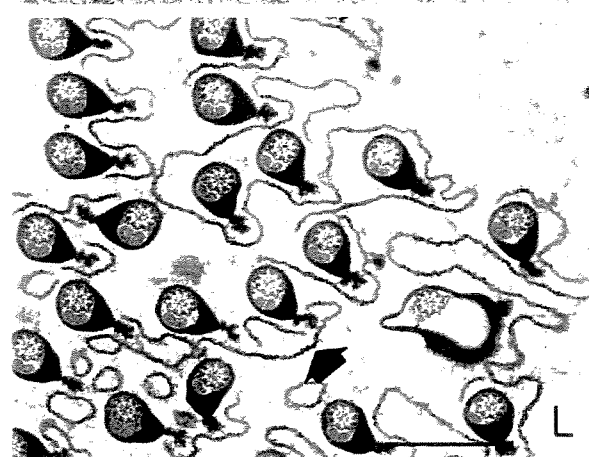
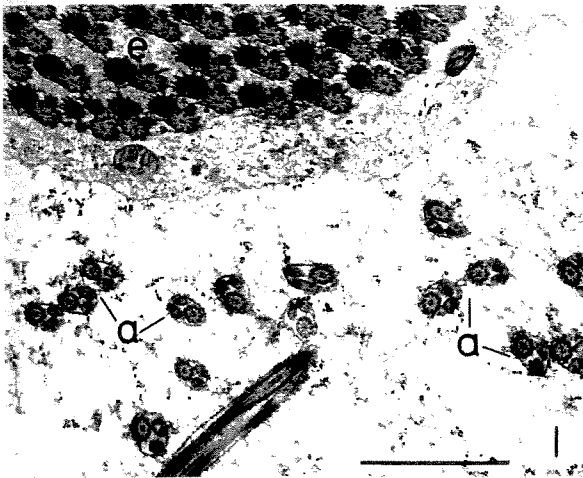
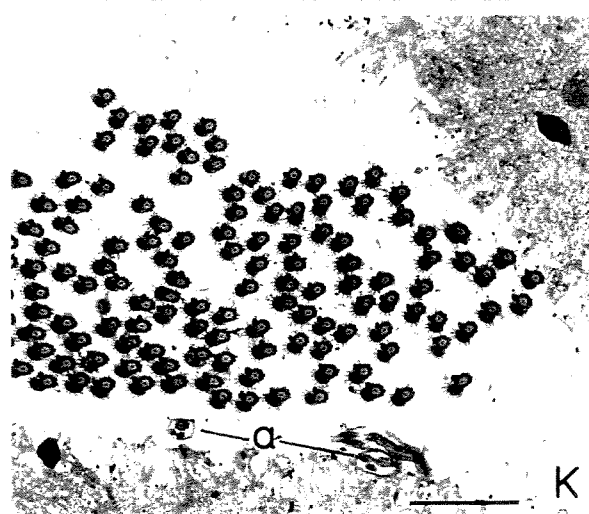
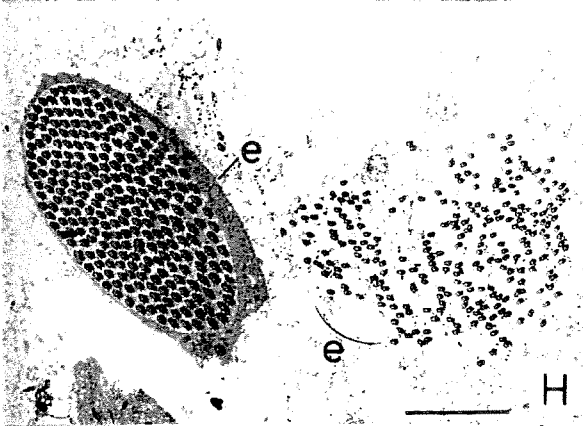
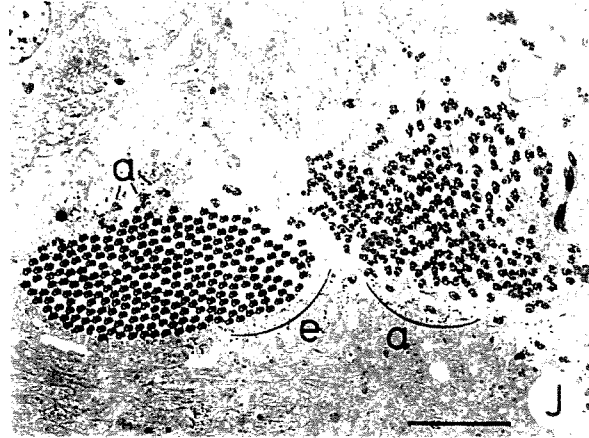
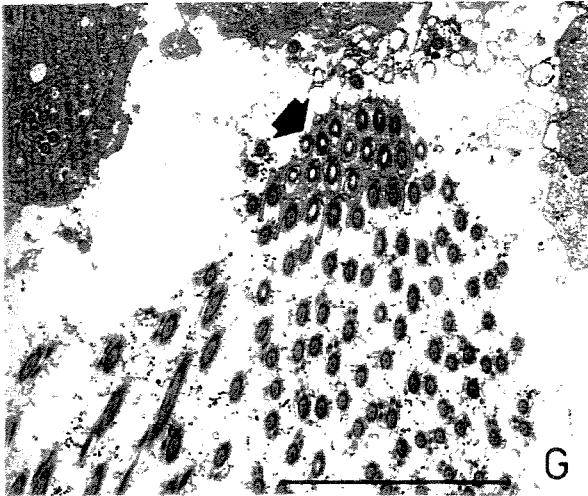
(G) Proximal deferent duct region. Apyrene spermatozoa aggregated by the embedding of their heads in a cystic cell (arrow).

(H) and (I) Proximal deferent duct region. Intact eupyrene (e) cyst and dispersed apyrene (a) and eupyrene (e) spermatozoa in the lumen.

(J) and (K) Proximal deferent duct region. Aggregated eupyrene (e) sperm without a cystic cell. Apyrene (a) spermatozoa dispersed in the lumen and near eupyrene ones.

(L) Medial deferent duct region. Aggregated eupyrene sperm partially surrounded by a fibrous material (arrow). Notice altered extracellular structures.

Scale bars: (G)-(H), (J): 5µm; (K): 2.5µm; (I): 2µm; (L): 1µm.



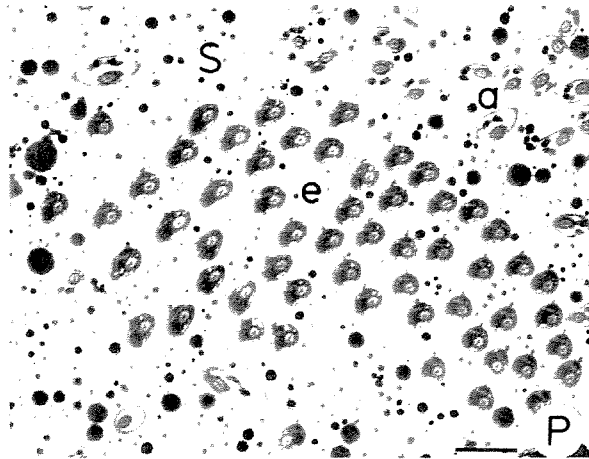
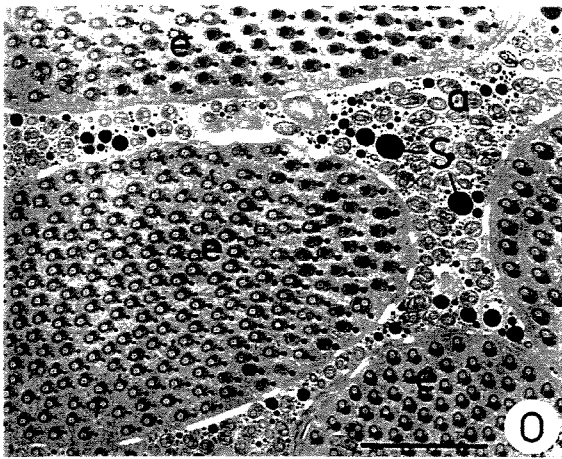
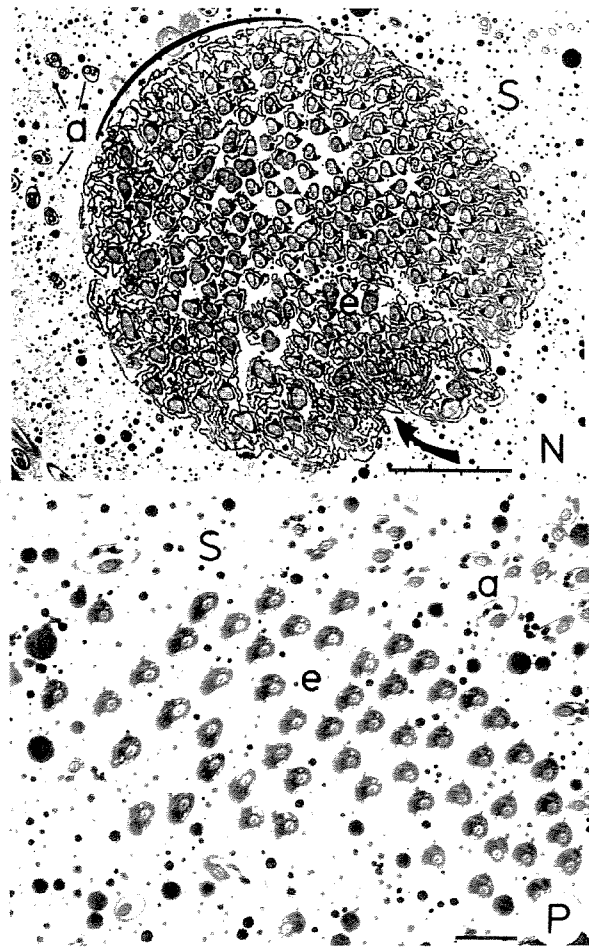
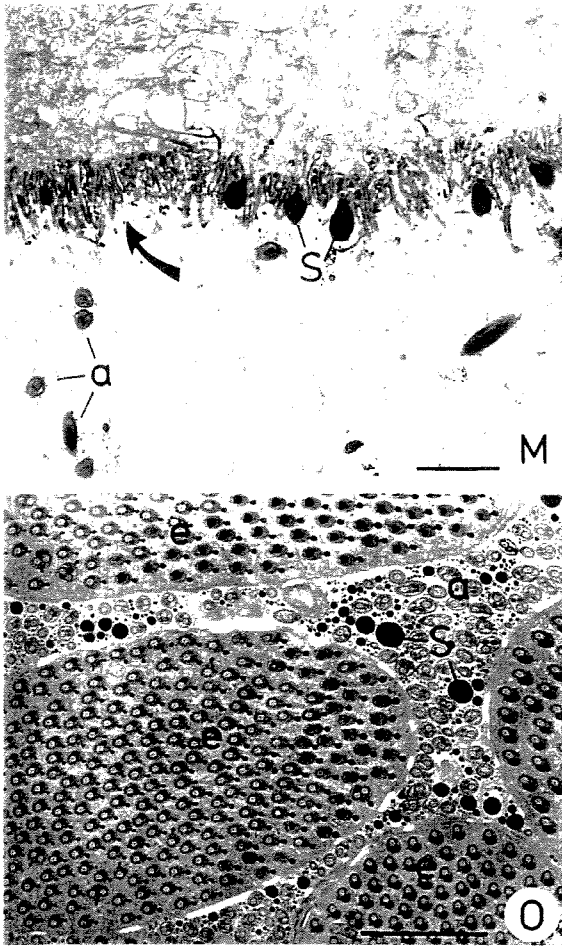
Figures 2M-P: Apyrene and Eupyrene sperm arrangement

(M) Distal deferent duct region. Secretion granules (S) secreted by the epithelium. Notice the abundant microvilli (arrow) and apyrene sperm (a).

(N) Distal deferent duct region. Aggregated eupyrene (e) sperm with abundant and uniform (arc) fibrous material (arrow). Dispersed apyrene (a) sperm in secretion (S).

(O) Seminal vesicle. Eupyrene bundles (e) and dispersed apyrene (a) sperm surrounded by secretion (S). **(P)** Ductus ejaculatorius. Eupyrene (e) and apyrene (a) sperm immersed in secretion (S).

Scale bars: (N)-(O): 5 μ m; (M): 2.5 μ m; (P): 1 μ m.



Figures 3A-H: Apyrene and Eupyrene sperm morphology

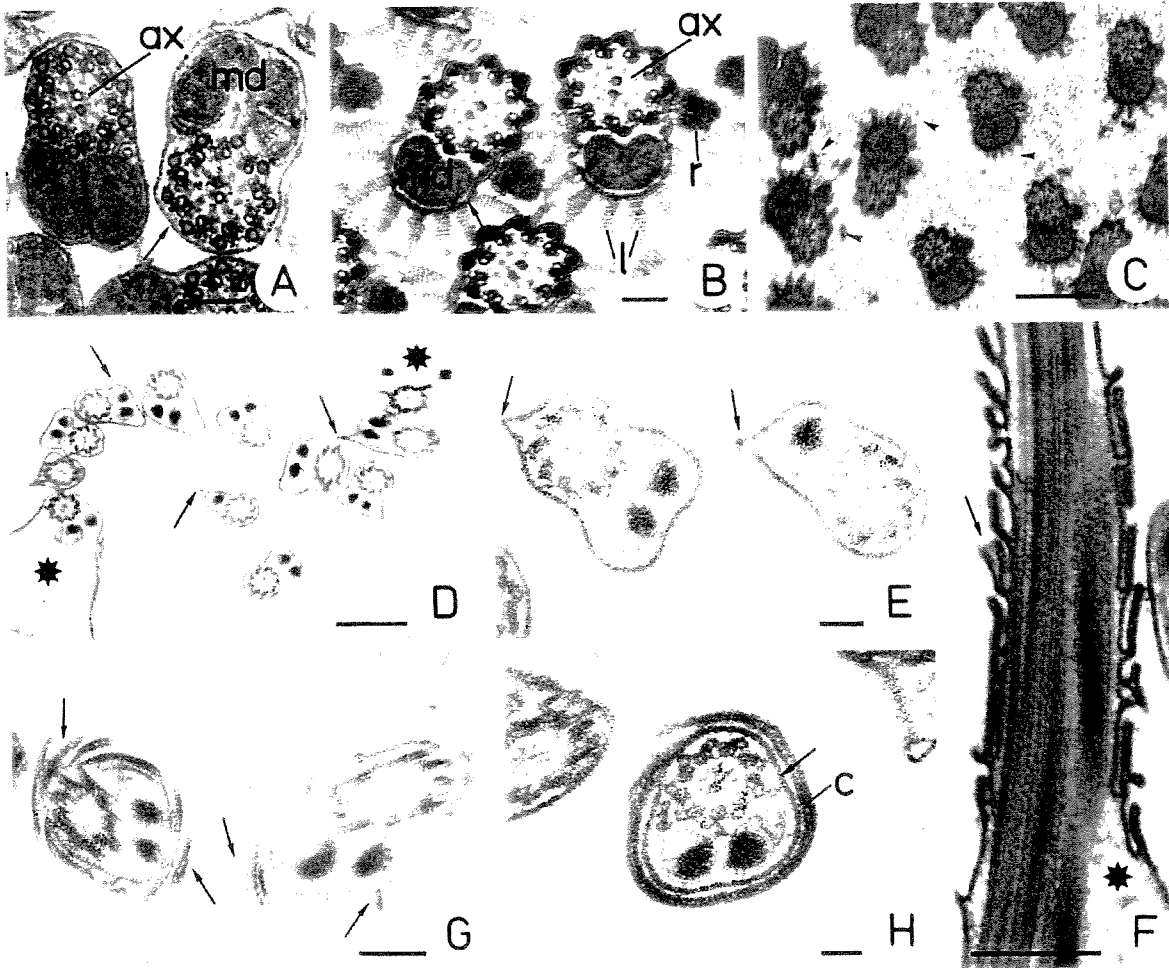
(A) Testicular apyrene spermatozoon. Axoneme (ax), mitochondrial derivatives (md) and plasma membrane (arrow).

(B) Testicular eupyrene spermatozoa. Axoneme (ax), mitochondrial derivatives (md), laciniate (l) and reticular (r) appendages and plasma membrane (arrow).

(C) Eupyrene sperm from basal testis region. Note the disintegration of the laciniate appendages (arrowheads).

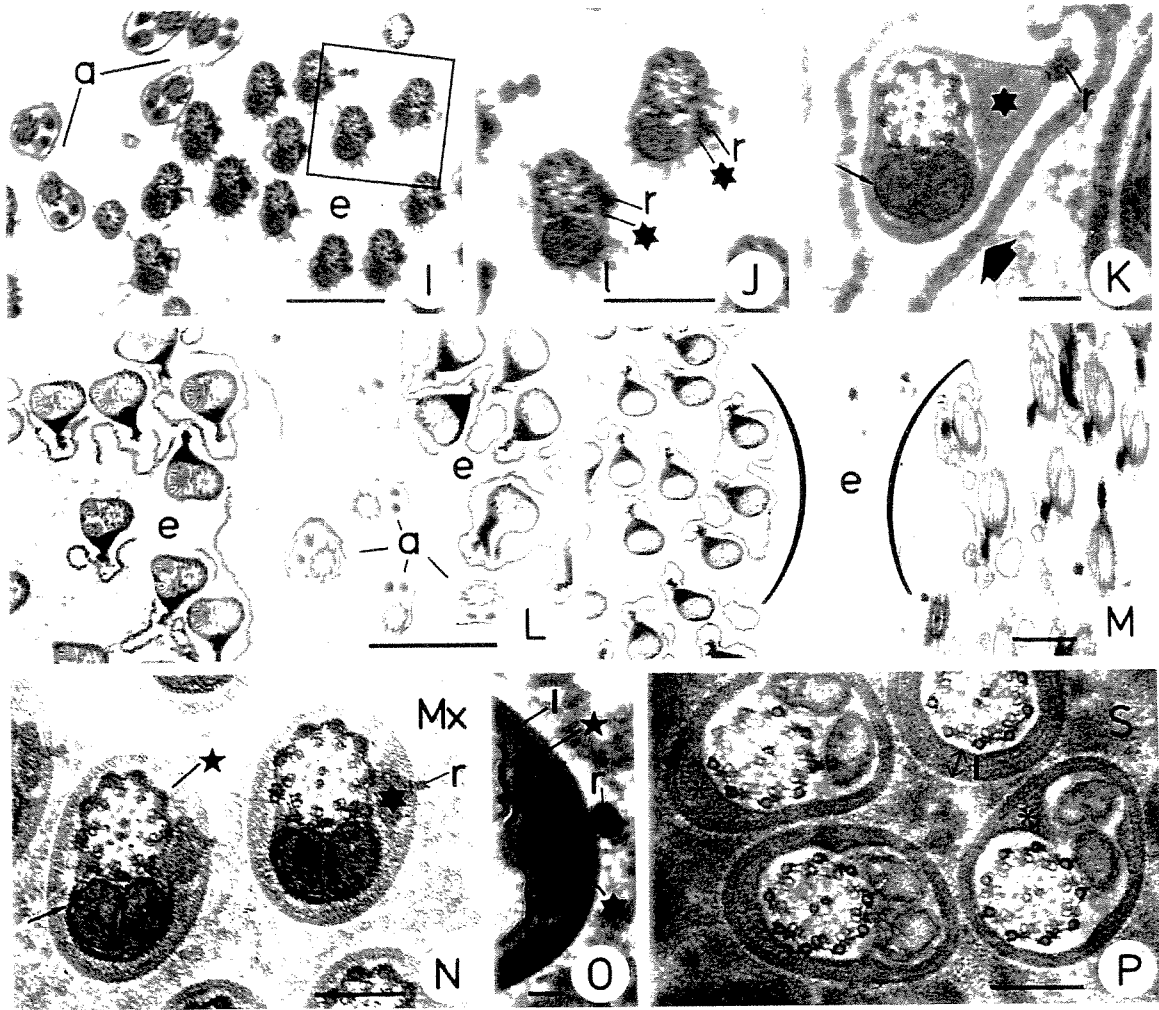
(D) to (H) Apyrene sperm from proximal deferent duct region. Development of concentric layers (arrow). (D) and (E) show initial pinching of superfluous membrane. (F) to (H) more abundant membrane folds into various layers and abundant intracellular material (eight pointed star).

Scale bars: (A), (B), (E), (H): 0.1 μm ; (G): 0.2 μm ; (C), (D), (F): 0.5 μm .



Figures 3I-P: Apyrene and Eupyrene sperm morphology

- (I) Eupyrene (e) and apyrene (a) spermatozoa from the proximal deferent duct. Apyrene sperm with completed concentric layers.
- (J) Higher magnification of fig. 2I (square) showing dense, amorphous material (six pointed star) next to the reticular appendage (r). Remains of laciniate appendages (l).
- (K) Eupyrene sperm from medial deferent duct. The coat presents an abundant amorphous material (six pointed star). External reticular appendage (r), plasma membrane (small arrow) and fibrous matrix material (large arrow).
- (L) Eupyrene (e) and apyrene (a) spermatozoa from medial deferent duct region. Eupyrene aggregations surrounded by fibrous matrix material twisting around coated sperm. Apyrene sperm with layers in formation.
- (M) Different developmental stages of eupyrene aggregation (e) from the medial deferent duct region: eupyrene sperm without a coat (right parenthesis) or with a coat (left parenthesis).
- (N) Eupyrene sperm from the seminal vesicle. A well-defined coat with amorphous material (five pointed star) covers the sperm and also contains a dense material (six pointed star) next to the reticular appendage (r). Cell membrane (arrow) and matrix (Mx).
- (O) Higher magnification of the eupyrene coat treated with tannic acid. The coat presents an external layer (l), an amorphous material (five pointed star) below the external layer and a dense material (six pointed star) located next to the reticular appendage (r).
- (P) Apyrene sperm from the seminal vesicle. Well-defined concentric layers (l) and an irregular amorphous material (asterisk) inside the layers. Secretion (S).
- Scale bars: (K), (P): 0.1 μm ; (N), (O): 0.2 μm ; (J): 0.5 μm ; (I), (L), (M): 1 μm .



CAPÍTULO 2

Citoquímica Ultra-estrutural dos Espermatozóides Apirenes e Eupirene ao Longo do Trato Reprodutor Masculino

2.1

Protein detection in spermatids and spermatozoa of the butterfly Euptoieta hegesia
(Lepidoptera: Nymphalidae)
(pp.83-107)

2.2

Carbohydrate localization in apyrene and eupyrene spermatozoa of the butterfly Euptoieta hegesia (Lepidoptera: Nymphalidae)
(pp. 108-127)

2.3

Lectin binding sites on the spermatids and spermatozoa of Euptoieta hegesia
(Lepidoptera: Nymphalidae)
(pp. 128-145)

2.4

Immunocytochemical evidence of tubulin isoforms in spermatids and spermatozoa of Euptoieta hegesia (Lepidoptera: Nymphalidae)
(pp. 146-167)

2.1

**Protein detection in spermatids and spermatozoa of the butterfly
Euptoieta hegesia (Lepidoptera: Nymphalidae)**

Mancini, K. and Dolder, H.

Running title: Proteins in spermatids and spermatozoa of Lepidoptera

Abstract

Due to the cytochemical reports on Lepidopteran sperm and their extracellular structures, this study was undertaken to detect protein components in both sperm types in *Euptoieta hegesia*. In apyrene spermatozoa head, the proteic cap presented an external ring and an internal dense content, evidenced by tannic acid; basic proteins were detected only in external portions. In the tail, the paracrystalline core of mitochondrial derivatives and the axoneme are rich in proteins. The extratesticular spermatozoa are covered by a proteic coat, which presented two distinct layers, detailed by tannic acid. In eupyrene spermatozoa, acrosome and nucleus were negative stained, probably because of their high compaction. In the tail, there is no paracrystalline core and the axoneme presented a very specific reaction for basic proteins. The laciniate and reticular appendages are composed of cylinder subunits and presented a light reaction to E-PTA and a strong reaction to tannic acid. A complex proteic coat also covers the extratesticular spermatozoa. We found similarities between both extratesticular coats, indicating a possible common origin. These results showed that both spermatozoa types are rich in proteins, especially the eupyrene appendages and the extratesticular coats. We believe that both coats are related to the maturation and capacitation sperm processes.

Keywords: ultrastructure – cytochemistry – apyrene – eupyrene.

Introduction

Butterflies and moths produce two sperm types, the eupyrene and apyrene ones, which are formed in different stages of testicular development. However, they can be found simultaneously in the imago (Leviatan and Friedländer, 1979; Friedländer and Benz, 1981; Katsuno, 1989).

The apyrene spermatozoa are devoid of a nucleus and the anterior end is composed only of a dense cap (Phillips, 1971; Friedländer and Gitay, 1972; Medeiros and Silveira, 1996; Mancini and Dolder, 2001a). Eupyrene spermatozoa, however, present a typical head, composed of a tubular acrosome and nucleus (Lai-Fook, 1982; Kubo-Irie *et al.*, 1998). Two mitochondrial derivatives and a 9+9+2 axoneme constitute the flagella of both sperm types.

In eupyrene spermatozoa, there are two types of extracellular appendages attached to the membrane, called laciniate and reticular, which extend along the entire sperm length (Phillips, 1970; Leviatan and Friedländer, 1979; Mancini and Dolder, 2001b). Both sperm types undergo several morphological changes after they leave the testis. The apyrene spermatozoa acquire several concentric layers while eupyrene ones acquire a complex coat and lose their laciniate appendages (Phillips, 1971; Riemann and Thorson, 1971; Lai-Fook *et al.*, 1982; Kubo-Irie *et al.*, 1998).

Despite the abundant morphological studies of Lepidoptera sperm, there are few analyses concerning their cytochemistry. Wolf and collaborators represent a very expressive contribution in immunolocalization in light microscopy of microtubules in spermatocytes of Lepidoptera (Wolf, 1992, 1996a, 1996b, 1997; Wolf and Bastmeyer, 1991a, 1991b; Wolf and Joshi, 1996). However, cytochemical studies involving apyrene and eupyrene spermatozoa, with their elaborate extracellular structures, are rare (Friedländer and Gershon, 1978; França and Báó, 2000).

The composition and functional significance of the eupyrene appendages and the extracellular coat of both sperm types are still unclear. Here we detected proteins (general and basic) through cytochemical methods in *Euptoieta hegesia* sperm, in an effort to

collaborate toward understanding the chemical composition and the ultrastructural transformations of these spermatozoa as they move along the male tract.

Materials and methods

Testis, deferent duct and seminal vesicle of adult *Euptoieta hegesia* butterflies were processed according to cytochemical methods for protein detection in Transmission Electron Microscopy:

Tannic acid for General Proteins (Dallai and Afzelius, 1990):

Specimens were fixed in 2,5% glutaraldehyde, 1 % tannic acid, 1,5% sucrose and 5 mM calcium chloride in 0.1 M sodium phosphate buffer for three days at 4°C. The materials were rinsed in buffer and contrasted in an aqueous solution of 1% uranyl acetate for 2 hours at room temperature. Finally, they were dehydrated and embedded in Epoxy Resin. The ultra thin sections were contrasted with solutions of uranyl acetate and lead citrate.

Ethanol-Phosphotungstic acid (E-PTA) for Basic Proteins (Modified of Bloom and Aghajanian, 1968):

Specimens were fixed in 2,5% glutaraldehyde, 1,5% sucrose and 5 mM calcium chloride in 0.1 M sodium phosphate buffer for 4 hours at 4°C. They were then rinsed in buffer, dehydrated in ethanol at 4°C and finally contrasted in 2% PTA (phosphotungstic acid) in absolute ethanol for 2 hours at room temperature or up to 24 hours at 4°C. The specimens were embedded in Epoxy Resin. The ultra thin sections were observed without further contrasting.

Results

Apyrene Spermatozoa

In apyrene spermiogenesis, early spermatids contain several micronuclei scattered in the cytoplasm as a result of an atypical meiotic division. These micronuclei contain amorphous chromatin, which presented an electron-dense reaction to E-PTA (Fig. 2A). In late spermatids, such micronuclei are degenerated and eliminated from the posterior tip.

The anterior end of apyrene cells, devoid of a nucleus, is composed of a long cap, which consists of an external ring and an internal dense material, strongly stained by tannic acid (Figs. 1A and B), when compared with conventional fixation methods (not shown). The presence of basic proteins was only detected in the external portions (Fig. 2B).

In the spermatid flagella, a positive reaction due to general and basic proteins was observed in the paracrystalline core of mitochondrial derivatives (Figs. 1C and 2C). However, it is not possible to clearly distinguish the paracrystalline arrangement of this structure. On the other hand, in spermatozoa, despite the positive reaction of the paracrystalline core using both techniques (Figs. 1E-G and 2D-F), it is only possible to clearly identify the paracrystalline substructure with tannic acid (Figs. 1E-G).

In the axoneme, the walls of the peripheral and accessory microtubules are very evident using E-PTA (Figs. 2C-F), if compared with the central ones. The lumen of one of the peripheral microtubules and, generally, one of the central pair, presented basic proteins (Figs. 2C and E). The proteins that link the axoneme elements do not have a positive reaction with this technique.

However, tannic acid reveals rich details of the axoneme proteins (Figs. 1C-G). The dynein arms and the radial spokes presented an electron-dense reaction and the microtubule walls can be easily identified as being composed of protofilaments. The accessory microtubules present 16 protofilaments and the central ones, 14 (Fig. 1D). The interior of the A microtubules of the peripheral pairs and, generally, one of the central microtubules stand out with an electron-dense reaction. Although the lumen of the accessory microtubules was not electron-dense, it was possible to identify, in cross section, 7-9

circular electron lucid sub-units (Fig. 1D). These sub-units are organized as a circle of micro cylinders surrounding a central micro cylinder.

The plasma membrane of apyrene spermatids and spermatozoa showed an electron-dense reaction with E-PTA (Figs. 2C-F). The reaction becomes more intense in the extra testicular spermatozoa, where a thick coat, composed of several concentric layers, is acquired (Fig. 2E).

Using tannic acid, this coat found on apyrene spermatozoa from the deferent duct and seminal vesicle, also presented a positive reaction for proteins (Figs. 1F and G). Especially in the deferent duct, the tannic acid technique indicated two regions in the coat: an external amorphous layer and an internal one, next to the cell membrane, that is divided into small dense, aligned cylinder sub-units (Fig. 1F)

Eupyrene Spermatozoa

The anterior region of eupyrene spermatozoa is made up of an acrosome and a nucleus. The acrosome is formed initially by a spherical vesicle that elongates and becomes a tubular structure in the spermatozoon. In early spermatids, the spherical acrosomal vesicle (Fig. 4A), as well as the following elongating phases (Figs. 4B and C) are E-PTA positive. However, in late spermatids and spermatozoa, where this structure has acquired its definitive tubular form, no positive reaction for E-PTA was observed (Figs. 4E and F). For general proteins in spermatids and spermatozoa, there was no reaction and the acrosome appears electron lucid (Figs. 3A, B and H).

Simultaneously to the acrosomal changes there are nuclear modifications. The spermatid nucleus, in different chromatin condensation phases presented a positive reaction to E-PTA (Figs. 4A-C and E). In spermatozoa, however, the compact nucleus is E-PTA negative (Figs. 4F and J). With tannic acid there was no evident reaction in spermatid and spermatozoon nuclei (Figs. 3A, C and H) that differ from those observed with conventional methods (not shown).

In the anterior region, besides the nucleus and acrosome, eupyrene cells present two types of extracellular appendages termed laciniate and reticular, which will later be discussed as to their cytochemical reactions.

The eupyrene flagella are composed of an axoneme and two mitochondrial derivatives. In contrast to apyrene flagella, the eupyrene mitochondrial derivatives do not present paracrystalline cores and no reaction was observed in this region, using both techniques.

The centriolar region, in the anterior flagellar extremity, presented a strongly electron-dense reaction to E-PTA (Fig. 4D). The proteins that link the axoneme elements were strongly marked with both techniques (Figs. 3D-F, I and 4G, H, K). The central microtubule wall is E-PTA negative, and the lumen of the A microtubules of the peripheral pairs and the central ones are E-PTA positive (Figs. 4G, H and K).

With the tannic acid method, the walls were expressively well evidenced, with 16 protofilaments in the accessory microtubules and 14 in the central ones (Fig. 3F). The lumen of the A microtubules of the peripheral pairs and the central ones were electron dense (Figs. 3D-F and I). No micro cylinder sub-units were observed in their lumen.

Exclusively external to the plasma membrane, the eupyrene sperm present appendages, called laciniate and reticular. The laciniate ones presented a positive reaction to E-PTA in the anterior regions, where they are well developed (Fig. 4F). However in the flagellar regions they presented a very light reaction (Fig. 4H). With tannic acid, these structures clearly showed a regular structure (Figs. 3C, E and F), which is much more defined than when observed using conventional fixation methods (not shown). In the square of the figure 3F is possible to note that this regular structure consists of aligned tubular sub-units.

The reticular appendage is present since early spermatid formation and presented a positive reaction to E-PTA only in the external portions (Figs. 4E-H). With tannic acid, this appendage was highly contrasted in the anterior region (Figs. 3A-C) and presented a paracrystalline organization only in the flagellar portion (Figs. 3D and E).

Eupyrene spermatozoa from the proximal deferent duct region start to acquire a coat, strongly contrasted by tannic acid. It is possible to distinguish two regions: an amorphous external layer and an internal one, next to the cell membrane, that also presents small cylinder sub-units, as seen for apyrene spermatozoa. Beyond this first coat, there is an

accumulation of dense material between the cell membrane and the reticular appendage. The laciniate appendages, still with a regular organization, start to disaggregate (Fig. 3G).

In the seminal vesicle, these spermatozoa are totally encapsulated by the coat, which presents an electron-dense reaction with both techniques (Figs. 3H-I and 4J-K). The laciniate appendages are absent.

Here, the anterior extremity does not have a coat, but is composed of a large globular structure, which is externally E-PTA positive (Fig. 4I). The anterior region, at the level of the nucleus and acrosome, and the flagellar region present a coat.

The internal layer next to the cell membrane, described in the deferent duct spermatozoa, is maintained in the seminal vesicle (white arrows in Figs. 3H and I) and the external one develops into a thick amorphous layer (large arrow in Fig. 3I). The dense material, next to the reticular appendage is well developed (white asterisk in Fig. 3I). Covering all the structures described above, except the reticular appendage, is an external layer of the coat (opened arrow, Figs. 3H and I) that shows a break (white arrowheads, Fig. 3I) where it contacts the reticular appendage. In the nuclear region, the amorphous material does not exist and the eupyrene coat is uniformly filled with dense material (Figs. 3H and 4J). It is interesting to notice the basic protein presence in the cytoplasmic material of these spermatozoa (star, Fig. 4K) and the absence of reaction of this material to tannic acid (star, Fig. 3I).

Discussion

There are several cytochemical studies involving spermiogenesis and/or spermatozoa of different insect orders: Coleoptera (Báo, 1991, 1996, 1998; Báo and Hamú, 1993; Craveiro and Báo, 1995; Fernandes and Báo, 1996), Diptera (Perotti, 1971, 1986; Perotti and Riva, 1988; Quagio-Grassiotto and Dolder, 1988; Báo and Dolder, 1990; Báo *et al.*, 1992; Báo and Souza, 1992, 1993, 1994; Cattaneo *et al.*, 1997; Perotti and Pasini, 1995; Pasini *et al.*, 1996, 1999;), Hemiptera (Báo, 1997; Fernandes *et al.*, 1998; Fernandes and

Báo, 1999, 2000), Orthoptera (Kierszenbaum and Tres, 1978) and Hymenoptera (Lino-Neto *et al.*, 1999, 2000).

In the Lepidoptera order, however, these cytochemical analyses are very rare (França and Báo, 2000; Friedländer and Gershon, 1978) and most of them are related to very immature cells (Wolf, 1992, 1996a, 1996b, 1997; Wolf and Bastmeyer, 1991a, 1991b; Wolf and Joshi, 1996). So, the discussion is mostly based on comparisons with other insect orders.

Because of the structural complexity of extracellular structures of apyrene and eupyrene spermatozoa and their various morphologic alterations along the male and female tracts, a cytochemical study contributes expressively toward the understanding of this elaborate sperm dimorphism.

Due to the excellent preservation of the tissue with the tannic acid method, images of conventionally fixed specimens were not included in the present work (see Mancini & Dolder, 2001a). The tannic acid method developed by Dallai and Afzelius (1990), specific for proteins, was revealed to be extremely interesting for the morphologic description, mainly in detailing elements of axoneme and the extracellular coat.

The anterior cap of apyrene spermatozoa of *Euptoieta hegesia* presented basic proteins in the most external region, in contrast with the observation of França and Báo (2000) and Medeiros (1997), which detected a homogeneous basic proteins reaction. The present research used different incubation times for E-PTA (2 to 24 hours), however, in none of them was the reaction homogeneous, as observed by the above authors. We believe this could reflect a difference in the compaction or the composition of this structure in different species. It is known that, in the testis, apyrene anterior regions are embedded in the cytoplasm of cystic cells. That could make E-PTA penetration difficult. In *E. hegesia* we observed a large quantity of rough endoplasmic reticulum in the cytoplasm of cystic cells and we believe that the cap could be a product of these sites of protein production.

The protein detection of the paracrystalline core of mitochondrial derivatives in apyrene flagella is similar to the observations of França and Báo (2000), Medeiros (1997) and Mancini and Dolder (2001a). The presence of a paracrystalline core in mitochondrial

derivatives is common to many orders of insects (Jamieson *et al.*, 1999) and its function is unclear.

In the eupyrene spermatozoa, the proteins that connect the axonemal elements were more strongly stained than in the apyrene ones. Because of the clear details of the axoneme seen with the tannic acid method, it was possible to count the protofilaments, as also observed by Medeiros (1997) in apyrene spermatozoa, and by Dallai and Afzelius (1990, 1995) and Jamieson *et al.* (1999) in eupyrene spermatozoa.

Observations of sub-units in the lumen of accessory microtubules in apyrene spermatozoa were made only by Medeiros (1997). Dallai and Afzelius (1990, 1995) also detected micro cylinder sub-units in many insect orders.

Studies of other insect groups also detected different reactions for the axoneme microtubules (Báo, 1991, 1996; Craveiro and Báo, 1995). Besides the possible presence of different types of tubulin in the axoneme (alfa, beta, gama, acetilated, tyrosinated), there are different proteins that link the axoneme elements and occur in the microtubule lumen. These differences may explain the distinct staining patterns.

The plasma membrane of intratesticular apyrene spermatozoa is revealed by both techniques. The cytochemical methods permit the conclusion that cell membranes of apyrene and eupyrene spermatozoa are rich in proteins and glycoproteins. Glycoproteins are molecules important in cellular recognition and specificity, two essential characteristics of germ cells.

Concentric layers, not always clearly distinguishable, cover the extratesticular apyrene spermatozoa. These layers, in deferent duct and seminal vesicle, presented a positive reaction to the techniques employed. In the present work, through the tannic acid technique, we found similarity between the extracellular coat of the apyrene and eupyrene spermatozoa in the deferent duct. Other authors (Phillips, 1971; Friedländer and Gitay, 1972; Riemann and Gassner, 1973; Riemann and Giebultowicz, 1992) had already found some similarity between the coat of apyrene and eupyrene extra testicular sperm. The formation of apyrene and eupyrene coats occurs simultaneously in the deferent duct, which could also indicate a common origin.

The laciniate and reticular appendages, exclusive of the eupyrene spermatozoa, contain protein. The reticular appendage presented a reaction for basic proteins only in the external regions, possibly due to the difficulty of penetration in this highly compact structure. Using the tannic acid technique, it was possible to notice a compact paracrystalline formation in these appendages, as observed by Dallai and Afzelius (1990) and Jamieson *et al.* (1999).

The laciniate appendages reacted positively to E-PTA, mainly in the anterior regions. França and Bão (2000) detected intense and homogeneous basic protein in both appendages of *Anticarsia gemmatilis*. Medeiros (1997), however, only found evident reticular appendages, also intense and homogeneous.

The globular structure at the anterior end of eupyrene spermatozoa in seminal vesicle was previously observed by Mancini and Dolder (2001a) and has a positive reaction to E-PTA only on its surface and on the surrounding layer.

The tubular acrosome did not react to either technique. França and Bão (2000), however, had detected a light positive reaction in *A. gemmatilis*. This tubular structure seems to be very compact, which makes penetration difficult for large molecules.

The nucleus did not have a positive reaction to the E-PTA in mature cells. However, in late spermatids, some areas were marked because of different degrees of chromatin condensation, which expose different sites for linking to basic nuclear proteins. Differences in nuclear reactions for basic proteins between spermatozoa and spermatids have been observed in Lepidoptera (França and Bão, 2000), Coleoptera (Bão and Hamú, 1993; Bão, 1996 and 1998), Orthoptera (Kierszenbaum and Tres, 1978) and Diptera (Quagio-Grassiotto and Dolder, 1988). The nucleus of *E. hegesia* spermatozoa is homogeneous and does not present compartments. Zama *et al.* (in preparation), studying *Meliponini* spermatozoa (Hymenoptera), detected a dense positive reaction to E-PTA in a specific crescent moon nuclear region.

When leaving the testis, in the proximal deferent duct, the eupyrene spermatozoa begin to lose their laciniate appendages (Riemann, 1970; Phillips, 1971; Lai-Fook, 1982; Riemann and Giebultowicz, 1992; Kubo-Irie *et al.*, 1998; Mancini and Dolder, 1999). Concomitantly, these spermatozoa acquire a surrounding layer with the reticular appendage

remaining external; both structures are strongly marked by tannic acid. Many authors suggest that the external layer could be the result of rearrangement of the laciniate appendages (Phillips, 1971; Friedländer and Gitay, 1972; Lai-Fook, 1982; Kubo-Irie *et al.*, 1998). We believe, that the laciniate appendages may contribute partially to coat formation, but mainly to the matrix formation, which surrounds the spermatozoa organized in bundles in the seminal vesicle.

In the seminal vesicle, the coat, with its three regions, is well developed and involves totally and homogenously the eupyrene spermatozoa. The break, detected in the external layer of the eupyrene coat, which permits extrusion of the reticular appendage, was identified in the seminal vesicle. This structure will later be occupied by the dense plate, which was observed in the spermathecae (Friedländer and Gitay, 1972; Riemann and Gassner, 1973).

The coat is rich in proteic components, mainly basic protein, as is the cytoplasmic material next to the mitochondrial derivatives. The matrix is also partially composed of protein, but the presence of basic protein is slight.

These results indicate that the extracellular structures of apyrene and eupyrene sperm are rich in proteins. Researches on *E. hegesia* sperm indicated presence of carbohydrate in these structures (Mancini and Dolder, in preparation). Laciniate appendages of eupyrene sperm and the coats of both sperm types presented positive reactions for the protein detection techniques applied. This could be an indication of laciniate rearrangement to contribute to the coats in the deferent duct. Besides their proteic composition, the similarity of apyrene and eupyrene extra testicular coats indicates that they could have a common origin.

The present study is part of our investigation to understand the various modifications in apyrene and eupyrene sperm types along the male and female tract of *Euptoieta hegesia*, which involves other cytochemical techniques (for carbohydrate detection), lectins method and immunocytochemistry (Mancini and Dolder, in preparation).

References

- Báo, S. N. 1991. Morphogenesis of the flagellum in the spermatids of *Coelomera lanio* (Coleoptera, Chrysomelidae): ultrastructural and cytochemical studies. **Cytobios** 66: 157-167.
- Báo, S. N. 1996. **Spermiogenesis in *Coelomera lanio* (Chrysomelidae: galerucinae): ultrastructural and cytochemical studies.** In: Jolivet PHA, Cox ML (eds) Chrysomelidae Biology: General Studies. Academic Publishers, Netherlands, pp. 119-132.
- Báo, S. N. 1997. Cytochemical localization of carbohydrate in the spermatid of *Rhodnius prolixus* (Hemiptera: Reduviidae). **Acta Microsc.** 6: 14-20.
- Báo, S. N. 1998. Ultrastructural and cytochemical studies on spermiogenesis of the beetle *Cerotoma arcuata* (Coleoptera, Chrysomelidae). **Biocell** 22: 35-44.
- Báo, S. N. and de Souza, W. 1992. Lectin binding sites on head structures of the spermatid and spermatozoon of the mosquito *Culex quinquefasciatus* (Diptera: Culicidae). **Histochem.** 98: 365-371.
- Báo, S. N. and de Souza, W. 1993. Ultrastructural and cytochemical studies of the spermatid and spermatozoon of *Culex quinquefasciatus* (Culicidae). **J. Submicrosc. Cytol. Pathol.** 25: 213-222.
- Báo, S. N. and de Souza, W. 1994. Cytochemical localization of enzymes in the spermatid and the spermatozoon of *Culex quinquefasciatus* say (Diptera: culicidae). **Int. J. Insect Morphol. Embryol.** 23: 57-67.
- Báo, S. N. and Dolder, H. 1990. Ultrastructural localization of acid phosphatase in spermatid cells of *Ceratitis capitata* (Diptera). **Histochem.** 93: 439-442.
- Báo, S. N. and Hamú, C. 1993. Nuclear changes during spermiogenesis in two chrysomelid beetles. **Tissue and Cell** 25: 439-445.
- Báo, S. N., Lins, U., Farina, M. and de Souza, W. 1992. Mitochondrial derivatives of *Culex quinquefasciatus* (Culicidae) spermatozoon: some new aspects evidenced by cytochemistry and image processing. **J. Struct. Biol.** 109: 46-51.

- Bloom, F. E. and Aghajanian, G. K. 1968. Fine structural and cytochemical analysis of the staining of synaptic junctions with phosphotungstic acid. **J. Ultrastruct. Res.** **22**: 361-375.
- Cattaneo, F., Pasini, M. E. and Perotti, M. E. 1997. Glycosidases are present on the surface of *Drosophila melanogaster* spermatozoa. **Mol. Reprod. Develop.** **48**: 276-281.
- Craveiro, D. and Báo, S. N. 1995. Localization of carbohydrates in spermatids of three chrysomelid beetles (Coleoptera, Chrysomelidae). **Biocell** **19**: 195-202.
- Dallai, R. and Afzelius, B. A. 1990. Microtubular diversity in insect spermatozoa: results obtained with a new fixative. **J. Struct. Biol.** **103**: 164-179.
- Dallai, R. and Afzelius, B. A. 1995. Phylogenetic significance of axonemal ultrastructure: examples from Diptera and Trichoptera. In: Jamieson BGM *et al.* (eds). Advances in spermatozoal phylogeny and taxonomy. **Mem. Mus. Natn. Hist. Nat.** **166**: 301-310.
- Fernandes, A. P. and Báo, S. N. 1996. Ultrastructural study of the spermiogenesis and localization of tubulin in spermatid and spermatozoon of *Diabrotica speciosa* (Coleoptera: Chrysomelidae). **Cytobios** **86**: 231-241.
- Fernandes, A. P. and Báo, S. N. 1999. Ultrastructural localization of enzymatic activity during spermiogenesis in two phytophagous bugs (Hemiptera: Pentatomidae). **Tissue and Cell** **31**: 349-356.
- Fernandes, A. P. and Báo, S. N. 2000. Ultrastructural and cytochemical studies of the spermatozoa of *Acrosternum aseadum* (Hemiptera: Pentatomidae). **J. Submicrosc. Cythol. Pathol.** **32**: 547-553.
- Fernandes, A. P., Curi, G. and Báo, S. N. 1998. Contribution of the Golgi complex – endoplasmic reticulum system during spermiogenesis in three species of phytophagous bugs (Hemiptera: Pentatomidae). **Int. J. Insect Morphol. Embryol.** **27**: 235-240.
- França, F. G. .R. and Báo, S. N. 2000. Dimorphism in spermatozoa of *Anticarsia gemmatilis* Hübner, 1918 (Insecta, Lepidoptera, Noctuidae). **Braz. J. Morphol. Sci.** **17**: 5-10.
- Friedländer, M. and Benz, G. 1981. The apyrene-eupyrene dichotomous spermatogenesis of Lepidoptera. Organ culture study on the timing of apyrene commitment in the codling moth. **Int. J. Invert. Reprod.** **3**: 113-120.

- Friedländer, M. and Gershon, J. 1978. Reaction of surface lamella of moth spermatozoa to vinblastine. **J. Cell Sci.** **30**: 353-361.
- Friedländer, M. and Gitay, H. 1972. The fate of the normal anucleated spermatozoa in inseminated female of the silkworm *Bombyx mori*. **J. Morphol.** **138**: 121-129.
- Jamieson, B. G. M., Dallai, R. and Afzelius, B. A. 1999. **Insects: their spermatozoa and phylogeny**. Enfield, New Hampshire (USA) Science Publishers, Inc.
- Katsuno, S. 1989. Spermatogenesis and the abnormal germ cells in Bombycidae and Saturniidae. **J. Fac. Agric. Hokkaido Univ.** **64**: 21-34.
- Kierszenbaum, A. L. and Tres, L. L. 1978. The packaging unit: a basic structural feature for the condensation of late cricket spermatid nuclei. **J. Cell Sci.** **33**: 265-383.
- Kubo-Irie, M., Irie, M., Nakazawa, T. and Mohri, H. 1998. Morphological changes in eupyrene and apyrene spermatozoa in the reproductive tract of the male butterfly *Atrophaneura alcinous* Klug. **Invert. Reprod. Develop.** **34**: 259-268.
- Lai-Fook, J. 1982. Structural comparison between eupyrene and apyrene spermiogenesis in *Calpododes ethlius* (Hesperiidae: Lepidoptera). **Can. J. Zool.** **60**: 1216-1230.
- Leviatan, R. and Friedländer, M. 1979. The eupyrene-apyrene dichotomous spermatogenesis of Lepidoptera. I. The relationship with postembryonic development and the role of the decline in juvenile hormone titer toward pupation. **Develop. Biol.** **68**: 515-524.
- Lino-Neto, J., Báo, S. N. and Dolder, H. 1999. Structure and ultrastructure of the spermatozoa of *Bephratelloides pomorum* (Fabricius) (Hymenoptera: Eurytomidae). **Int. J. Insect Morphol. Embryol.** **28**: 253-259.
- Lino-Neto, J., Báo, S. N. and Dolder, H. 2000. Structure and ultrastructure of the spermatozoa of *Trichogramma pretiosum* Riley and *Trichogramma atopovirilia* Oatman and Platner (Hymenoptera: Trichogrammatidae). **Acta Zool. (Stockholm)** **81**: 205-211.
- Mancini, K. and Dolder, H. 1999. Ultrastructural modifications in apyrene and eupyrene spermatozoa of *Euptoieta hegesia* (Lepidoptera: Nymphalidae) along the male reproductive tract. **Acta Microsc.**, p 567-568.

- Mancini, K. and Dolder, H. 2001a. Ultrastructure of a pyrene and eupyrene spermatozoa from the seminal vesicle of *Euptoieta hegesia* (Lepidoptera: Nymphalidae). **Tissue and Cell** 33: 301-308.
- Mancini, K. and Dolder, H. 2001b. Extracellular appendages of lepidopteran spermatozoa. **Acta Microsc.**, p 301-302.
- Medeiros, M. 1997. **Estudo ultra-estrutural da espermiogênese dicotômica de *Alabama argillacea* Hübner, 1818** (Doctor Thesis). Instituto de Biociências, Universidade Estadual de São Paulo.
- Medeiros, M. and Silveira, M. 1996. Ultrastructural study of a pyrene spermatozoa of *Alabama argillacea* (Insecta, Lepidoptera, Noctuidae) with tannic acid containing fixative. **J. Submicrosc. Cytol. Pathol.** 28: 133-140.
- Pasini, M. E., Redi, C. A., Caviglia, O. and Perotti, M. E. 1996. Ultrastructural and cytochemical analysis of sperm dimorphism in *Drosophila subobscura*. **Tissue and Cell** 28: 165-175.
- Pasini, M. E., Cattaneo, F., Pinto, M. R., Santis, R. and Perotti, M. E. 1999. Plasma membrane association and preliminary characterization of *Drosophila* sperm surface glycosidases. **Mol. Reprod.** 52: 166-173.
- Perotti, M. E. 1971. Microtubules as components of *Drosophila* male paragonia secretion. An electron microscopic study, with enzymatic tests. **J. Submicrosc. Cytol.** 3: 255-282.
- Perotti, M. E. 1986. Identification and localization of carbohydrates in the plasma membrane of *Drosophila* spermatozoon. **Develop Growth Differ** 28 (supplement): 55.
- Perotti, M. E. and Pasini, M. 1995. Glycoconjugates of the surface of the spermatozoa of *Drosophila melanogaster*: a qualitative and quantitative study. **J. Exp. Zool.** 271: 311-318.
- Perotti, M. E. and Riva, A. 1988. Concanavalin A binding sites on the surface of *Drosophila melanogaster* sperm: a fluorescence and ultrastructural study. **J. Ultrastruct. Mol. Struct. Res.** 100: 173-182.
- Phillips, D. M. 1970. Insect sperm: their structure and morphogenesis. **J. Cell Biol.** 44: 243-277.

- Phillips, D. M. 1971. Morphogenesis of the laciniate appendages of lepidopteran spermatozoa. **J. Ultrastruct. Res.** **34**: 567-585.
- Quagio-Grassiotto, I. and Dolder, H. 1988. The basic nucleoprotein E-PTA reaction during spermiogenesis of *Ceratitis capitata* (Diptera: Tephritidae). **Cytobios** **53**: 153-158.
- Riemann, J. G. 1970. **Metamorphosis of sperm of the cabbage looper *Trichoplusia ni* during passage from the testes to the female spermatheca.** In: Baccetti, B. Comparative Spermatology. Academic Press. New York. pp. 321-331.
- Riemann, J. G. and Gassner, G. 1973. Ultrastructure of Lepidopteran sperm within spermathecae. **Ann. Entomol. Soc. Am.** **66**: 154-159.
- Riemann, J. G. and Giebultowicz, J. M. 1992. Sperm maturation in the *vasa deferentia* of the gypsy moth, *Lymantria dispar* L. (Lepidoptera: Lymantriidae). **Int. J. Insect Morphol. Embryol.** **21**: 271-284.
- Riemann, J. G. and Thorson, B. J. 1971. Sperm maturation in the male and female genital tracts of *Anagasta kuhniella* (Lepidoptera: Pyralidae). **Int. J. Insect Morphol. Embryol.** **1**: 11-19.
- Wolf, K. W. 1992. Spindle membranes and microtubules are coordinately reduced in apyrene relative to eupyrene spermatocyte of *Inachis io* (Lepidoptera: Nymphalidae). **J. Submicrosc. Cytol. Pathol.** **24**: 381-394.
- Wolf, K. W. 1996a. Cytology of Lepidoptera VIII. Acetylation of alfa-tubulin in mitotic and meiotic spindles of two Lepidoptera species, *Ephestia kuehniella* (Pyralidae) and *Pieris brassicae* (Pieridae). **Protoplasma** **190**: 88-98.
- Wolf, K. W. 1996b. Immunocytochemical evidence of a tubulin reserve at the tip of growing flagella in spermatogenesis of the Mediterranean Mealmoth, *Ephestia kuehniella* Z. (Pyralidae, Lepidoptera, Insecta). **Acta Zool. (Stockholm)** **77**: 79-84.
- Wolf, K. W. 1997. Centrosome structure is very similar in eupyrene and apyrene spermatocyte of *Ephestia kuehniella* (Pyralidae: Lepidoptera: Insecta). **Invert. Reprod. Develop.** **31**: 39-46.
- Wolf, K. W. and Bastmeyer, M. 1991a. Cytology of Lepidoptera. V. The microtubule cytoskeleton in eupyrene spermatocyte of *Ephestia kuehniella* (Pyralidae), *Inachis io* (Nymphalidae) and *Orgyia antiqua* (Lymantriidae). **Eur. J. Cell Biol.** **55**: 225-237.

- Wolf, K. W. and Bastmeyer, M. 1991b. Cytology of Lepidoptera. VI. Immunolocalization of microtubules in detergent-extracted apyrene spermatocytes of *Ephesia kuehniella* Z. **Eur. J. Cell Biol.** **55**: 238-247.
- Wolf, K. W. and Joshi, H. C. 1996. Microtubule organization and distribution of gamma-tubulin in male meiosis of Lepidoptera. **Mol. Reprod. Develop.** **45**: 547-559.

Figure legends

(1) Apyrene spermatozoa with the tannic acid method

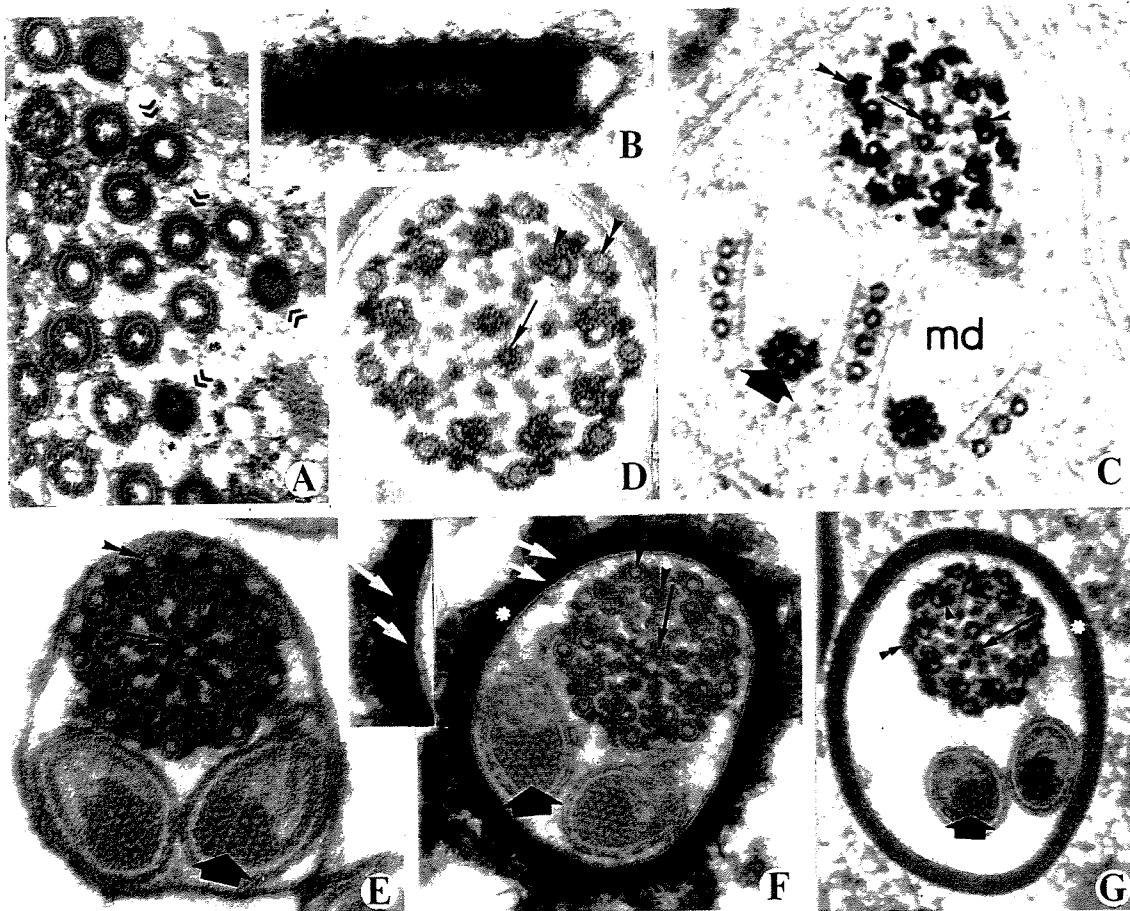
Figs. A and B: Cross and longitudinal sections, respectively, of the spermatid anterior cap (double arrowheads). 22000x; 62000x

Fig. C: Spermatid flagellum with positive reaction in the paracrystalline core (arrow) of the mitochondrial derivatives (md). On the axoneme, the electron density lumen of the accessory microtubules (double arrowhead) and one of the peripheral (arrowhead). Notice the electron dense reaction in one of the central pair microtubules (arrow). 85000x

Fig. D: Axoneme detail, showing the electron density of the central pair lumen (arrow), peripheral lumen (arrowhead). Notice the electron lucid circular sub units within the accessory microtubules (double arrowhead). 170000x

Fig. E: Spermatozoon from testis. On the axoneme: accessory microtubules with electron lucid cores (double arrowhead), peripheral (arrowhead) and one of central pair (arrow) with electron dense reaction. Notice the heavy staining of axoneme and membrane proteins. Paracrystalline core (large arrow). 130000x

Figs. F and G: Spermatozoa from deferent duct and seminal vesicle, respectively. Notice the thick external coat (white asterisk). In the deferent duct, this coat presents two regions: an external amorphous layer (longer arrow) and an internal one divided into small dense, aligned sub-units (small arrow). On the axoneme: accessory microtubules have electron lucid cores (double arrowhead); peripheral (arrowhead) and one of central pair (arrow) are electron dense. Paracrystalline core (large arrow). 119000x; 80000x



(2) Apyrene Spermatozoa with E-PTA method

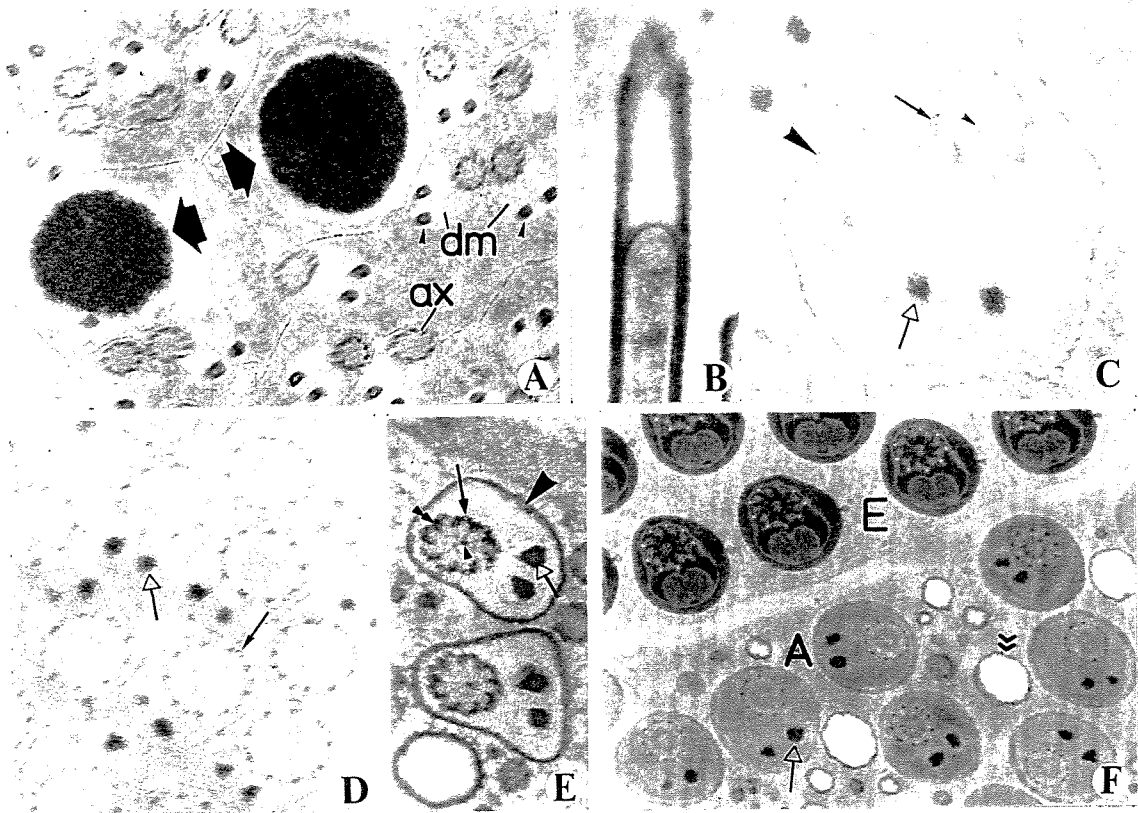
Fig. A: Spermatids with E-PTA positive micronuclei (arrows). Light staining occurs on axoneme (ax) and the paracrystalline core (arrowhead) of mitochondrial derivatives (dm). 20000x

Fig. B: Basic proteins on the surface of the anterior cap. 85000x

Fig. C: Spermatid flagellum with an E-PTA positive paracrystalline core (open arrow) and plasma membrane (large arrowhead). On the axoneme: accessory microtubules (arrow) and one of the central pair (arrowhead) are electron dense. 50000x

Fig. D: Spermatozoa flagellum from testis. Paracrystalline core (open arrow) and accessory microtubules (arrow) of axoneme are E-PTA positive. 50000x

Figs. E and F: Apyrene spermatozoa (A) and Eupyrene sperm bundles (E) from seminal vesicle. Apyrene coat (arrowhead) and paracrystalline core (open arrow) show an electron-dense reaction. Accessory microtubules, peripheral (arrow) and one of the central pair (arrowhead) are E-PTA positive. Secretion globule (double arrowhead) with basic proteins marked on its surface. 42000x; 20000x.



(3) Eupyrene Spermatozoa with Tannic Acid method

Figs. A and B: Anterior regions of spermatid and spermatozoon from testis, respectively.

Electron lucid acrosome (a), nucleus (n), laciniate (l) and reticular (r) appendages. In fig. (A) the dense amorphous mass (star). Cystic cell (C). 52000x; 58000x

Fig. C: Region anterior to the nucleus, showing the elaborate laciniate (l) and reticular (r) appendages, this last one with an electron-dense reaction. Cystic cell (C). 95000x

Fig. D: Spermatid flagellum from the testis with reticular appendage (r) and mitochondrial derivatives (md) surrounded by microtubules. 50000x

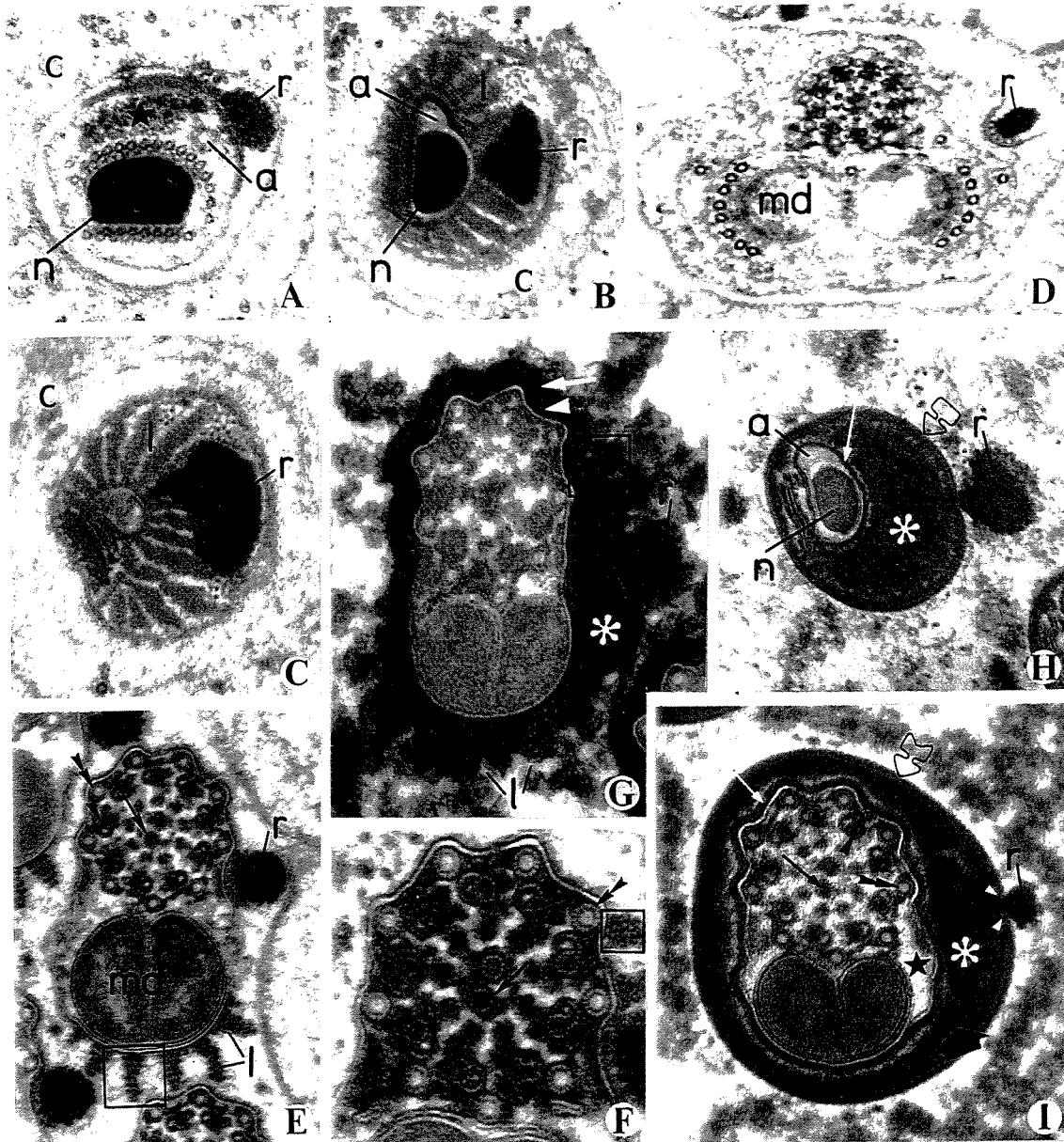
Fig. E: Spermatozoon flagellum from the testis. Laciniate appendages (l) with aligned tubular sub-units (square) and paracrystalline reticular appendage (r). Electron density of microtubules of central pair (arrow) and of A-sub-units of the peripheral (arrowhead); accessory microtubules have electron lucid cores (double arrowhead). Mitochondrial derivatives (md). 90000x

Fig. F: Axoneme detail. Electron density of the central pair (arrow), peripheral (arrowhead) and accessory (double arrowhead) microtubules. Notice the tubular sub-units of laciniate appendages (square). 150000x

Fig. G: Spermatozoa from the proximal deferens duct. Electron-dense reaction of the extracellular portions: first coat with an external thin amorphous layer (white arrow) and an internal one (white arrowhead), dense material (asterisk), paracrystalline reticular (r) and laciniate (l) appendages with tubular sub-units (square). 120000x

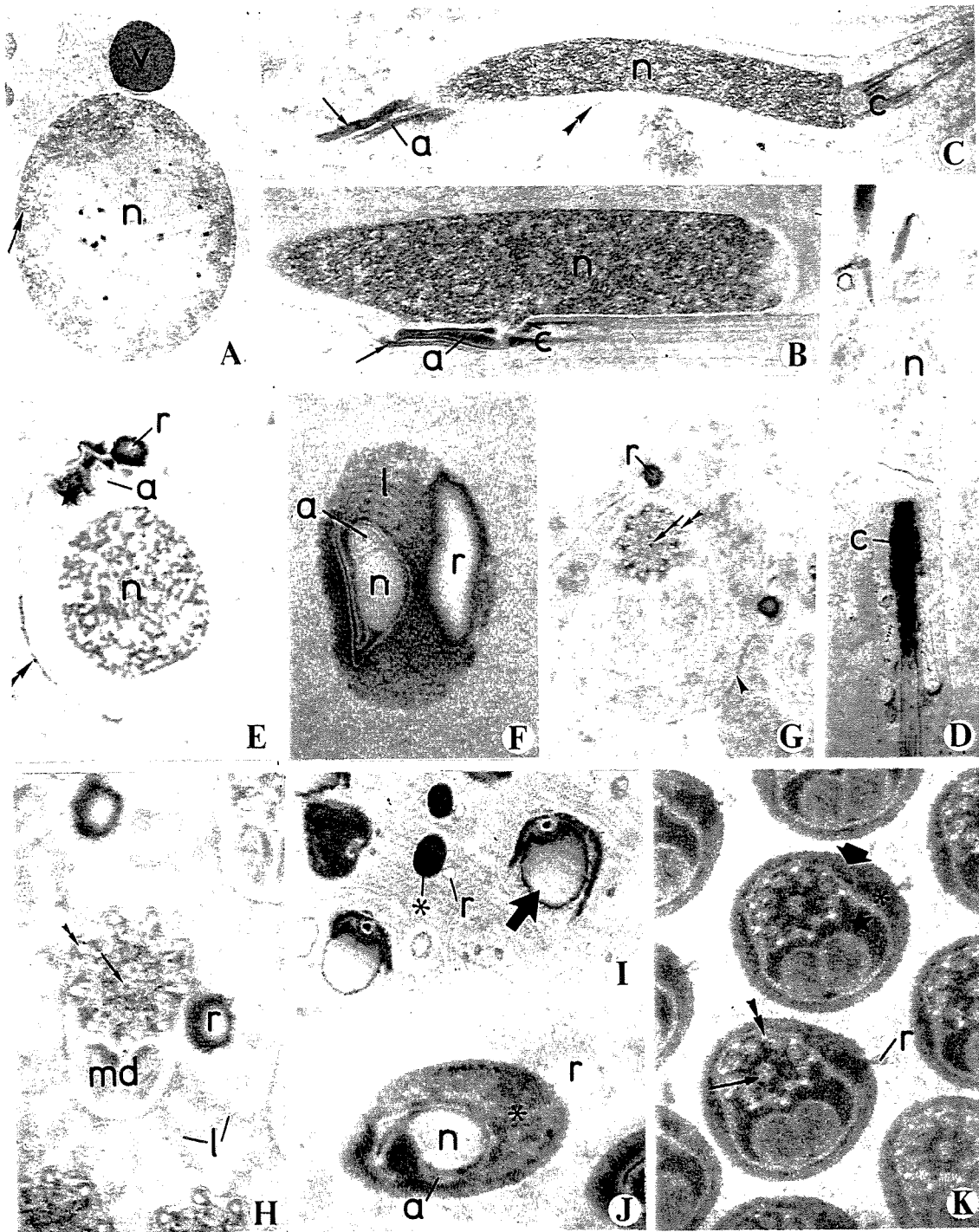
Fig. H: Spermatozoon head region from the seminal vesicle. The coat can be divided into: external layer (open arrow), dense material (asterisk) and internal layer (white arrow). Electron lucid acrosome (a), nucleus (n), paracrystalline reticular appendage (r). 80000x

Fig. I: Spermatozoon flagellum from the seminal vesicle. In the coat: external layer (open arrow) with a break (white arrowheads), amorphous material (large arrow), dense material (white asterisk) and internal layer (white arrow). In the axoneme: central pair (arrow), peripheral (arrowhead) and accessory (double arrowhead) microtubules. Reticular appendage (r). Notice that cytoplasmic material is not marked (star). 95000x



(4) Eupyrene Spermatozoa with E-PTA method

- Fig. A:** Early spermatid with spherical nucleus (n) and an E-PTA positive acrosomal vesicle (v). Notice the positive reaction on the nucleus periphery (arrow). 15000x
- Figs. B and C:** Longitudinal section of spermatids with an E-PTA positive nucleus (n). The tubular acrosome (a), reticular appendage (arrow), centriolar region (c) are E-PTA positive. A very light reaction occurs on the membrane (double arrowhead). 15000x
- Fig. D:** Longitudinal section of spermatid with an E-PTA negative nucleus (n) and centriolar region (c) with abundant basic protein. 15000x
- Fig. E:** Transverse section of spermatid with electron dense nucleus (n) and electron lucid acrosome (a). Reticular appendage (r) and amorphous material (star) with positive electron dense reaction. Cellular membrane (double arrowhead). 50000x
- Fig. F:** Spermatozoa from testis. Nucleus (n) and acrosome (a) are electron lucid. Reticular appendage (r) with basic protein evident at the surface. Lacinate appendages (l) are E-PTA positive. 100000x
- Fig. G:** Spermatid flagellum. Positive reaction in reticular appendage (r). In the axoneme: the lumen of central pair (arrow) and walls of the accessory microtubules (double arrowhead) are electron dense. Cellular membrane (arrowhead). 50000x
- Fig. H:** Spermatozoon flagellum from the testis. Axoneme with basic protein; electron dense accessory microtubule wall (double arrowhead); central pair (arrow) with dense lumen and electron lucid wall. Reticular appendage (r) is E-PTA positive on the surface. Mitochondrial derivatives (md) and lacinate appendages (l) show a light reaction. 100000x
- Fig. I:** Anterior ends of seminal vesicle spermatozoa. The globular structure (arrow) has a heterogeneous distribution of basic proteins. Spermatozoon coat (asterisk) and electron lucid reticular appendage (r). 20000x
- Fig. J:** Anterior region of the seminal vesicle spermatozoon. Acrosome (a), reticular appendage (r) and nucleus (n) are E-PTA negative. Dense coat (asterisk). 50000x
- Fig. K:** Spermatozoa flagella from the seminal vesicle with electron-dense reaction in the coat (large arrow), principally in the dense material (asterisk), in the cytoplasmic material (star). In the axoneme: dense core of central pair of microtubules (arrow) and clear accessory and peripheral microtubules (double arrowhead). 52000x



2.2

Carbohydrate localization in apyrene and eupyrene spermatozoa of the butterfly *Euptoieta hegesia* (Lepidoptera: Nymphalidae)

Mancini, K. and Dolder, H.

Running Title: Carbohydrates in Lepidoptera sperm

Abstract

Cytochemical studies on dimorphic Lepidopteran sperm are rare, and the chemical composition and function of their extracellular structures are unknown. Testis, deferent duct and seminal vesicle of *Euptoieta hegesia* butterflies were processed with cytochemical methods for carbohydrate detection in Transmission Electron Microscopy, using Ruthenium Red, Thiéry and Cuprolinic Blue techniques. Apyrene and eupyrene cell membranes presented carbohydrates, probably associated with proteins and lipids. The lumen and wall of the axonemal microtubules of both sperm types stain differently. In **apyrene spermatozoa**, carbohydrate residues are shown in the paracrystalline cores of the mitochondrial derivatives. The extratesticular apyrene coat was positive for carbohydrates, marked by all techniques. In **eupyrene spermatozoa**, no nuclear reaction was observed, probably because of the degree of chromatin condensation. The acrosome gave a positive reaction for general carbohydrates and negative for acid carbohydrates. Both eupyrene appendages, laciniate and reticular, contain carbohydrate residues. The reticular appendage was strongly stained by cuprolinic blue and presented a paracrystalline arrangement with ruthenium red. The laciniate appendages, which appear to be composed by circular subunits, were well defined by ruthenium red. The extratesticular eupyrene coat was positive for carbohydrates, evidenced by all techniques. The carbohydrate residues in apyrene and eupyrene extratesticular coats are probably related to the maturation and capacitation processes.

Keywords: ultrastructure – cytochemistry – apyrene – eupyrene.

Introduction

Euptoieta hegesia, as occurs with other butterflies and moths, produces simultaneously two types of spermatozoa, called eupyrene and apyrene sperm (Mancini and Dolder, 1999, 2001). The eupyrene spermatozoa present nucleus and acrosome in the head region (Phillips, 1970; Lai-Fook, 1982; Kubo-Irie *et al.*, 1998) and are directly responsible for egg fertilization. The apyrene spermatozoa, however, do not present nucleus and acrosome (Friedländer and Gitay, 1972; Friedländer and Miesel, 1977) and participate indirectly in egg fertilization. Research has demonstrated that apyrene spermatozoa are involved in the mechanism of sperm competition (Drummond, 1984; Silberglie *et al.*, 1984). In this case, males tailor their ejaculate volume and composition in response to sperm competition risk and intensity. Thus, apyrene sperm fill the spermathecae, retarding female receptivity, diminishing the sperm competition risk and increasing paternal success (Gage, 1994; Snook, 1997, 1998; Cook and Wedell, 1996, 1999).

Both sperm types undergo some morphologic modifications along the male and female reproductive tract (Riemann, 1970; Riemann and Thorson, 1971; Friedländer and Gitay, 1972; Kubo-Irie *et al.*, 1998). These modifications occur in the extracellular structures and involve the exclusive eupyrene appendages (reticular and laciniate) and the coat of both sperm types.

Carbohydrate residues can form integral parts of larger glycoconjugates, such as glycoproteins, glycolipids or polysaccharides. Glycoconjugates have functions in a wide range of biological activities, including forming and maintaining a stable tertiary structure for proteins, aiding the secretion of extracellular materials, immunomodulation, promoting interaction between cells, as well as between cells and extracellular matrix and the regulation of proteolytic activities (Varki, 1993). They are also important molecules for the specificity of gamete recognition, adhesion and fusion (Nicolson and Yanagimachi, 1972; Koehler, 1978; Sharon and Lis, 1993).

Several studies describe the morphology of apyrene and eupyrene spermatozoa (Phillips, 1970, 1971; Riemann, 1970; Riemann and Thorson, 1971; Friedländer and Gitay, 1972; Lai-Fook, 1982; Kubo-Irie *et al.*, 1998; Jamieson *et al.*, 1999; Mancini and Dolder,

1999; Garvey *et al.*, 2000) however the cytochemical analyses still remain unknown. Only a few ultrastructural studies have developed some cytochemical aspects (Friedländer, 1976; Friedländer and Gershon, 1978; Medeiros, 1986, 1997; França and Bão, 2000; Mancini and Dolder, in preparation).

In Lepidopteran sperm, the origin, function and chemical composition of eupyrene appendages as well as the extracellular coat of apyrene and eupyrene spermatozoa still have not been elucidated. Here, cytochemical methods for carbohydrate detection were used on apyrene and eupyrene spermatozoa of the butterfly *Euptoieta hegesia*, for a better understanding of the chemical composition and functions of the ultrastructural transformations in these spermatozoa.

Materials and methods

Testis, deferent duct and seminal vesicle of the adults butterfly *Euptoieta hegesia* were processed for distinct Transmission Electron Microscopy methods.

Conventional

Specimens were fixed in 2.5% glutaraldehyde, 4% paraformaldehyde, 1.5% sucrose, 5mM CaCl₂ in 0.1M sodium phosphate buffer for 12 hours at 4°C. After fixation, they were rinsed in buffer, post-fixed in 1% osmium tetroxide in sodium phosphate buffer for 3-5 hours at 4°C. Finally, they were dehydrated in acetone and included in Epoxy resin.

Cytochemistry

General Glycoproteins

Ruthenium Red

Specimens were fixed in 2.5% glutaraldehyde, 1% ruthenium red in 0.1M cacodylate buffer for 2 hours, in the dark, at room temperature and then washed in the same

buffer. They were post-fixed in 1% osmium tetroxide in cacodylate buffer for 1 hour, followed by 1% osmium tetroxide, 1% ruthenium red in cacodylate buffer, in the dark, at room temperature and then washed in the same buffer. Finally, the specimens were dehydrated in acetone and included in Epoxy resin (modified from Luft, 1971 in Mancini *and* Dolder, 2001).

Thiery method

Specimens were fixed according to the conventional method, without osmium tetroxide. Ultrathin sections were collected on gold grids, incubated in 1% periodic acid for 30 minutes at room temperature and washed in water from 10 to 30 minutes. The gold grids were incubated in 1% tiosemicarbazide in 10% acetic acid for 72 hours for glycoproteins. Subsequently, the gold grids were washed in 10% acetic acid (3x5 minutes), 5% (5 minutes), 2% (5 minutes) and water (3x5 minutes). Finally, the grids were immersed in 1% silver proteinate (Fluka) for 30 minutes in the dark (De Souza *et al.*, 1998).

Glycosaminoglycans (Acid Glycoproteins)

Cuprolinic Blue

Specimens were fixed in 2.5% glutaraldehyde, 0.2% cuprolinic blue, drops of 0.2M magnesium chloride in 0.05M sodium acetate buffer for 24 hours at 4°C. The specimens were washed in the same buffer and post-fixed in 1% sodium tungstate for 24 hours at 4°C. Then they were dehydrated in 30% ethanol + 1% tungstate for 30 minutes at 4°C; 50% ethanol + 1% tungstate overnight at 4°C; 70% ethanol; 90% ethanol and 100% ethanol for 15 minutes each solution. Finally, they were included in Epoxy resin (Modified from Scott *et al.*, 1989).

In all the cytochemical methods used, the ultra thin sections were contrasted with uranyl acetate and lead citrate solutions.

Results

Eupyrene spermatozoa

The head region of intratesticular eupyrene spermatozoa is composed of a compacted, elongated nucleus and a tubular acrosome. External to the plasma membrane, these spermatozoa present two elaborated and exclusive appendages, denominated laciniate and reticular appendages (Fig. 1A).

When compared with the conventional fixation method (Fig. 1A), the nuclei of *E. hegesia* did not present an evident reaction to carbohydrates. However, the acrosome presented an electron dense reaction to ruthenium red (Fig. 1C) and no reaction to cuprolinic blue (Fig. 1B).

The reticular appendage, in the head region, presented acid glycoproteins (glycosaminoglycans) demonstrated by the positive reaction to cuprolinic blue, becoming as electron dense as the nucleus (Fig. 1B). The laciniate appendages, well developed in this region, were not considered positive for cuprolinic blue, while they present a slight reaction to ruthenium red (Figs. 1B and C, respectively).

The tail of eupyrene spermatozoa contains two apposed, parallel mitochondrial derivatives, a 9+9+2 axoneme, in which the central pairs and accessory microtubules have denser lumens, and the extracellular reticular and laciniate appendages (Fig. 1D).

In the axoneme, the accessory microtubule walls presented a positive reaction to cuprolinic blue, while their lumens appear electron lucid (Fig. 1I). The accessory microtubules lumens appear electron dense when the Thiéry (Figs. 1J and P) and ruthenium red (Figs. 1E and F) methods were employed, as well as in the conventional fixation method (Fig. 1D). The central microtubule pair's lumens became electron dense when treated with ruthenium red and cuprolinic blue methods (Figs. E and I, respectively). The mitochondrial derivatives showed little reaction on the external regions when treated with cuprolinic blue (Figs. 1H and I).

The reticular appendage was the outstanding structure when ruthenium red was used (Figs. 1E-G) and reacted even more strongly with cuprolinic blue (Figs. 1H and I).

technique. The Figure 1 G shows the very dense reaction to ruthenium red even without section contrasting. It is possible to notice a compact paracrystalline formation of this appendage when submitted to cuproinic blue (Fig. 1I) and, this is even clearer with ruthenium red (Figs. 1E-G). The reticular appendage did not react with the Thiéry method (Fig. 1J). It is possible to observe a U-shaped support between the cell membrane and the reticular appendage (Figs. 1 D-F and I), which is better shown with ruthenium red and cuproinic blue methods (Figs. 1E-F and I).

The laciniate appendages were observed in fine detail with the ruthenium red technique, showing a regular paracrystalline organization, with circular sub units found in transversal sections (Figs. 1E-F). With cuproinic blue these structures were well defined while the Thiéry method showed a poor image of these appendages (Figs. 1H-I and J, respectively). The cell membrane was strongly marked by the cuproinic blue (Fig. 1I) and Thiéry methods (Fig. 1J).

In eupyrene intratesticular cysts, it is possible to observe a dispersed material, detected between the spermatozoa with conventional fixation (not shown) and with cytochemical methods (large circles, Figures 1D-F and I). This material presents structural similarity to the circular sub unit of the laciniate appendages.

When they leave the testis, the eupyrene spermatozoa lose their cystic organization and the laciniate appendages that surrounded the cell membrane. From the deferent duct to the end of the reproductive tract these spermatozoa gradually develop a dense coat.

In the seminal vesicle, these spermatozoa are maintained in an organized sheath by a matrix and are totally covered by an individual coat, with the external reticular appendage still present (Fig. 1L). In the eupyrene anterior region, acrosome, coat and reticular appendage presented a positive reaction to ruthenium red (Fig. 1K). In the sperm tail region, the coat presented distinct dense regions and layers when treated with Thiéry (Fig. 1P) and even more so with ruthenium red (Figs. 1M-N) methods. It is possible to identify a thin external, Thiéry positive layer; an amorphous mass distributed inside the layer and an amorphous material, located between the reticular appendage and the cell membrane. This material next to the reticular appendage was more strongly stained by ruthenium red (Fig. 1M-N) and appears less dense with the Thiéry method (Fig. 1P).

With cuproline blue, the coat of eupyrene spermatozoa from the deferent duct presented a uniform electron dense reaction. The disorganized reticular appendage was also stained (Fig. 1O). The matrix that maintains the eupyrene spermatozoa in the seminal vesicle was positive for carbohydrates with all cytochemical methods (Figs. 1K, N-P).

Apyrene spermatozoa

The apyrene spermatozoa from the testis possess a dense cap in the anterior region, a structure that is standard for many Lepidoptera. This structure presented an electron dense reaction with the Thiéry method (Fig. 2A). The other techniques employed did not show an evident reaction when compared with the conventional fixation method.

The tail region, observed with the conventional fixation, is composed of two mitochondrial derivatives and an axoneme, in which the accessory microtubules and one of the central pair have a dense lumen (Fig. 2B). The paracrystalline core of the mitochondrial derivatives was well evidenced by ruthenium red (Figs. 2C-E) and cuproline blue (Fig. 2F) techniques. In the axoneme, the accessory microtubule walls were electron dense with cuproline blue (Fig. 2F), as was seen in the eupyrene spermatozoa. The accessory microtubule lumen presented an electron dense reaction to ruthenium red (Figs. 2D-E), with the conventional fixation method. When cuproline blue was employed, the accessory microtubule lumen did not present electron density (Fig. 2F). With the ruthenium red method, one of the central pair's lumen became electron dense (Fig. 2E). None of the microtubules were marked by the Thiéry method (Fig. 2G).

Cell membranes were conspicuous with the three techniques employed (Figs. 2 E-G). The extra testicular apyrene spermatozoa gradually acquire concentric layers that become very developed in the seminal vesicle (Fig. 2H). These layers presented a positive reaction to the three techniques employed (Figs. 2I-J). Only with the conventional fixation method (Fig. 2H) was it possible to identify an intracellular material of irregular distribution; none of the other techniques detected this material.

Discussion

The results obtained in this research demonstrated that apyrene and eupyrene spermatozoa from *Euptoieta hegesia* present different glycoconjugates.

According to Hayat (1993), the ruthenium red can be applied for general glycoproteins detection, while cuproinic blue is more specific, being used for the sulfated (acid) glycoproteins detection, such as the glycosaminoglycans. These cytochemical affinities were observed in our micrographs. The material was homogeneously stained by ruthenium red, when compared with cuproinic blue, for which the intense stain was restricted to the reticular appendage, rich in acid glycoproteins.

The Thiéry method was extremely exigent. After several repetitions, convincing results were only obtained with the silver proteinate of the Fluka company. The ultra thin sections, submitted to this technique, which does not use osmium tetroxide, lose considerable resolution and this makes the identification of structures difficult.

Several proteins present in the nucleus are related to the structural determination of genomic properties, the chromosomal compaction and the processes of duplication and transcription of the genetic material. Studies have demonstrated that many of these macro proteins are glycosaminoglycans and glycoproteins (Stein *et al.*, 1975). In *Euptoieta hegesia* no evident nuclear reaction was observed; probably the level of nuclear condensation and genetic inactivity were factors contributing to the absence of an identifiable reaction.

The acrosome showed a positive reaction for general carbohydrates and a negative reaction for glycosaminoglycans or acid glycoproteins. In fact, the acrosomal surface and many acrosomal enzymes possess glycoconjugates (Ahluwalia *et al.*, 1990; Bão and de Souza, 1992). Apyrene and eupyrene cell membranes presented carbohydrates associated to proteins and lipids. Craveiro and Bão (1995), using the Thiéry method, also observed a positive reaction in the sperm membranes of three species of Coleoptera.

The cytochemical methods employed permitted the identification of different categories of axonemal microtubules. In the apyrene and eupyrene spermatozoa of *E. hegesia* the accessory microtubule walls presented acid carbohydrate residues. The central

pair lumen of apyrene and eupyrene microtubular axonemes also presented carbohydrate residues, demonstrated by ruthenium red and cuproinic blue. The association of carbohydrates to accessory microtubules and to one of the central pair was also described in Coleoptera (Báo, 1991, 1996; Craveiro and Báo, 1995) and Diptera (Báo and de Souza, 1993). Our observations in apyrene and eupyrene early spermatids showed a different carbohydrate distribution on the axoneme, suggesting a gradual deposition of carbohydrates after axoneme formation.

The reticular appendage contains carbohydrates, made evident by cuproinic blue and ruthenium red methods. Medeiros (1986) observed a positive reaction in the reticular appendage with the ruthenium red method. Previous studies demonstrated proteic residues in these appendages with the E-PTA method (Medeiros, 1986; França and Báo, 2000; Mancini and Dolder, in preparation) and tannic acid (Jamieson *et al.*, 1999; Mancini and Dolder, in preparation). The thin U-shaped structure, observed between the cell membrane and the reticular appendage, seems to represent an anchorage for this appendage onto the cell membrane.

The laciniate appendages reacted strongly to the ruthenium red method, showing a regular organization, which suggests the presence of glycoconjugates. There are evidences of the predominance of proteic residues in these appendages (França and Báo, 2000; Medeiros, 1997; Mancini and Dolder, in preparation). The organization found with ruthenium red is similar to that observed with tannic acid. We suggest that the laciniate appendages present predominantly protein, while the reticular appendages present carbohydrate. The similarity between the laciniate appendage structure and the material dispersed around the eupyrene spermatozoa from the testis, suggests that this material originates from the disintegration of the laciniate appendages.

The eupyrene spermatozoon coat in the seminal vesicle showed the presence of carbohydrates. With the ruthenium red technique, distinct regions were observed, probably because of different carbohydrate residues. In the deferent duct, this distinction does not occur, possibly because the layer is still not completed. Many authors suggest that this coat could be the result of the rearrangement and reorganization of the laciniate appendages, which occurs in the deferent duct (Phillips, 1971; Friedländer and Gitay, 1972; Lai-Fook,

1982; Kubo-Irie *et al.*, 1998). The present work did not find evidences for this hypothesis; however, we believe that the laciniate appendages contribute partially to the coat and to matrix formations.

The mitochondrial paracrystalline core of apyrene spermatozoa from *Euptoieta hegesia* is emphasized by cytochemical methods for carbohydrate detection. These carbohydrates are probably associated to proteic residues found in these structures (Medeiros, 1997; França and Bão, 2000; Mancini and Dolder, in preparation). Bão (1991), with the ruthenium red technique, also showed this mitochondrial paracrystalline core in Coleoptera sperm.

In the seminal vesicle, concentric membranes presented carbohydrates in their composition, since membranes are rich in proteic and carbohydrate residues associated to the lipidic layer.

In the female's spermatheca, the eupyrene sperm lose their extracellular coat before egg fertilization. In this case, the coat is not necessary for gamete recognition. We agree with Riemann (1970) that all these morphological changes of extracellular structures described here are probably related to the maturation and capacitation processes of both sperm types. We also believe that reticular and laciniate appendages are involved in eupyrene sperm aggregation in the testis.

Because of the few cytochemical studies regarding butterfly and moth spermatozoa, the results presented here are an important contribution to Lepidoptera sperm structural composition.

References

- Ahluwalia, B., Farshori, P., Jamuar, M., Baccetti, B. and Anderson, W. A. 1990. Specific localization of lectins in boar and bull spermatozoa. **J. Submicrosc. Cytol. Pathol.** 22: 53-62.

- Báo, S. N. 1991. Morphogenesis of the tail in the spermatids of *Coelomera lanio* (Coleoptera, Chrysomelidae): ultrastructural and cytochemical studies. **Cytobios** 66: 157-167.
- Báo, S. N. 1996. **Spermiogenesis in *Coelomera lanio* (Chrysomelidae: galerucinae): ultrastructural and cytochemical studies**. In: Jolivet, P. H. A. and Cox, M. L. (Eds.), Chrysomelidae Biology: General Studies. Academic Publishers, Netherlands, pp. 119-132.
- Báo, S. N. and de Souza, W. 1992. Lectin binding sites on head structures of the spermatid and spermatozoon of the mosquito *Culex quinquefasciatus* (Diptera: Culicidae). **Histochem.** 98: 365-371.
- Báo, S. N. and de Souza, W. 1993. Ultrastructural and cytochemical studies of the spermatid and spermatozoon of *Culex quinquefasciatus* (Culicidae). **J. Submicrosc. Cytol. Pathol.** 25: 213-222.
- Cook, P. A. and Wedell, N. 1996. Ejaculate dynamics in butterflies: a strategy for maximizing fertilization success. **Proc. Royal Soc. London B** 263: 1047-1051.
- Cook, P. A. and Wedell, N. 1999. Non-fertile sperm delay female remating. **Nature** 397: 486.
- Craveiro, D. and Báo, S. N. 1995. Localization of carbohydrates in spermatids of three chrysomelid beetles (Coleoptera, Chrysomelidae). **Biocell** 19: 195-202.
- De Souza, W. 1998. **Técnicas Básicas de Microscopia Eletrônica Aplicada às Ciências Biológicas**. Sociedade Brasileira de Microscopia.
- Drummond, B. A. 1984. **Multiple mating and sperm competition in the lepidoptera**. In: Smith, R.L. Sperm competition and the evolution of animal mating systems. Academic Press, London. pp 291-370.
- França, F. G. R. and Báo, S. N. 2000. Dimorphism in spermatozoa of *Anticarsia gemmatilis* Hübner, 1918 (Insecta, Lepidoptera, Noctuidae). **Braz. J. Morphol. Sci.** 17: 5-10.
- Friedländer, M. 1976. The role of transient perinuclear microtubules during spermiogenesis of the warehouse moth *Ephestia cautella*. **J. Submicrosc. Cytol.** 8: 319-326.

- Friedländer, M. and Gitay, H. 1972. The fate of the normal anucleated spermatozoa in inseminated female of the silkworm *Bombyx mori*. *J. Morphol.* 138: 121-129.
- Friedländer, M. and Miesel, S. 1977. Spermatid anucleation during the normal atypical spermiogenesis of the warehouse moth *Ephestia cautella*. *J. Submicrosc. Cytol.* 9: 173-185.
- Friedländer, M. and Gershon, J. 1978. Reaction of surface lamella of moth spermatozoa to vinblastine. *J. Cell Sci.* 30: 353-361.
- Gage, M. J. G. 1994. Associations between body size, mating pattern, testis size and sperm lengths across butterflies. *Proc. Royal Soc. London B* 258: 247-254.
- Garvey, L. K., Gutierrez, G. M. and Krider, H. M. 2000. Ultrastructure and morphogenesis of the apyrene and eupyrene spermatozoa in the gypsy moth. *Ann. Entomol. Soc. Am.* 93: 1147-1155.
- Hayat, M. A. 1993. **Stain and cytochemical methods**. Plenum Press.
- Jamieson, B. G. M., Dallai, R. and Afzelius, B. A. 1999. **Insects: their spermatozoa and phylogeny**. Enfield, New Hampshire (USA) Science Publishers, Inc.
- Koehler, J. K. 1978. The mammalian sperm surface. Studies with specific labeling techniques. *Int. Rev. Cytol.* 54: 73-195.
- Kubo-Irie, M., Irie, M., Nakazawa, T. and Mohri, H. 1998. Morphological changes in eupyrene and apyrene spermatozoa in the reproductive tract of the male butterfly *Atrophaneura alcinous* Klug. *Invert. Reprod. Develop.* 34: 259-268.
- Lai-Fook, J. 1982. Structural comparison between eupyrene and apyrene spermiogenesis in *Calpododes ethlius* (Hesperiidae: Lepidoptera). *Can. J. Zool.* 60: 1216-1230.
- Mancini, K. and Dolder, H. 1999. Ultrastructural modifications in apyrene and eupyrene spermatozoa of *Euptoieta hegesia* (Lepidoptera: Nymphalidae) along the male reproductive tract. *Acta Microsc.* 8, Supplement C, 567-568.
- Mancini, K. and Dolder, H. 2001. Ultrastructure of apyrene and eupyrene spermatozoa from the seminal vesicle of *Euptoieta hegesia* (Lepidoptera: Nymphalidae). *Tissue and Cell* 33: 301-308.
- Medeiros, M. 1986. **Caracterização ultra-estrutural de espermatozóides eupirenes e apirenes de *Alabama argillacea* Hübner, 1818 (Lepidoptera: Noctuidae), ao nível dos**

- testículos e das vias genitais de imagos machos e fêmeas até a espermateca.** Instituto de Biologia, Universidade Estadual de Campinas (Master Thesis).
- Medeiros, M. 1997. **Estudo ultra-estrutural da espermiogênese dicotômica de *Alabama argillacea* Hübner, 1818.** Instituto de Biociências, Universidade Estadual de São Paulo (Doctor Thesis).
- Nicolson, G. L. and Yanagimachi, R. 1972. Terminal saccharides on sperm plasma membranes: identification by specific agglutinins. **Science** 197: 276-279.
- Phillips, D. M. 1970. Insect sperm: their structure and morphogenesis. **J. Cell Biol.** 44: 243-277.
- Phillips, D. M. 1971. Morphogenesis of the laciniate appendages of lepidopteran spermatozoa. **J. Ultrastruct. Res.** 34: 567-585.
- Riemann, J. G. 1970. **Metamorphosis of sperm of the cabbage looper *Trichoplusia ni* during passage from the testes to the female spermatheca.** In: Baccetti, B. Comparative Spermatology. Academic Press. New York. pp. 321-331.
- Riemann, J. G. and Thorson, B. J. 1971. Sperm maturation in the male and female genital tracts of *Anagasta kuhniella* (Lepidoptera: Pyralidae). **Int. J. Insect Morphol. Embryol.** 1: 11-19.
- Scott, J. E., Haigh, M., Nusgens, B. and Lapiere, C. M. 1989. Proteoglycan: collagen interactions in dermatosparatic skin and tendon. An electron histochemical study using cupromeronic blue in a critical electrolyte concentration method. **Matrix** 9: 437-442.
- Sharon, N. and Lis, H. 1993. Carbohydrates in cell recognition. **Scientific American**, pp. 74-81.
- Silberglie, R. E., Shepherd, J. G. and Dickinson, J. L. 1984. Eunuchs: the role of apyrene sperm in lepidoptera? **Am. Nat.** 123: 255-265.
- Snook, R. R. 1997. Is the production of multiple sperm types adaptive? **Evolution** 51: 797-808.
- Snook, R. R. 1998. The risk of sperm competition and the evolution of sperm heteromorphism. **An. Behav.** 56: 1497-1507.

Stein, G. S., Roberts, R. M., Davis, J. L., Head, W. J., Stein, J. L., Thrall, C. L., Van Veen J. and Welch, D. W. 1975. Are glycoproteins and glycosaminoglycans components of the eukaryotic genome? **Nature** **258**: 639-641.

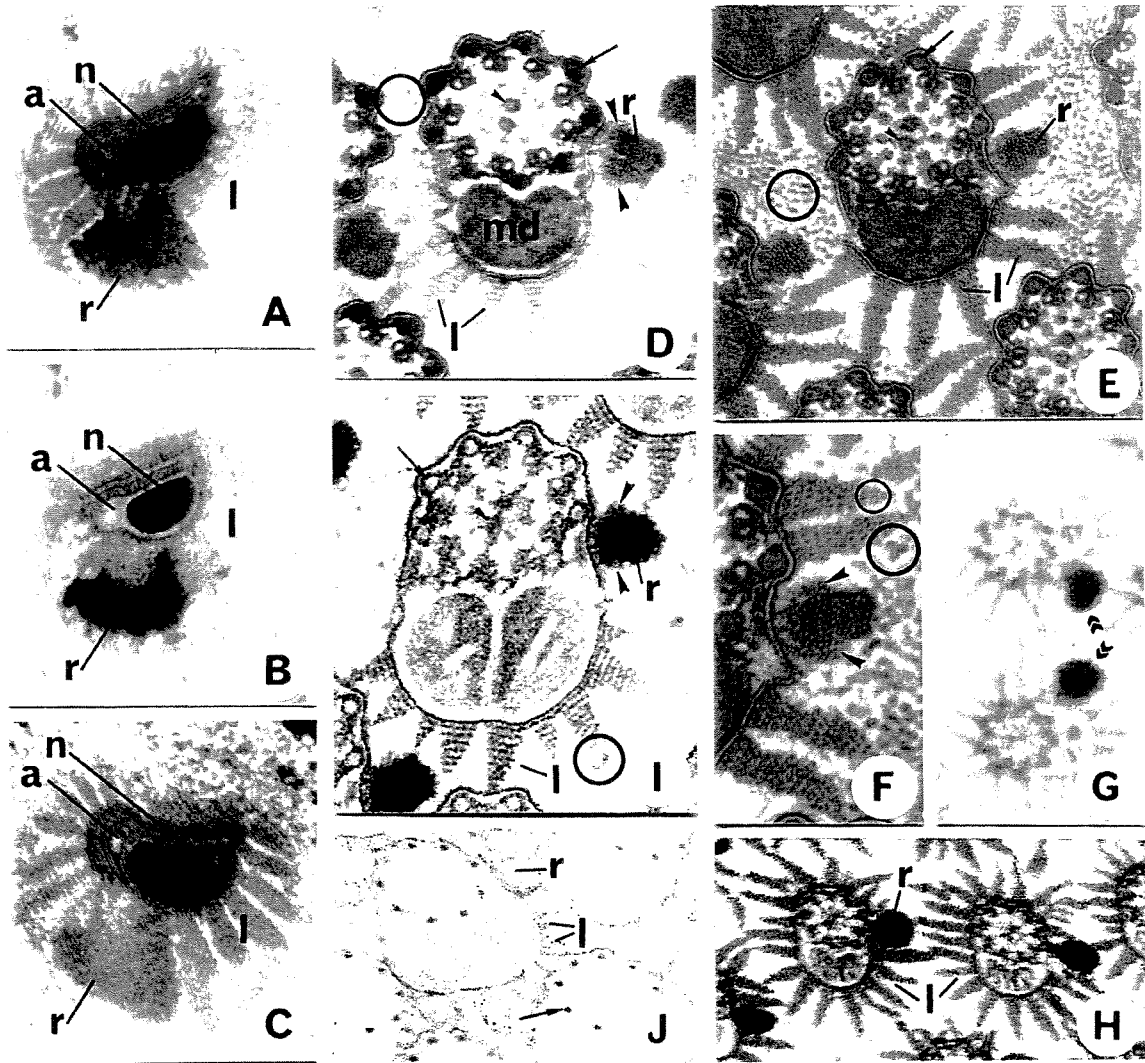
Varki, A. 1993. Biological roles of oligosaccharides: all of the theories are correct. **Glycobiology** **3**: 97-130.

Figure Legends

(C) – Convencional (CB) – Cuprolinic Blue
(RR) – Ruthenium Red (TH) – Thiery

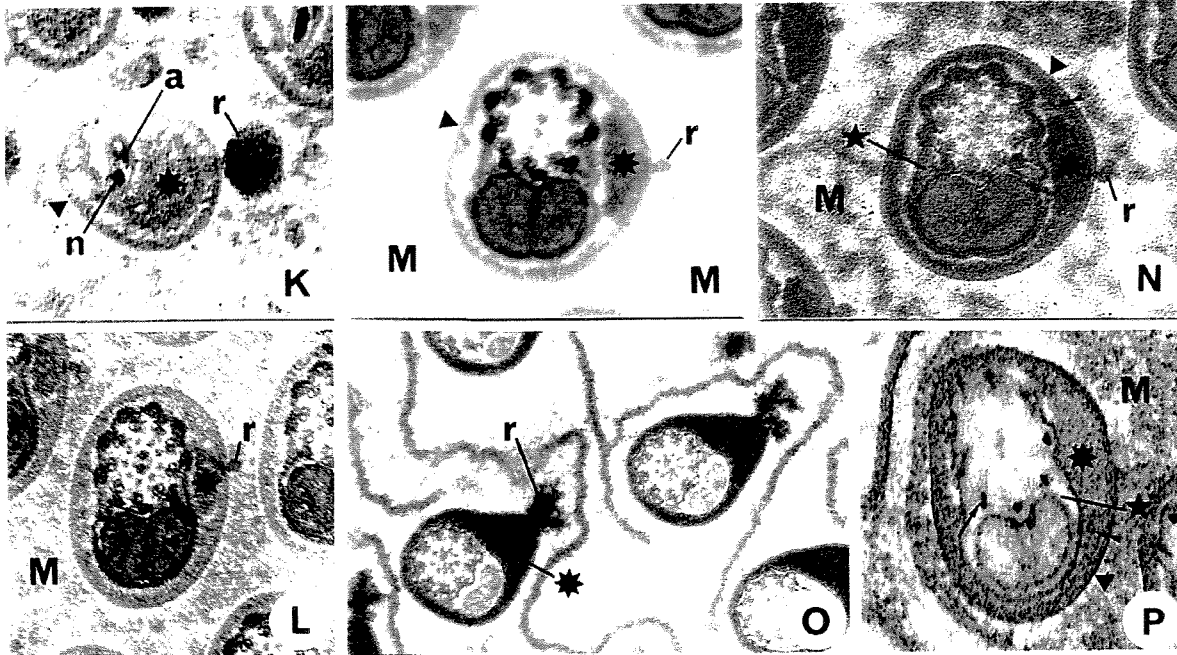
Figures 1A-J: Eupyrene Spermatozoa from Testis

Fig. A: (C). Anterior region of eupyrene spermatozoon. Tubular acrosome (a), nucleus (n), laciniate (l) and reticular (r) appendages. 70000x **Fig. B: (CB).** Similar region as in Fig. 1A. Electron dense reaction of the reticular appendage (r) and lack of reaction in the acrosome (a). 86.000x **Fig. C: (RR).** Head region as in Fig. 1A. Reaction product is observed in the laciniate appendages (l) and acrosome (a). 72000x **Fig. D: (C).** Eupyrene spermatozoa tail. In the axoneme: electron density of the accessory microtubules (arrow) and central pairs (arrowhead) was found. Also electron dense structures include the mitochondrial derivatives (md), the reticular appendage (r) with its U-shaped support (arrowhead); laciniate appendages (l). Notice dispersed material (circle). 82000x **Fig. E: (RR).** Similar region as in Fig. 1D. Notice the electron density of the accessory microtubules (arrow) and central pairs (arrowhead). Laciniate (l) and reticular (r) appendages with regular organization. Dispersed material (circle). 82000x **Fig. F: (RR).** Detail of the Figure 1E showing the regularity of the organization of the appendages, the U-shaped support (arrowhead) and the structural similarity between the laciniate appendage units (small circle) and the dispersed material (large circle). 115000x **Fig. G: (RR – without section contrast).** Intense stain of the reticular appendage (double arrowheads). 40000x **Figs. H and I: (CB).** Spermatozoa tail showing the intense stain of laciniate (l) and, mainly, the reticular appendages (r). Axoneme with electron density of the central pair of microtubules (arrowhead) and electron lucid accessory ones (arrow). 50000x; 100000x **Fig. J: (TH).** Spermatozoon tail showing very light stain of laciniate appendages (l); and dense accessory microtubules (arrow); while the reticular appendage (r) is negatively stained. 68000x



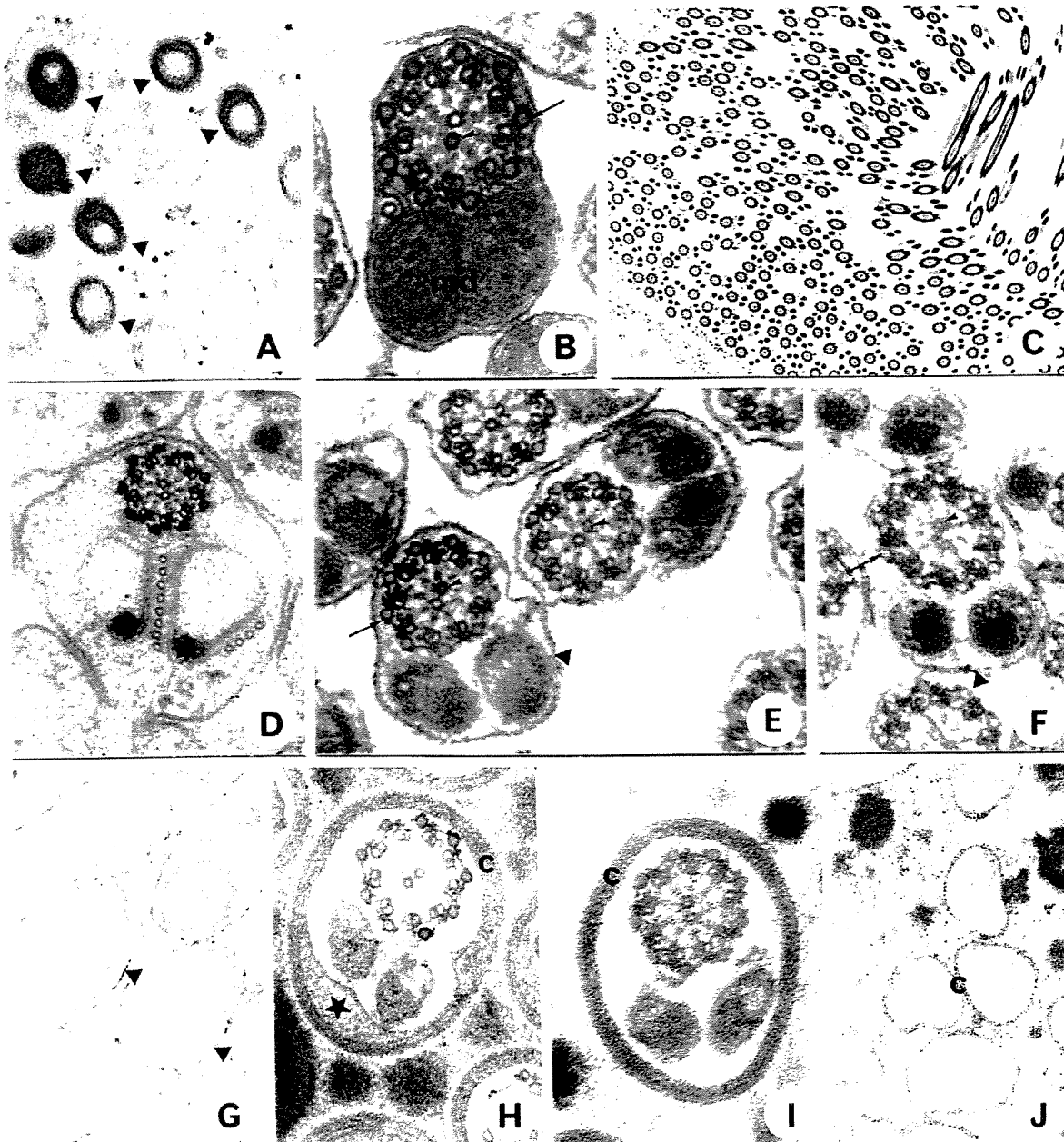
Figures 1K-P: Extra testicular Eupyrene Spermatozoa

Fig. K: (RR). Anterior region of eupyrene sperm from the seminal vesicle showing the dense reaction of the reticular appendage (r) and acrosome (a). The coat is composed of an external layer (arrowhead) and an amorphous dense material (asterisk). Nucleus (n). 66000x **Fig. L: (C).** Spermatozoon tail from seminal vesicle. Inside the coat, is an amorphous dense material (asterisk). Reticular appendage (r) and matrix (M). 50000x **Fig. M: (RR - without section contrast).** Same region as in Fig. 1L. Amorphous dense material (asterisk) was stained. Matrix (M) was negatively stained. External layer (arrowhead) and reticular appendage (r). 70000x **Fig. N: (RR).** Same region as in Fig. 1M, showing details of the coat, with the external layer (arrowhead), a mass below this layer (double arrowhead) and the amorphous dense material (asterisk). Matrix (M) and cytoplasmic material (star) stained. 65000x **Fig. O (CB).** Spermatozoa tail from deferent duct. Early coat with dense material (asterisk) and reticular appendage (r) electron dense. 50000x **Fig. P: (TH).** Spermatozoon tail from seminal vesicle. Product reaction in the coat: external layer (arrowhead), internal mass (double arrowhead) and amorphous material (asterisk). Dense accessory microtubules (arrow) and clear cytoplasmic material electron lucid (star). Matrix (M) is electron dense. 70000x



Figures 2A-J: Intra and Extra testicular Apyrene Spermatozoa

Fig A: (TH). Anterior end of intratesticular spermatozoa showing the dense cap sectioned at different levels (arrowhead). 40000x **Fig. B: (C).** Tail of testis spermatozoa. Mitochondrial derivatives (md) and axoneme in which accessory microtubules (arrow) and one of the central pair (arrowhead) are electron dense. 130000x **Fig. C: (RR).** Spermatozoa cyst showing the microtubules of the axoneme and the mitochondrial derivatives' paracrystalline cores. 8600x **Fig. D: (RR).** Spermatid tail. Electron density of the mitochondrial derivatives' paracrystalline cores (asterisk). 60000x **Figs. E-F-G: (RR-CB-TH, respectively).** Tail of testis spermatozoa. Cell membranes (arrowhead) are electron dense, mainly with Thiéry method. (E) and (F) with dense paracrystalline cores (asterisk); accessory (arrow) and central pair (arrowhead) of microtubules show different electron densities. 85000x; 85000x; 70000x **Figs. H-I-J: (C-RR-TH, respectively).** Spermatozoa tail from seminal vesicle showing the stained concentric membranes (C). Identification of amorphous material of irregular distribution (star) is only seen in (H). 80000x; 85000x; 30000x



2.3

**Lectin binding sites on the spermatids and spermatozoa of
Euptoieta hegesia (Lepidoptera: Nymphalidae)**

Mancini, K. and Dolder, H

Running title: Lectin on spermatids and spermatozoa of *Euptoieta hegesia*.

Abstract

The present research analyzed the presence of carbohydrate residues as revealed by lectin labeling in the spermatids and spermatozoa of the *Euptoieta hegesia* butterfly (including PNA, GS-I, GS-II, HPA, UEA-I and WGA). In **apyrene cells**, the micronucleus was the structure most frequently labeled, since it was labeled by all lectins, except by WGA. Spermatid cytoplasm was intensely labeled with GS-I and GS-II. The anterior dense cap showed GS-I, GS-II and HPA binding. PNA and GS-I marked the paracrystalline core of the mitochondrial derivative. The plasma membrane was labeled with HPA in spermatids and spermatozoa, while the coat of extratesticular spermatozoa was intensely labeled with GS-I, GS-II and HPA. In **eupyrene cells**, the acrosomal vesicle showed labeling by HPA and WGA but no lectin labeling was found for the tubular acrosome. The lectins GS-I, GS-II, PNA and HPA were very evident in the nuclei of spermatids while the spermatozoon nucleus was labeled with these same lectins, as well as UEA-I. The plasma membrane was intensely labeled only with HPA. The reticular appendages showed the richest labeling, with the presence of PNA, GS-I, GS-II and HPA, while the laciniate appendages were marked for the same lectins, except for PNA. The coat acquired in the extratesticular region was labeled with HPA, GS-I and GS-II. This study demonstrates that lectin specific sugars are widely distributed in apyrene and eupyrene spermatids and spermatozoa of *Euptoieta hegesia*. Thus, the less well-known structures, including the apyrene cap, the eupyrene extracellular appendages, especially the reticular appendage, and the apyrene and eupyrene coats, which are exclusive for Lepidoptera, presented carbohydrate residues.

Key words: glycoconjugates – lectin – apyrene – eupyrene.

Introduction

It is well established that almost all cells carry carbohydrates on their surfaces in the form of glycoproteins, glycolipids, and polysaccharides (Sharon and Lis, 1989). These glycoconjugates have an important role in several biological processes.

Recognition is the first step in numerous processes based on cell-cell interactions, such as fertilization, embryogenesis, cell migration, organ formation, immune defense, and microbial infection (Sharon and Lis, 1989).

In germ cells, numerous studies have demonstrated that carbohydrates mediate the interaction between gametes and they are components of the cell surface of spermatozoa and ovules. Their complementarity is responsible for gamete recognition, specificity and adhesion (Nicolson and Yanagimachi, 1972; Koehler, 1978; Perotti and Riva, 1988).

Lectins have been largely used for identification, characterization and localization of carbohydrate-containing molecules because they can selectively recognize sugar residues. This class of proteins or glycoproteins is not confined to plants, as originally believed, but is found on cell surfaces and intracellular particles (Sharon and Lis, 1989).

There are many studies with carbohydrate detection in vertebrates, especially in mammals (Martínez-Menárguez *et al.*, 1992). In invertebrates, insects are the group most studied as to the physiology of reproduction, gamete structure and morphogenesis. However, there is little research regarding sperm cytochemistry.

Especially in the Lepidoptera order, where the most evident phenomenon of sperm dimorphism occurs, there are few studies of the composition of both sperm types (Medeiros 1986, 1997; França and Bão, 2000).

The eupyrene and the apyrene sperm types present complex extracellular structures and go through several morphological changes along the male reproductive tract. The eupyrene spermatozoa contain two exclusive and elaborate extracellular appendages, known as laciniate and reticular.

The chemical composition and the role of these appendages remain unclear. On the other hand, in the apyrene spermatozoa there are no appendages, but they have extracellular structures such as an anterior dense cap and a coat with several concentric layers.

The present research analyzed the presence of carbohydrate residues in the spermatids and spermatozoa of the *Euptoieta hegesia* butterfly by lectin labeling.

Materials and Methods

Adults of the *Euptoieta hegesia* butterfly were collected on the Campus of Universidade Estadual de Campinas, SP, Brazil. Testis, vas deferens and vesicula seminalis were processed for Transmission Electron Microscopy to evaluate carbohydrate detection using different lectins (Sigma).

The reproductive tract was fixed in 0.5% glutaraldehyde (EMS), 4% paraformaldehyde, 0.2% picric acid (EMS), 3% sucrose and 5mM calcium chloride in 0.1M sodium phosphate buffer for 3 hours. After rising in the same buffer, free aldehyde groups were blocked in 50mM glycine in 0.2M sodium phosphate buffer overnight at 4°C and contrasted with 2% uranyl acetate (EMS) in 15% acetone for 2 hours also at 4°C. The specimens were dehydrated in acetone, embedded and finally included in LR White resin (EMS).

Ultrathin sections were collected on nickel grids and pre-incubated in PBS solution containing 1% bovine serum albumin/BSA (Sigma) and 0.1% Tween 20 for 1 hour at room temperature. Subsequently, the sections were incubated in PBS-BSA containing different gold-labeled lectins (Table 1), at a dilution of 1:5 for 1 hour at room temperature. The sections were washed in PBS and distilled water and contrasted in solutions of uranyl acetate (EMS) and lead citrate (EMS). The controls were made with the addition of the competing sugars (Sigma).

Results

Different labeling patterns were observed for the lectins used and the results are summarized in Table 2. The micronucleus was the structure most frequently labeled in apyrene cells. In eupyrene cells, the nucleus and the reticular appendages were the structures most frequently and intensely labeled. GS-I and GS-II were the lectins that presented the most intensely labeling. The lectin WGA was less detected in both apyrene and eupyrene cells. The HPA was the lectin that labeled the plasma membrane and all extracellular structures.

Apyrene Spermatids and Spermatozoa

Numerous micronuclei and a large cytoplasmic volume characterize apyrene spermatids. The micronucleus was the structure most intensely labeled (figs. A1-4) since it was labeled by all lectins, except by WGA. The cytoplasm of spermatids was intensely labeled only with GS-I (not shown) and GS-II (fig. A2), the other lectins present a very scattered marking. The plasma membrane showed N-acetilgalactosamine residues using HPA in the spermatids (figs. A1 and 5) and spermatozoa (fig. A6).

An anterior dense cap, an axoneme and two mitochondrial derivatives that present a paracrystalline core characterize apyrene spermatozoa. This anterior dense cap presented α -galactosamine, α -galactose residues, binding to GS-I and GS-II (not shown), and N-acetilgalactosamine residues, marked by HPA (figs. B11 and 12). The paracrystalline core of each mitochondrial derivative was labeled with PNA (not shown) and GS-I (fig. A7). The axoneme was not labeled by any lectin. In the extratesticular regions, these spermatozoa acquire several concentric layers around the plasma membrane that was intensely labeled with GS-I, GS-II (not shown) and HPA (fig. A9).

Eupyrene Spermatids and Spermatozoa

Early eupyrene spermatids are characterized by an acrosomal vesicle attached to the spherical nucleus and a large cytoplasmic volume. The acrosomal vesicle presented N-acetylglucosamine and N-acetylgalactosamine, evidenced by HPA (fig. B1) and WGA (fig. B2), respectively. No other acrosomic carbohydrates were identified (figs. B3 and 4). The nucleus of late spermatids was intensely labeled by GS-I and GS-II (fig. B4) and lightly labeled by PNA and HPA. The cytoplasm presented only α -galactosamine and α -galactose residues, marked by GS-I and GS-II (not shown).

Eupyrene spermatozoa contain an anterior region composed of a tubular acrosome and an elongated, compacted nucleus followed by a flagellar region composed of an axoneme and two mitochondrial derivatives without paracrystalline cores. They also have two elaborate extracellular structures, called laciniate and reticular appendages that extend for the entire sperm length and are well developed in the anterior region.

The nucleus was intensely labeled with GS-I (fig. B5), GS-II (fig. B6), PNA (fig. B7), UEA-I (figs. B8 and 9) and HPA (fig. B10). The tubular acrosome was apparently not labeled by any lectin. The plasma membrane of spermatids was intensely labeled with HPA (figs. C1 and 2). The reticular appendages presented D-galactose marked with PNA (fig. B7), α -galactosamine, α -galactose with GS-I and GS-II (figs. B5 and 6) and N-acetylgalactosamine with HPA (fig. B10) residues. These labels were very intense in the anterior region, where these two appendages are well developed. However, the HPA and GS-II lectins presented the same binding pattern for the reticular appendages in both the anterior (figs. B6 and 10) and flagellar regions (figs. C1 to 5). The laciniate appendages were labeled with GS-I (fig. B5), GS-II (fig. B6) and HPA (figs. C3 and 4). In the vas deferens, the spermatozoa lose their laciniate appendages, some of them being cast off intact from the membrane, while others gradually disintegrate into filaments. Both intact appendages and filaments were labeled with HPA (figs. C6 and 7), GS-I and GS-II (not shown). In the vesicula seminalis, eupyrene spermatozoa acquire a complex coat, with different electron densities, that presented α -galactosamine, α -galactose, shown by GS-I

(fig. C9) and GS-II, and N- acetyl galactosamine, by HPA (fig. C8). However, a dense region of this coat was not labeled by any lectins.

Discussion

The results of this study indicate that lectin specific sugars are widely distributed in apyrene and eupyrene spermatids and spermatozoa of *Euptoieta hegesia*.

The major concentration of lectin binding sites occurred in the **nucleus** of eupyrene spermatozoa. Of the six lectins studied, only WGA did not label this structure. Biochemical and cytochemical studies have shown the presence of sugar residues in the intracellular compartment, especially the nucleus (Stein *et al.*, 1975; Kan and Pinto da Silva, 1986; Londono and Bendayan, 1987; Báó and de Souza, 1992, 1993; Craveiro and Báó, 1995; Báó *et al.*, 2001). The nucleus of eupyrene spermatids, however, not presented an intense labeling. In fact, with the progressive chromatin condensation, labeling of the nuclear compartment gradually increases so that intense labeling is observed in the spermatozoa. The same labeling patterns were observed also in invertebrate (Coleoptera and Diptera, Craveiro and Báó, 1995 and Báó and de Souza, 1992, respectively) and vertebrate sperm (Anura, Báó *et al.*, 2001). This differential nuclear distribution suggests the involvement of glycoproteins in the process of nuclear condensation. Also, qualitative and quantitative variation of lectins in the nucleus can be correlated with changes in the nuclear activities.

The **micronucleus** of apyrene spermatids was labeled with all lectins, except with WGA, while the nucleus of eupyrene spermatids was labeled with GS-I, GS-II and UEA-I. These distinct lectin binding sites may be involved in the elongation process of the eupyrene nucleus and the degeneration of the apyrene ones. Light microscope studies have shown that, in elongated eupyrene nuclei, lysine rich nucleoproteins are replaced with arginine rich ones, while in apyrene nucleus only lysine rich nucleoproteins are detected. This differential protein distribution may reflect functional differences between the two types of cysts and is probably related to the regulation of dichotomy in lepidopteran spermiogenesis (Friedländer and Hauschteck-Jungen, 1982).

The anterior dense **cap** of the apyrene spermatozoa presented α -galactosamine, α -galactose (GS-I and GS-II) and N-acetilgalactosamine (HPA) residues; this last one was very labeled. In fact, previous cytochemical studies demonstrated the presence of protein (Craveiro and B  o, 1995; Medeiros, 1997; Mancini and Dolder, in preparation) and carbohydrates (Mancini and Dolder, in preparation) in this anterior cap. The origin of this structure is unknown. We believe that has extracellular components, because the HPA was the lectin that labeled all extracellular structures in apyrene and eupyrene sperm and also labeled this cap very strongly.

The **plasma membrane** of apyrene and eupyrene spermatids was intensely labeled with HPA, indicating that D-galactose residues are important components found in glycoproteins and glycolipids located on the surface cell, which are involved in the recognition, specificity and adhesion of gametic cells. Spermatozoa membranes are rich in sugar residues (Perotti and Riva, 1988; B  o and Souza, 1993; Perotti and Pasini, 1995). In *E. hegesia*, sperm membranes did not present asymmetry as was found for the sperm membrane of *Drosophila melanogaster* (Perotti and Riva, 1988) with Con-A labeling.

As a rule, the **acrosomal complex** is intensely labeled by different lectins that indicate glycosylated components of the acrosomal enzymes (Ahluwalia *et al.*, 1990; B  o and de Souza, 1992; Mart  nez-Men  rguez *et al.*, 1992; Craveiro and B  o, 1995; B  o *et al.*, 2001;). These components also have an important role in the enzymatic activation process, as well as in cell recognition and specificity. In *E. hegesia*, the detection of N-acetilgalactosamine and N-acetilglucosamine in the acrosomal vesicle indicates the probable participation of these carbohydrates in gamete recognition as well in the enzymatic activity of the acrosome. This detection, however, was only evident in the acrosomal vesicle and absent in the spermatozoon acrosome where this structure appears tubular and thin. Morphological and chemical modifications of this structure could result in the differential labeling observed.

The **reticular appendage** was more intensely labeled in the anterior region than along the flagellum, where it appears very small and compact. This differential morphology and compaction along the sperm length may explain the heterogeneous labeling. With high compaction, the sugar sites cannot be displayed, blocking the lectin sites. However, these

appendages could also present a heterogeneous distribution of carbohydrate residues along the sperm length. Previous studies demonstrated protein (Medeiros, 1986; Jamieson *et al.*, 1999; França and Bão, 2000; Mancini and Dolder, in preparation) and carbohydrate residues (Mancini and Dolder, in preparation) in these appendages.

The **laciniate appendages** were less labeled than the reticular appendage. This extracellular structure was intensely labeled with HPA along the entire sperm length but was also labeled with GS-I and GS-II. França and Bão (2000) detected intense and homogeneous basic protein in these appendages.

We believe that the laciniate appendages present predominantly proteic residues, while the reticular appendages present more carbohydrate residues. The present study did not find any evidence for an intracellular origin of both appendages. In fact, we observed that is no relation between the composition of these appendages and the intracellular compartment of eupyrene cells.

In the vesicula seminalis, some authors suggest that the eupyrene coat represents the rearrangement of the **laciniate appendages** (Phillips, 1971; Friedländer and Gitay, 1972; Kubo-Irie *et al.*, 1998). Here, the laciniate appendages and the coat of eupyrene spermatozoa were labeled with the same lectins, GS-I, GS-II and HPA. These results corroborate the hypothesis of rearrangement of the laciniate appendages within the male tract. We believe that these appendages contribute partially to the eupyrene coat in the vesicula seminalis, since this coat presents different regions, probably as a result of different components or degree of condensation. The dense region of the coat was not labeled by any lectin, also suggesting a different chemical composition. The apyrene coat was labeled with the same lectins as was the eupyrene coat, but we believe that these two coats are not of common origin, since the coat of apyrene sperm is formed by concentric layers of plasma membrane (Mancini and Dolder, in preparation).

The spermatozoa in Lepidoptera present several evident morphological modifications throughout the male and female reproductive tracts. Probably, these modifications are related to the maturation and capacitation of these cells, originating different glycosylated domains on the surface of the spermatozoa within the reproductive tract.

Acknowledgments

We would like to thank A. V. L. Freitas for supplying the butterfly and Sonia Nair Bão for help with the lectin method. This research was supported by the Brazilian Agency FAPESP (01/01049-6).

References

- Bão, S. N. and de Souza, W. 1992. Lectin binding sites on head structures of the spermatid and spermatozoon of the mosquito *Culex quinquefasciatus* (Diptera: Culicidae). **Histochem.** **98**: 365-371.
- Bão, S. N. and de Souza, W. 1993. Ultrastructural and cytochemical studies of the spermatid and spermatozoon of *Culex quinquefasciatus* (Culicidae). **J. Submicrosc. Cytol. Pathol.** **25**: 213-222.
- Bão, S. N., Vieira, G. H. C. and Fernandes, A. P. 2001. Spermiogenesis in *Melanophryniscus cambaraensis* (Amphibia, Anura, Bufonidae): ultrastructural and cytochemical studies of carbohydrates using lectins. **Cytobios** **106**: 203-216.
- Craveiro, D. and Bão, S. N. 1995. Localization of carbohydrates in spermatids of three chrysomelid beetles (Coleoptera, Chrysomelidae). **Biocell** **19**: 195-202.
- França, F. G. R. and Bão, S. N. 2000. Dimorphism in spermatozoa of *Anticarsia gemmatalis* Hübner, 1918 (Insecta, Lepidoptera, Noctuidae). **Braz. J. Morphol. Sci.** **17**: 5-10.
- Friedländer, M. and Gitay, H. 1972. The fate of the normal anucleated spermatozoa in inseminated female of the silkworm *Bombyx mori*. **J. Morphol.** **138**: 121-129.
- Friedländer, M. and Hauschteck-Jungen, E. 1982. Differential basic nucleoprotein kinetics in the two kinds of Lepidoptera spermatids: nucleate (eupyrene) and anucleate (apyrene). **Chromosoma (Berlin)** **85**: 387-398.
- Jamieson, B. G. M., Dallai, R. and Afzelius, B. A. 1999. **Insects: their spermatozoa and phylogeny**. Enfield, New Hampshire (USA) Science Publishers, Inc.

- Kan, F. W. K. and Silva, P. P. 1986. Preferential association of glycoproteins to the euchromatin regions of cross-fractured nuclei is revealed by fracture-label. **J. Cell Biol.** **102**: 576-586.
- Koehler, J. K. 1978. The mammalian sperm surface. Studies with specific labeling techniques. **Int. Rev. Cytol.** **54**: 73-195.
- Kubo-Irie, M., Irie, M., Nakazawa, T. and Mohri, H. 1998. Morphological changes in eupyrene and apyrene spermatozoa in the reproductive tract of the male butterfly *Atrophaneura alcinous* Klug. **Invert. Reprod. Develop.** **34**: 259-268.
- Londono, I. and Bendayan, M. 1987. Ultrastructural localization of mannoside residues on tissue sections: comparative evaluation of the enzyme-gold and the lectin-gold approaches. **Eur. J. Cell Biol.** **45**: 88-96.
- Martínez-Menárguez, J. A., Ballesta, J., Avilés, M., Castells, M. T. and Madrid, J. F. 1992. Cytochemical characterization of glycoproteins in the developing chromosome of rats. **Histochem.** **97**: 439-449.
- Medeiros, M. 1986. **Caracterização ultra-estrutural de espermatozóides eupirenes e apirenes de *Alabama argillacea* Hübner, 1818 (Lepidoptera: Noctuidae), ao nível dos testículos e das vias genitais de imagos machos e fêmeas até a espermateca.** Master Thesis. Instituto de Biologia, Universidade Estadual de Campinas.
- Medeiros, M. 1997. **Estudo ultra-estrutural da espermiogênese dicotômica de *Alabama argillacea* Hübner, 1818.** Doctor Thesis. Instituto de Biociências, Universidade Estadual de São Paulo.
- Nicolson, G. L. and Yanagimachi, R. 1972. Terminal saccharides on sperm plasma membranes: identification by specific agglutinins. **Science** **197**: 276-279.
- Perotti, M. E. and Riva, A. 1988. Concanavalin A binding sites on the surface of *Drosophila melanogaster* sperm: a fluorescence and ultrastructural study. **J. Ultrastruct. Mol. Struct. Res.** **100**: 173-182.
- Perotti, M. E. and Pasini, M. 1995. Glycoconjugates of the surface of the spermatozoa of *Drosophila melanogaster*: a qualitative and quantitative study. **J. Exp. Zool.** **271**: 311-318.

- Phillips, D. M. 1971. Morphogenesis of the laciniate appendages of lepidopteran spermatozoa. **J. Ultrastruct. Res.** 34: 567-585.
- Stein, G. S., Roberts, R. M., Davis, J. L., Head, W. J., Stein, J. L., Thrall, C. L., Van Veen, J. and Welch, D. W. 1975. Are glycoproteins and glycosaminoglycans components of the eukaryotic genome? **Nature** 258 (18): 639-641.
- Sharon, N and Lis, A. 1989. Lectins as cell recognition molecules. **Science** 246: 227-234.

Table 1: Lectins used as cytochemical probes and their sugar specificity.

Lectins	Sugar specificity
<i>Arachis hypogaea</i> (PNA)	D-galactose
<i>Griffonia simplicifolia</i> (GS I)	α -galactosamine, α -galactose
<i>Griffonia simplicifolia</i> (GS II)	α -galactosamine, α -galactose
<i>Helix pomatia</i> (HPA)	N-acetilgalactosamine
<i>Ulex europeus I</i> (UEA I)	L-fucose
<i>Triticum vulgaris</i> (WGA)	N-acetilglucosamine

Table 2: Summary of the labeling of ultrathin sections of LR White embedded spermatids and spermatozoa.

Lectins	Apyrene						Eupyrene						
	Spermatid			Spermatozoon			Spermatid			Spermatozoon			
	M	Mn	Ct	Cp	Pc	C	N	Av	Ct	N	Ra	La	C
PNA	-	+	-	-	+	-	-	-	-	++	+	-	-
GS I	-	+	+	+	+	+	+	-	+	++	++	+	+
GS II	-	+	+	+	-	+	+	-	+	++	+	+	+
HPA	+	+	-	+	-	+	-	+	-	+	++	+	+
UEA I	-	+	-	-	-	-	+	-	-	+	-	-	-
WGA	-	-	-	-	-	-	-	+	-	-	-	-	-

Abbreviations: Membrane (M); Micronucleus (Mn); Cytoplasm (Ct); Cap (Cp); Paracrystalline core (Pc); Coat (C); Nucleus (N); Acrosomal vesicle (Av); Reticular appendages (Ra) and Laciniate appendages (La).

Symbols: (-) represent the absence or very few particles; (+) and (++) represent the degree of particle concentration.

Figure Legends

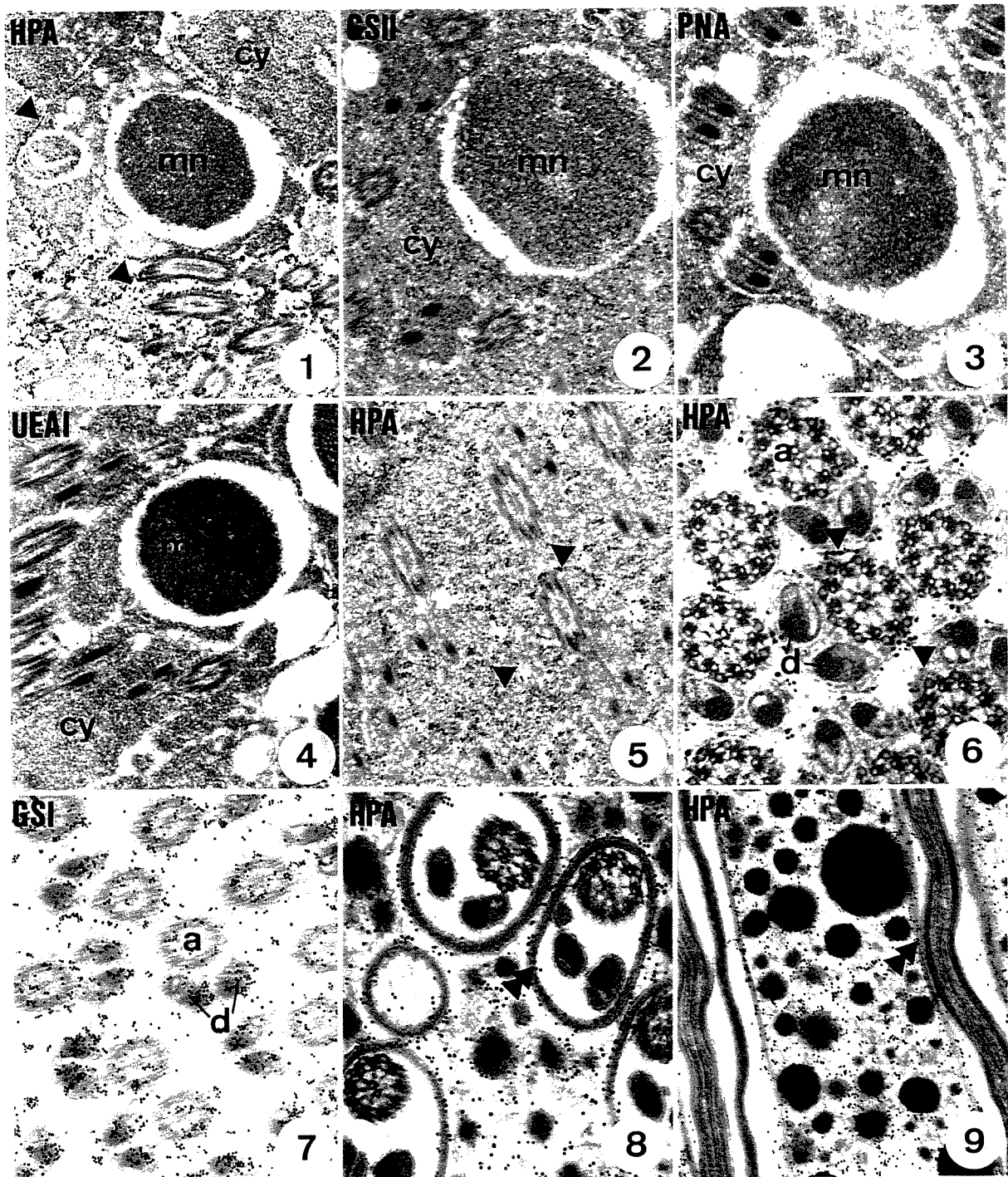
Figures A1 to 9: Apyrene Spermatids and Spermatozoa

Figs. 1 to 4: Spermatids showing the labeling of micronucleus (mn), and cytoplasm (cy) with HPA, GS-II, PNA and UEA-I, respectively. Note in fig. 1 the intense labeling of the plasma membrane (arrowhead) with HPA. 26000x

Figs. 5 and 6: Flagella of spermatids and spermatozoa, respectively, showing the plasma membrane (arrowhead) labeled with HPA. Axoneme (a) and mitochondrial derivatives (d). (5) 25000x; (6) 45000x

Fig. 7: Flagella of spermatozoa showing the labeling of the paracrystalline core of the mitochondrial derivatives (d) with GS-I. Axoneme (a). 30000x

Figs. 8 and 9: Flagella of spermatozoa from the vesicula seminalis showing the labeling of the apyrene coat (double arrowhead) with HPA. Note the labeling of the secretion that surrounds the spermatozoa. (8) 40000x; (9) 30000



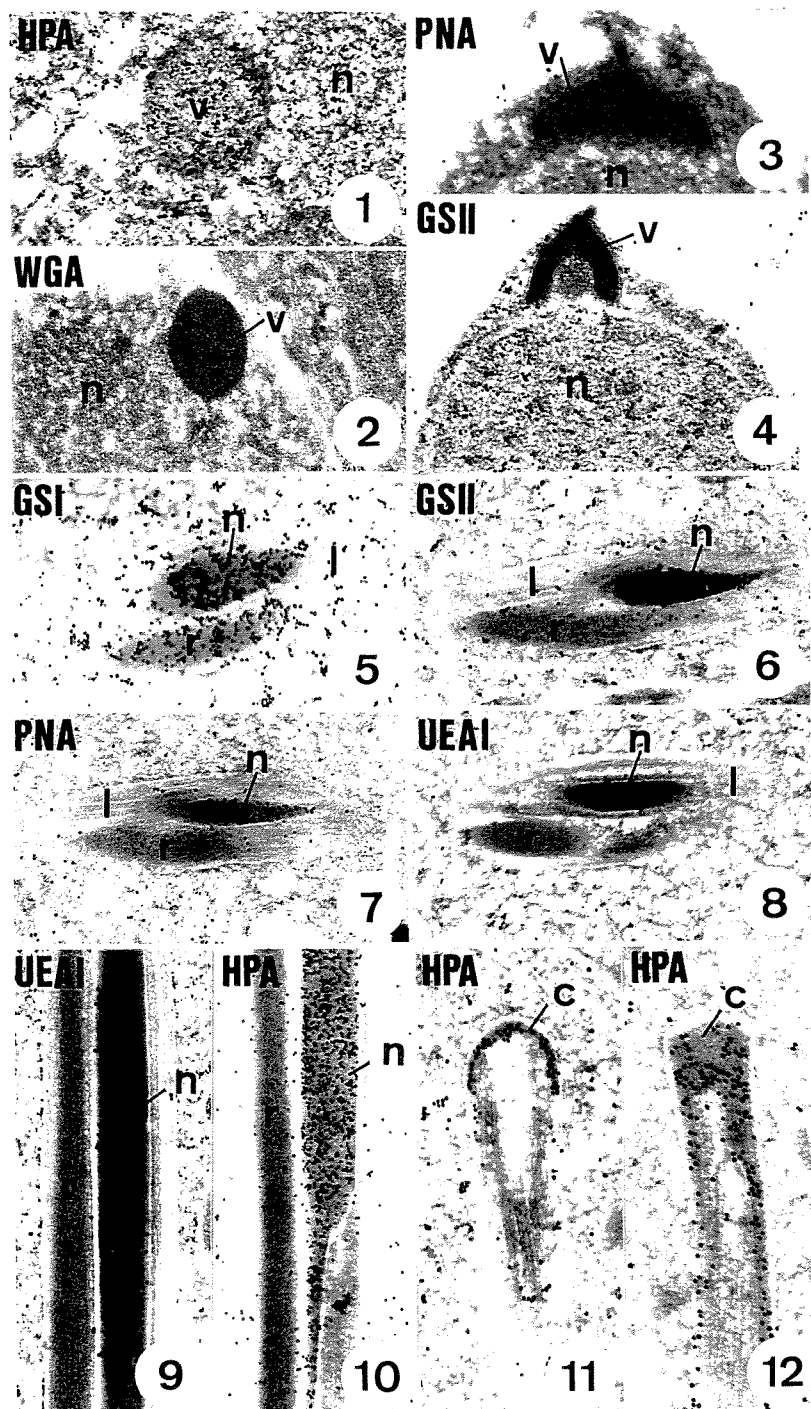
Figures B1 to 12: Anterior Region of apyrene and eupyrene cells

Figs. 1 to 4: Acrosomal vesicle (v) of eupyrene spermatids labeled with HPA (1) and WGA (2). PNA (3) while GS-II (4) does not present labeling. Note the differential labeling of the nucleus (n). (1) and (4) 30000x; (2) 54000x; (3) 50000x

Figs. 5 to 8: Anterior region of eupyrene spermatozoa showing differential labeling for nucleus (n), reticular (r) and laciniate (l) appendages with GS-I, GS-II, PNA and UEA-I, respectively. (5) 45000x; (6) and (7) 32000x; (8) 28000x

Figs. 9 and 10: Longitudinal sections of anterior region of eupyrene cells showing the labeling of nucleus (n) with UEA-I and HPA, respectively. The UEA-I (9) did not label the reticular appendage (r). (9) 42000x; (10) 76000x

Figs. 11 and 12: Longitudinal section of apyrene spermatid (11) and spermatozoa (12) showing the labeling of the cap (c) with HPA. (11) 42000x; (12) 50000



Figures C1 to 9: Eupyrene Spermatids and Spermatozoa

Fig. 1: Spermatids showing labeling of the plasma membrane (arrowhead) and the reticular appendage (r) with HPA. 32000x

Fig. 2: Flagella of spermatids showing the labeling of the reticular appendage (r) and the plasma membrane (arrowhead) with HPA. 25000x

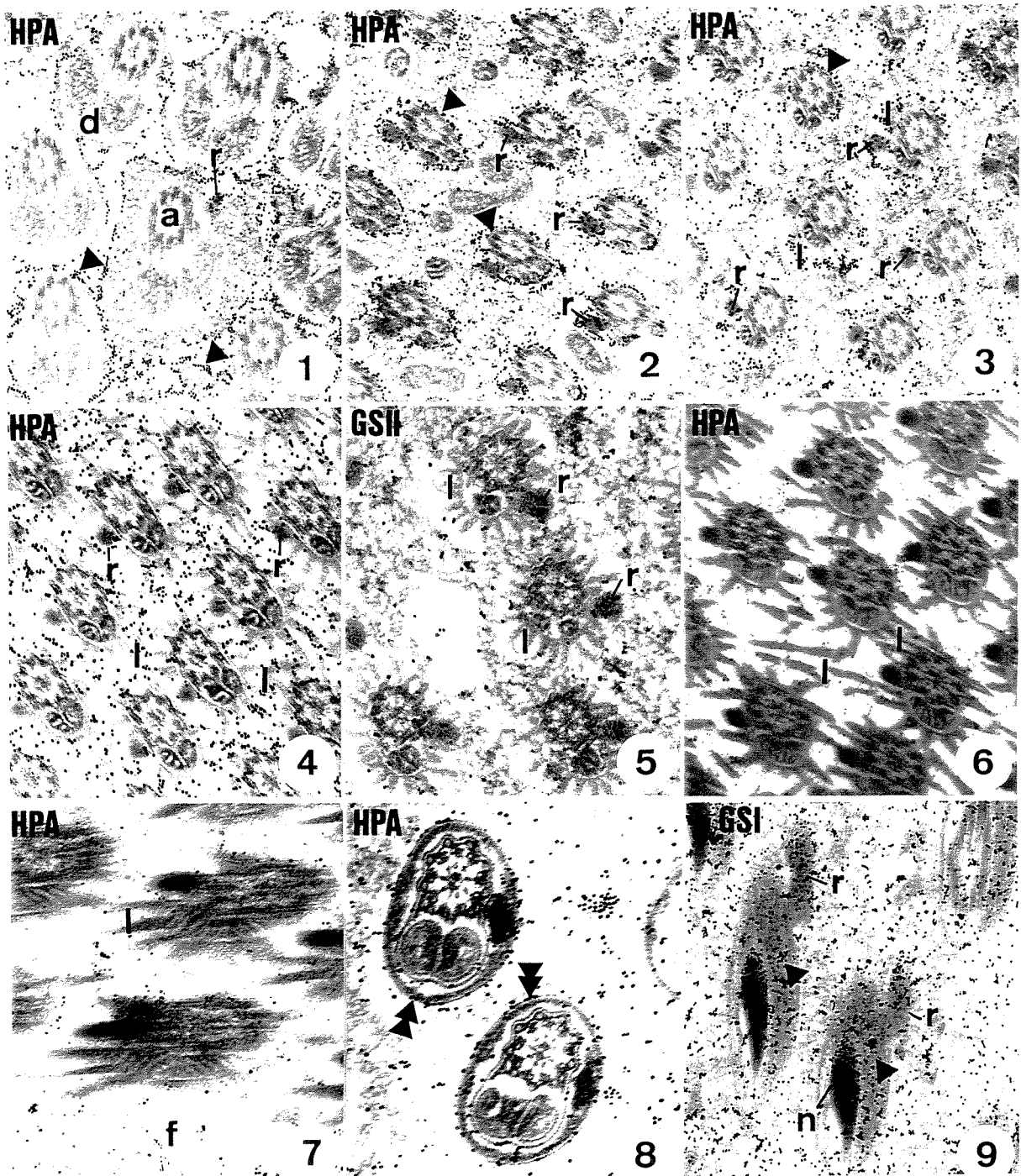
Figs. 3 and 4: Flagella of spermatozoa showing the labeling of reticular (r) and laciniate (l) appendages with HPA. (3) 32000x; (4) 42000x

Fig. 5: Flagella of spermatozoa showing the labeling of reticular appendages (r) with GS-II. Note the labeling of the cyst cell. 43000x

Figs. 6 and 7: Flagella of spermatozoa with labeled laciniate appendages (l) attached to the membrane, disconnected (6) or reduced to filaments (f). (6) 42000x; (7) 70000x.

Fig. 8: Eupyrene spermatozoa from the vesicula seminalis showing the labeling of the complex coat (double arrowhead) with HPA. Note the labeling of the matrix that surrounds the spermatozoa. 54000x.

Fig. 9: Eupyrene spermatozoa from the vesicula seminalis showing the labeling of the complex coat (arrowhead), reticular appendage (r) and nucleus (n) with GS-II. Note the labeling of the matrix that surrounds the spermatozoa. 25000x



2.4

Immunocytochemical Evidence of Tubulin Isoforms in Spermatids and Spermatozoa of *Euptoieta hegesia* (Lepidoptera: Nymphalidae)

Mancini K¹, Fernandes AP² and Dolder H¹

Running title: Tubulin in Lepidoptera Sperm

Institutions:

¹Departamento de Biologia Celular, IB, 6109, Unicamp, 13084-971, Campinas, SP, Brasil.

²Departamento de Biologia Celular, IB, UnB, 70919-970, Brasília, DF, Brasil

Abstract

A comparative analysis of the distribution of tubulin isoforms in apyrene and eupyrene sperm of *Euptoieta hegesia* butterflies was carried out, also verifying the presence of tubulin in laciniate appendages of the eupyrene sperm. Ultra thin sections of LR White embedded spermatids and spermatozoa were labeled for alpha, beta, gamma, alpha-acetylated and alpha-tyrosinated tubulin. Apyrene and eupyrene spermatids show the same antibody recognition pattern for tubulin isoforms. All tubulin isoforms were detected in axonemal microtubules. Alpha and gamma tubulin were also detected on the cytoplasmic microtubules. However, for beta and tyrosinated tubulin only scattered labeling was detected on cytoplasmic microtubules and acetylated tubulin was not detected. In apyrene and eupyrene spermatozoa only the axoneme labeling was analyzed because the cytoplasmic microtubules had been eliminated. Alpha, beta and tyrosinated tubulin were easily detected on the apyrene and eupyrene axoneme; gamma tubulin was strongly marked on eupyrene axonemes but was scattered on the apyrene ones. Acetylated tubulin appeared with scattered labeling on the axoneme of both sperm types. Our results demonstrate significant differences in tubulin isoform distribution in apyrene and eupyrene axonemal and cytoplasmic microtubules. Extracellular structures were not labeled by antibodies against for any tubulin isoforms. The extracellular structures, especially the laciniate appendages, are not formed of tubulin.

Keywords: immunocytochemistry – tubulin – apyrene – eupyrene – laciniate appendages.

Introduction

The best-known case of sperm polymorphism occurs in butterflies and moths, which produce two distinct sperm types called apyrene and eupyrene spermatozoa (Riemann, 1970; Katsuno, 1977; Lai-Fook, 1982; Kubo-Irie *et al.*, 1998; Jamieson *et al.*, 1999; França and Bão, 2000; Mancini and Dolder, 2001). In general, eupyrene spermatozoa contain a nucleus and an acrosome, constituting an elongated head, and a long tail, whereas apyrene spermatozoa have a proximal tip covered by a dense cap and also a long tail.

However, the most evident difference is the elaborate extracellular structures present in eupyrene spermatozoa, which undergo morphological modifications along the male and female reproductive tract (Riemann, 1970; Phillips, 1971; Riemann and Thorson, 1971; Friedländer and Gitay, 1972; Lai-Fook, 1982; Kubo-Irie *et al.*, 1998). In the testis, they possess two exclusive appendages, called the laciniate and reticular appendages (Phillips, 1970, 1971; Jamieson *et al.*, 1999).

In the extra testicular regions, the eupyrene sperm lose their laciniate appendages and acquire a complex coat (Phillips, 1971; Riemann and Thorson, 1971; Lai-Fook, 1982; Kubo-Irie *et al.*, 1998; Mancini and Dolder, 2001). The apyrene spermatozoa, however, present a less complex extracellular coat, acquired only in the extra testicular regions (Phillips, 1971; Friedländer and Gitay, 1972; Kubo-Irie *et al.*, 1998; Garvey *et al.*, 2000; Mancini and Dolder, 2001).

The chemical composition of these appendages as well as the coats of both sperm types still remains unclear. Previous ultrastructural studies suggested that the laciniate appendages were tubulin-containing structures; its mean, intracellular formations being derived from transient microtubules of elongating eupyrene spermatids (Friedländer, 1976; Friedländer and Gershon, 1978; Jamieson *et al.*, 1999).

Microtubules are found in almost all eukaryotes cell types associated with many cellular functions, such as cell division, morphogenesis, flagellar and ciliary motility, intracellular transport and cytoskeletal organization. This multiplicity of functions is thought to rely on the differentiation of various intracellular microtubule populations. These populations are generated by tubulin isoforms, as products of multigenic families, as well

as post-translational modifications of tubulins and differential binding of associated proteins (Schulze *et al.*, 1987; MacRae, 1997; Ludueña, 1998).

Microtubules are comprised of heterodimeric complexes of alpha and beta tubulin isotypes (Fosket and Morejohn, 1992; Ludueña, 1998). The third isotype, the gamma tubulin, has a 28-35% sequence identical to the classical alpha and beta tubulin (Oakley and Oakley, 1989; Ludueña, 1998). In addition, alpha and beta tubulin undergo a variety of post-translational modifications that include: (1) acetylation or (2) tyrosination /detyrosination of alpha tubulin and (3) phosphorylation, (4) polyglutamylation or (5) polyglycylation of alpha and beta tubulins (McRae, 1997; Ludueña, 1998). The functional significance of these isoforms is being elucidated. Tubulin in highly stable microtubules is almost invariably acetylated and tyrosinated, although the relationship between post-translational modifications and stability remains unclear (Bulinski and Gudersen 1991).

Here, we made a comparative analysis of tubulin isoform distribution in a pyrene and eupyrene sperm of *Euptoieta hegesia* butterflies and a verification of the possible presence of tubulins in laciniate appendages.

Materials and methods

Adult males of the butterfly *Euptoieta hegesia* were collected on the Campus of the Universidade Estadual de Campinas (SP – Brazil). Testis and seminal vesicle were dissected and used for transmission electron microscope and immunocytochemistry.

Transmission Electron Microscopy

(1) Specimens were fixed in 2.5% glutaraldehyde, 4% paraformaldehyde, 1.5% sucrose, 5mM CaCl₂ in a 0.1M sodium phosphate buffer for 12 hours at 4°C. After fixation, they were rinsed in the same buffer, post-fixed in 1% osmium tetroxide for 3-5 hours at 4°C, dehydrated in acetone and embedded in Epoxy resin.

(2) Specimens were fixed in 2,5% glutaraldehyde, 1% tannic acid, 1,5% sucrose and 5mM calcium chloride in 0.1M sodium phosphate buffer for three days at 4°C. The materials were rinsed in the same buffer and contrasted in an aqueous solution of 1% uranyl acetate for 2 hours at room temperature (Dallai and Afzelius 1990). They were dehydrated in acetone and embedded in Epoxy Resin.

(3) Specimens were fixed in 2.5% glutaraldehyde, 1% ruthenium red in 0.1M sodium cacodylate buffer for 2 hours, in the dark, at room temperature and then washed in the same buffer. They were post-fixed in 1% osmium tetroxide in sodium cacodylate buffer for 1 hour, followed by 1% osmium tetroxide, 1% ruthenium red in sodium cacodylate buffer, in the dark, at room temperature and then washed in the same buffer. They were dehydrated in acetone and embedded in Epoxy resin.

The ultra thin sections obtained for the three methods were contrasted with uranyl acetate and lead citrate and observed in a transmission electron microscope (LEO 906).

Immunocytochemistry

Specimens were fixed in 0.5% glutaraldehyde, 4% paraformaldehyde, 0.2% picric acid, 3% sucrose and 5mM calcium chloride in 0.1M sodium phosphate buffer for 3 hours at room temperature. After rising in the same buffer, free aldehyde groups were quenched with 50mM glycine in 0.2M sodium phosphate buffer overnight at 4°C and contrasted with 2% uranyl acetate in 15% acetone for 2 hours also at 4°C. The specimens were dehydrated in acetone and embedded in LR White resin.

The ultrathin sections were collected on nickel grids, pre-incubated in phosphate buffered saline (PBS) containing 1.5% bovine albumin (PBS-BSA) and 0.01% Tween 20, and subsequently incubated for 1 hour in monoclonal antibodies against alpha-tubulin (clone DMIA), alpha-acetylated-tubulin (clone 6-11B-1), alpha-tyrosinated-tubulin (clone TUB-1A2), beta-tubulin (clone TUB 2.1) and gamma-tubulin (clone GTU-88) at a dilution of 1:100 (British Biocell International, England). After washing with PBS-BSA, the grids

were incubated for 1 hour with the respective labeled secondary antibody-Au (mouse or rabbit-IgG-Au-conjugated 10nm) at a dilution of 1:20. After incubation, the grids were washed with PBS and distilled water, stained with uranyl acetate and lead citrate and observed in a transmission electron microscope.

Results

Ultrathin sections of LR White embedded spermatids and spermatozoa were labeled against alpha, beta, gamma, alpha-acetylated and alpha-tyrosinated tubulins. The results are summarized in Table 1.

Apyrene and Eupyrene Spermatids

Abundant cytoplasm, a 9+9+2 axoneme type, two mitochondrial derivatives and the reticular appendage attached to the plasma membrane characterize the tail of eupyrene spermatids (fig. 1A). Apyrene spermatids are characterized by a large amount of cytoplasm, a 9+9+2 axoneme type and two mitochondrial derivatives with paracrystalline cores (fig. 1B). Both spermatids types also present cytoplasmic microtubules layers that surround the developing mitochondrial derivatives (figs. 1A-B).

Apyrene and eupyrene spermatids show the same antibody recognition pattern for tubulin isoforms. Alpha-tubulin was detected on the axonemal microtubules as well as on the cytoplasmic microtubules that surround the mitochondrial derivatives (fig. 1C). Beta-tubulin was detected on the axonemal microtubules but their occurrence on the cytoplasmic microtubules appears to be scattered (fig. 1D). Gamma-tubulin was detected on the axoneme and on the cytoplasmic microtubules that surround mitochondrial derivatives (fig. 1E) and nucleus (fig. 1H). Acetylated tubulin was detected scattered on the axoneme but not in the cytoplasm (fig. 1F). Tyrosinated tubulin was detected on the axoneme and scattered in the cytoplasmic microtubules of the tail (fig. 1G), as well as on the head cytoplasmic microtubules that surround the nucleus (fig. 1I).

Apyrene and Eupyrene Spermatozoa

The tail of apyrene and eupyrene spermatozoa is characterized by a 9+9+2 axoneme type and two mitochondrial derivatives (figs. 2A and 3A-B, respectively). The eupyrene one also presents two exclusive extracellular structures, denominated reticular and laciniate appendages, which present a paracrystalline organization, with circular subunits observed in transverse sections, when the tannic acid and ruthenium red techniques are applied (figs. 3A-B, respectively). In the extra testicular regions, the eupyrene sperm lack the laciniate appendages, and both sperm types acquire an extracellular coat (figs. 2B and 3H).

In apyrene and eupyrene spermatozoa, only the axoneme was labeled (figs. 2C-J and 3C-G, I-K). The cytoplasmic layers of microtubules, which surrounded the nucleus and the mitochondrial derivatives, had been eliminated. The labeling pattern for tubulin isoforms on axonemal microtubules of apyrene and eupyrene spermatozoa was similar. In general, alpha tubulin was most intensely labeled (figs. 2C and 3C) and beta tubulin was also clearly detected (fig. 2D and 3D). Gamma tubulin was strongly marked on eupyrene axonemes (fig. 3E) but it was scattered on apyrene ones (fig. 2E). Acetylated tubulin label was sparsely scattered on both apyrene (fig. 2F) and eupyrene (fig. 3F) axonemal microtubules. Tyrosinated tubulin, however, was clearly detected on eupyrene axonemes (fig. 3G), as well as on apyrene ones (fig. 2G).

Extracellular structures were not labeled by antibodies against any tubulin isoforms. Reticular and laciniate appendages of intratesticular eupyrene spermatozoa did not show any labeling (figs. 3C-G) as also happens with the apyrene and eupyrene coats acquired in extra testicular regions (figs. 2H-J and 3I-K). Axonemal microtubules of apyrene (figs. 2H-J) and eupyrene (3I-K) spermatozoa from the seminal vesicle show similar tubulin distribution as seen in these cell types from the testis.

Discussion

The sperm polymorphism that occurs in the Lepidoptera order results in two sperm types, which differ in morphology and function. The eupyrene sperm are responsible for egg fertilization, while the apyrene ones, which are devoid of a nucleus, are involved in sperm competition (Drummond, 1984; Silberglied *et al.*, 1984; Gage, 1994; Cook and Wedell, 1996, 1999; Snook, 1997, 1998). The situation becomes more complicated due to the presence of exclusive eupyrene appendages, whose chemical composition and functions are still not elucidated. Besides this, both sperm types, especially the eupyrene one, undergo several extracellular modifications along the reproductive tracts and the importance of these structures remains unclear.

Only few ultrastructural studies developed some cytochemical aspects on apyrene and eupyrene sperm (Friedländer, 1976; Friedländer and Gershon, 1978; França and Bão, 2000). Wolf (1992, 1996a, 1996b, 1997) and Wolf and collaborators (1988, 1991a, 1991b, 1996) made important studies using immunofluorescence for tubulin distribution on Lepidoptera spermatocytes and early spermatids.

Here, we carried out a comparative analysis of tubulin isotypes (alpha, beta and gamma) and their post-translational modifications (alpha-acetylated and alpha-tyrosinated) distributed in late spermatids and spermatozoa from the testis and seminal vesicle of *Euptoieta hegesia* butterflies. Our results demonstrate differences in tubulin isoform types and their post-translational modifications in apyrene and eupyrene axonemal and cytoplasmic microtubules.

The compartmentalization of distinct tubulin isoforms has been demonstrated within several classes of cytoplasmic microtubules (Delgado-Viscogliosi *et al.*, 1996; Lopes *et al.*, 2001) and axonemal microtubules (Fouquet *et al.*, 1996; Gagnon *et al.*, 1996; Multigner *et al.*, 1996; Kann *et al.*, 1998; Johnson, 1998; Fernandes and Bão, 2001; Mencarelli *et al.*, 2000).

All tubulin isoforms applied are present in the axonemal microtubules of *E. hegesia*. In fact, previous cytochemical studies (Mancini and Dolder, in preparation) reported

differential labeling for carbohydrate and protein in axonemal microtubules of apyrene and eupyrene spermatozoa.

Alpha and beta tubulins were the most strongly labeled isoforms on apyrene and eupyrene axonemal microtubules of spermatids and spermatozoa. In fact, these tubulin isotypes are known to form the heterodimeric unit that assembles the microtubules. Cytoplasmic microtubules presented alpha tubulin but not beta tubulin isoform. In contrast, in spermatids of the phytophagous bugs, alpha tubulin was detected only in the axoneme and beta tubulin was detected in both axoneme and cytoplasmic microtubules (Fernandes and B áo, 2001). In the beetle *Diabrotica speciosa* spermatids, alpha tubulin was clearly detected in both axonemal and cytoplasmic microtubules (Fernandes and B áo, 1996). The differential alpha and beta tubulin contents of axonemal and cytoplasmic microtubules indicate a distinct composition for these microtubules.

Gamma tubulin is involved in microtubule nucleation. It appears in the microtubules organizing centers (Joshi, 1994), as the spindle pole body (Oakley *et al.*, 1990), the pericentriolar material (Fuller *et al.*, 1995), and the basal body (Liang *et al.*, 1996). It binds to their minus ends (Li and Joshi, 1995) and can self-assemble into a novel tubular structure (Shu and Joshi, 1995). Here, this isotype is well distributed on both axonemal microtubules and on cytoplasmic microtubules of eupyrene and apyrene spermatozoa. In the phytophagous bug spermatids, this tubulin isoform is not present on the axoneme microtubules (Fernandes and B áo, 2001).

Acetylation seems to occur in tubulin after it has been incorporated into microtubules (Sasse and Gull, 1988; Wilson and Forer, 1989). It has been correlated with flagellar assembly (L'Hernault and Rosenbaum, 1985). It is, generally, an indicator of stable microtubules and is particularly notable in axonemal microtubules (Schulze *et al.*, 1987; Webster and Borisy, 1989; Takemura *et al.*, 1992; Ludueña, 1998). Nevertheless, in unicellular organisms such as *Trichomonas vaginalis*, *T. foetus* and *Trypanosoma brunei* acetylated tubulin has been demonstrated in instable microtubules during the elongating phase and mitosis (Sasse and Gull 1988; Delgado-Viscogliosi *et al.* 1996; Lopes *et al.* 2001). Here, we detected scattered acetylated tubulin on the axonemal stable microtubules. No labeling was observed on cytoplasmic microtubules.

Tyrosination has been seen reported in a variety of cytoplasmic microtubules in vertebrates (Gudersen *et al.* 1984; Arregui and Barra 1995) and is common in the interphase network and in the spindle (Ludueña 1998). It was detected in the A-tubules of the peripheral doublets of *Chamydomonas* (Johnson 1998) and sea urchin axonemes (Multigner *et al.* 1996). In the *Apis mellifera* sperm axoneme, the accessory microtubules presented less tyrosinated alpha tubulin than the other axonemal microtubules (Mencarelli *et al.* 2000). The functional significance of this isotype has not been elucidated. In *E. hegesia*, these post-translational modifications were detected on both axonemal and cytoplasmic microtubules; in the latter it was very scattered.

There was no labeling for tubulins on any extracellular structure of apyrene and eupyrene spermatozoa. Previous observations in *E. hegesia* sperm indicate that carbohydrates and proteins compose the extracellular structures: reticular and laciniate appendages and extra testicular coat of both sperm types (Mancini and Dolder, in preparation). According to Friedländer (1976) the laciniate appendages are transitory forms of tubulin, which are destined to generate these appendages or other non-microtubular structures. They may generate these structures after having contributed to the process of nuclear elongation. Additional support for this theory was supplied by treatment in vivo with the antimitotic agent vinblastine sulphate by Friedländer and Gershon (1978). The laciniate appendages react to vinblastine, as do tubulin-containing structures. The laciniate appendages appeared to be microtubular derivatives, although they lacked the structure of any of the known polymorphic tubulin forms. Here, we did not find any evidence for this theory.

The cytoplasmic microtubules are located surrounding the nucleus of eupyrene sperm and mitochondrial derivatives of both sperm types. In fact, for the eupyrene spermatozoa the microtubular living corresponds to the extracellular location of laciniate appendages. We disagree with Friedländer (1976) and Friedländer and Gershon (1978) that these appendages are formed of tubulin. However, these cytoplasmic microtubules could contribute to the formation and orientation of the laciniate appendages. The differential distribution among microtubules of different cytoplasmic regions suggests that the isoforms

and their post-translational modifications play a role in determining the biochemical and functional specificity of microtubules.

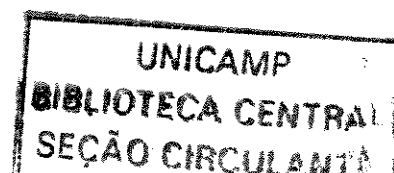
References

- Arregui, C. O. and Barra, H. S. 1995. Segmented pattern of tyrosinated microtubules assembly in neuritis of chick retinal neurons. **Biocell** **19**: 49-55.
- Bulinski, J. C. and Gudersen, G. G. 1991. Stabilization and post-translational modification of microtubules during cellular morphogenesis. **Bioessays** **13**: 285-293.
- Cook, P. A. and Wedell, N. 1996. Ejaculate dynamics in butterflies: a strategy for maximizing fertilization success. **Proc. Royal Soc. London B** **263**: 1047-1051.
- Cook, P. A. and Wedell, N. 1999. Non-fertile sperm delay female remating. **Nature** **397**: 486.
- Dallai, R. and Afzelius, B. A. 1990. Microtubular diversity in insect spermatozoa: results obtained with a new fixative. **J. Struct. Biol.** **103**: 164-179.
- Delgado-Viscogliosi, P., Brugerolle, G. and Viscogliosi, E. 1996. Tubulin post-translational modifications in the primitive protist *Trichomonas vaginalis*. **Cell Motil. Cytoskel.** **33**: 288-297.
- Drummond, B. A. 1984. **Multiple mating and sperm competition in the lepidoptera**. In: Smith RL. Sperm competition and the evolution of animal mating systems. Academic Press, London. pp 291-370.
- Fernandes, A. P. and Báo, S. N. 1996. Ultrastructural study of the spermiogenesis and localization of tubulin in spermatid and spermatozoon of *Diabrotica speciosa* (Coleoptera: Chrysomelidae). **Cytobios** **86**: 231-241.
- Fernandes, A. P. and Báo, S. N. 2001. Immunoelectron microscopy detection of tubulins during the spermiogenesis of phytophagous bugs (Hemiptera: Pentatomidae). **Invert. Reprod. Develop.** **40**: 163-170.
- Fosket, D. E. and Morejohn, L. C. 1992. Structural and functional organization of tubulin. **Annu. Rev. Plant Physiol. Plant Mol. Biol.** **43**: 201-240.

- Fouquet, P.-J., Eddé, B. and Kann, M. L. 1996. Comparative immunogold analysis of tubulin isoforms in the mouse sperm flagellum: unique distribution of glutamylated tubulin. **Mol. Reprod. Dev.** **43**: 358-365.
- França, F. G. R. and Báó, S. N. 2000. Dimorphism in spermatozoa of *Anticarsia gemmatalis* Hübner, 1918 (Insecta, Lepidoptera, Noctuidae). **Braz. J. Morphol. Sci.** **17**: 5-10.
- Friedländer, M. 1976. The role of transient perinuclear microtubules during spermiogenesis of the warehouse moth *Ephestia cautella*. **J. Submicrosc. Cytol.** **8**: 319-326.
- Friedländer, M. and Gershon, J. 1978. Reaction of surface lamella of moth spermatozoa to vinblastine. **J. Cell Sci.** **30**: 353-361.
- Friedländer, M. and Gitay, H. 1972. The fate of the normal anucleated spermatozoa in inseminated female of the silkworm *Bombyx mori*. **J. Morphol.** **138**: 121-129.
- Fuller, S. D., Gowen, B. E., Reinsch, S., Sawyer, A., Buendia, B., Wepf, R. and Karsenti, E. 1995. The core of the mammalian centriole contains gamma-tubulin. **Curr. Biol.** **5**: 1384-1393.
- Gage, M. J. G. 1994. Associations between body size, mating pattern, testis size and sperm lengths across butterflies. **Proc. Royal Soc. London B** **258**: 247-254.
- Gagnon, C., White, D., Cosson, J., Huitorel, P., Eddé, B., Desbruyères, E., Paturle-Lafanechère, L., Multigner, L., Jod, D. and Cibert, C. 1996. The polyglutamylated lateral chain of alpha-tubulin plays a key role in flagellar motility. **J. Cell Sci.** **109**: 1545-1553.
- Garvey, L. K., Gutierrez, G. M. and Krider, H. M. 2000. Ultrastructure and morphogenesis of the apyrene and eupyrene spermatozoa in the gypsy moth. **Ann. Entomol. Soc. Am.** **93**: 1147-1155.
- Gudersen, G. G., Kalmoski, M. H., Bulinski, J. C. 1984. Distinct populations of microtubules: tyrosinated and nontyrosinated alpha tubulin are distributed differently in vivo. **Cell** **38**: 779-789.
- Jamieson, B. G. M., Dallai, R. and Afzelius, B. A. 1999. **Insects: their spermatozoa and phylogeny**. Enfield, New Hampshire (USA) Science Publishers, Inc.

- Johnson, K. A. 1998. The axonemal microtubules of the *Chlamydomonas* flagellum differ in tubulin isoform content. **J. Cell Sci.** **111**: 313-320.
- Joshi, H. C. 1994. Microtubules organizing center and gamma-tubulin. **Curr. Opin. Cell Biol.** **6**: 55-62.
- Kann, M., Prigent, Y., Levilliers, N., Bré, M. and Fouquet, J. 1998. Expression of glycylation tubulin during the differentiation of spermatozoa in mammals. **Cell Motil. Cytoskel.** **41**: 341-352.
- Katsuno, S. 1977. Studies on eupyrene and apyrene spermatozoa in the silkworm *Bombyx mori* L. (Lepidoptera: Bombycidae) III. The post-testicular behavior of the spermatozoa at various stages from pupa to the adult. **Appl. Entomol. Zool.** **12**: 241-247.
- Kubo-Irie, M., Irie, M., Nakazawa, T. and Mohri, H. 1998. Morphological changes in eupyrene and apyrene spermatozoa in the reproductive tract of the male butterfly *Atrophaneura alcinous* Klug. **Invert. Reprod. Develop.** **34**: 259-268.
- Lai-Fook, J. 1982. Structural comparison between eupyrene and apyrene spermiogenesis in *Calpodus ethlius* (Hesperiidae: Lepidoptera). **Can. J. Zool.** **60**: 1216-1230.
- L'Hernault, S. W. and Rosenbaum, J. L. 1985. Chlamydomonas alpha-tubulin is posttranslationally modified by acetylation on the Sigma-amino group of a lysine. **Biochem.** **24**: 473-478.
- Li, Q. and Joshi, H. C. 1995. Gamma tubulin is a minus end-specific microtubule binding protein. **J. Cell Biol.** **131**: 207-214.
- Liang, A., Ruiz, F., Heckmann, K., Klotz, C., Tollon, Y., Beisson, J. and Wright, M. 1996. Gamma tubulin is permanently associated with basal bodies in ciliates. **Eur. J. Cell Biol.** **70**: 331-338.
- Lopes, L. C., Ribeiro, K. C. and Benchimol, M. 2001. Immunolocalization of tubulin isoforms and post-translational modification in the protists *Tritrichomonas foetus* and *Trichomonas vaginalis*. **Histochem. Cell Biol.** **116**: 17-29.
- Ludueña, R. F. 1998. Multiple forms of tubulin: different gene products and covalent modifications. **Int. Rev. Cytol.** **178**: 207-275.

- Mencarelli, C., Bré, M., Levilliers, N. and Dallai, R. 2000. Accessory tubules and axonemal microtubules of *Apis mellifera* sperm flagellum differ in their tubulin isoform content. **Cell Motil. Cytoskel.** **47**: 1-12.
- MacRae, T. H. 1997. Tubulin post-translational modifications. Enzymes and their mechanisms of action. **Eur. J. Biochem.** **244**: 265-278.
- Mancini, K. and Dolder, H. 2001. Ultrastructure of apyrene and eupyrene spermatozoa from the seminal vesicle of *Euptoieta hegesia* (Lepidoptera: Nymphalidae). **Tissue and Cell** **33**: 301-308.
- Multigner, L., Pignot-Paintrand, I., Saoudi, Y., Job, D., Plessmann, U., Rüdiger, M. and Weber, K. 1996. The A and B tubules of the outer doublets of sea urchin sperm axonemes are composed of different tubulin variants. **Biochem.** **35**: 10862-10871.
- Oakley, C. E. and Oakley, B. R. 1989. Identification of gamma-tubulin, a new member of the tubulin superfamily encoded by *mipA* gene in *Aspergillus nidulans*. **Nature** **338**: 662-664.
- Oakley, B. R., Oakley, C. E., Ion, Y. and Jung, M. K. 1990. Gamma tubulin is a component of the spindle pole body that is essential for microtubule function in *Aspergillus nidulans*. **Cell** **61**:1289-1301.
- Phillips, D. M. 1970. Insect sperm: their structure and morphogenesis. **J. Cell Biol.** **44**: 243-277.
- Phillips, D. M. 1971. Morphogenesis of the laciniate appendages of lepidopteran spermatozoa. **J. Ultrastruc. Res.** **34**: 567-585.
- Riemann, J. G. 1970. **Metamorphosis of sperm of the cabbage looper *Trichoplusia ni* during passage from the testes to the female spermatheca.** In: Baccetti, B. Comparative Spermatology. Academic Press. New York. pp. 321-331.
- Riemann, J. G. and Thorson, B. J. 1971. Sperm maturation in the male and female genital tracts of *Anagasta kuhniella* (Lepidoptera: Pyralididae). **Int. J. Insect Morphol. Embryol.** **1**: 11-19.
- Sasse, R. and Gull, K. 1988. Tubulin post-translational modifications and the construction of microtubular organelles in *Trypanosoma brunei*. **Cell Sci.** **90**: 577-589.



- Schulze, E., Asai, D. J., Bulinski, J. C. and Kirschner, M. 1987. Post-translational modification and microtubule stability. **J. Cell Biol.** **105**: 2167-2177.
- Shu, H-B. and Joshi, H. C. 1995. Gamma-tubulin can both nucleate microtubule assembly and self-assemble into novel tubular structures in mammalian cells. **J. Cell Biol.** **130**: 1137-1147.
- Silberglied, R. E., Shepherd, J. G. and Dickinson, J. L. 1984. Eunuchs: the role of apyrene sperm in lepidoptera? **Am. Nat.** **123**: 255-265.
- Snook, R. R. 1997. Is the production of multiple sperm types adaptive? **Evolution** **51**: 797-808.
- Snook, R. R. 1998. The risk of sperm competition and the evolution of sperm heteromorphism. **An. Behav.** **56**: 1497-1507.
- Takemura, R., Okabe, S., Umeyama, T., Kanai, Y., Cowan, N. and Hirokawa, N. 1992. Increased microtubule-stability and alpha-tubulin acetylation in cells transfected with microtubule-associated proteins MAP1B, MAP2 or tau. **J. Cell Sci** **103**: 953-964.
- Webster, D. L. and Borisy, G. G. 1989. Microtubules are acetylated in domains that turnover slowly. **J. Cell Sci.** **92**: 57-65.
- Wilson, P. J. and Forer, A. 1989. Acetylated alpha-tubulin in spermatogenic cells of the crane fly *Nephrotoma suturalis*: kinetochore microtubules are selectively acetylated. **Cell Motil. Cytoskel.** **14**: 237-250.
- Wolf, K. W. 1992. Spindle membranes and microtubules are coordinately reduced in apyrene relative to eupyrene spermatocyte of *Inachis io* (Lepidoptera: Nymphalidae). **J. Submicrosc. Cytol. Pathol.** **24**: 381-394.
- Wolf, K. W. 1996a. Cytology of Lepidoptera VIII. Acetylation of alpha-tubulin in mitotic and meiotic spindles of two Lepidoptera species, *Ephesia kuehniella* (Pyralidae) and *Pieris brassicae* (Pieridae). **Protoplasma** **190**: 88-98.
- Wolf, K. W. 1996b. Immunocytochemical evidence of a tubulin reserve at the tip of growing flagella in spermatogenesis of the Mediterranean Mealmoth, *Ephesia kuehniella* Z. (Pyralidae, Lepidoptera, Insecta). **Acta Zool. (Stockholm)** **77**: 79-84.

- Wolf, K. W. 1997. Centrosome structure is very similar in eupyrene and apyrene spermatocyte of *Ephesia kuehniella* (Pyrilidae: Lepidoptera: Insecta). **Invert. Reprod. Develop.** **31**: 39-46.
- Wolf, K.W., Baumgart, K. and Traut, W. 1988. Cytology of Lepidoptera. II. Fine structure of eupyrene and apyrene primary spermatocytes in *Orgyia thyellina*. **Eur. J. Cell Biol.** **44**: 57-67.
- Wolf, K. W. and Bastmeyer, M. 1991a. Cytology of Lepidoptera. V. The microtubule cytoskeleton in eupyrene spermatocyte of *Ephesia kuehniella* (Pyrilidae), *Inachis io* (Nymphalidae) and *Orgyia antiqua* (Lymantriidae). **Eur. J. Cell Biol.** **55**: 225-237.
- Wolf, K. W. and Bastmeyer, M. 1991b. Cytology of Lepidoptera. VI. Immunolocalization of microtubules in detergent-extracted apyrene spermatocytes of *Kuehniella* Z. **Eur. J. Cell Biol.** **55**: 238-247.
- Wolf, K. W. and Joshi, H. C. 1996. Microtubule organization and distribution of gamma-tubulin in male meiosis of Lepidoptera. **Mol. Reprod. Develop.** **45**: 547-559.

Table 1: Quantitative approach of tubulins isoforms detection

<u>Antibodies</u> (anti-tubulins)	<u>Spermatid</u>		<u>Spermatozoa</u>		
	Axoneme	Cytoplasm	Axoneme		Extracellular structures
			Apy	Eup	
Alpha	++++	+++	++++	++++	-
Beta	++++	+	++++	+++	-
Gamma	+++	++	+	++	-
Alpha-acetylated	+	-	+	+	-
Alpha-tyrosinated	++	+	++	++	-

The signals represent the approximated number of particles per region (axoneme and cytoplasm): (+): 1-5; (++) : 6-10; (+++) : 11-15; (++++): 15-20; (-) particles not found.

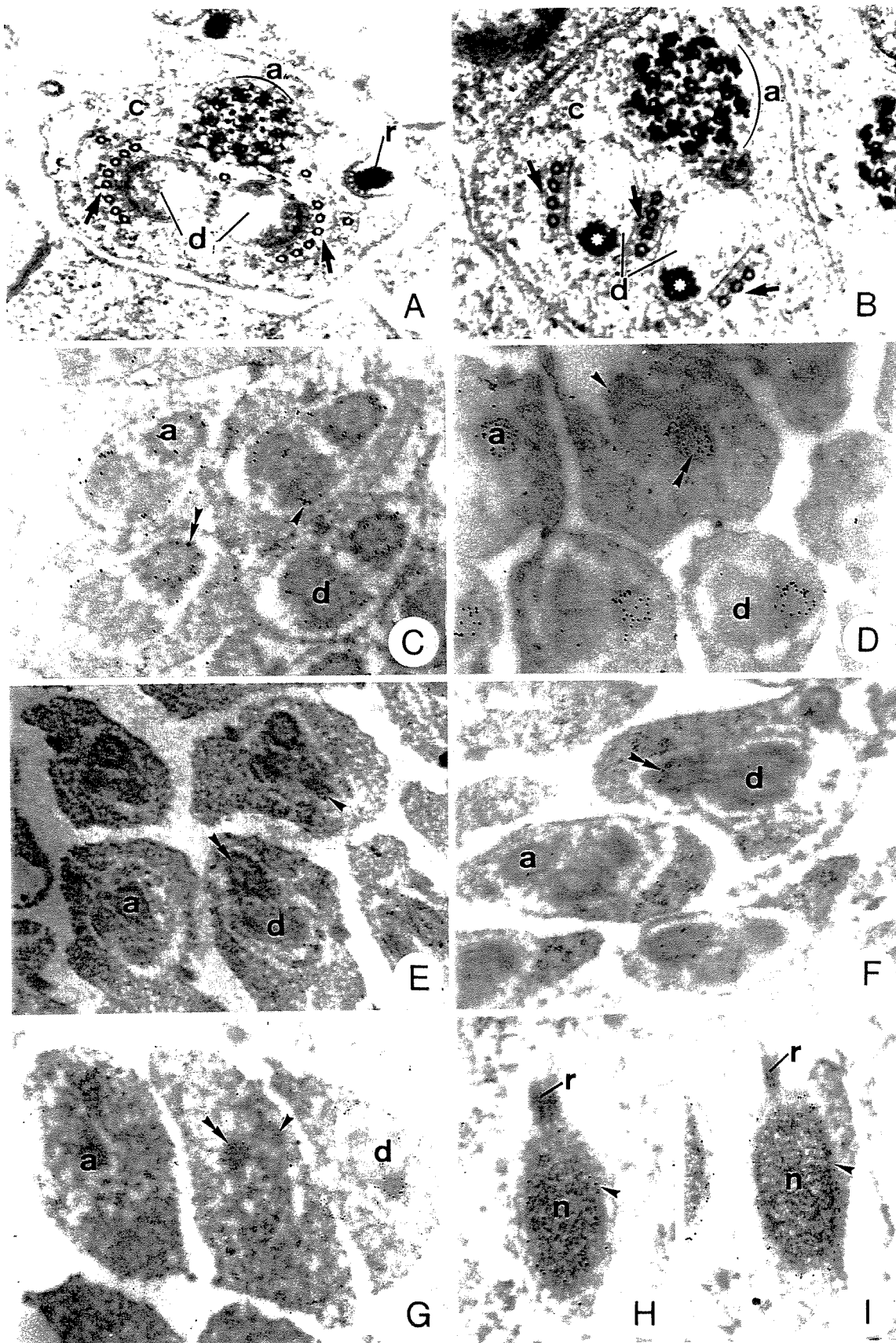
Figure Legends

Figs. 1: Apyrene and Eupyrene Spermatids

Figs. A and B: Conventional method (tannic acid). Transverse sections on the tail of eupyrene (A) and apyrene (B) spermatids. Axoneme (a), mitochondrial derivatives (d), with paracrystalline core (white asterisk) in the apyrene spermatid, and the reticular appendage (r) on the eupyrene one. In the cytoplasm (c) notice the cytoplasmic microtubules (arrows). (A) 50000x; (B) 70000x

Figs. C to G: Immunocytochemical method. Transverse sections of the tails of spermatids labeled for alpha (C), beta (D), gamma (E), alpha-acetylated (F) and alpha-tyrosinated (G) tubulins. Axoneme (a) with different labeling (double arrowhead); cytoplasmic microtubules (arrowhead) surrounding mitochondrial derivatives (d). (C) 40000x; (D) 38000x; (E) 20000x; (F) 30000x; (G) 20000x

Figs. H and I: Immunocytochemical method. Transverse sections on the head of eupyrene spermatids labeled for gamma (H) and alpha-tyrosinated (I) tubulins. Cytoplasmic microtubules (arrowhead) surrounding the nucleus (n). Reticular appendage (r). 9000x

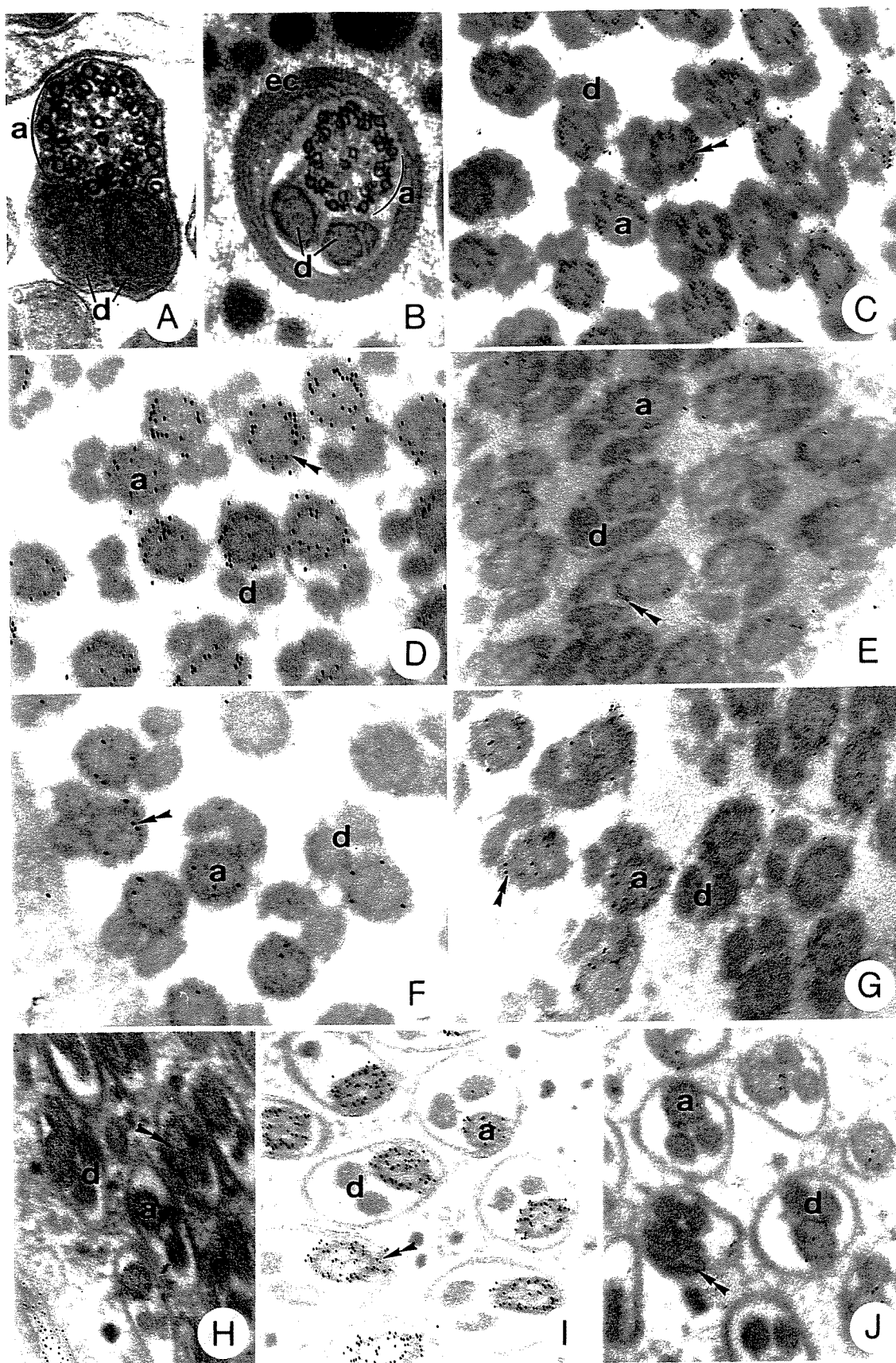


Figs. 2: Apyrene Spermatozoa

Figs. A and B: Conventional method. Transverse sections on the tail of apyrene spermatozoon. (A): Apyrene spermatozoa from testis. (B): Apyrene spermatozoa from the seminal vesicle with an extracellular coat (ec). Axoneme (a), mitochondrial derivatives (d). (A) 85000x; (B) 65000x

Figs. C to G: Immunocytochemical method. Transverse sections of the tails of apyrene spermatozoa labeling against alpha (C), beta (D), gamma (E), alpha-acetylated (F) and alpha-tyrosinated (G) tubulins. Axoneme (a) with different labeling (double arrowhead); no cytoplasmic microtubules surround mitochondrial derivatives (d). (C) 40000x; (D) 42000x; (E) 42000x; (F) 45000x; (G) 40000

Figs. H to J: Immunocytochemical method. Transverse sections of the tail of apyrene spermatozoa from the seminal vesicle labeled for alpha (H), beta (I) and alpha-acetylated (J) tubulins. Axoneme (a) with different intensity of labeling; no labeling on the coat. (H) 22000x; (I) 30000x; (J) 30000



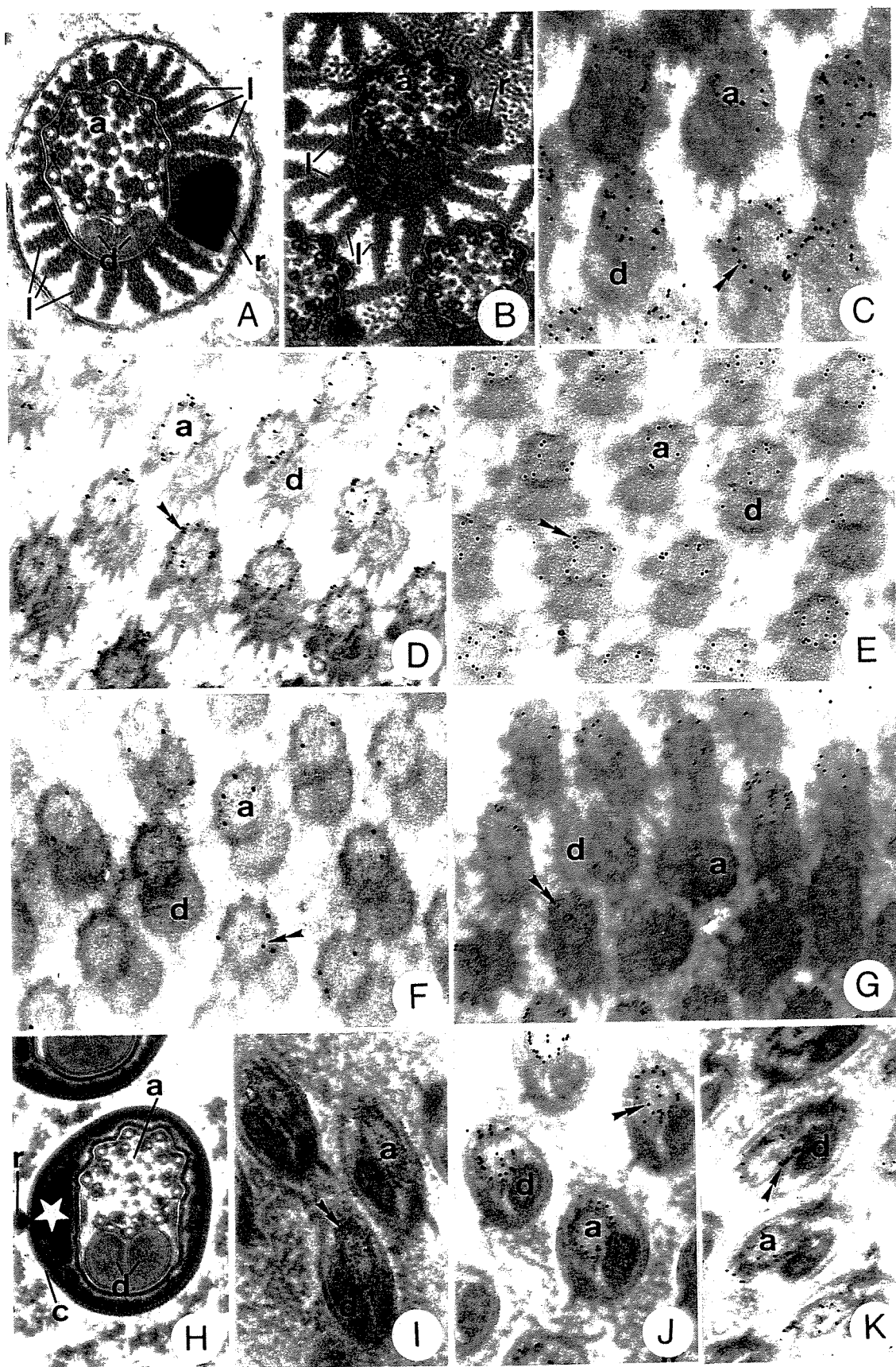
Figs. 3: Eupyrene Spermatozoa

Figs. A and B: Conventional methods, tannic acid (A) and ruthenium red (B). Transverse sections of the tail of eupyrene spermatozoa from the testis. Axoneme (a), mitochondrial derivatives (d), reticular (r) and laciniate (l) appendages with paracrystalline organization. (A) 92000x; (B) 65000x

Figs. C to G: Immunocytochemical method. Transverse sections of the tail of eupyrene spermatozoa labeled for alpha (C), beta (D), gamma (E), alpha-acetylated (F) and alpha-tyrosinated (G) tubulins. Axoneme (a) with different labeling; no cytoplasmic microtubules surround mitochondrial derivatives (d). No labeling on reticular (r) and laciniate (l) appendages. (C) 40000x; (D) to (G) 26000x

Fig. H: Conventional method (tannic acid). Transverse section of the tail of eupyrene spermatozoa from the seminal vesicle. Axoneme (a), mitochondrial derivatives (d), reticular appendage (r) and extracellular coat (c) with dense material (star). 66000x

Figs. I to K: Immunocytochemical method. Transverse sections on the tail of eupyrene spermatozoa from seminal vesicle labeling against alpha (I), beta (J) and alpha-tyrosinated (K) tubulins. Axoneme (a) with different labeling, mitochondrial derivatives (d), no labeling on the coat. 24000x



CAPÍTULO 3

Estrutura e Ultra-estrutura da Espermateca e dos Espermatozóides em Fêmeas

3.1

Morphology of the spermatheca and the spermatozoa found in *Euptoieta hegesia* females

(Lepidoptera: Nymphalidae)

(pp. 169-197)

3.1

Morphology of the spermatheca and the spermatozoa found in *Euptoieta hegesia* females (Lepidoptera: Nymphalidae)

Mancini, K. and Dolder, H.

Running title: Spermatheca and spermatozoa in *Euptoieta hegesia* females

Introduction

Sperm storage by females is especially common and well developed in insects. This ability to store sperm releases females from the risk and energy expenditure involved in finding subsequent mates. In Lepidoptera, the sperm are transferred by a spermatophore sac (Osanai *et al.*, 1987; Watanabe and Sato, 1993). After mating, many female store sperm for months or even years within a specialized reservoir called spermatheca where they remain until used for fertilization (Englemann, 1970). The critical and poorly known aspect of female reproduction is the maintenance of sperm viability and function during their storage.

The spermathecae of insect present a great diversity in number, shape and constitution. But, in general, these organs contain a structure for sperm storage and a glandular epithelium, which can constitute a separate gland or a component of the spermatheca wall.

Lepidoptera males produce simultaneously two distinct sperm types, called apyrene and eupyrene. Both sperm types are transferred to the female during the mating and then storage in the spermatheca (Riemann, 1970; Phillips, 1971; Friedländer and Gitay, 1972; Lai-Fook, 1982). The spermatheca of Lepidoptera is in general composed by two lobules, denominate *utriculus* and *lagena* (Riemann, 1970; Haüser, 1993; Karube and Kobayashi, 1999; Watanabe *et al.*, 2000). The *utriculus* presents more eupyrene sperm while the *lagena* posses more apyrene sperm (Riemann, 1970).

The eupyrene sperm is responsible for the egg fertilization while the apyrene one, since it not presents nucleus and acrosome, is not able to fertilize the eggs. The first studies suggested that the apyrene spermatozoa was related to the eupyrene transport until the female reproductive tract (Friedländer and Gitay, 1972; Friedländer and Miesel, 1977; Riemann, 1970), to the dissociation of the eupyrene sperm bundles along the male reproductive tract (Osanai *et al.*, 1987) and to the nutrition of the eupyrene sperm in the female (Riemann and Gassner, 1973). However, these hypotheses not presented any experimental support. Research has demonstrated that apyrene spermatozoa are involved in the mechanism of sperm competition (Drummond, 1984; Silberglied *et al.*, 1984). In this case, males tailor their ejaculate volume and composition in response to sperm competition

risk and intensity. Thus, apyrene sperm fill the spermathecae, retarding female receptivity, diminishing the sperm competition risk and increasing paternal success (Gage, 1994; Snook, 1997, 1998; Cook and Wedell, 1996, 1999).

Apyrene and eupyrene sperm pass through several morphological modifications along the male and female reproductive tracts, which exclusively involve extracellular components. But both sperm types acquire an extratesticular coat along the entire sperm length (Riemann, 1970; Phillips, 1971; Friedländer and Gitay, 1972; Lai-Fook, 1982; Medeiros, 1986, 1997; Kubo-Irie *et al.*, 1998). In the spermatheca, the apyrene sperm maintain the same extratesticular morphology while the eupyrene one loss their complex coat before the fertilization.

The ultrastructure of apyrene and eupyrene sperm into the spermatheca was previous described in *Trichoplusia ni* (Riemann, 1970), *Anagasta kühniella* (Riemann and Thorson, 1971), *Bombyx mori* (Friedländer and Gitay, 1972), *Calpodes ethlius* (Lai-Fook, 1982), *Manduca sexta* (Friedländer *et al.*, 2001) and in other five Lepidoptera species (Riemann and Thorson, 1973). However, the spermatheca ultrastructure was not described yet. The present study described the morphology of the spermatheca and their spermatozoa in female of the butterflies *Euptoieta hegesia*.

Material and Methods

Spermatheca of adult's female of the butterflies *Euptoieta hegesia* were dissected to anatomic description and transmission electron microscopy.

Anatomic description

The spermatheca were fixed in 4% paraformaldehyde and then photographed in stereoscopy.

Transmission electron microscopy

Most specimens were fixed in 2.5% glutaraldehyde, 4% paraformaldehyde, 1.5% sucrose, 5mM CaCl₂ in a 0.1M sodium phosphate buffer for 12 hours at 4°C. After fixation, they were rinsed in buffer, post-fixed in 1% osmium tetroxide for 3-5 hours at 4°C, dehydrated in acetone and finally embedded in LR White resin (for better embedding). The ultrathin sections were stained with uranyl citrate and lead acetate solutions and then observed in Transmission Electron Microscope.

Results

General Morphology

The internal female reproductive system of *Euptoieta hegesia* consists of 2 ovaries with four ovarioles each connected to a common oviduct. Connected also to this oviduct and near to the ovopositor there is the spermatheca and the *bursa copulatrix* (fig. A). The *bursa copulatrix* is a transparent large bulb, about 2 mm long and 1,5 mm in diameter. The spermatheca is also a transparent organ about 1 mm long and located just dorsal to the oviduct. It consists two lobules, called *utriculus* and *lagena*, with a common spiral duct and a gland connected to the *utriculus* (fig. B). The *utriculus* is the largest lobule while the *lagena* is the smaller one and is membranous. Because it is transparent it is not readily recognized during dissection. These spermathecal structures present an external muscular sheath.

Spermathecal Epithelium

Utriculus

The *utriculus* epithelium has been schematically drawn in figure C. The *utriculus* has a secretory epithelium composed by three cell types: a columnar secretory cell, a duct-forming cell and a cuticle-forming cell (fig. D1).

The secretory cells lie directly on the basal lamina and end near the lumen. They possess a cytoplasm rich in granular endoplasmic reticulum and mitochondria, and a large nucleus that is located in the basal region, with a conspicuous nucleolus (fig. D2). In the apical regions, the cytoplasm contains several dense secretory bodies and numerous microvilli (figs. D3 to 6) formed by the apical plasma membrane that are organized in an invagination (reservatory) (figs. D4 and 6). This cavity is almost entirely filled with dense secretion that is eliminated in the end apparatus with the duct of the duct-forming cells (figs. D3 to 6).

The duct-forming cells are located between the columnar and the cuticle-forming cells (figs. D3 and 7) and produce the chitin duct walls. These cells possess an irregular shape since they form projections toward the lumen and the reservatory of the secretory cells (figs. D3, 4 and 9) where the secretion builds up and flows into the lumen. The duct is wrapped around by the duct-forming cell and its closely nucleus (figs. D3, 6 and 7).

The cuticle-forming cells are lined with a large dense cuticle close to the lumen that project toward the duct-forming cells (figs. D7 to 9). These cells possess an irregular shape but also form a homogenous large layer around the cuticle (figs. D6 and 9). The cytoplasm is rich in membranous bodies and vesicles that produce the cuticle (fig. D10). Here, the duct is wrapped around by the cuticle-forming cells and possesses the same components as in the duct-forming cell level (figs. D6 to 9).

The cuticle is composed by a thin epicuticle and an endocuticle that varies in thickness (figs. D8 to 10) and is penetrated by several secretion ducts (figs. D8 and 9) that pass through the cuticle liberating the secretion in the lumen.

The lumen has a regular shape, its surrounded by the large dense cuticle and possesses a dense secretion in which the spermatozoa are immersed (figs. D1, 7 to 10).

Lagena

The lagena presents a very thin epithelium when compared to the *utriculus* and only one cell type occurs which is not secretory. The cells are elongated and the cytoplasm is rich in mitochondria. The nucleus is also elongated and contains a very evident nucleolus.

This lobule possesses a very irregular lumen composed of a dense secretion with spermatozoa and surrounded by a thin cuticle (fig. D11).

Spermathecal glands

The spermathecal gland (not shown) contains an epithelial structure similar to the *utriculus*, with the columnar secretory cells and duct-forming cells. The lumen is filled only with secretion.

Spiraling duct

The spiraling duct contains a non-secretory epithelium composed of columnar cells. The lumen is regular, surrounded by a large cuticle composed by an inner lucid epicuticle and a dense procuticle (fig. D12). The spermatozoa are immersed in a clear secretion.

Ultrastructure of the spermatozoa

Apyrene and eupyrene spermatozoa were found in both spermathecal lobules and in the spiraling duct. In these regions, the volume of eupyrene sperm is bigger than apyrene population one. Both sperm types are dispersed in the lumen immersed in secretion; however, the eupyrene spermatozoa are loosely aggregated and aligned.

The apyrene morphology in the spermatheca is similar to that found in the male extratesticular regions. They contain a dense anterior cap and the flagellum is composed by a 9+9+2 axoneme and two mitochondrial derivatives. They also conserve their extracellular coat of concentric membranes, which surround the entire sperm length. They contain an evident intracellular lucid area around the axoneme and the mitochondrial derivatives (fig. E1). In the spiraling duct, this coat is absent and the apyrene spermatozoa are covered only by the plasma membrane (fig. E2).

The eupyrene morphology is different from that found in the male extratesticular region and additional extracellular modification occur in the spermatheca. The sperm anterior region is composed of a tubular acrosome and a nucleus while the flagellar region is composed by a 9+9+2 axoneme and two mitochondrial derivatives (fig. E3). They are

entirely covered by a complex coat, similar to that found in the male seminal vesicle. The reticular appendage is absent and in its place there is a dense plate (figs. E3 to 6). The coat is composed of an external layer and an amorphous matrix filling, both extracellular. The external layer presents three regions: two thin dense layers separated by a large less-dense layer (fig. E3). The coat presents about 20° of rotation in relation to the sperm cell when compared with the sperm in the seminal vesicle. In some spermathecal regions, where the secretion is very dense, the morphology of the eupyrene sperm was complex (fig. E4). The above description of eupyrene sperm is applicable to both spermathecal lobules.

In the *utriculus*, a large number of eupyrene spermatozoa were observed in different degeneration stages, with axonemal disorganization, membranous structures, due to mitochondrial derivative degeneration, and decomposition of the coat into an amorphous dense mass (fig. E5).

In the basal region of the *utriculus* and the *lagena*, near the spiraling duct, the coat of eupyrene sperm presented a small projection next the axoneme (fig. E6). At this small projection the eupyrene coat breaks to liberate the bare sperm. So, in the spiraling duct, the eupyrene lose their coat and maintain only the plasma membrane (figs. E7 to 12). The three types were observed in the same spermathecal: eupyrene sperm with coat, eupyrene sperm without a coat and the empty coat (fig. E8). In the medial spiraling duct, there are a great number of empty coats composed of the external layer and the amorphous matrix, and also bare eupyrene sperm (figs E11 and 12). It was not observed apyrene degeneration or lose of their coat.

Discussion

During mating, Lepidopteran males transfer a spermatophore to the female *bursa copulatrix*, which contains both sperm types. Secretions of the male accessory gland are also transferred into the female. Then, apyrene and eupyrene spermatozoa are transferred and stored in the spermatheca until the egg fertilization. In the present study spermathecae

of *Euptoieta hegesia* females were dissected for anatomic description and then for transmission electron microscopy.

The female reproductive tract and the spermathecal organization of *Euptoieta hegesia* are similar to that described for the majority Lepidopteran species (Häuser, 1993; Karube and Kobayashi, 1999; LaMunyon, 2000) differing principally as to the small dimension of its spermatheca. However, this is the first detailed description of the spermathecal epithelium, including the two lobules, the gland and the duct. The spermathecal epithelium of *E. hegesia*, with the secretory cells and the duct-forming cells were comparable to the description of *Drosophila melanogaster* (Diptera) (Filosi and Perotti, 1975), *Frankliniella occidentalis* (Thysanoptera) (Dallai *et al.*, 1996) *Logusta migratoria migratorioides* (Orthoptera) (Lay *et al.*, 1999). The spermatheca organization, with three cell types, similar to *E. hegesia* was described in four species of *Microcoryphina* (Bitsch, 1989).

The spermatheca of the majority of the Lepidoptera species is composed of two lobes, the *utriculus* and the *lagna* (Riemann, 1970; Karube and Kobayashi, 1999; Watanabe *et al.*, 2000). Riemann (1970) observed differences of apyrene and eupyrene distribution between the two lobules: in the *utriculus* he observed more eupyrene spermatozoa while in the *lagna* he found more apyrene sperm. In this study, we did not find any difference between the contents of the lobules.

The species were collected in the field and immediately dissected. Therefore we did not control the mating time in the inseminated females. Studies with control of mating time demonstrated that the eupyrene spermatozoa are transferred in bundles to the *bursa copulatrix* and then they dispersed together with apyrene (Riemann, 1970; Holt and North, 1970; Riemann and Thorson, 1971; Friedländer and Gitay, 1972; Riemann and Gassner, 1973; Watanabe *et al.*, 2000). The apyrene sperm present more motility/vibration than the eupyrene ones (Katsuno, 1978; Cook and Wedell, 1996).

We did not find any differences between apyrene and eupyrene motility in the *E. hegesia* female. The stronger apyrene motility supports the hypothesis of eupyrene transport by apyrene sperm up to the female (Friedländer and Gitay, 1972; Friedländer and Miesel, 1977; Riemann, 1970). However, the hypothesis most accepted today is that

apyrene sperm are related to sperm competition, where males are able to vary the volume and their composition of the sperm in response to the intensity of competition between males (Cook and Wedell, 1999). In the case, of high competition, apyrene sperm fill the spermatheca, diminishing the female receptivity for the next mating. Therefore, the risk of sperm competition is lowered and the success of the paternity increases (Cook and Wedell, 1996, 1999; Wedell and Cook, 1998, 1999a, b).

Quantitative studies show a variation in the composition of the ejaculated sperm, where the volume of the apyrene is bigger than the eupyrene spermatozoa (Cook and Wedell, 1996, 1999; Wedell and Cook, 1998, 1999a, b; Watanabe *et al.*, 2000). Watanabe *et al.* (2000) showed that the apyrene sperm pass through the spermatheca before eupyrene ones. Therefore they are dispersed in the male and present high motility.

In the spermatheca, apyrene and eupyrene sperm initiate a degeneration process. The apyrene spermatozoa degenerate faster than the eupyrene. In *Papilio xuthus*, apyrene sperm remain in the spermatheca for 12 hours, while the eupyrene sperm is found up to 1 week after mating (Watanabe *et al.*, 2000). In *E. hegesia*, only eupyrene degeneration was observed. However, more eupyrene than apyrene sperm were observed, which may indicate earlier apyrene degeneration. Friedländer and Gitay (1972) described the distribution and morphology of the apyrene and eupyrene spermatozoa in the female of *Bombyx mori* and found only eupyrene spermatozoa in the *canaliculus fecundans*, where the eggs are fertilized. This also appears to corroborate the suggestion that apyrene sperm degenerate first.

Eupyrene sperm in the *E. hegesia* female present an extracellular coat composed of an external layer and an internal amorphous matrix. The reticular appendage is absent and a dense plate appears in its contact point with the coat. The intracellular structures do not present any modifications, continuing similar to that found in the male. This is according to the general description of eupyrene spermatozoa in the spermatheca as given for other Lepidoptera (Riemann, 1970; Riemann and Thorson 1971; Phillips, 1971; Friedländer and Gitay, 1972; Riemann and Gassner, 1973; Lai-Fook, 1982; Medeiros, 1986, 1997). The intracellular components of the eupyrene spermatozoa, such as the acrosome, nucleus, axoneme and mitochondrial derivatives, remain without modification. Some authors

observed small changes in the axonemal elements (Riemann and Gassner, 1973; Medeiros, 1986). The presence of an extracellular coat, as well as the absence of the reticular appendage in the eupyrene spermatozoa was reported in all species analyzed (Riemann, 1970; Riemann and Thorson, 1971; Phillips, 1971; Friedländer and Gitay, 1972; Riemann and Gassner, 1973; Medeiros, 1986). In the external layer of the coat, the presence of a dense plate seems to occur in all eupyrene spermatozoa in females. This plate has the same location as of the reticular appendage in the seminal vesicle. A rotation of the coat was observed in other Lepidopteran species; it is about 20° in *Anagasta kuhniella* (Riemann and Thorson, 1971), as in *E. hegesia*, up to 120° in *Trichoplusia ni* (Riemann, 1970). The meaning of this rotation still is unknown.

Some authors report the presence of an electron dense area internal to the coat, next to the dense plate (Riemann, 1970; Riemann and Thorson, 1971; Riemann and Gassner III, 1973). This area was poorly observed in the present study, since it corresponds to the dense material found in the seminal vesicle (Mancini and Dolder, 2001).

The majority of the reports show that the rupture point for the eupyrene sperm release is located at the dense plate (Riemann and Thorson, 1971; Friedländer and Gitay, 1972). The present work found this rupture point next to the axoneme, similar to the description of Medeiros (1986) in *Alabama argillacea*. After the rupture, several empty coats and bare eupyrene sperm were found, as observed in *Bombyx mori* (Fiedlander and Gitay, 1972), *Anagasta kuehniella* (Riemann and Thorson, 1971) and *Alabama argillacea* (Medeiros, 1986). In agreement with Fiedlander and Gitay (1972), the coat could have the function of eupyrene sperm protection along the reproductive tract and therefore upon arriving finally in spermatheca they lose this protection, which is longer necessary and would represent a barrier to the fertilization process.

References

- Bitsch, J. 1989. The glandular units of the spermatheca of machilids (microcoryphia): ultrastructure and modifications during moulting. **Int. J. Insect Morphol. Embryol.** 18: 97-110.
- Cook, P. A. and Wedell, N. 1996. Ejaculate dynamics in butterflies: a strategy for maximizing fertilization success. **Proc. Royal Soc. London B** 263: 1047-1051.
- Cook, P. A. and Wedell, N. 1999. Non-fertile sperm delay female remating. **Nature** 397, 486.
- Dallai, R. Del Bene, G. and Lupetti, P. 1996. Fine structure of spermatheca and accessory gland of *Frankliniella occidentalis* (Pergande) (Thysanoptera: Thripidae). **Int. J. Insect Morphol. Embryol.** 25: 317-330.
- Drummond, B. A. 1984. Multiple mating and sperm competition in the lepidoptera. In: Smith, R.L. **Sperm competition and the evolution of animal mating systems.** Academic Press, London.
- Engelmann, F. 1970. **The physiology of insect reproduction.** Pergamon, Oxford.
- Filosi, M. and Perotti, M. E. 1975. Fine structure of the spermatheca of *Drosophila melanogaster* Meig. **J. Submicrosc. Cytol.** 7: 259-270.
- Friedländer, M. and Gitay, H. 1972. The fate of the normal anucleated spermatozoa in inseminated female of the silkworm *Bombyx mori*. **J. Morphol.** 138: 121-129.
- Friedländer, M. and Miesel, S. 1977. Spermatid anucleation during the normal atypical spermiogenesis of the warehouse moth *Ephestia cautella*. **J. Submicrosc. Cytol.** 9: 173-185.
- Friedländer, M., Jeshtadi, A. and Reynolds, S. E. 2001. The structural mechanism of trypsin-induced intrinsic motility in *Manduca sexta* spermatozoa in vitro. **J. Insect Physiol.** 47: 245-255.
- Gage, M. J. G. 1994. Associations between body size, mating pattern, testis size and sperm lengths across butterflies. **Proc. Royal Soc. London B** 258: 247-254.

- Häuser, C. L. 1993. Die inneren weiblichen genitalorgane der tagfalter (Rhopalocera): vergleichende morphologie und phylogenetische interpretation (Insecta, Lepidoptera). **Zool. Jb. Syst.** 120: 389-439.
- Holt, G. G. and North, D. T. 1970. Spermatogenesis in the cabbage looper *Trichoplusia ni* (Lepidoptera: Noctuidae). **Ann. Entomol. Soc. Am.** 63: 501-507.
- Karube, F. and Kobayashi, M. 1999. Presence of eupyrene spermatozoa in vestibulum accelerates oviposition in the silkworm moth, *Bombyx mori*. **J. Insect Physiol.** 45: 947-957.
- Katsuno, S. 1978. Studies on eupyrene and apyrene spermatozoa in the silkworm *Bombyx mori* L. (Lepidoptera: Bombycidae) VII. The motility of sperm bundles and spermatozoa in the reproductive organs of males and females. **Appl. Ent. Zool.** 13: 91-96.
- Kubo-Irie, M., Irie, M., Nakazawa, T. and Mohri, H. 1998. Morphological changes in eupyrene and apyrene spermatozoa in the reproductive tract of the male butterfly *Atrophaneura alcinous* Klug. **Invert. Reprod. Develop.** 34: 259-268.
- Lai-Fook, J. 1982. Structural comparision between eupyrene and apyrene spermiogenesis in *Calpodus ethlius* (Hesperiidae: Lepidoptera). **Can. J. Zool.** 60: 1216-1230.
- LaMunyon, C. W. 2000. Sperm storage by females of the polyandrous noctuid moth *Heliothis virescens*. **An. Behav.** 59: 395-402.
- Lay, M., Zissler, D. and Hartmann, R. 1999. Ultrastructural and functional aspects of the spermatheca of the African migratory locust *Locusta migratoria migratorioides* (Reiche and Fairmaire) (Orthoptera: Acrididae). **Int. J. Insect Morphol. Embryol.** 28:349-361.
- Mancini, K. and Dolder, H. 2001. Ultrastructure of apyrene and eupyrene spermatozoa from the seminal vesicle of *Euptoieta hegesia* (Lepidoptera: Nymphalidae). **Tissue and Cell** 33: 301-308.
- Medeiros, M. 1986. **Caracterização ultra-estrutural de espermatozóides eupirenes e apirenes de *Alabama argillacea* Hübner, 1818 (Lepidoptera: Noctuidae), ao nível dos testículos e das vias genitais de imagos machos e fêmeas até a espermateca.** Tese (Mestrado). Instituto de Biologia, Universidade Estadual de Campinas.

- Medeiros, M. 1997. **Estudo ultra-estrutural da espermiogênese dicotômica de *Alabama argillacea* Hübner, 1818.** Tese (doutorado). Instituto de Biociências, Universidade Estadual de São Paulo.
- Osanai, M., Kasuga, H and Aigaki, T. 1987. Physiological role of apyrene spermatozoa of *Bombyx mori*. **Experientia** **43**: 593-596.
- Phillips, D. M. 1971. Morphogenesis of the laciniate appendages of lepidopteran spermatozoa. **J. Ultrastruct. Res.** **34**: 567-585.
- Riemann, J. G. 1970. Metamorphosis of sperm of the cabbage looper *Trichoplusia ni* during passage from the testes to the female spermatheca. In: Baccetti, B. **Comparative Spermatology**. Academic Press. New York. pp. 321-331.
- Riemann, J. G. and Gassner, G. 1973. Ultrastructure of Lepidopteran sperm within spermathecae. **Ann. Entomol. Soc. Am.** **66**: 154-159.
- Riemann, J. G. and Thorson, B. J. 1971. Sperm maturation in the male and female genital tracts of *Anagasta kuehniella* (Lepidoptera: Pyralididae). **Int. J. Insect Morphol. Embryol.** **1**: 11-19.
- Silberglied, R. E., Shepherd, J. G. and Dickinson, J. L. 1984. Eunuchs: the role of apyrene sperm in lepidoptera? **Am. Nat.** **123**: 255-265.
- Snook, R. R. 1997. Is the production of multiple sperm types adaptive?. **Evolution** **51** (3): 797-808.
- Snook, R. R. 1998. The risk of sperm competition and the evolution of sperm heteromorphism. **An. Behav.** **56**: 1497-1507.
- Watanabe, M. and Sato, K. 1993. A spermatophore structure in the bursa copulatrix of the small white *Pieris rapae* (Lepidoptera, Pieridae) during copulation, and its sugar content. **J. Res. Lepid.** **32**: 26-36.
- Watanabe, M., Bonno, M. and Hachisuka, A. 2000. Eupyrene sperm migrates to spermatheca after apyrene sperm in the swallowtail butterfly, *Papilio xuthus* L. (Lepidoptera: Papilionidae). **J. Ethol.** **18**: 91-99.
- Wedell, N. and Cook, P. A. 1998. Determinants of paternity in a butterfly. **Proc. Royal Soc. London B** **265**: 625-630.

- Wedell, N. and Cook, P. A. 1999. Butterflies tailor their ejaculate in response to sperm competition risk and intensity. **Proc. Royal Soc. London B** 266: 1033-1039.
- Wedell, N. and Cook, P. A. 1999. Strategic sperm allocation in the small white butterfly *Pieris rapae* (Lepidoptera: Pieridae). **Funct. Ecol.** 13: 85-93.

Fig. A: Diagram of the internal reproductive organs of the female *Euptoieta hegesia*. AG – Accessory glands; BC – *Bursa copulatrix*; CA – Calix; CO – Common oviduct; DB – *Ductus bursae*; DS – *Ductus seminalis*; LG – Lagna; LO – Lateral oviduct; OB – *Ostium bursae*; OL – Ovarioles; OP – Ovipositor; OV – Ovary; SD – Spermathecal duct; SG – Spermathecal gland; ST – Spermatheca; UT – *Utriculus*.

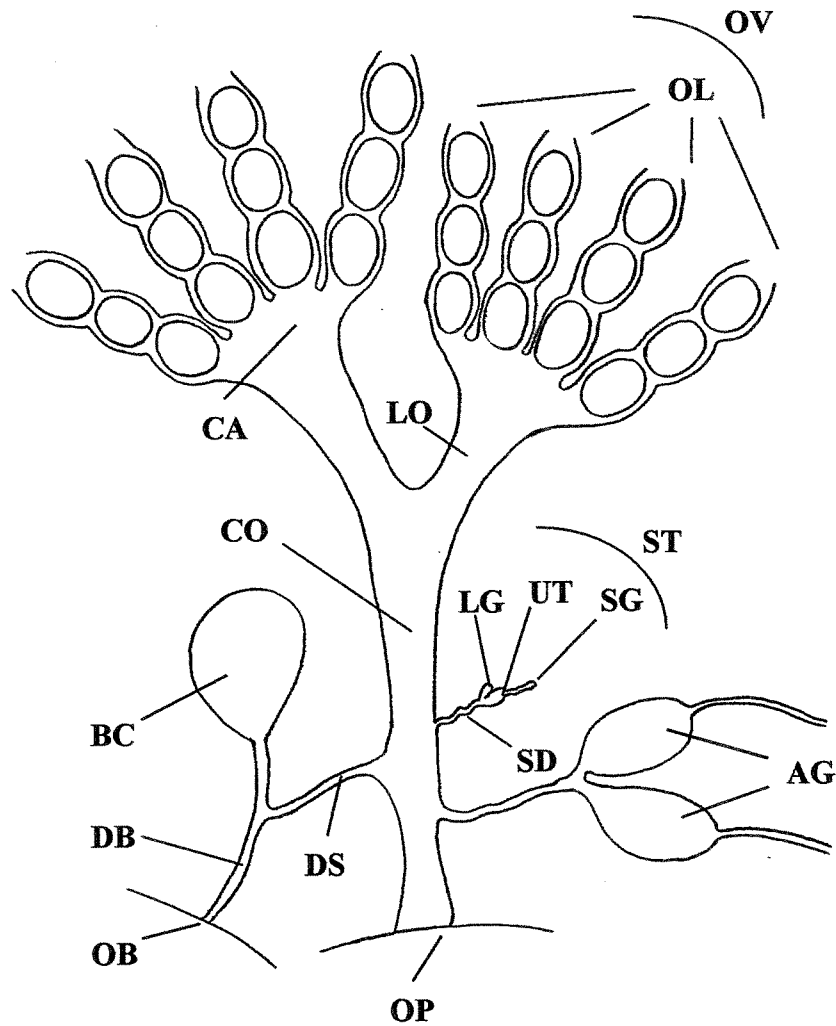
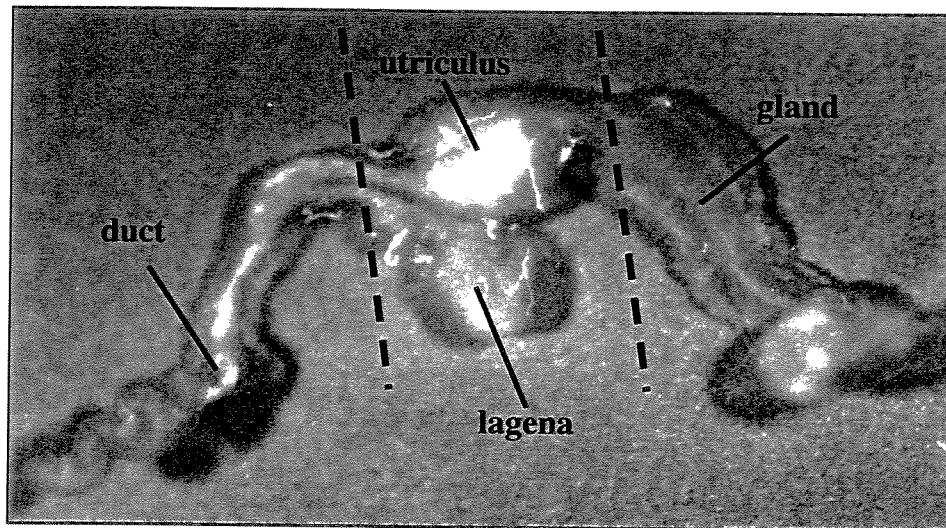
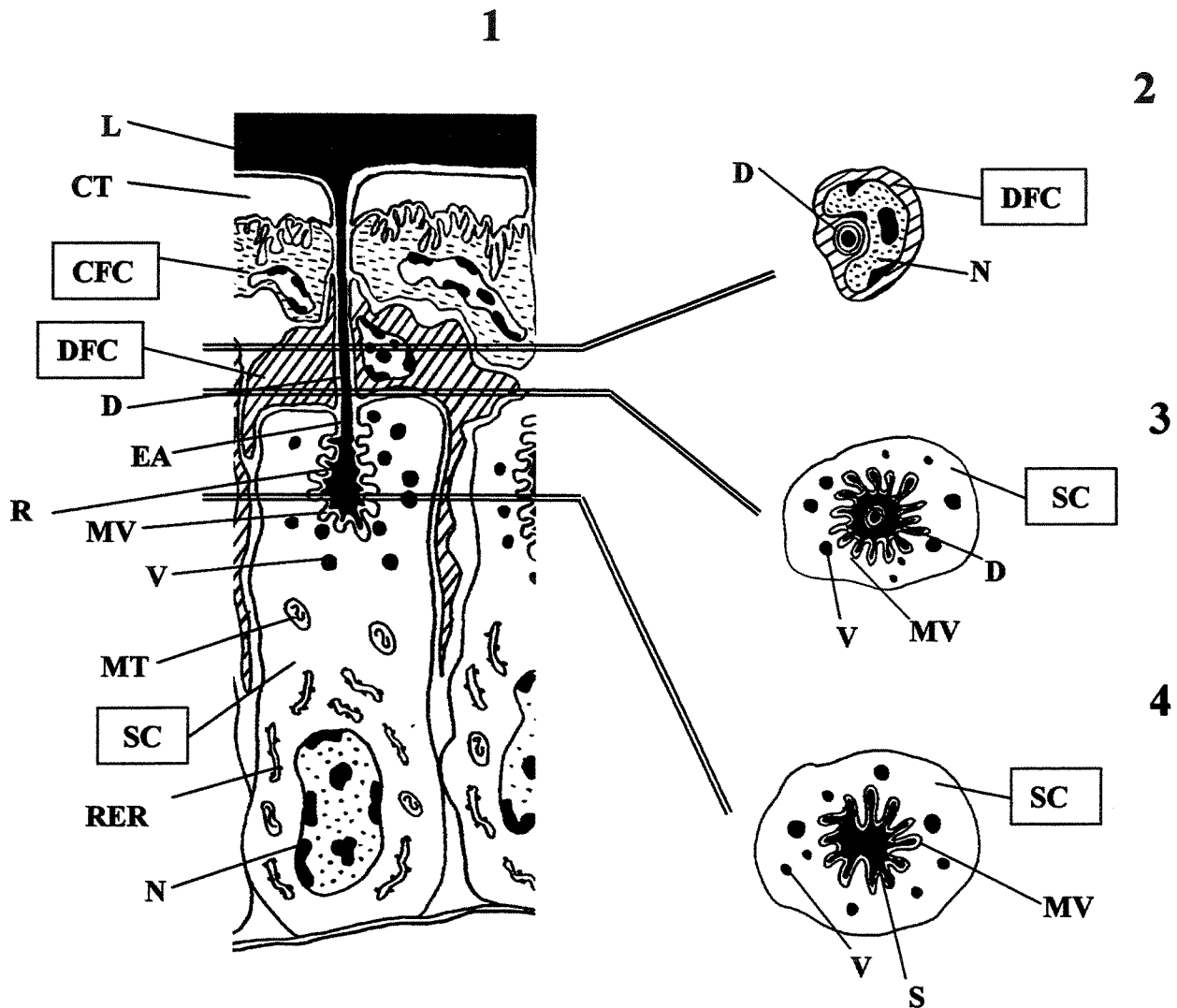


Fig. B: Spermatheca of *Euptoieta hegesia* and their compartments



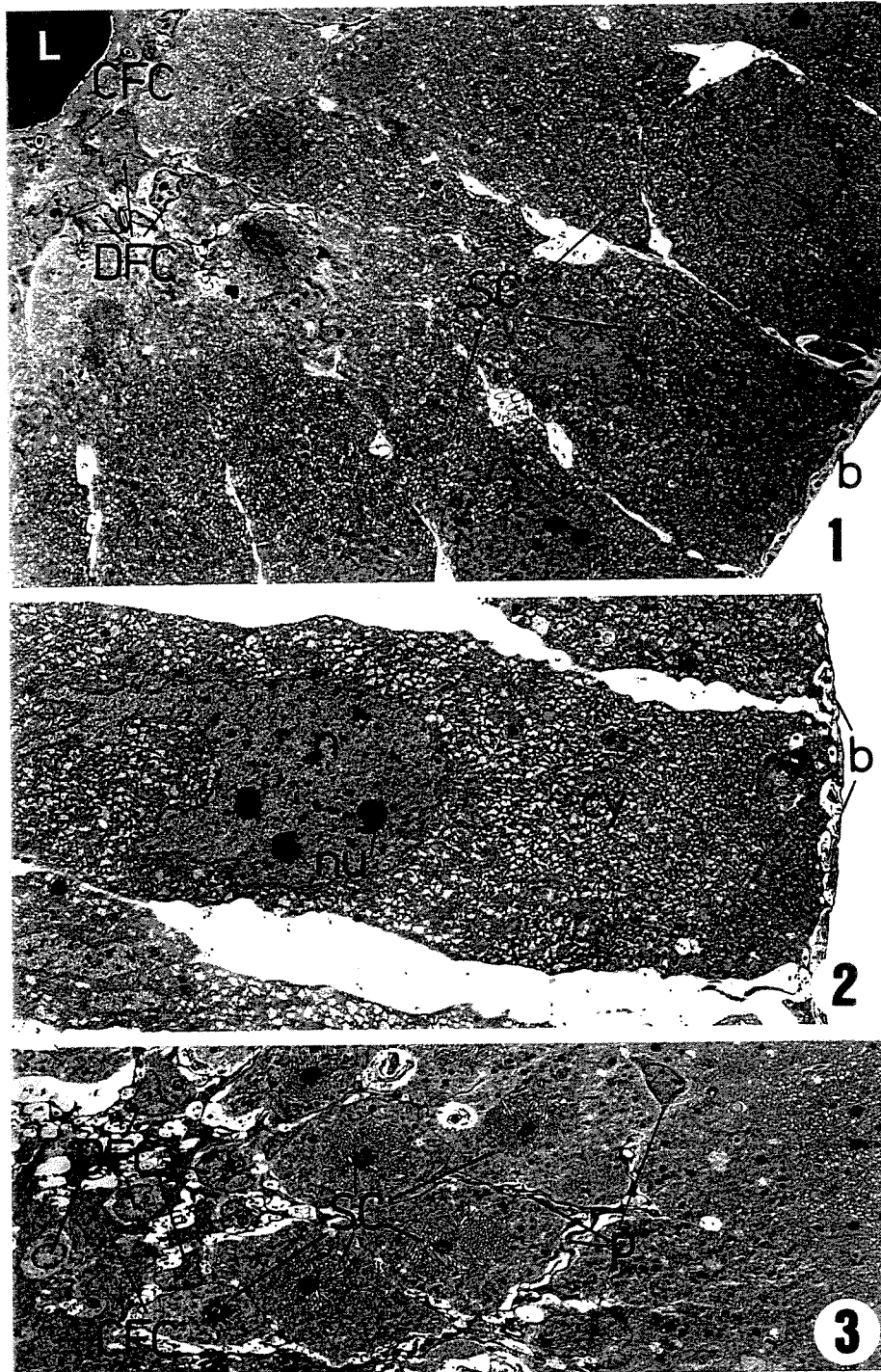
Figs. C1 to 4: Diagrammatic reconstructions of the secretory epithelium in spermatheca of *Euptoieta hegesia* based on ultrastructural observations. (1) Longitudinal diagram; (2) to (4) Transversal diagrams.

SC – Secretory Cell; CFC – Cuticle-forming cell; CT – Cuticle; D – Duct; DFC – Duct-forming Cell; EA – End Apparatus; L – Lumen; MT – Mitochondria; MV – Microvilli; N – Nucleus; R – Reservatory; RER – Rough Endoplasmic Reticulum; V – Vesicle of secretion.



Figs. D1 to 3: Spermathecal epithelium (*Utriculus*).

- (1): Secretory epithelium composed by the cuticle-forming cells (CFC), the duct-forming cells (DFC), the secretory cells (SC) and the basal lamina (b). Lumen (L). 2000x.
- (2): Basal region of columnar cell showing the nucleus (n) with evident nucleolus (nu). The cytoplasm (cy) is rich in rough endoplasmic reticulum and mitochondria. 4000x.
- (3): Medial region of secretory epithelium showing the secretory cells (SC), the duct-forming cell (DFC) and their projection (p) and the cuticle-forming cells (CFC). 27000x.

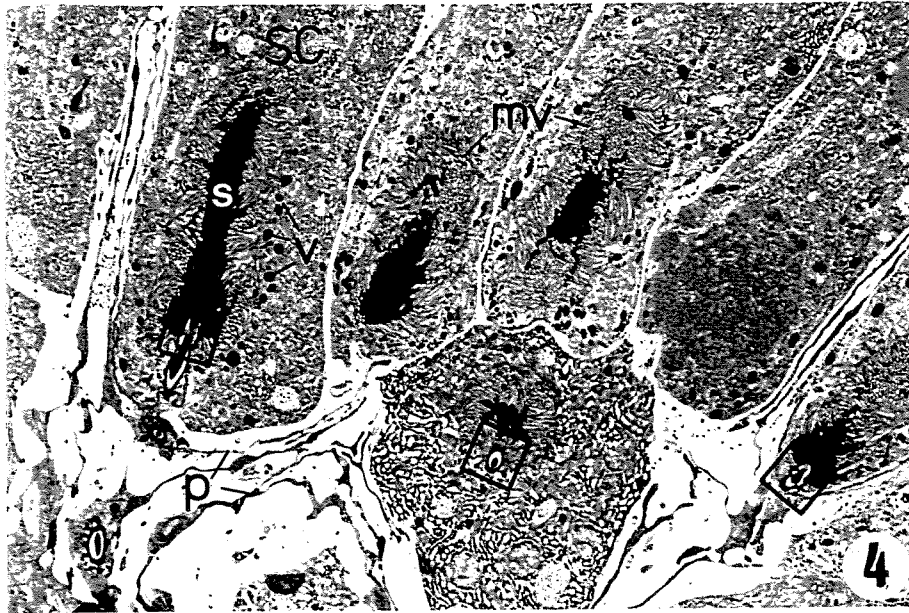


Figs. D4 to 6: Spermathecal epithelium (*Utriculus*).

(4): Longitudinal section of the apical region of the secretory cells (SC) showing the secretion (s) in reservatory with the end apparatus (squares). Microvillis (mv). 4300x.

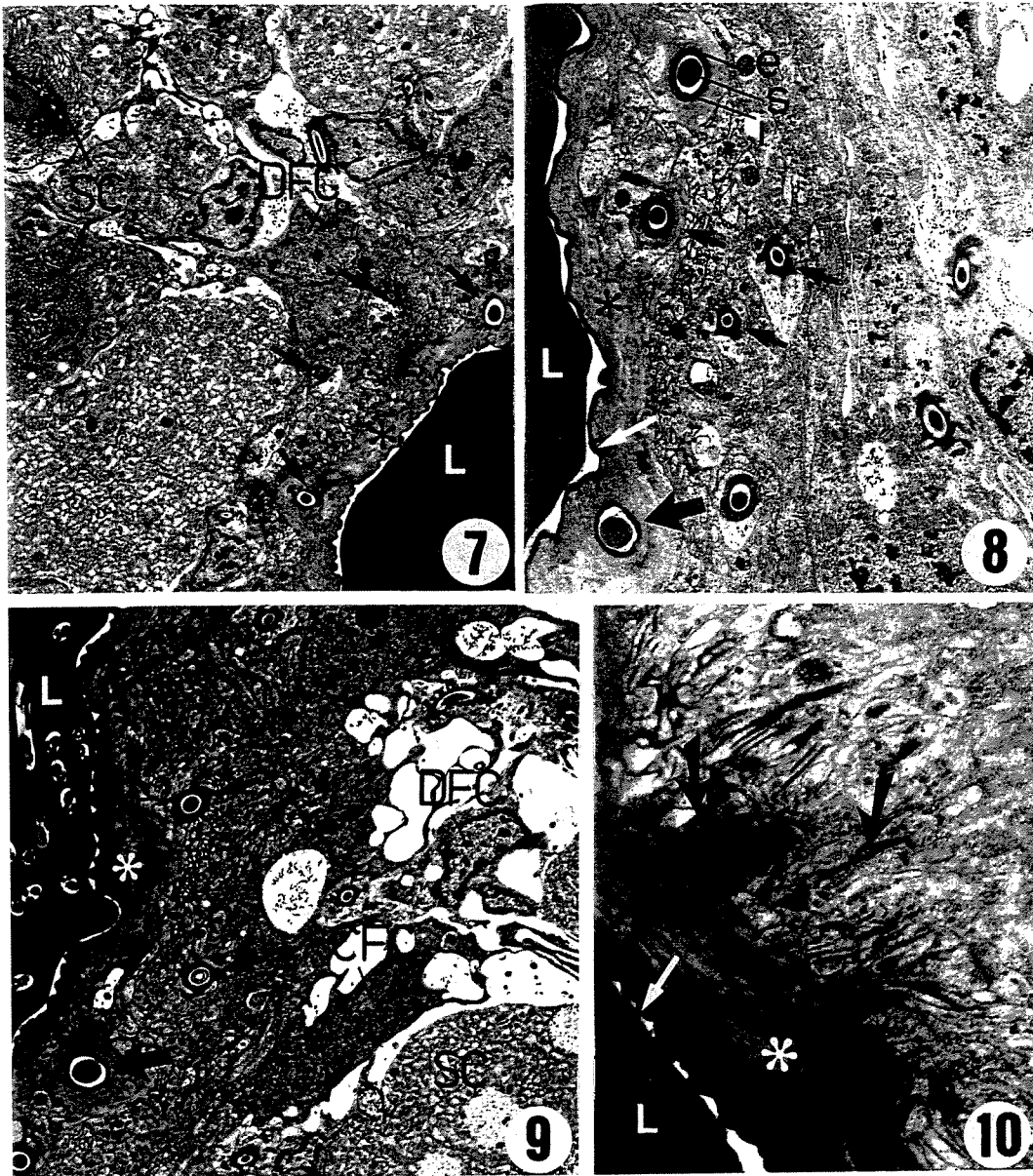
(5): Secretory cells (SC) and the closely association with the duct-forming cells (white arrows) and the cuticle-forming cells (black arrows). Secretion (s) in the reservatory with microvillis (mv). 4300x.

(6): Duct-forming cells (DFC) with nucleus and clearly cytoplasm that surround the duct (arrowheads). End apparatus (square), microvillis (mv), secretion (s) in the reservatory and cuticle-forming cells (arrows). 5500x.



Figs. D7 to 10: Spermathecal epithelium (*Utriculus*).

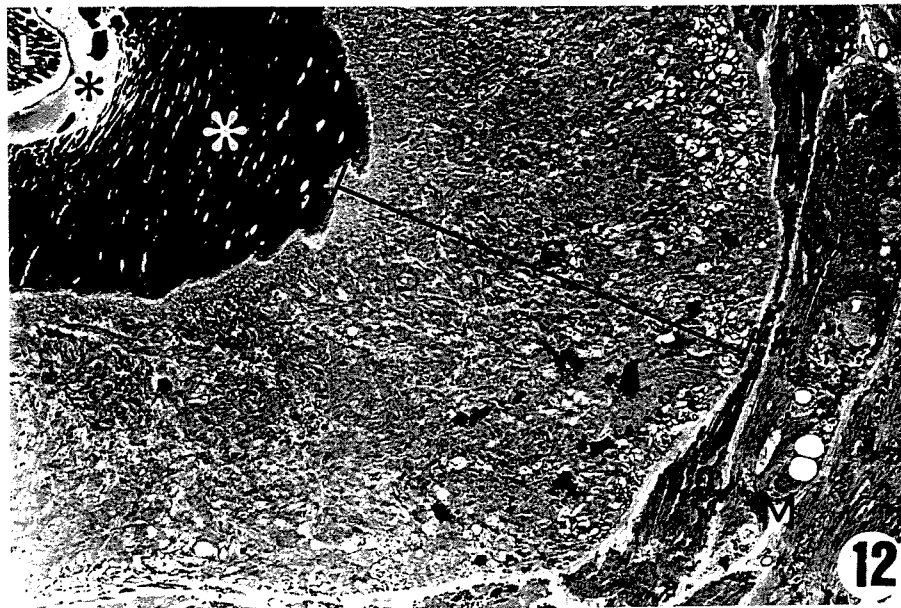
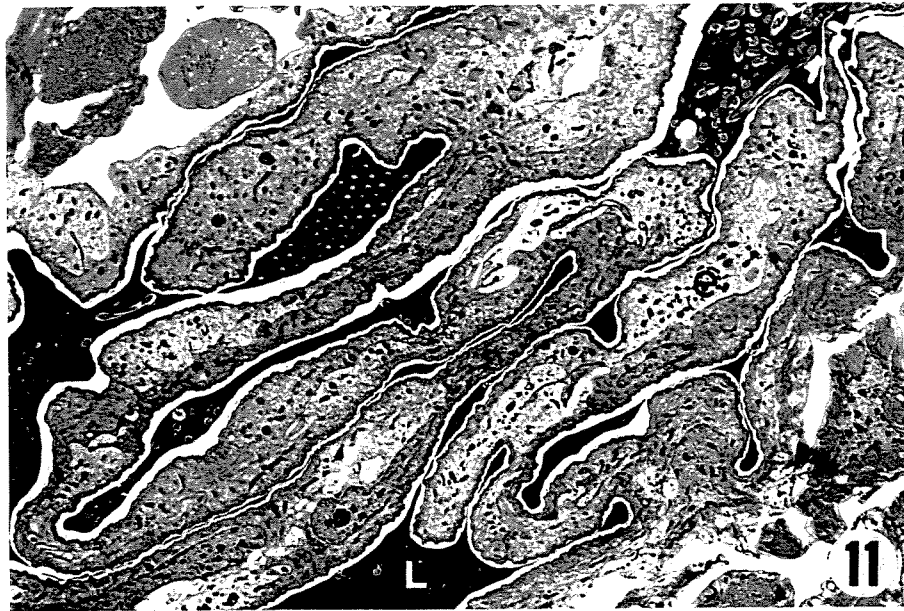
- (7): Ducts (arrows) wrapped by the cuticle-forming cells and by the duct-forming cells (DFC). Secretory cells (SC), cuticle (black asterisk) and lumen (L). 5500x.
- (8): Cuticle-forming cells with immersed ducts (black arrows). The duct presents an inner dense layer (i), an external large layer (e) and the secretion (s). In the cuticle, the duct (large black arrow) loss the external layer. The cuticle presents a thin epicuticle (white arrow) and a large endobcuticle (black asterisk). 8900x
- (9): Ducts (arrows) wrapped by the duct-forming cells (DFC). Cuticle-forming cells (CFC) and the endocuticle (white asterisk). Secretory cell (SC). 4300x.
- (10): Detail of the cuticle with an inner thin epicuticle (white arrow) and a large endocuticle (white asterisk). Note the several anchorage projections. 11500x.



Figs. D11 and 12: Spermathecal epithelium (*Lagena*) and Spiraling duct

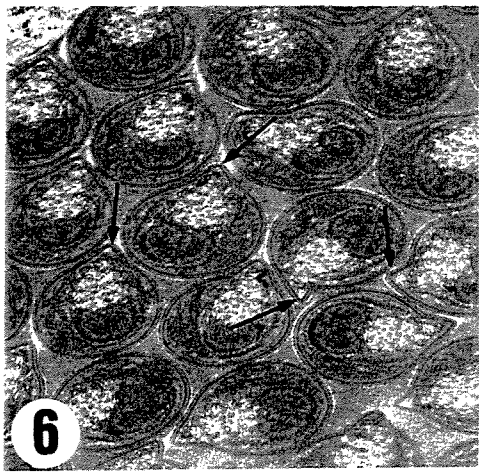
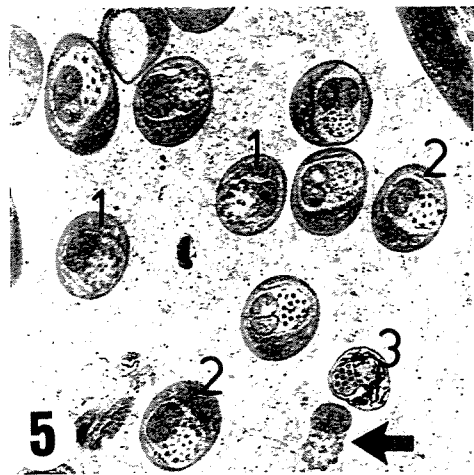
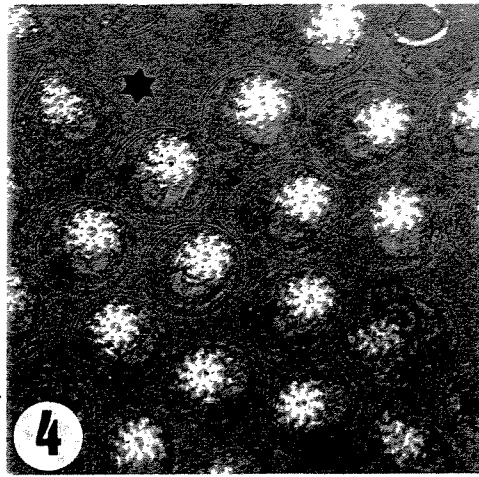
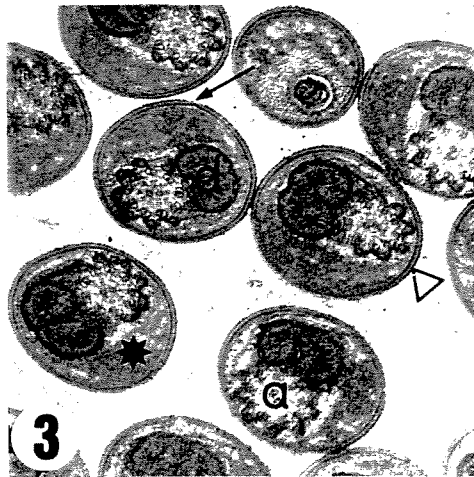
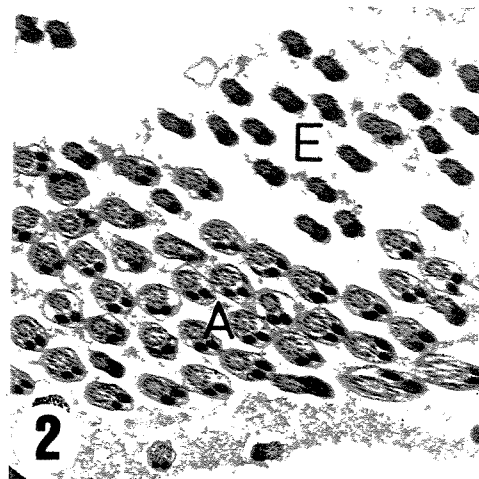
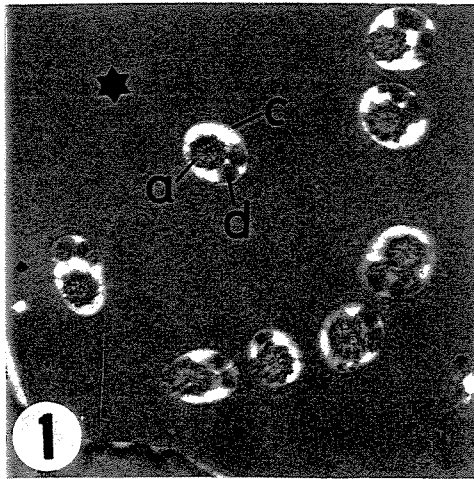
(11): Lagena. The epithelium (e) is formed by non-secretory elongated cells. The lumen (L) is very irregular. 2600x.

(12): Spiraling duct. The epithelium (e) has only columnar cells. The cuticle is very large and present a large dense (white asterisk) and a thin lucid (black arrow) layers. The lumen (L) is small and regular. Note the external muscles fibers (M). 2600x.



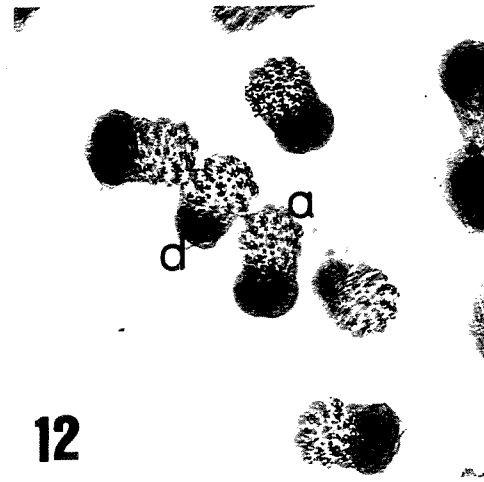
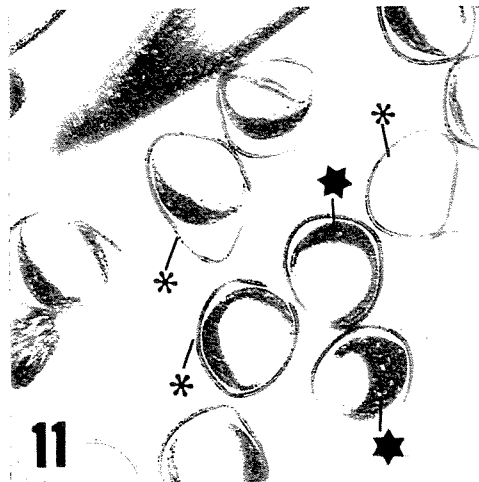
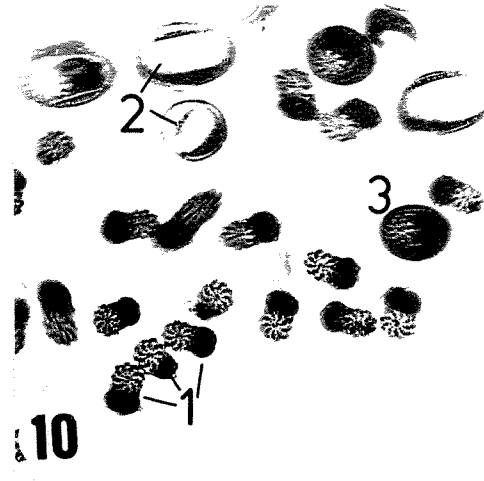
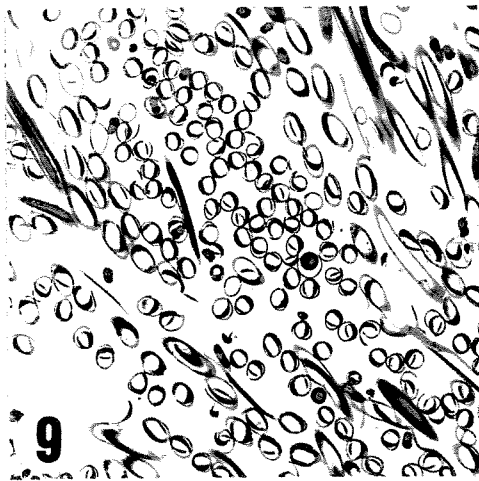
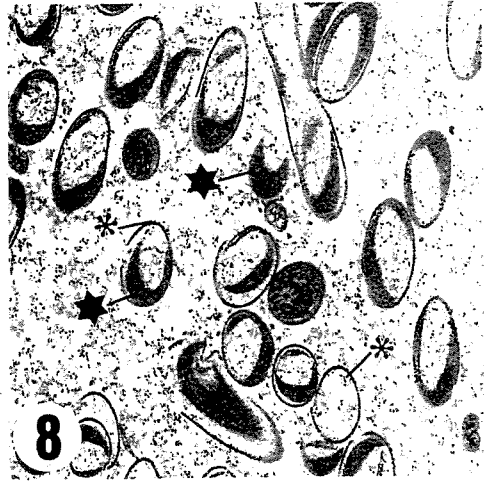
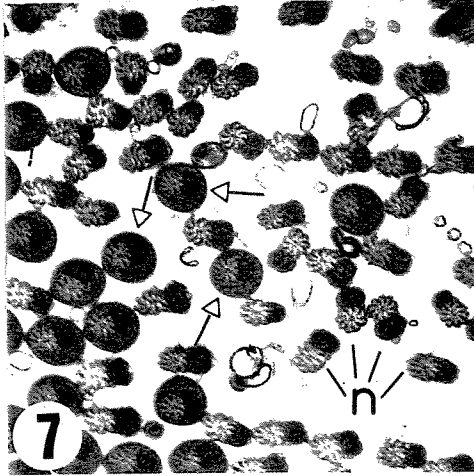
Figs. E1 to 6: Apyrene and Eupyrene Spermatozoa

- (1): Apyrene spermatozoa from the *utriculus*. Axoneme (a), mitochondrial derivatives (d), extracellular coat (c). Secretion (star). 15000x.
- (2): Apyrene (A) spermatozoa from the spiral duct showing the absence of the coat. Eupyrene spermatozoa (E). 9000x.
- (3) Eupyrene spermatozoa from the *utriculum*. The flagella are composed by an axoneme (a), mitochondrial derivatives (d) and the coat, which contains an amorphous matrix (star) and an external layer (open arrowhead) with the dense plate (arrow). 50000x.
- (4): Eupyrene spermatozoa from the *lagena*. The morphology is similar to fig. (3) but there is a great volume of secretion (star). 35000x.
- (5): Degenerating stages of eupyrene spermatozoa from the *utriculus*: 1 - normal cells; 2 - axoneme disorganization; 3 - total degenerated cell. The arrow indicates an eupyrene without a coat. 25000x.
- (6): Eupyrene spermatozoa from the *utriculus* showing the projections (arrows) of the coat. 45000x.



Figs. E6 to 12: Apyrene and Eupyrene Spermatozoa

- (7): Eupyrene spermatozoa from the *utriculus* near the spiral duct showing the spermatozoa with coat (arrows) and bare ones (n). 24000x.
- (8): Eupyrene coats with the external layer (asterisks) and the amorphous matrix (star). 24000x.
- (9): Large quantity of empty eupyrene coats in the spiraling duct. 4500x.
- (10): Three phases of eupyrene spermatozoa: 1 – naked cells; 2 – coats; 3 – coated eupyrene. 31000x.
- (11): Detail of the eupyrene coat with an amorphous matrix (star) and an external layer (asterisk). 50000x.
- (12): Bare eupyrene spermatozoa from the spiraling duct. Detail of the axoneme (a) and the mitochondrial derivatives (d). 50000x



CONCLUSÕES

- ✓ O processo de espermiogênese dicotômica em *E. hegesia* é semelhante àquele descrito para a maioria das espécies de lepidópteros estudada.
- ✓ As modificações sofridas por ambos os tipos de espermatozóides ao longo dos tratos reprodutores masculino e feminino estão relacionadas ao processo de maturação e capacitação destes tipos celulares e envolvem exclusivamente estruturas extra-celulares.
- ✓ O envoltório eupirene parece ser parcialmente resultado do rearranjo dos apêndices laciniados.
- ✓ A desagregação precoce dos espermatozóides apirenes contribui com o transporte dos agregados eupirenes ao longo do trato reprodutor masculino.
- ✓ O envoltório extra-celular eupirene não está relacionado ao processo de reconhecimento gamético, uma vez que tal estrutura é perdida na espermateca antes do processo de fertilização.
- ✓ Ocorrem diferenças na distribuição de proteínas e carboidratos no lúmen dos microtúbulos e nos elementos de ligação que compõem o axonema, nas membranas celulares e principalmente nas estruturas extra-celulares de ambos os tipos de espermatozóides.
- ✓ Nos espermatozóides apirenes ainda foram detectadas proteínas e carboidratos no capuz anterior e nas regiões paracristalinas dos derivados mitocondriais.
- ✓ Nos espermatozóides eupirenes, os apêndices laciniados apresentaram, principalmente, componentes protéicos, enquanto os apêndices reticulados parecem ser compostos principalmente por carboidratos.

- ✓ Ambos os tipos de apêndices apresentaram organização paracristalina, sendo formados por sub-unidades cilíndricas.
- ✓ A semelhança de reação à técnica de ácido tânico, para detecção de proteínas, entre os envoltórios apirene e eupirene sugere uma origem comum entre essas estruturas.
- ✓ A presença dos mesmos glicoconjugados nos apêndices laciniados e nos envoltórios apirene e eupirene sugere uma origem destes envoltórios a partir deste apêndice.
- ✓ Os apêndices laciniados não são estruturas derivadas de microtúbulos.
- ✓ A morfologia da espermateca de *E. hegesia* apresenta semelhanças àquela conhecida para algumas das espécies de insetos já estudadas.